

AQUADUCT
AB INITIO QUANTUM DYNAMICS
USING COUPLED CLUSTER IN TIME

by

Sebastian Gregorius Winther-Larsen

THESIS
for the degree of
MASTER OF SCIENCE



Faculty of Mathematics and Natural Sciences
University of Oslo

September 17, 2019

Abstract

We advance the Coupled Cluster method's in the time-dependent realm, by implementing a robust solver based on the orbital-adaptive time-dependent Coupled Cluster (OATDCC)[1] method. This involves implementing both a simplified static orbital time-dependent coupled cluster solver with single and double excitations (TDCCSD) and an orbital-adaptive scheme with double excitations (OATDCCD). To supplement the time-dependent methods we implement several ground state solvers based on the Lagrangian Coupled Cluster formulation, with single and double excitations, as well as a non-orthogonal orbital-optimised Coupled Cluster (NOCC) solver[2].

We construct several quantum dot basis sets with different potential functions in one- and two dimensions, including interactions with magnetic fields. What is more, we also implement an interface with popular quantum chemistry software modules PySCF[3] and Psi4[4] for extraction of additional basis sets for atoms and molecules. The quantum systems are allowed to vary with time by addition of a time-dependent term to the Hamiltonian, with which we simulate a laser field in the dipole approximation.

As a validation we reproduce results from the scientific literature, both for atoms, molecules and quantum dots. We show that our methods lead to convergence in the ever-increasing basis set size limit, for simple quantum dot systems. For the same quantum dot system, we show how sensitive a system is to changes in the frequency of a driving oscillating field. Frequencies closer to the resonant frequency lead to extiations and increased energy. We are able to simulate systems that are fairly large - quantum dots in one- and two dimensions with up to twelve electrons. For systems that meander far from the reference state, we show that the orbital-adaptive method has far superior stability, compared with the method with static orbitals.

For all quantum dot systems we find strong conformity with the harmonic potential theorem[5], yet we see a slight many-body effect for a two-dimensional double dot system. By subjecting the two-dimensional quantum dots to a homogenous, static magnetic field in the form of an angular momentum operator, we see two frequencies in the dipole spectrum, instead of one frequency. This is also in accordance with the harmonic potential theorem. The difference between the two frequencies in the new spectrum is the same as the Larmor frequency of the magnetic field, within acceptable tolerance levels.

Acknowledgements

As a project such as this eventually comes to an end, for better or for worse¹, the custom is to devote some words in a message of gratitude. After all, there are people in one's life that make everything a bit more enjoyable through their support - be it scientific or spiritual.

Firstly, I would like to thank my supervisor Morten. You welcomed me, willingly, with open arms, and despite of my previous background in finance, into the computational physics group. I value your unterminable optimism - after a chat with you I always feel invigorated and motivated. You bring great inspiration to your students and others around you.

Words of emphatic thanks are also imparted in the direction of my serendipitous co-supervisor Håkon. Your aid and insights have proven invaluable beyond a doubt. I consider myself very lucky to have someone examine my work as closely as you have done. More than that, I am delighted to have a friend like you.

To my partner in despair, Øyvind, who has been invaluable in all respects. You have that one personal trait that I look up to with high regard: unbounded resolve and grit that makes for true strength of character. I have found it motivating to work beside you and I am thankful for your friendship over the the many months (years!) we have struggled with very difficult physics together.

I would like to give my regards to the amazing people that make up the computational physics graduate students. If nothing more, you definitely make for the most enjoyable luncheons that oft-times include pristine philosophical discussions. The tales of the camaraderie of this gang of nonconformists will undoubtedly become material for an operette or at least some form of low-budget musical theatre.

I am also thankful to the two troupes of troubadours I have been affiliated with during my time as a student at the University of Oslo. It was in the ranks² of Studentorkestert Biørneblæs where I first picked up the saxophone, and here I found tremendous musical joy. Eventually I was head-hunted to become Il Maestro of Blinder Haarn oc Blaese. An event that actually *was* the basis of some form of very low-budget musical theatre. One should never let the (low) quality of the music be hindrance to a great orchestral experience.

To Vilde: I feel fortunate to have someone like you as my companion. The adventures we've had make up some of my most treasured memories, and I hope we will have many more together. Thank you for your patience, love and encouragement throughout these extra-ordinary months.

Collaboration details The software that has been developed as part of this thesis was developed in joint effort between Schøyen[6] and myself. As such, it exists as only one product, as we saw fit to join forces instead of manufacturing two duplicates of the same invention.

¹I have always believed that even an existence with severe stress is preferred compared to an existence without purpose.

²I am not sure if "rank" is the best word, because if Biørneblæs were even able to line up, it would more closely resemble a pile of overcooked spaghetti than ranks and files.

Contents

1	Introduction	1
1.1	The Quantum Many-Body Problem	2
1.2	Goals	3
1.3	Our Contributions	4
1.4	Structure of this Thesis	4
I	Fundamentals	7
2	Quantum Mechanics	9
2.1	Classical Mechanics	9
2.2	Canonical Quantisation	10
2.2.1	The Dirac-von Neumann Postulates	11
2.3	The Quantum Hamiltonian	14
2.3.1	Angular Momentum and Intrinsic Spin	16
2.3.2	Atomic Units	19
2.4	Indistinguishable Particles	20
2.5	Density Operators	22
3	Second Quantisation	23
3.1	Slater Determinants	23
3.2	Creation and Annihilation Operators	24
3.3	Anticommutator Relations	26
3.4	Representation of Operators	27
3.5	Normal Order and Wick's Theorem	28
3.5.1	Normal ordering and contractions	28
3.5.2	Wick's Theorem	29
3.5.3	Particle-Hole Formalism	30
3.5.4	Wick's theorem relative to the Fermi vacuum	31
II	Quantum Many-Body Approximations	33
4	Hartree-Fock Theory	35
4.1	Deriving the Hartree-Fock Equations	36

4.2	The Roothan-Hall Equations	38
4.3	Restricted Hartree-Fock Theory	40
4.4	Unrestricted Hartree-Fock Theory	42
4.5	Time-Dependent Hartree-Fock	44
5	Perturbation Theory	47
5.1	Formal perturbation theory	47
5.1.1	Energy- and Wavefunction Expansion	48
5.1.2	Projection Operators	49
5.1.3	The Resolvent	50
5.2	Brillouin-Wigner Perturbation Theory	51
5.3	Rayleigh-Schrödinger Perturbation Theory	52
6	Coupled Cluster	55
6.1	The Cluster Operator	56
6.2	Coupled-Cluster Doubles	57
6.3	The Coupled Cluster Equations	64
6.4	A Variational Formulation of Coupled Cluster	67
6.4.1	The Hellmann-Feynman Theorem	68
6.4.2	The Lagrangian Formulation of Coupled Cluster	70
6.4.3	The Bivariational Principle	71
6.5	Generalisation in Time	72
6.5.1	Equations of Motion	76
III	Implementation	81
7	Quantum Systems	83
7.1	Quantum System Abstract Base Class	85
7.2	Quantum Dots	86
7.2.1	One Dimension	87
7.2.2	Two Dimensions	91
7.2.3	Two-Dimensional Double Well	95
7.2.4	Two-Dimensional Magnetic Quantum dots	98
7.3	Constructing a Custom System	99
7.4	Time Evolution	100
8	Coupled Cluster	105
8.1	Ground State Computations	107
8.1.1	Representation of Amplitudes	107
8.1.2	Coupled Cluster Base Class	108
8.1.3	Coupled Cluster Doubles	110
8.1.4	Coupled Cluster Singles Doubles	112
8.1.5	Orbital-Adaptive Coupled Cluster	113
8.1.6	Mixing of Amplitude Vectors	116
8.2	Time Development	119

8.2.1	TDCCSD	122
8.2.2	OATDCCD	125
8.2.3	Integrators and ODE Solvers	128
IV	Results	135
9	Validation	137
9.1	Instantaneous dipole in H_2	137
9.2	Ground State Probability in 1D Quantum Dot	139
9.3	Dipole Spectrum of Helium	141
9.4	Ionisation of 1D Beryllium	142
10	Quantum Dots	147
10.1	Harmonic Oscillators in One Dimension	147
10.1.1	Dipole spectrum	150
10.1.2	Resonance Sensitivity	150
10.2	Two-dimensional Quantum Dot	153
10.2.1	Dipole Spectrum	156
10.2.2	Resonance Sensitivity	157
10.3	Two-dimensional Double Dot	158
10.4	Two-dimensional Magnetic Quantum Dot	160
10.4.1	Many-particle Magnetic Quantum Dots	162
V	Conclusion	165
11	Summary Remarks	167
11.1	Further Studies	168
VI	Appendices	171
A	Quantum Dot Results	173
A.1	One Dimension	174
A.2	Two Dimensions	179
A.3	Two Dimensions with Magnetic Field	180
B	Coupled Cluster	183
B.1	CC and CI correspondence	183
B.2	Slater-Condon Rules	184
B.3	Configuration space derivation of CCD	187
B.4	CCSD Equations	190
B.5	CCSD Lagrangian	192
B.6	Kappa Doubles Equations	193

C	Code Listings	195
C.1	2D Coulomb elements	195
C.2	Function for constructing system from Psi4	197
C.3	Function for constructing system from PySCF	198
D	Solving the Schrödinger Equation Analytically	203
D.1	The Schrödinger Equation in Spherical Coordinates	203
D.1.1	The Angular Equation	204
D.1.2	The Radial Equation	206
D.2	Quantum Systems	206
D.2.1	The Quantum Harmonic Oscillator	207

Chapter 1

Introduction

The aim and raison d'être of this thesis is to implement methods that enable the study of many-body quantum systems in time. The word ‘implement’ entails construction of numerical solvers on a computer. Such computational modelling have since its inception around the middle of the last century become present in all of the natural sciences, and have since made its foray in the social sciences as well. In the natural sciences, one could argue that computation plays as big a role as the two conventional congregations of theory and experiment. In physics, computations are a central component in a vast area of fields so diverse as quantum chromodynamics[7, 8], molecular dynamics[9, 10] and astrophysics[11].

Quantum mechanics is the description of the behaviour of matter and light in all its details, and in particular of the happenings on an atomic scale. A state of a quantum system is described by a wavefunction $\Psi(\mathbf{r}, t)$, which provides us with all there is to know about a particular system. We can determine $\Psi(\mathbf{r}, t)$ at any point in the future by solving the Schrödinger equation, given the initial state of the system $\Psi(\mathbf{r}, t_0)$,

$$i\hbar \frac{\partial}{\partial t} \Psi(\mathbf{r}, t) = \hat{H} \Psi(\mathbf{r}, t). \quad (1.1)$$

Our ability to solve the Schrödinger equation analytically is constrained to only a few quantum systems, and vanishes rapidly as the number of constituent particles in such a system exceed just a few. It has therefore been necessary to extend the proverbial chalk and blackboard with numerics and a computer.

This thesis deals specifically with the electronic quantum many-body problem, which is the central topic in quantum chemistry. The underlying theory for all of chemistry is well-known and has been known for more than half a century, but the only element we are able to solve analytically is the very simplest element, hydrogen. Adding an electron to the quantum model for the hydrogen atom results in an analytically unsolvable Schrödinger equation. As such, in order to actually *solve* chemistry we need numerical approximations.

1.1 The Quantum Many-Body Problem

We have established that solving the Schrödinger equations exactly with hand, mind, pencil and paper is impossible in the overwhelming majority of interesting cases. For this reason, a plethora of computational, approximative methods have been developed aiming to solve the many-body Schrödinger equation. Starting from first principles, or *ab initio*, the goal of such algorithms is to procure some information about a quantum system in a reasonable amount of time. In order to accomplish this, some sacrifices must be made in the form of simplifications.

The Hartree-Fock method [12–14] which has seen extensive use since its inception in 1930 employs a mean-field approximation, which provides an efficiently computed result, but not a very accurate one. The most popular approximative method is without doubt the density functional theory (DFT), developed by Kohn and Sham in 1965 [15]. Density functional theory simplifies the quantum many-body problem by reformulating it in terms of electron number density. However, DFT is also insufficient if one requires a high degree of accuracy.

It is possible to solve a quantum many-body problem “correctly” by direct diagonalisation of the matrix representation of the Hamiltonian, best known as a Full Configuration Interaction (FCI) computation. Such a method will yield an absolutely accurate result in the limit of an infinite orbital basis set, but it suffers from exponential complexity scaling [16]. A sophisticated Monte-Carlo scheme, like Diffusion Monte-Carlo (DMC) can in principle also provide the exact solution to the Schrödinger equation by imaginary time-evolution of an initial wave function ansatz [17]. However, the high dependence on the initial guess is problematic. What is more, the method often requires the input of another less accurate method as a starting point. Another example of a similar method is the Variational Monte-Carlo (VMC) method, which is simpler and faster than DMC, but not as accurate.

Since the Hartree-Fock method is the earliest of methods designed to solve the quantum many-body problem, it has become the purpose of all subsequent many-body methods to describe *electron correlation*, defined as the difference between the Hartree-Fock description of the electronic wavefunction and the exact solution of the Schrödinger equation. The simplest approach to treat electron correlations is by performing a Configurations Interaction (CI) expansion,

$$\Psi = \Phi_{\text{HF}} + \sum_{ia} C_a^i \Phi_i^a + \sum_{\substack{i < j \\ a < b}} C_{ab}^{ij} \Phi_{ij}^{ab} + \dots, \quad (1.2)$$

where Φ_i^a is a *singly excited* configuration and C_a^i is the matrix of coefficients associated with this configuration. We obtain the exact, Full Configuration Interaction (FCI), by including all terms in the CI expansion. It is common to perform a truncation of this expansion after some purposefully pre-determined excitation level. Truncating after double-excitation level, for instance, produces Configuration Interaction Singles Doubles (CISD), which is the most common choice in quantum chemistry. We will understand presently why such a truncation is problematic for the Configuration Interaction method.

Two important properties that a many-body method must incorporate is *size-extensivity* and *size-consistency*. A quantum-mechanical model is said to be *extensive* if the energy of the system computed with this model scales with the size of the system [18]. For systems of non-interacting helium atoms, for instance, we must have that $E(N\text{He}) = NE(\text{He})$. Moreover, a model is *size-consistent* if the energies of two systems A and B and of the combined system AB , with A and B very far apart, computed in equivalent ways, satify $E(AB) = E(A) + E(B)$ [19]. It can be shown that truncated Configuration Interaction does *not* comply with the concept of extensivity [20].

A class of methods of which most constituents provide proper *extensive* model descriptions is Many Body Perturbation Theory (MBPT) [21]. Many-body perturbation theory can also be truncated at a certain excitation level, in the same manner as truncated Configuration Interaction. The linked-diagram theorem [22], states that a particular perturbation expansion can be expressed by “linked terms” only¹, leading to the Coupled Cluster method [23, 24]. Coupled Cluster has become one of the most prevalent methods in quantum chemistry, as it is very accurate, whilst maintaining size-consistency and size-extensivity. The Coupled Cluster method also has elegant truncation levels, similar to the truncated Configuration Interaction method².

Computational scaling of *ab initio* quantum mechanical models range from $\mathcal{O}(N!)$ for Full Configuration Interaction (FCI), via $\mathcal{O}(N^6)$ for Coupled Cluster Singled Doubles with Perturbed Triples (CCSD(T)) to $\mathcal{O}(N^4)$ for formal Hartree-Fock (HF) [25].

1.2 Goals

The specific task of this thesis is to study the time evolution of quantum mechanical systems using the Coupled Cluster method. In particular this pertains to the study of time-dependent electronic systems, with an emphasis on quantum dots [26]. By use of proper object-orientation the implementation can also be used to study simple atoms and molecules in three dimensions. The aim was to extend the formalism and algorithms developed in the thesis of Kristiansen [27].

The thesis progression milestones have been split into the following steps,

1. Write a Coupled Cluster Doubles code with double excitations (CCD) capable of solving a system of two electrons in two or three dimensions in a single harmonic oscillator well.
2. Extend the Coupled Cluster solver to include single excitations (CCSD) and time evolution with static orbitals (TDCCSD). Moreover, expand system implementations to include more interesting systems, for example double potential wells or simple atoms.
3. Include orbital dependencies in the time-dependent coupled cluster solver, as discussed by Kvaal[1], in an Orbital Adaptive Time-Dependent Coupled Cluster Doubles (OATDCCD) solver.

¹A thorough treatment of these terms are found in the end of chapter 5

²Coupled Cluster and Configuration Interaction has an elegant correspondence, see section B.1

1.3 Our Contributions

There already exists an abundance of optimised and well-tested ab initio quantum chemistry software packages. As such we do not seek to build software meant to compete with such software, but to function as a supplement. As far as we know there is currently no software that allows for time-dependent Coupled Cluster computations in widespread use, making our contribution worthwhile. The interest we have seen for our work at the Hylleraas centre at the University of Oslo is testament to this[28].

We construct two modules for use with the Python programming language that works well in conjunction, but can also be used separately. The module `coupled_cluster`, as the name suggests contains all our Coupled Cluster solvers, both ground state and time-dependent. The module `quantum_systems` provides basis sets designed to work with the `coupled_cluster` module. The `quantum_systems` module also contains functions for extracting basis sets from the very popular quantum chemistry modules PySCF[3] and Psi4[4]. The source code for the `coupled_cluster` module can be found at github.com/Schoyen/coupled-cluster³ and documentation at www.coupledcluster.com. The source code for the `quantum_systems` module can be found at github.com/Schoyen/quantum-systems and documentation at Schoyen.github.io/quantum-systems.

We choose Python as a development language for a couple of reasons. First, even though Python is essentially a “scripting language”, in the sense that it is usually slower than a compiled language like C++, most of our computations are matrix or tensor computations which are very fast in Python. We do matrix multiplications and linear algebra in NumPy, which is highly optimised because of its use of Basic Linear Algebra Subprograms (BLAS) [29] and Linear Algebra PACKage (LAPACK) [30]. Both implemented in Fortran, BLAS consists of a low-level matrix and vector arithmetic operations, while LAPACK is a collection of common algorithms used in linear algebra, such as routines for solving systems of linear equations. For heavy operations that are not vectorisable, we have found just-in-time compilations with Numba very beneficial [31].

Second, Python is a high level language which has sped up development greatly compared to developing in a lower level language. For this reason we have a feeling that we have accomplished more than we would have otherwise. The drawback of developing in a higher level language is the lack of low level control, like memory management. All things considered, we are satisfied with the choice of development language, with the benefits outweighing the necessary sacrifices.

1.4 Structure of this Thesis

This thesis consists of five main parts. The first part, *Fundamentals* introduces the basis of quantum mechanics as well as the second quantisation formalism.

In the second part, *Quantum Many-Body Approximation*, we thoroughly present three many-body methods, each in its own chapter. We start with chapter 4 on *Hartree-Fock Theory*, because this is the first ab initio many-body method that saw

³At the time this document is first printed, the source code may not be public. We plan to make the source code open and public as soon as possible.

truly widespread use, but also because the Lagrange multiplier path we take to derive the method is similar to what we will do later, when we introduce the Lagrangian formulation of Coupled Cluster. We also introduce a time-dependent Hartree-Fock scheme in this chapter. Next, we present many-body *Perturbation Theory* in chapter 5, which is a method often used as a supplement to other many-body methods as well as on its own. Deriving the Rayleigh-Schrödinger perturbation theory also highlights the origins of the Coupled Cluster method, the topic of the following chapter.

In chapter 6 we provide a detailed derivation of the Coupled Cluster equations, before detailing the problems caused by the method's non-variational nature. This leads naturally to the Lagrangian formulation of Coupled Cluster[32] and the bivariational principle[33]. Lastly, we introduce time-dependent Coupled Cluster theory, with both static and adaptive orbitals[1].

In *Implementation*, the third part of the thesis, we bestow upon the reader a specification of the two python modules, `quantum_systems` in chapter 7 and `coupled_cluster` in chapter 8. Furthermore, we seek to explain the machinery in the two python modules, and their functionality. As the code base is somewhat extensive, it is not feasible to go through every aspect of the modules, but we provide a sufficient overview of the ideologies used in developments, the class structure hierarchy and the possibilities available to the user and future developer.

In the fourth part of the thesis, we provide *Results* generated with the coupled cluster solvers we have implemented. We start by a validation against some existing literature on time-dependent ab initio solvers in chapter 9. This includes the reproduction of several results from relatively well-known articles. Chapter 10 contains the central results of this thesis. Here we provide results from simulations of one- and two-dimensional quantum dots, as well as two-dimensional quantum dots affected by a homogenous, static magnetic field. Because this study has been conducted in close conjunction with Schøyen, more results that are computed with the same solvers, relating to atoms and molecules can be found in ref. [6].

Finally, in the fifth and final section we present a *Conclusion* in chapter 11. Here we also put forward some suggestions for future work in the same field of study as this thesis.

Part I

Fundamentals

Chapter 2

Quantum Mechanics

Here we present basic and foundational quantum theory, a theory that seeks to describe the nature at the smallest scales of energy. The name “quantum” stems from the need to see energy not as continuous and infinitely divisible , but rather as a sum of discrete quantities of equal size. Quantum mechanics came to the rescue when classical physics was unable to explain phenomena such as the mysterious sodium line, the ultraviolet catastrophe, and the bewildering photo-electric effect. With the new theory came new challenges like an axiomatic uncertainty, the wave-particle duality of light and a probabilistic interpretation of nature. In this chapter we will not be so hubristic as to delve into the philosophical particulars, but hope only to revitalise the reader’s faculties with the principal ideas on which this thesis is built.

2.1 Classical Mechanics

The formalism used in quantum mechanics largely stems from William Rowan Hamilton’s formulation of classical mechanics. Through the process of canonical quantisation any classical model of a physical system is turned into a quantum mechanical model.

In Hamilton’s formulation of classical mechanics, a complete description of a system of N particles is described by a set of canonical coordinates $q = (\vec{q}_1, \dots, \vec{q}_N)$ and corresponding conjugate momenta $p = (\vec{p}_1, \dots, \vec{p}_N)$. Together, each coordinate-momentum pair forms a point $\xi = (q, p)$ in phase space, which is the space of all possible states of the system. Moreover, pairs of generalised coordinates and conjugate momenta are canonical if they satisfy the Poisson brackets so that $\{q_i, p_k\} = \delta_{ij}$. The Poisson bracket of two functions is defined as

$$\{f, g\} = \frac{\partial f}{\partial q} \frac{\partial g}{\partial p} - \frac{\partial f}{\partial p} \frac{\partial g}{\partial q}. \quad (2.1)$$

The governing equations of motion in a classical system is Hamilton’s equations,

$$\dot{q} = \frac{\partial}{\partial p} \mathcal{H}(q, p) \quad (2.2)$$

$$\dot{p} = -\frac{\partial}{\partial q} \mathcal{H}(q, p) \quad (2.3)$$

where $\mathcal{H}(q, p)$ is the Hamiltonian, a function for the total energy of the system. Hamilton's equations may also be stated in terms of the Poisson brackets,

$$\frac{dp_i}{dt} = \{p_i, \mathcal{H}\}, \quad \frac{dq_i}{dt} = \{q_i, \mathcal{H}\}. \quad (2.4)$$

A system consisting of N particles of equal mass m , subject to forces caused by an external potential, as well as acting on each other with forces stemming from a central potential $w(q_i, q_j)$ has the following Hamiltonian,

$$\mathcal{H}(\mathbf{q}, \mathbf{p}) = \mathcal{T} + \mathcal{V} + \mathcal{W} = \frac{1}{2m} \sum_i |\vec{p}_i|^2 + \sum_i v(\vec{q}_i) + \frac{1}{2} \sum_{i < j} w(\vec{q}_i, \vec{q}_j), \quad (2.5)$$

where the sum over $i < j$ implies sum over different indices. This Hamiltonian conveniently contains several parts - the kinetic energy, the external potential energy and the interaction energy; denoted by \mathcal{T} , \mathcal{V} and \mathcal{W} respectively.

2.2 Canonical Quantisation

In order to transition from a classical system to a quantum system, we move from the classical phase space to the Hilbert space, through the procedure known as canonical, or first¹-, quantisation. Whilst the state of a classical system is a point in phase space, a quantum state is a complex-valued state vector in discrete, infinite-dimensional, Hilbert space. A physicist would define a Hilbert space as a complete vector space equipped with an inner product. This space is most commonly chosen to be the space of square-integrable functions Ψ , dependent on all coordinates

$$\Psi = \Psi(x_1, x_2, \dots, x_N). \quad (2.6)$$

These functions are dubbed wavefunctions and are maps from a point (x_1, \dots, x_N) in configuration space to the complex vector space,

$$\Psi : X^N \rightarrow \mathbb{C}. \quad (2.7)$$

It has been widely discussed how such an object can represent the state of a particle. One answer is provided by Max Born's probabilistic interpretation, which says that $|\Psi(x_1, \dots, x_N)|^2$, gives the probability of finding the particle at a certain position. For a situation with one particle in one dimension we have,

$$\int_a^b |\Psi(x)|^2 dx = \left\{ \begin{array}{l} \text{probability of finding the} \\ \text{particle between } a \text{ and } b \end{array} \right\} \quad (2.8)$$

while $|\Psi(x_1, x_2, \dots, x_N)|^2$ is the probability density for locating all particles at the point $(x_1, \dots, x_N) \in X^N$. Since the total probability must be 1, we are provided with a normalisation condition for the wavefunction,

¹Second quantisation comes later.

$$\int_{X^N} |\Psi(x_1, x_2, \dots, x_N)|^2 dx_1 dx_2 \dots dx_N = 1. \quad (2.9)$$

The relation between a classical- and quantum description of a mechanical system is most clearly seen when the two descriptions are expressed in terms of the same variables. In fact, we may apply *quantisation* of the classical variables to produce the quantum equivalent of the system. The classical phase space variables are changed into quantum observables,

$$q_i \rightarrow \hat{q}_i, \quad p_i \rightarrow \hat{p}_i. \quad (2.10)$$

The quantum observables are required to satisfy the Heisenberg commutation relation,

$$[\hat{q}_i, \hat{p}_j] = i\hbar\delta_{ij}, \quad (2.11)$$

instead of the Poisson bracket from Equation 2.1. Here \hbar is the reduced Planck's constant. For any general variables A and B , this transition can be expressed by substitution between Poisson brackets for the classical variables and commutators for the quantum observables,

$$\{A, B\} \rightarrow \frac{1}{i\hbar} [\hat{A}, \hat{B}]. \quad (2.12)$$

This correspondence between the classical and quantum dynamical equations is directly related to *Ehrenfest's theorem*, which states that the classical dynamical equations keep their validity also in the quantum theory, with the classical variables replaced by their corresponding quantum expectation values[34].

2.2.1 The Dirac-von Neumann Postulates

The following postulates, or axioms, provide a precise and concise description of quantum mechanics in terms of operators on the Hilbert space. There are many variations of these postulates, two of which were introduced by the namesakes of the postulates, Paul Adriene Maurice Dirac [35] and John von Neumann [36].

Hilbert Space

A quantum state of an isolated physical system is described by a vector with unit norm in a Hilbert space \mathcal{H} , a complex vector space equipped with an inner product. The inner product associates a scalar value, which may be either real or complex, with any pair of state vectors.

The inner product can be defined as

$$\langle \psi_\alpha | \psi_\beta \rangle = \int \psi_\alpha^*(x) \psi_\beta(x) dx, \quad (2.13)$$

where ψ^* is the complex conjugate of ψ . Here we have introduced Dirac notation, which is very common when describing quantum states. For each quantum state $|\psi_\alpha\rangle$ there exists a dual state $\langle\psi_\alpha|$. We refer to these two vectors as *bra* and *ket* vectors, respectively. Some properties of an inner product, written in Dirac's style, read

$$\langle \psi_\alpha | \psi_\beta \rangle = \langle \psi_\beta | \psi_\alpha \rangle^* \quad (2.14)$$

$$\langle \psi_\alpha | (z_1 |\psi_\beta\rangle + z_2 |\psi_\beta\rangle) = z_1 \langle \psi_\alpha | \psi_\beta \rangle + z_2 \langle \psi_\alpha | \psi_\beta \rangle \quad (2.15)$$

$$\langle \psi_\alpha | \psi_\alpha \rangle \geq 0, \quad (2.16)$$

where $z_n = a_n + ib_n$ is a complex number. Notice that in these properties, a superposition of a state wavefunction in the form of linear combination of two other states have appeared. Such superpositions are generally written

$$|\psi_\gamma\rangle = z_1 |\psi_\alpha\rangle + z_2 |\psi_\beta\rangle, \quad (2.17)$$

where we have produced a new quantum state from two other states. Any two or more states may be superposed to produce a new state in this manner. Superposition is of fundamental importance to quantum mechanics, and even though the concept is similar to the classical superposition principle for waves in classical physics, "the superposition that occurs in quantum mechanics is of an essentially different nature from any occurring in the classical theory" according to Dirac [35].

To conclude the description of quantum states for now; a state function ψ is said to be *normal* if its innerproduct with itself is one, $\langle \psi | \psi \rangle = 1$. Two different state functions are *orthogonal* if their inner product is zero. We have orthogonal functions if $\langle \psi_\alpha | \psi_\beta \rangle = \delta_{\alpha\beta}$, where $\delta_{\alpha\beta}$ is the Kronecker delta.

Observables

Each physical observable of a system is associated with a *Hermitian* operator acting on the Hilbert space. The eigenstates of each such operator define a *complete, orthonormal* basis set of vectors \mathcal{B} for the d -dimensional Hilbert space,

$$\mathcal{B} = \{|i\rangle\}_{i=1}^d. \quad (2.18)$$

Completeness of the basis set \mathcal{B} means,

$$\sum_{i=1}^d |i\rangle \langle i| = \mathbb{1}. \quad (2.19)$$

With \hat{O} an operator, *hermiticity* means,

$$\langle \phi | \hat{O} \psi \rangle = \langle \hat{O} \phi | \psi \rangle \equiv \langle \phi | \hat{O} | \psi \rangle. \quad (2.20)$$

This implies that the operator \hat{O} must be its own Hermitian conjugate,

$$\hat{O}^\dagger = \hat{O}. \quad (2.21)$$

Some properties of the Hermitian conjugate read,

$$(z\hat{O})^\dagger = z^* \hat{O}^\dagger \quad (2.22)$$

$$(\hat{O}_1 + \hat{O}_2)^\dagger = \hat{O}_1^\dagger + \hat{O}_2^\dagger \quad (2.23)$$

$$(\hat{O}_1 \hat{O}_2)^\dagger = \hat{O}_2^\dagger \hat{O}_1^\dagger. \quad (2.24)$$

Measurements

Physically measurable values, associated with an observable \hat{O} are defined by the eigenvalues o_n of the observable,

$$\hat{O} |n\rangle = o_n |n\rangle, \quad (2.25)$$

where $|n\rangle$ are the eigenvectors of the same observable \hat{O} . The probability for finding a particular eigenvalue in the measurement is

$$p_n = |\langle n|\psi\rangle|^2, \quad (2.26)$$

with the system in state $|\psi\rangle$ before the measurement, and $|n\rangle$ as the eigenstate corresponding to the eigenvalue o_n . If the observable \hat{O} is Hermitian, we can write the operators as a spectral decomposition

$$\hat{O} = \sum_{n=1}^d o_n |n\rangle\langle n|, \quad (2.27)$$

where d is the dimensionality of the Hilbert space.

Time Evolution

In the *Schrödinger picture* time evolution of the state vector, $|\psi\rangle = |\psi(t)\rangle$, is given by the Schrödinger equation,

$$i\hbar \frac{d}{dt} |\psi(t)\rangle = \hat{H} |\psi(t)\rangle. \quad (2.28)$$

Note that any superposed state, as described by 2.17, will also be a solution to the Schrödinger equation due to its linearity.

The Schrödinger equation is first order in the time derivative, meaning that the time evolution $|\psi\rangle = |\psi(t)\rangle$ is uniquely determined by some initial condition $|\psi_0\rangle = |\psi(t_0)\rangle$. \hat{H} is the Hamiltonian of the system, which is a *linear, hermitian* operator. The Hamiltonian gives rise to the time evolution, which is a *unitary* mapping between quantum states in time,

$$|\psi(t)\rangle = \hat{\mathcal{U}}(t, t_0) |t_0\rangle. \quad (2.29)$$

The time evolution operator $\hat{\mathcal{U}}$ is determined by the Hamiltonian through the equation

$$i\hbar \frac{\partial}{\partial t} \hat{\mathcal{U}}(t, t_0) = \hat{H} \hat{\mathcal{U}}(t, t_0), \quad (2.30)$$

which follows from the Schrödinger equation. For a time-independent Hamiltonian it is given by

$$\hat{\mathcal{U}}(t, t_0) = e^{-i\hat{H}(t-t_0)/\hbar}. \quad (2.31)$$

We see that this time-propagator is Hermitian

$$\hat{\mathcal{U}}\hat{\mathcal{U}}^\dagger = \hat{\mathcal{U}}^\dagger\hat{\mathcal{U}} = 1. \quad (2.32)$$

If however \hat{H} is time-dependent, so that the operator at different times do not commute, we may use a more general integral expression for the time-propagator,

$$\hat{\mathcal{U}}(t, t_0) = \sum_{n=0}^{\infty} \left(-\frac{i}{\hbar}\right)^n \int_{t_0}^t \int_{t_0}^{t_1} dt_1 \int_{t_0}^{t_1} dt_2 \cdots \int_{t_0}^{t_{n-1}} dt_n \hat{H}(t_1) \hat{H}(t_2) \cdots \hat{H}(t_n). \quad (2.33)$$

A unitary transformation of states and observables

$$|\psi\rangle \rightarrow |\psi'\rangle = \hat{U}|\psi\rangle, \quad \hat{O} \rightarrow \hat{O}' = \hat{U}\hat{O}\hat{U}^\dagger, \quad \hat{U}^\dagger\hat{U} = 1. \quad (2.34)$$

leads to a different, but equivalent representation of a quantum system. The transition to the *Heisenberg picture* is defined by a special time-dependent unitary transformation,

$$\hat{U} = \hat{\mathcal{U}}^\dagger(t, t_0), \quad (2.35)$$

which is the inverse of the time-evolution operator. When applied to the time-dependent state vector of the Schrödinger picture it will cancel the time-dependence

$$|\psi\rangle_H = \hat{\mathcal{U}}^\dagger(t, t_0)|\psi(t)\rangle_S = |\psi(t_0)\rangle_S. \quad (2.36)$$

The time-dependence is now carried by the observables, rather than the state vectors,

$$\hat{O}_H = \hat{\mathcal{U}}^\dagger(t, t_0)\hat{O}_S\hat{\mathcal{U}}(t, t_0), \quad (2.37)$$

and the Schrödinger equation is replaced by the Heisenberg equation

$$\frac{d}{dt} = \frac{i}{\hbar}[\hat{H}, \hat{O}_H] + \frac{\partial}{\partial t}\hat{O}_H. \quad (2.38)$$

There is a third representation called the *interaction picture*, but we will remain firmly rooted in the Schrödinger picture and halt this general introduction to time-development here.

2.3 The Quantum Hamiltonian

The full Hamiltonian for a quantum many-body system can be a large and unwieldy thing. In this study we will constrain ourselves to the study of electronic systems. On a phenomenological basis, one would include nuclear terms in the Hamiltonian as well. In this study however, we will stay within the Born-Oppenheimer approximation and treat the nuclei as stationary, thereby refraining from introducing terms that involve the motion of nuclei.

The full molecular electronic Breit-Pauli Hamiltonian, thoroughly described in Helgaker et al.[37], contains the following types of terms

$$\hat{H}_{\text{mol}}^{\text{BP}} = \begin{cases} \hat{H}_{\text{kin}} & \leftarrow \text{kinetic energy} \\ +\hat{H}_{\text{cou}} & \leftarrow \text{Coulomb interactions} \\ +\hat{H}_{\text{ee}} & \leftarrow \text{external electric field interaction} \\ +\hat{H}_Z & \leftarrow \text{Zeeman interactions} \\ +\hat{H}_{\text{so}} & \leftarrow \text{spin-orbit interactions} \\ +\hat{H}_{\text{ss}} & \leftarrow \text{spin-spin interactions} \\ +\hat{H}_{\text{oo}} & \leftarrow \text{orbit-orbit interactions} \\ +\hat{H}_{\text{dia}} & \leftarrow \alpha^4 \text{ diamagnetic interactions} \end{cases} \quad (2.39)$$

We will not be working the full Breit-Pauli Hamiltonian, but we will go into some of the most important terms that an electronic Hamiltonian can constitute.

Kinetic energy The general kinetic energy operator is given by

$$\hat{H}_{\text{kin}} = -\frac{\hbar}{2m} \sum_i \nabla_i^2, \quad (2.40)$$

where ∇ is the differential operator and the sum is over all electrons in the system. This term is an example of what we call a one-particle operator as it remains the same for all electrons and contains no terms that would represent interactions between particles. For a free particle or a gas of non-interacting particles, Equation 2.40 is sufficient to describe the entire system.

Potential terms Adding a confining potential to the Hamiltonian in addition to the kinetic energy term in Equation 2.40,

$$\hat{H} \supset \hat{H}_{\text{kin}} + \hat{V} \quad (2.41)$$

gives rise to much more interesting systems and is the beginning of an approximation of reality. Perhaps the most common is the harmonic oscillator potential, which in one dimension reads

$$\hat{V}(x) = \frac{1}{2}m\omega^2 x^2, \quad (2.42)$$

where m is the mass of the particles and ω is the (angular) frequency of oscillation.

This is a very popular confining potential because virtually any oscillatory motion can be approximated by it, if the amplitude of the oscillations is sufficiently small. This parabolic, harmonic potential is the basis of a quantum dot which is a central part of this study. In quantum chemistry we only consider potentials derived from particle-particle interactions, and not such external potentials.

Coulomb interactions The electrostatic interaction between particles in a molecule or atom is modelled by Coulomb terms in the Hamiltonian.

$$\hat{H}_{\text{cou}} = - \sum_{iK} \frac{k_e Z_K e^2}{r_{iK}} + \frac{1}{2} \sum_{i \neq j} \frac{k_e e^2}{r_{ij}} + \frac{1}{2} \sum_{K \neq L} \frac{k_e Z_K Z_L e^2}{R_{KL}}, \quad (2.43)$$

where e is the elementary particle charge and $k_e = 1/4\pi\epsilon_0$ is the Coulomb constant. The first term is the potential between nuclei and electrons, the second term is the potential between electrons and the last term is the potential between nuclei.

External electric field interactions Now comes the time to go through, in broadest of strokes, a quantisation of an electromagnetic field. For a thorough derivation see for instance Joachain *et al.*[38]. When we include an electromagnetic field in the model it is necessary to include terms in the Hamiltonian that model the effects of an externally

applied scalar potential $\phi = \phi(\mathbf{r}, t)$ and a vector potential $\mathbf{A} = \mathbf{A}(\mathbf{r}, t)$. This will also affect the kinetic energy of the particles, which we therefore include at first,

$$\hat{H}_{\text{ef}} \subset \frac{1}{2m}(e\mathbf{A} - \hat{\mathbf{p}})^2 + e\phi = \frac{\hat{\mathbf{p}}^2}{2m} - \frac{e}{2m}(\mathbf{A} \cdot \hat{\mathbf{p}} + \hat{\mathbf{p}} \cdot \mathbf{A}) + \frac{e^2}{2m}\mathbf{A}^2 + e\phi. \quad (2.44)$$

This Hamiltonian now describes a free particle subject to an external electric field. Since we have already included a term for kinetic energy we now wish to remove it, keeping only the new terms,

$$\hat{H}_{\text{ef}} = -\frac{e}{2m}(\mathbf{A} \cdot \hat{\mathbf{p}} + \hat{\mathbf{p}} \cdot \mathbf{A}) + \frac{e^2}{2m}\mathbf{A}^2 + e\phi. \quad (2.45)$$

We assume that the external field has sufficiently large wavelength compared to the system, making the vector potential uniform in space $\mathbf{A}(\mathbf{r}, t) = \mathbf{A}(t)$. This approximation is very reasonable, considering visible light has a wavelength of $\lambda \sim 5000\text{\AA}$ and the diameter of an atom is around 1\AA . In the dipole approximation we can write the vector potential as

$$\mathbf{A}(t) = \mathbf{A}_0 e^{-i\omega_k t} + \mathbf{A}_0^* e^{i\omega_k t}, \quad (2.46)$$

where \mathbf{A}_0 and \mathbf{A}_0^* are photon creation and annihilation operators, and ω_k is the angular frequency of the field. The photon creation and annihilation operators allow for spontaneous emission and absorption of photons without the presence of a field, but we will disregard such phenomena and stick to a semi-classical description. We therefore rewrite the vector potential as

$$\mathbf{A}(t) = \epsilon A_0 \sin(\omega_k t), \quad (2.47)$$

where ϵ is the polarisation vector. This expression is the same as Equation 2.46 up to a phase. In the Coulomb gauge we have

$$\mathbf{E} = -\frac{d}{dt}\mathbf{A}, \quad (2.48)$$

which gives us an expression for the E-field

$$\mathbf{E}(t) = \epsilon \mathbf{E}_0 \cos(\omega_k t), \quad (2.49)$$

where $\mathbf{E}_0 = -\omega_k A_0$ and we can approximate the external field time-dependent electric field by

$$\hat{H}_{\text{ef}} = -\hat{\mathbf{d}} \cdot \epsilon \mathbf{E}_0 \cos \omega_k t, \quad (2.50)$$

where $\hat{\mathbf{d}} = q\hat{\mathbf{r}}$, is the dipole operator, dictating the allowed transitions.

2.3.1 Angular Momentum and Intrinsic Spin

In general, modelling of interactions with magnetic fields necessitates the use of operators for intrinsic angular momentum ($\hat{\mathbf{S}}$) and extrinsic angular momentum ($\hat{\mathbf{L}}$). These are often referred to as *spin* and *angular momentum*, respectively. We will spend some time here elaborating on such terms.

Angular momentum

In a classical system, the angular momentum of a particle with respect to the origin is given as

$$\mathbf{L} = \mathbf{r} \times \mathbf{p}, \quad (2.51)$$

which broken down into components becomes,

$$L_x = yp_z - zp_y, \quad L_y = yp_x - xp_z, \quad L_z = xp_y - yp_x. \quad (2.52)$$

From this we can obtain the quantum mechanical description by promotion to operators, and inserting the representation for the momentum operator in position space, $p_x \rightarrow i\hbar\partial/\partial x$.

The commutators of the angular momentum operators obey the following cyclic permutation of indices rule,

$$[\hat{L}_x, \hat{L}_y] = i\hbar\hat{L}_z, \quad [\hat{L}_y, \hat{L}_z] = i\hbar\hat{L}_x, \quad [\hat{L}_z, \hat{L}_x] = i\hbar\hat{L}_y. \quad (2.53)$$

We see that they do not commute with each other, but the square of the total angular momentum, defined by

$$\hat{L}^2 \equiv \hat{L}_x^2 + \hat{L}_y^2 + \hat{L}_z^2, \quad (2.54)$$

does

$$[\hat{L}^2, \hat{L}_x] = 0, \quad [\hat{L}^2, \hat{L}_y] = 0, \quad [\hat{L}^2, \hat{L}_z] = 0. \quad (2.55)$$

In spherical coordinates, which is better suited for our needs, the angular momentum operator is given by

$$\hat{\mathbf{L}} = -i\hbar\hat{\mathbf{r}} \times \nabla. \quad (2.56)$$

Given the gradient in spherical coordinates,

$$\nabla = e_r \frac{\partial}{\partial r} + e_\theta \frac{1}{r} \frac{\partial}{\partial \theta} + e_\phi \frac{1}{r \sin \theta} \frac{\partial}{\partial \phi} \quad (2.57)$$

and $\mathbf{r} = re_r$ we get

$$\begin{aligned} \hat{\mathbf{L}} &= -i\hbar \left[r(e_r \times e_r) \frac{\partial}{\partial r} + (e_r \times e_\theta) \frac{\partial}{\partial \theta} + (e_r \times e_\phi) \frac{1}{\sin \theta} \frac{\partial}{\partial \phi} \right] \\ &= -i\hbar \left(e_\phi \frac{\partial}{\partial \theta} - e_\theta \frac{1}{\sin \theta} \frac{\partial}{\partial \phi} \right). \end{aligned} \quad (2.58)$$

Now, with a bit of algebra we get

$$\hat{L}_x = i\hbar \left(\sin \phi \frac{\partial}{\partial \theta} + \cos \phi \cot \theta \frac{\partial}{\partial \phi} \right) \quad (2.59)$$

$$\hat{L}_y = i\hbar \left(\cos \phi \frac{\partial}{\partial \theta} + \sin \phi \cot \theta \frac{\partial}{\partial \phi} \right) \quad (2.60)$$

$$\hat{L}_z = -i\hbar \frac{\partial}{\partial \phi} \quad (2.61)$$

The squared operator becomes

$$\hat{L}^2 = -\hbar^2 \left[\frac{1}{\sin \theta} \frac{\partial}{\partial \theta} \left(\sin \theta \frac{\partial}{\partial \theta} \right) + \frac{1}{\sin^2 \theta} \frac{\partial^2}{\partial \phi^2} \right]. \quad (2.62)$$

The eigenvalue equations of \hat{L}^2 and \hat{L}_z are

$$\hat{L}^2 \psi = \hbar^2 l(l+1) \psi, \quad \hat{L}_z \psi = \hbar m \psi, \quad (2.63)$$

where $\psi = Y_l^m(\theta, \phi)$ are the spherical harmonics,

$$Y_l^m(\theta, \phi) = \epsilon \sqrt{\frac{(2l+1)}{4\pi} \frac{(l-|m|)!}{(1+|m|)!}} e^{im\theta} P_l^m(\cos \theta), \quad (2.64)$$

and P_l^m are the associated Legendre polynomials.

Spin

In classical mechanics, intrinsic spin ($\mathbf{S} = I\omega$) is associated with an object's motion about its centre of mass. A similar thing goes on in quantum mechanics, but it has nothing to do with motion in space. In quantum mechanics spin is seen as a property that particles can carry, but is analogous with its classical counterpart only in name.

Algebraically, *spin* is the same as *angular momentum*, beginning with the commutator relations,

$$[\hat{S}_x, \hat{S}_y] = i\hbar \hat{S}_z, \quad [\hat{S}_y, \hat{S}_z] = i\hbar \hat{S}_x, \quad [\hat{S}_z, \hat{S}_x] = i\hbar \hat{S}_y, \quad (2.65)$$

while the eigenvectors of \hat{S}^2 and S_z satisfy

$$\hat{S}^2 |s m_s\rangle = \hbar^2 s(s+1) |s m_s\rangle, \quad \hat{S}_z |s m_s\rangle = \hbar m |s m_s\rangle. \quad (2.66)$$

Here, $|s m_s\rangle$ is an eigenstate determined by the quantum numbers s and m_s .

Because the quantum mechanical spin has nothing to do with motion in space and is independent of any coordinates r , θ or ϕ , there is no reason to exclude half-integer values of s and m_s ,

$$s = 0, \frac{1}{2}, 1, \frac{3}{2}, \dots, \quad m_s = -s, s+1, \dots, s-1, s. \quad (2.67)$$

As it would turn out, every elemental particle has a specific and immutable value of s , and the most important one is $s = \frac{1}{2}$ (!) as it is the spin-value for all leptons, including the electron, all quarks as well as protons and neutrons. Since our particle of scrutiny is the electron our interest lies in spin-half systems, i.e.

$$s = \frac{1}{2}, \quad m_s = \pm \frac{1}{2}. \quad (2.68)$$

In such a system there are only two spin eigenstates,

$$\left| \frac{1}{2}, +\frac{1}{2} \right\rangle = |\uparrow\rangle = |+\rangle, \quad \left| \frac{1}{2}, -\frac{1}{2} \right\rangle = |\downarrow\rangle = |-\rangle. \quad (2.69)$$

This means that the Hilbert space \mathcal{H} for spin-half particles has two dimensions, and that any state can be expressed as a two-dimensional vector called a spinor,

$$|\chi\rangle = \begin{pmatrix} a \\ b \end{pmatrix} = a |\uparrow\rangle + b |\downarrow\rangle = a \begin{pmatrix} 1 \\ 0 \end{pmatrix} + b \begin{pmatrix} 0 \\ 1 \end{pmatrix}. \quad (2.70)$$

The probability of finding a particle represented by the state vector $|\chi\rangle$ in the spin up or spin down state is $|a|^2$ and $|b|^2$, respectively. This requires a normalisation, such that $|a|^2 + |b|^2 = 1$.

In the basis of $|\uparrow\rangle$ and $|\downarrow\rangle$ the operators \hat{S}^2 , \hat{S}_x , \hat{S}_y and \hat{S}_z are represented by two-dimensional matrices,

$$\hat{S}^2 = \frac{3}{4}\hbar^2 \begin{pmatrix} 1 & 0 \\ 0 & 1 \end{pmatrix} \quad (2.71)$$

$$\hat{S}_x = \frac{\hbar}{2}\sigma_x, \quad \hat{S}_y = \frac{\hbar}{2}\sigma_y, \quad \hat{S}_z = \frac{\hbar}{2}\sigma_z, \quad (2.72)$$

where the Pauli matrices are given by,

$$\sigma_x = \begin{pmatrix} 0 & 1 \\ 1 & 0 \end{pmatrix} \quad \sigma_y = \begin{pmatrix} 0 & -i \\ i & 0 \end{pmatrix} \quad \sigma_z = \begin{pmatrix} 1 & 0 \\ 0 & -1 \end{pmatrix}. \quad (2.73)$$

2.3.2 Atomic Units

It is common practice to switch to a set of units that are easier to work with, in essence setting $\hbar = m_e = e = \dots = 1$. In this study we use atomic units, a form of such dimensionless units. To see how these units arise, consider the time-independent Schrödinger equation for a Hydrogen atom,

$$\left(-\frac{\hbar^2}{2m_e} \nabla^2 - \frac{e^2}{4\pi\epsilon_0 r} \right) \phi = E\phi, \quad (2.74)$$

where \hbar is the reduced Planck constant, equal to Planck's constant divided by 2π ; m_e is the mass of the electron, $-e$ is the charge of the electron, ϵ_0 is the permittivity of free space and ∇ is the many-dimensional differential operator. We make this equation dimensionless by letting $r \rightarrow \lambda r'$,

$$\left(-\frac{\hbar^2}{2m_e\lambda^2} \nabla'^2 - \frac{e^2}{4\pi\epsilon_0\lambda r'} \right) \phi' = E\phi'. \quad (2.75)$$

We can factor out the constants in front of the operators, if we choose λ so that,

$$\frac{\hbar^2}{m_e\lambda^2} = \frac{e^2}{4\pi\epsilon_0\lambda} = E_a \rightarrow \lambda \frac{4\pi\epsilon_0\hbar^2}{m_e e^2} = a_0 \quad (2.76)$$

where E_a is the atomic unit of energy that chemists call Hartree. Incidentally, we see that λ is just the Bohr radius, a_0 . If we let $E' = E/E_a$, we obtain the dimensionless Schrödinger equation,

$$\left(-\frac{1}{2} \nabla'^2 - \frac{1}{r'} \right) \phi' = E' \phi'. \quad (2.77)$$

Some conversion factors between atomic units and SI units can be found in Table 2.1.

Table 2.1: Conversion of atomic units to SI units.

Physical quantity	Conversion factor	Value
Length	a_0	$5.2918 \times 10^{-11} m$
Mass	m_e	$9.1095 \times 10^{-31} kg$
Time	\hbar/E_a	$2.4189 \times 10^{-17} s$
Charge	e	$1.6022 \times 10^{-19} C$
Energy	E_a	$4.3598 \times 10^{-18} J$
Velocity	$a_0 E_a / \hbar$	$2.1877 \times 10^6 ms^{-1}$
Angular momentum	\hbar	$1.0546 \times 10^{-34} Js$
Electric dipole moment	ea_0	$8.4784 \times 10^{-30} Cm$
Electric polarizability	$e^2 a_0^2 / E_a$	$1.6488 \times 10^{-41} C^2 m^2 J^{-1}$
Electric field	$E_a / (ea_0)$	$5.1423 \times 10^{11} V m^{-1}$
Wave function	$a_0^{-3/2}$	$2.5978 \times 10^{15} m^{-3/2}$

2.4 Indistinguishable Particles

In classical mechanics, although particles are indistinguishable, one typically regards particles as individuals because a permutation of particles is counted as a new arrangement and something different than the initial configuration. This was called “Transcendental Individuality” by Heinz Post[39]. In quantum mechanics, on the other hand, a permutation is not regarded as giving rise to a new arrangement. It follows that quantum objects are very different from anything else we know from everyday life, and must be considered “non-individual”. This idea has its origin from the uncertainty principle, stating that no sharply defined particle exist. If we take this idea to its extreme one may postulate that all particles of a given type are one and the same. Here from Richard Feynman’s Nobel lecture[40]: “I received a telephone call one day at the graduate college at Princeton from Professor Wheeler, in which he said, ‘Feynman, I know why all electrons have the same charge and the same mass’ ‘Why?’ ‘Because, they are all the same electron!’ ”

Following the brief discussion above one may begin to postulate that, the probability density for the location of particles in a system must be permutation invariant,

$$|\Psi(x_1, x_2, \dots, x_i, x_j, \dots, x_N)|^2 = |\Psi(x_1, x_2, \dots, x_j, x_i, \dots, x_N)|^2, \quad (2.78)$$

where Ψ represents a wavefunction description of N particles For any arbitrary permutation, this is equivalent to

$$\Psi(x_1, \dots, x_N) = e^{i\alpha(\sigma)} \Psi(x_{\sigma(1)}, x_{\sigma(2)}, \dots, x_{\sigma(N)}), \quad (2.79)$$

where $\sigma \in S_N$ is some permutation of N indices and α is some real number that may be dependent on σ . The same relation can be written by way of a linear permutation operator,

$$(\hat{P}_\sigma \Psi)(x_1, \dots, x_N) = \Psi(x_{\sigma(1)}, x_{\sigma(2)}, \dots, x_{\sigma(N)}). \quad (2.80)$$

The ‘indistinguishability postulate’ states that if a permutation P is applied to a state representing an assembly of particles, there is no way of distinguishing between the permuted state and the original, by means of an observation at any time.

One can show that the resulting wavefunction that has undergone a permutation operation falls into two categories,

$$\hat{P}_\sigma \Psi = \begin{cases} \Psi & \forall \sigma \in S_N, \\ (-1)^{|\sigma|} \Psi & \end{cases} \quad (2.81)$$

where $|\sigma|$ is the number of transpositions in σ and the sign will be $(-1)^{|\sigma|} = \pm 1$. In the former case, when the sign is +, the wavefunction is “totally symmetric with respect to permutations”; while in the latter case, when the sign is −, the wavefunction is “totally anti-symmetric.” We show this result with a simple permutation operator \hat{P}_{ij} that exchanges coordinates of particle i and j , i.e.

$$\hat{P}_{ij} \Psi(x_1, x_2, \dots, x_i, x_j, \dots, x_N) = \Psi(x_1, x_2, \dots, x_j, x_i, \dots, x_N). \quad (2.82)$$

Applying this permutation operator twice will return us to the initial wavefunction,

$$\hat{P}_{ij} \hat{P}_{ij} = 1, \quad (2.83)$$

which implies that the permutation operator is Hermitian and unitary. Moreover, the Permutation operator must commute with any operator \hat{O} ,

$$[\hat{P}_{ij}, \hat{O}] = 0. \quad (2.84)$$

Consider an eigenvalue equation for the permutation operator \hat{P}_{ij} ,

$$\hat{P}_{ij} \Psi = \lambda_{ij} \Psi, \quad (2.85)$$

from which it follows that

$$\Psi = \hat{P}_{ij}^2 \Psi = \lambda_{ij}^2 \Psi \rightarrow \lambda_{ij}^2 = 1. \quad (2.86)$$

This leads us to another postulate in quantum theory, that we have only two types of basic particles. *Bosons* have totally symmetric wavefunctions only, while *fermions* have totally anti-symmetric wavefunctions only. “The physical consequences of this postulate seems to be in good agreement with experimental data” [41]. Moreover, all particles with integer spin are bosons, and all particles with half-integer spin are fermions [42, 43]. This can be proved in relativistic quantum mechanics, but must be accepted as an axiom in nonrelativistic theory [44]. Generally, the degeneracy of a state for a given energy ϵ is divided into three categories,

$$n(\epsilon) = \begin{cases} e^{-(\epsilon-\mu)/k_B T} & \text{Maxwell-Boltzmann} \\ \frac{1}{e^{-(\epsilon-\mu)/k_B T} + 1} & \text{Fermi-Dirac} \\ \frac{1}{e^{-(\epsilon-\mu)/k_B T} - 1} & \text{Bose-Einstein.} \end{cases} \quad (2.87)$$

The Maxwell-Boltzmann distribution is the classical result, for *distinguishable* particles; the Fermi-Dirac distribution applies to *identical fermions*, and the Bose-Einstein distribution is for *identical bosons*. Here, T is the temperature, k_B is Boltzmann’s constant and μ is the chemical potential.

To this day, particles with no other spin has been found, but the norwegian physicists Jon Magne Leinaas and Jan Myrheim discovered that in one- and two dimensions, more general permutation symmetries are possible. They dubbed this third class of fundamental particles "anyons" [41].

2.5 Density Operators

Density operators will become very useful, especially later when we use them to compute expectation values. A formal introduction to this concept is therefore warranted. Consider a system that is described not by a single state vector, but by an ensemble of state vectors $\{|\psi\rangle_1, |\psi\rangle_2, \dots, |\psi\rangle_n\}$ with a probability distribution $\{p_1, p_2, \dots, p_m\}$ defined over the ensemble. We may consider this ensemble to contain *quantum probabilities* carried by the state vectors $\{|\psi\rangle_k\}$ and classical probabilities carried by the distribution $\{p_k\}$. A system described by an ensemble state is said to be in a *mixed state*.

The expectation value of a quantum observable in a state described by an ensemble of state vectors is

$$\langle \hat{O} \rangle = \sum_{k=1}^n p_k \langle \hat{O} \rangle_k = \sum_{k=1}^n p_k \langle \psi_k | \hat{O} | \psi_k \rangle. \quad (2.88)$$

This expression motivates the introduction of the *density operator* associated with the mixed state,

$$\hat{\rho} = \sum_{k=1}^n p_k |\psi_k\rangle\langle\psi_k|. \quad (2.89)$$

The corresponding matrix, defined by reference to an orthogonal basis $\{|\phi_i\rangle\}$, is called the *density matrix*,

$$\rho_{ij} = \sum_{i=1}^n p_k \langle \phi_i | |\psi_k\rangle\langle\psi_k| | \phi_j \rangle. \quad (2.90)$$

An important note is that all measurable information about the system is contained in its density operator. We can for instance compute expectation values using the density operator,

$$\begin{aligned} \langle \hat{O} \rangle &= \sum_{k=1}^n p_k \sum_i \langle \psi_k | \hat{O} | \phi_i \rangle \langle \phi_i | \psi_k \rangle \\ &= \sum_i \sum_{k=1}^n p_k \langle \phi_i | \psi_k \rangle \langle \psi_k | \hat{O} | \phi_i \rangle = \text{tr}\{\hat{\rho}\hat{O}\}. \end{aligned} \quad (2.91)$$

There are certain general properties that any density operator has to satisfy,

$$\begin{aligned} p_k = p_k^* &\rightarrow \hat{\rho} = \hat{\rho}^\dagger \quad \text{Hermiticity} \\ p_k \geq 0 &\rightarrow \langle \chi | \hat{\rho} | \chi \rangle \forall \chi \quad \text{Positive semi-definite} \\ \sum_k p_k = 1 &\rightarrow \text{tr}\{\hat{\rho}\} = 1 \quad \text{Normalisation.} \end{aligned} \quad (2.92)$$

We also note that

$$\text{tr } \hat{\rho}^2 = \sum_k p_k^2 \rightarrow \text{tr } \hat{\rho}^2 \leq 1, \quad (2.93)$$

because all eigenvalues are $p_k \leq 1$, which means that $\text{tr } \hat{\rho}^2 \leq \text{tr } \hat{\rho}$. The pure state is a special case where one of the probabilities p_k is equal to one, and the others are 0. In this case, the density operator will be equivalent to a projection operator onto this single state. Moreover, $\text{tr } \hat{\rho}^2 = 1$ for a pure state, while for a mixed state we have $\text{tr } \hat{\rho}^2 < 1$.

Chapter 3

Second Quantisation

The second-quantisation formalism is a very useful tool used in the description of many-body systems. Here the particles themselves are discrete quanta created and destroyed by *creation-* and *annihilation* operators. We start by introduction of the Slater determinant, a very useful description of an anti-symmetric wavefunction, in order to build a nomenclature for describing the many-electron systems with which we are concerned.

3.1 Slater Determinants

For some smaller systems it can be satisfactory or even provident to use a single, special function to describe the entire system. Here however, we introduce the Slater determinant which is a way to write a product of wavefunctions. We will only consider many-electron wavefunctions that can be written as a single Slater determinant or as a linear combination of several Slater determinants.

We define an *orbital*¹ which is the wavefunction for a single particle, or more precisely a single electron. The wavefunction for a larger group of electrons, for instance those electrons that surround an atom or molecule, we call the *molecular orbital*. We also discriminate between spatial orbitals which are functions of spatial coordinates; and spin-orbitals, which are functions of the space and spin coordinates (typically a product of a spatial orbital and a spin function). A very complete description and thorough discussion of various aspects concerning electronic structure wavefunctions is given by Szabo & Ostlund [14].

The best description for a multiple-electron wavefunction, given by the independent-particle approximation is the Slater determinant,

$$\Phi(x_1, x_2, \dots, x_N) = \frac{1}{\sqrt{N!}} \begin{vmatrix} \phi_1(x_1) & \phi_2(x_1) & \dots & \phi_N(x_1) \\ \phi_1(x_2) & \phi_2(x_2) & \dots & \phi_N(x_2) \\ \vdots & \vdots & \ddots & \vdots \\ \phi_1(x_N) & \phi_2(x_N) & \dots & \phi_N(x_N) \end{vmatrix} \quad (3.1)$$
$$\equiv \langle x_1, x_2, \dots, x_N | \phi_1, \phi_2, \dots, \phi_N \rangle$$

¹Sometimes also called a single-particle function, a single-particle orbital, a single-electron orbital or similar. There is a chance that these terms will be used interchangably throughout this text without warning.

where $\phi_i(x_\mu)$ is a spinorbital indexed by i , at coordinates x_μ . The spin-orbitals, are single-particle functions in the proper two-dimensional Hilbert space and they are not necessarily orthonormal. The Slater determinant in Equation 3.1 defines an N -electron system. Adding a column and a row to the determinant in Equation 3.1 corresponds to adding a particle to the system, and we obtain an $N + 1$ -electron Slater determinant. Similarly, removing a columns and a row from the determinant corresponds to removing a particle from the system, and we obtain an $N - 1$ Slater determinant. In the final expression in Equation 3.1, a compact notation is introduced. Here the normalisation constant and labels for the fermion coordinates are understood – only the wavefunctions are exhibited.

To illustrate why this is a good approximation of the electronic wave function, consider first the two-electron case,

$$\Phi_{N=2} = \frac{1}{\sqrt{2}}(\phi_1(1)\phi_2(2) - \phi_1(2)\phi_2(1)). \quad (3.2)$$

We see from this relatively simple expression that if the electrons were to occupy the same state the wavefunction would equal zero, in effect forbidding such a state. This ensures that the Pauli exclusion principle for fermions is satisfied [45]. Moreover, if we switch coordinates of any two single-particle functions (spin-orbitals), corresponding to the interchange of rows in Equation 3.1, the result is a change of sign. This attribute of a determinant accommodates the total anti-symmetry necessary for a fermionic wavefunction. Conversely, a bosonic wavefunction can be constructed as a *permanent*.

We usually write a Slater determinant in a much more simple way,

$$|\Phi\rangle = |\phi_i\phi_j\phi_k\dots\phi_z\rangle = |ijk\dots z\rangle. \quad (3.3)$$

The N single-particle functions $\phi_i\dots\phi_z$, that make up this Slater determinant now form a basis for an N -particle Hilbert space \mathcal{H}_N .

3.2 Creation and Annihilation Operators

The introduction of creation- and annihilation operators are what establishes the second quantisation formalism. As we will see, such operators make the construction of N -particle wavefunctions as symmetrised or anti-symmetrised products redundant, because these symmetry properties are encompassed in the anticommutation properties of the operators. This is a great advantage of the second quantisation framework. Another advantage is the relatively easy management of many-particle systems.

The notation of creation and annihilation operators vary,

$$\begin{aligned} &\text{creation operator for spinorbital } \phi_i, \hat{X}_i^\dagger, \hat{a}_i^\dagger, \hat{c}_i^\dagger, \hat{i}^\dagger; \\ &\text{annihilation operator for spinorbital } \phi_i, \hat{X}_i, \hat{a}_i, \hat{c}_i, \hat{i}. \end{aligned}$$

Herein, \hat{a}_i^\dagger , \hat{a}_i is used and, if there is no chance of confusion, \hat{i}^\dagger , \hat{i} .

The Creation Operator For every single-particle index q , we define the creation operator \hat{a}_i^\dagger acting on the vacuum state by

$$\hat{a}_i^\dagger |0\rangle = |i\rangle. \quad (3.4)$$

For any slater determinant with $N > 0$, the action is defined by

$$\hat{a}_i^\dagger |jk\dots z\rangle = |ijk\dots z\rangle, \quad (3.5)$$

$$\hat{a}_i^\dagger |ijk\dots z\rangle = 0. \quad (3.6)$$

We see that this is the same as inserting a column into the matrix-form of the Slater determinant in Equation 3.1.

The Annihilation Operator It is sufficient to state that the annihilation operator \hat{a}_i is the hermitian adjoint of the creation operator \hat{a}_i , but to be specific we need

$$\hat{a}_i |0\rangle = 0, \quad (3.7)$$

as there is no particle in the vacuum state to annihilate. For any arbitrary Slater determinant, we have

$$\hat{a}_i |ijk\dots z\rangle = |ij\dots z\rangle, \quad (3.8)$$

$$\hat{a}_i |jk\dots z\rangle = 0. \quad (3.9)$$

The creation- and annihilation operators map wavefunctions between Hilbert spaces of different dimensionality, or particle number;

$$\hat{a}_i^\dagger : \mathcal{H}_N \rightarrow \mathcal{H}_{N+1} \quad (3.10)$$

$$\hat{a}_i : \mathcal{H}_N \rightarrow \mathcal{H}_{N-1}, \quad (3.11)$$

where \mathcal{H}_N is the Hilbert space for N particles. The space comprising all Hilbert spaces of different particles numbers is called the Fock space, defined as a direct sum of all Hilbert spaces

$$\mathcal{F} = \bigoplus_{N=0}^{\infty} \mathcal{H}_N. \quad (3.12)$$

The creation- and annihilation operators act on this Fock space.

We can now build a Slater determinant as the result of successive operations of several creation operators \hat{a}_q^\dagger on the vacuum state $|0\rangle$,

$$\hat{a}_i^\dagger \hat{a}_j^\dagger \hat{a}_k^\dagger \dots \hat{a}_z^\dagger |0\rangle = |ijk\dots z\rangle. \quad (3.13)$$

It is convenient to arrange the spin-orbitals in a Slater determinant in alphabetical order, as in Equation 3.13. This makes it necessary to ascertain the effects a creation or annihilation operator will have on a Slater determinant when the affected orbital is not at the beginning of the string of orbitals in the Slater determinant. Generally we have,

$$\hat{P} |ijk\dots z\rangle = (-1)^{\sigma(\hat{P})} |ijk\dots z\rangle, \quad (3.14)$$

where \hat{P} permutes the string of orbitals and $\sigma(\hat{P})$ is the parity of the permutation \hat{P} . We have

$$\hat{a}_p^\dagger |ijk \dots z\rangle = (-1)^{\eta_p} |ijk \dots p \dots z\rangle, \quad (3.15)$$

$$\hat{a}_p |ijk \dots p \dots z\rangle = (-1)^{\eta_p} |ijk \dots z\rangle, \quad (3.16)$$

where η_p is the number of orbitals preceding the orbital ϕ_p , pertaining to the creation (annihilation) operator, in the Slater determinant.

3.3 Anticommutator Relations

To show how the anticommutator relations are built into the creation- and annihilation operators, we start by considering two arbitrary creation operators acting on a Slater determinant,

$$\begin{aligned} \hat{a}_p^\dagger \hat{a}_q^\dagger |ijk \dots\rangle &= |pqijk \dots\rangle, \\ \hat{a}_q^\dagger \hat{a}_p^\dagger |ijk \dots\rangle &= |qpijk \dots\rangle = -|pqijk \dots\rangle. \end{aligned} \quad (3.17)$$

We demand that these two operations be equivalent, or that

$$\begin{aligned} \hat{a}_p^\dagger \hat{a}_q^\dagger &= -\hat{a}_q^\dagger \hat{a}_p^\dagger, \\ \{\hat{a}_p^\dagger, \hat{a}_q^\dagger\} &\equiv \hat{a}_p^\dagger \hat{a}_q^\dagger + \hat{a}_q^\dagger \hat{a}_p^\dagger = \hat{0}. \end{aligned} \quad (3.18)$$

This is the first of three anti-commutator relations we are going to derive.

The logical next step is to perform a similar operation with annihilation operators,

$$\begin{aligned} \hat{a}_p \hat{a}_q |qpijk \dots\rangle &= \hat{a}_p |pijk \dots\rangle = |ijk \dots\rangle, \\ \hat{a}_q \hat{a}_p |qpijk \dots\rangle &= -\hat{a}_q \hat{a}_p |pqijk \dots\rangle = -\hat{a}_q |qijk \dots\rangle = -|ijk \dots\rangle. \end{aligned} \quad (3.19)$$

We also require these two operations to be equivalent,

$$\begin{aligned} \hat{a}_p \hat{a}_q &= -\hat{a}_q \hat{a}_p, \\ \{\hat{a}_p, \hat{a}_q\} &\equiv \hat{a}_p \hat{a}_q + \hat{a}_q \hat{a}_p = \hat{0}. \end{aligned} \quad (3.20)$$

One case remains, when a creation operator and an annihilation operator is applied together on a Slater determinant,

$$\hat{a}_p^\dagger \hat{a}_q |qijk \dots\rangle = \hat{a}_p^\dagger |ijk \dots\rangle = |pijk \dots\rangle. \quad (3.21)$$

This operation will replace ϕ_q by ϕ_p even if ϕ_p would have been somewhere else in the interior of the Slater determinant. Any sign change as an effect of moving the orbital to the front of the string would be negated when the orbital is moved back to the original position. Exchanging the order of the operators however, gives

$$\hat{a}_q \hat{a}_p^\dagger |qijk \dots\rangle = \hat{a}_q |pqijk \dots\rangle = -\hat{a}_q |qpijk \dots\rangle = -|pijk \dots\rangle. \quad (3.22)$$

We again see a sign change and have,

$$\{\hat{a}_p^\dagger, \hat{a}_q\} = \hat{0} \quad (p \neq q). \quad (3.23)$$

If, on the other hand, $p = q$ we have

$$\begin{aligned}\hat{a}_p^\dagger \hat{a}_p |pijk\dots\rangle &= |pijk\dots\rangle, \\ \hat{a}_p \hat{a}_p^\dagger |pijk\dots\rangle &= 0,\end{aligned}\tag{3.24}$$

and if the orbital ϕ_p in question does not appear in the Slater determinant,

$$\begin{aligned}\hat{a}_p^\dagger \hat{a}_p |ijk\dots\rangle &= 0, \\ \hat{a}_p \hat{a}_p^\dagger |ijk\dots\rangle &= \hat{a}_p |pijk\dots\rangle = |ijk\dots\rangle.\end{aligned}\tag{3.25}$$

For all cases we have that,

$$(\hat{a}_p^\dagger \hat{a}_p + \hat{a}_p \hat{a}_p^\dagger) |\dots\rangle = |\dots\rangle,\tag{3.26}$$

or

$$\{\hat{a}_p^\dagger, \hat{a}_p\} = \{\hat{a}_p, \hat{a}_p^\dagger\} = \hat{1}.\tag{3.27}$$

In conclusion, the anti-commutator relations of the creation and annihilation operators are,

$$\{\hat{a}_p, \hat{a}_q\} = \hat{0},\tag{3.28}$$

$$\{\hat{a}_p^\dagger, \hat{a}_q^\dagger\} = \hat{0},\tag{3.29}$$

$$\{\hat{a}_p^\dagger, \hat{a}_q\} = \{\hat{a}_p, \hat{a}_q^\dagger\} = \delta_{pq},\tag{3.30}$$

where δ_{pq} is the Kronecker delta.

3.4 Representation of Operators

Here we shall see that it is very useful to express operators in terms of creation- and annihilation operators. We introduce a general one- and two-body operator. It is possible to create operators pertaining to any number of particles, but these are very uncommon to see in quantum chemistry, which is our domain.

A second-quantised one-body operator is written like

$$\hat{h} = \sum_{i=1}^N \hat{h}(i) = \sum_{ij} \langle i | \hat{h} | j \rangle \hat{a}_i^\dagger \hat{a}_j,\tag{3.31}$$

where in general, $\langle p | \hat{h} | q \rangle$ is the matrix element of the single-particle operator \hat{h} in a given one-particle basis,

$$h_q^p = \langle p | \hat{h} | q \rangle = \int dx \phi_p(x)^* \hat{h} \phi_q(x).\tag{3.32}$$

More accurately, we see from Equation 3.31, that \hat{h} weighs each occupied orbital of a Slater determinant with the appropriate matrix element.

A second-quantised two-body operator is written like

$$\hat{u} = \sum_{i,j}^N \hat{u}(i,j) = \frac{1}{2} \sum_{ijkl} u_{rs}^{pq} \hat{a}_i^\dagger \hat{a}_j^\dagger \hat{a}_l \hat{a}_k, = \frac{1}{4} \sum_{ijkl} \langle ij | \hat{u} | kl \rangle_{\text{AS}} \hat{a}_i^\dagger \hat{a}_j^\dagger \hat{a}_l \hat{a}_k, \quad (3.33)$$

where

$$\langle ij | \hat{u} | kl \rangle \equiv \int \int \phi_i^*(x_1) \phi_j^*(x_2) u(x_1, x_2) \phi_k(x_1) \phi_l(x_2) dx_1 dx_2. \quad (3.34)$$

Notice the transposed order of indices in 3.33. The interpretation of the expression is that a fermion is removed from state $|k\rangle$ and $|l\rangle$ and created in state $|i\rangle$ and $|j\rangle$, with the probability $\langle ij | \hat{u} | kl \rangle$. The antisymmetric two-electron integral for \hat{u} is abbreviated,

$$\langle ij | \hat{u} | kl \rangle - \langle ij | \hat{u} | lk \rangle = \langle ij | \hat{u} | kl \rangle_{\text{AS}} \quad (3.35)$$

We see that a full second-quantised Hamiltonian can be written,

$$\hat{H} = \hat{h} + \hat{u} = \sum_{ij} \hat{h}_{ij} \hat{a}_i^\dagger \hat{a}_j + \frac{1}{4} \langle ij | \hat{u} | kl \rangle_{\text{AS}} \hat{a}_i^\dagger \hat{a}_j^\dagger \hat{a}_l \hat{a}_k. \quad (3.36)$$

3.5 Normal Order and Wick's Theorem

We have built the foundations necessary to describe wavefunctions in terms of creation- and annihilation operators as well as a simple way of writing a general electronic Hamiltonian in the second-quantised manner. The following is a necessity to be able to compute vacuum expectation values $\langle - | \hat{A} \hat{B} \dots | - \rangle$ of products of creation- and annihilation operators. Such expectation values are very important for several computational methods, see Harris *et al.* [46].

3.5.1 Normal ordering and contractions

The normal-ordered product of a string of operators $\hat{A}_1, \hat{A}_2, \hat{A}_3, \dots$, is defined as the rearranged product of operators such that all the creation operators are to the left of all the annihilation operators, including a phase factor corresponding to the parity of the permutation, producing the rearrangement

$$\begin{aligned} n[\hat{A}_1 \hat{A}_2 \dots \hat{A}_n] &\equiv (-1)^{|\sigma|} \hat{A}_{\sigma(1)} \hat{A}_{\sigma(2)} \dots \hat{A}_{\sigma(n)} \\ &= (-1)^{\sigma(\hat{P})} \hat{P}(\hat{A}_1 \hat{A}_2 \dots \hat{A}_n) \\ &= (-1)^{|\sigma|} [\text{creation operators}] \cdot [\text{annihilation operators}] \\ &= (-1)^{|\sigma|} \hat{a}^\dagger \hat{b}^\dagger \dots \hat{u} \hat{v}, \end{aligned} \quad (3.37)$$

where \hat{P} is a permutation operator acting on the product of operators, and σ is the parity of the permutation. One should bear in mind that this definition is by no means unique. Here are some examples,

$$n[\hat{a}^\dagger \hat{b}] = \hat{a}^\dagger \hat{b} \quad n[\hat{b} \hat{a}^\dagger] = -\hat{a}^\dagger \hat{b}$$

$$\begin{aligned} n[\hat{a}\hat{b}] &= \hat{a}\hat{b} = -\hat{b}\hat{a} \\ n[\hat{a}^\dagger\hat{b}^\dagger] &= \hat{a}^\dagger\hat{b}^\dagger = -\hat{b}^\dagger\hat{a}^\dagger \\ n[\hat{a}^\dagger\hat{b}\hat{c}^\dagger\hat{d}] &= -\hat{a}^\dagger\hat{c}^\dagger\hat{b}\hat{d} = \hat{c}^\dagger\hat{a}^\dagger\hat{b}\hat{d} = \hat{a}^\dagger\hat{c}^\dagger\hat{d}\hat{b} = -\hat{c}^\dagger\hat{a}^\dagger\hat{d}\hat{b}. \end{aligned}$$

Note that the second quantised Hamiltonian in Equation 3.36 is already on normal-ordered form.

For two arbitrary creation and annihilation operators, we define their contraction as

$$\overline{\hat{A}\hat{B}} \equiv \langle - | \hat{A}\hat{B} | - \rangle, \quad (3.38)$$

or equivalently,

$$\overline{\hat{A}\hat{B}} \equiv \hat{A}\hat{B} - n[\hat{A}\hat{B}]. \quad (3.39)$$

For a creation- and annihilation operator there are four possible contractions,

$$\begin{aligned} \overline{\hat{a}^\dagger\hat{b}^\dagger} &= \langle - | \hat{a}^\dagger\hat{b}^\dagger | - \rangle = \hat{a}^\dagger\hat{b}^\dagger - n[\hat{a}^\dagger\hat{b}^\dagger] = 0 \\ \overline{\hat{a}\hat{b}} &= \langle - | \hat{a}\hat{b} | - \rangle = \hat{a}\hat{b} - n[\hat{a}\hat{b}] = 0 \\ \overline{\hat{a}^\dagger\hat{b}} &= \langle - | \hat{a}^\dagger\hat{b} | - \rangle = \hat{a}^\dagger\hat{b} - n[\hat{a}^\dagger\hat{b}] = 0 \\ \overline{\hat{a}\hat{b}^\dagger} &= \langle - | \hat{a}\hat{b}^\dagger | - \rangle = \hat{a}\hat{b}^\dagger - n[\hat{a}\hat{b}^\dagger] = \hat{a}\hat{b}^\dagger - (-\hat{b}^\dagger\hat{a}) = \{\hat{a}, \hat{b}^\dagger\} = \delta_{ab}. \end{aligned} \quad (3.40)$$

We see that all contractions between creation- and annihilation operators are a number, most of them are zero and only those with an annihilation operator to the left and a creation operator to the right can be one.

Contractions inside a normal ordered product is defined as follows,

$$n[\hat{A}\hat{B}\hat{C}\dots\hat{R}\dots\hat{S}\dots\hat{T}\dots\hat{U}\dots] = (-1)^\sigma \overline{\hat{R}\hat{T}\hat{S}\hat{U}\dots} n[\hat{A}\hat{B}\hat{C}\dots], \quad (3.41)$$

where all contracted operator pairs are moved to the front of the normal ordered product, and σ is the parity of the permutations required for this relocation. The result will be zero, or plus or minus the normal ordered product without the contracted operator pairs.

3.5.2 Wick's Theorem

Wick's theorem states that every string of creation and annihilation operators can be written as a sum of normal-ordered products with all possible contractions,

$$\begin{aligned} \hat{A}\hat{B}\hat{C}\hat{D}\dots &= n[\hat{A}\hat{B}\hat{C}\hat{D}\dots] + n[\overline{\hat{A}\hat{B}\hat{C}\hat{D}\dots}] + n[\overline{\hat{A}\hat{B}\hat{C}\hat{D}\dots}] + n[\overline{\hat{A}\hat{B}\hat{C}\hat{D}\dots}] \\ &\quad + \dots + n[\overline{\hat{A}\hat{B}\hat{C}\hat{D}\dots}] + n[\overline{\hat{A}\hat{B}\hat{C}\hat{D}\dots}] + \dots + n[\overline{\hat{A}\hat{B}\hat{C}\hat{D}\dots}] + \dots + \\ &\quad + n[\overline{\hat{A}\hat{B}\hat{C}\hat{D}\dots}] + n[\overline{\hat{A}\hat{B}\hat{C}\hat{D}\dots}] + n[\overline{\hat{A}\hat{B}\hat{C}\hat{D}\dots}] + \dots, \end{aligned} \quad (3.42)$$

where eventually all possible contractions of one, two pairs etc, are included.

Especially when computing vacuum expectation values of normal-ordered products Wick's theorem becomes very important. The reason for this is that each contraction will not contribute to the result, unless it is a fully contracted operator string,

$$\langle |\hat{A}\dots\hat{B}\dots\hat{C}\dots\hat{D}\dots| \rangle = \sum_{\text{all possible contractions}} \langle |n[\overbrace{\hat{A}\dots\hat{B}\dots\hat{C}\dots\hat{D}\dots}]| \rangle. \quad (3.43)$$

Most vacuum expectation values contain operator strings that already have substrings that are on normal-ordered form. This warrants a very useful generalisation of Wick's theorem for such strings,

$$\begin{aligned} n[\hat{A}_1\hat{A}_2\dots]n[\hat{B}_1\hat{B}_2\dots]\dots n[\hat{Z}_1\hat{Z}_2\dots] &= n[\hat{A}_1\hat{A}_2\dots:\hat{B}_1\hat{B}_2\dots:\dots:\hat{Z}_1\hat{Z}_2\dots] \\ &+ \sum_{(1)} n[\hat{A}_1\hat{A}_2\dots:\hat{B}_1\hat{B}_2\dots:\dots:\hat{Z}_1\hat{Z}_2\dots] + \dots + \sum_{(n)} n[\hat{A}_1\hat{A}_2\dots:\hat{B}_1\hat{B}_2\dots:\dots:\hat{Z}_1\hat{Z}_2\dots] \hat{Z}_N, \end{aligned} \quad (3.44)$$

where we sum over all combinations of contractions that each involve operators from different substrings, starting with one contractions and up to when all operators, or as many as possible, are contracted.

3.5.3 Particle-Hole Formalism

We see that a Slater determinant can be built recursively with creation operators,

$$\Phi = \hat{i}_1\hat{i}_2\dots\hat{i}_N = \hat{i}_1^\dagger\hat{i}_2^\dagger\dots\hat{i}_N^\dagger | \rangle. \quad (3.45)$$

Instead of rewriting Slater determinants with operators applied to the vacuum state in this manner we will introduce the reference state, or Fermi vacuum,

$$|0\rangle = |\Phi_0\rangle = |ijk\dots n\rangle. \quad (3.46)$$

We will define other Slater determinants relative to this reference state. For instance,

$$|\Phi_i^a\rangle \equiv \hat{a}^\dagger\hat{i}|\Phi_0\rangle = |ajk\dots n\rangle \quad (3.47)$$

$$|\Phi_{ij}^{ab}\rangle \equiv \hat{a}^\dagger\hat{b}^\dagger\hat{j}\hat{i}|\Phi_0\rangle = |abk\dots n\rangle \quad (3.48)$$

$$|\Phi_i\rangle \equiv \hat{i}|\Phi_0\rangle = |jk\dots n\rangle \quad (3.49)$$

$$|\Phi^a\rangle \equiv \hat{a}^\dagger|\Phi_0\rangle = |aijk\dots n\rangle \quad (3.50)$$

where equations 3.47, 3.48 3.49 and 3.50 constitute a single excitation, a double excitation, an electron removal and an electron attachment, respectively. Note that the reference state Slater determinants excited relative to the Fermi vacuum have the following properties,

$$|\Phi_{ij}^{ab}\rangle = |\Phi_{ji}^{ba}\rangle = -|\Phi_{ij}^{ba}\rangle = -|\Phi_{ji}^{ab}\rangle. \quad (3.51)$$

Take note of the specific letters used for creating and annihilating electrons in the example above. i, j, k, l, \dots are letters restricted to indices of *hole* states, and a, b, c, d, \dots

are letters restricted to indices of *particle* states, while p, q, r, \dots are for general use, indicating any state. Notice that

$$\begin{aligned} \hat{i}^\dagger |0\rangle &= 0 & \hat{a}|0\rangle &= 0, \\ \langle 0| \hat{i} &= 0 & \langle 0| \hat{a}^\dagger &= 0. \end{aligned} \quad (3.52)$$

Whenever we try to insert an electron where there already is one, or when we try to remove an electron that is not there, we get zero as result.

3.5.4 Wick's theorem relative to the Fermi vacuum

Now we will modify the concepts of normal-ordering, contractions and Wick's theorem so that they relate to the reference state and the Fermi vacuum, instead of the physical vacuum. First we introduce the pseudo-operators,

$$\begin{aligned} \hat{b}_i &= \hat{i}^\dagger, & \hat{b}_i^\dagger &= \hat{i} \\ \hat{b}_a &= \hat{a}, & \hat{b}_a^\dagger &= \hat{a}^\dagger, \end{aligned} \quad (3.53)$$

where \hat{b}_i^\dagger is a hole creation operator and \hat{b}_i is a particle creation operator, but only for vacant spaces below the fermi level. The reason for introducing such operators is to be able to work with the fermi vacuum in the same manner as regular operators work with the physical vacuum. Excited Slater determinants can easily be written using pseudo-operators,

$$|\Phi_i^a\rangle \equiv \hat{b}_a^\dagger \hat{b}_i^\dagger |\Phi_0\rangle \quad (3.54)$$

$$|\Phi_{ij}^{ab}\rangle \equiv \hat{b}_b^\dagger \hat{b}_j^\dagger \hat{b}_a^\dagger \hat{b}_i^\dagger |\Phi_0\rangle. \quad (3.55)$$

We introduce a new type of normal ordering for the pseudo-operators and for the actual operators that they represent,

$$\{\hat{A}\hat{B}\hat{C}\} = (-1)\hat{b}_p^\dagger \hat{b}_q^\dagger \dots \hat{b}_u^\dagger \hat{b}_v. \quad (3.56)$$

We write a contraction in the same manner,

$$\overline{\hat{A}\hat{B}} = \hat{A}\hat{B} - \{\hat{A}\hat{B}\}. \quad (3.57)$$

A normal-ordered product with contractions inside is also defined in the same way. We see that the only non-zero contractions are

$$\overline{\hat{b}_i \hat{b}_j^\dagger} = \overline{\hat{i}^\dagger \hat{j}} = \delta_{ij}, \quad \overline{\hat{b}_a \hat{b}_b^\dagger} = \overline{\hat{a} \hat{b}^\dagger} = \delta_{ab}. \quad (3.58)$$

Here we are also made aware of the benefit of pseudo-operators, as we now have only have non-zero contributions from contractions that have a creation operator to the right, and an annihilation operator to the left. More generally we have the anticommutator relations

$$\{\hat{b}_p, \hat{b}_q^\dagger\} = \delta_{pq}, \quad \{\hat{b}_p, \hat{b}_q\} = 0. \quad (3.59)$$

Part II

Quantum Many-Body Approximations

Chapter 4

Hartree-Fock Theory

In 1927, soon after the discovery of the Schrödinger equation in 1926, Douglas R. Hartree introduced a procedure which he called the self-consistent field method [12]. Hartree sought to do without empirical parameters and to solve the many-body time-independent Schrödinger equation from fundamental principles, *ab initio*. A year later John C. Slater and John A. Gaunt provided a sounder theoretical basis for the Hartree method by applying the variational principle to a trial wave function as a product of single-particle functions [47][48]. Slater later pointed out, with support from Vladimir A. Fock, that the method merely applied the Pauli exclusion principle in its older, incorrect formulation; forbidding presence of two electrons in the same state, but neglecting quantum statistics [49][13]. It was shown that a Slater determinant satisfies the anti-symmetric property of the exact solution and would be a suitable ansatz for applying the variational principle. Later, Hartree reformulated the method for calculations [50].

The Hartree-Fock methods makes the following simplifications to the multi-electron atomic (molecular) problem,

- The full molecular wavefunction is constrained to a function of the coordinates of only the electrons in the molecule. In not so many words, the Born-Oppenheimer approximation is inherent in the method.
- Any relativistic effects are completely ignored, i.e. the momentum operator is assumed to be completely non-relativistic.
- A variational solution is assumed to be a linear combination of a basis set, which is assumed to be approximately complete. This set of basis functions is usually non-orthogonal.
- Some electron correlation effects are ignored, as the methods implies a mean-field approximation. Coulomb correlations are fully incorporated in the Hartree-Fock method, but the method ignores Fermi correlations and is therefore unable to describe some effects, like London dispersion¹.
- The ground state is approximated by a single Slater determinant.

¹Named after Fritz London; London dispersion forces (LDF) are a type of force between atoms and molecules[51]

Relaxation of the last two simplifications give rise to the large group of many-body methods commonly referred to as post-Hartree-Fock methods.

4.1 Deriving the Hartree-Fock Equations

Consider a Hamiltonian for some system

$$\hat{H} = \hat{h} + \hat{u} \quad (4.1)$$

where the ground state of \hat{h} is a Slater determinant consisting of N single-particle functions,

$$\Phi = |\phi_1\phi_2\dots\phi_N\rangle, \quad \langle\phi_i|\phi_j\rangle = \delta_{ij}, \quad (4.2)$$

If \hat{u} is only a limited perturbation to the system, it is reasonable to assume that the actual ground state of the full system can also be represented by a Slater determinant. Because the Hartree-Fock theory includes a mean-field approximation, each particle moves independently of the others interacting with the remaining electrons only indirectly through an average potential \hat{v}^{HF} .

The expectation value of the Hamiltonian in Equation 4.1 is

$$\begin{aligned} \langle\Phi|\hat{H}|\Phi\rangle &= \sum_i \langle\phi_i|\hat{h}|\phi_i\rangle + \frac{1}{2} \sum_{ij} \langle\phi_i\phi_k|\hat{u}|\phi_i\phi_j - \phi_j\phi_i\rangle \\ &= \sum_i \langle\phi_i|\hat{h}|\phi_i\rangle + \frac{1}{2} \sum_{ij} \langle\phi_i\phi_k|\hat{u}|\phi_i\phi_j\rangle_{\text{AS}}, \end{aligned} \quad (4.3)$$

where

$$\langle\phi_i\phi_j|\hat{u}|\phi_k\phi_l\rangle = \int \int \bar{\phi}_i(x_1)\bar{\phi}_j(x_2)\hat{u}(x_1, x_2)\phi_k(x_1)\phi_l(x_2)dx_1dx_2$$

Now we want to minimise the energy (Equation 4.1) under the constraint of orthonormal single-particle functions, that is $\langle\phi_i|\phi_k\rangle = \delta_{ij}$. The minimum solution is called the Hartree-Fock state, $|\Phi_{\text{HF}}\rangle$. An optimisation problem with a constraint begs the formulation of a Lagrangian functional with a Lagrange multiplier for each constraint,

$$\begin{aligned} \mathcal{L}(\phi_1, \dots, \phi_n, \lambda) &= \langle\Phi|\hat{H}|\Phi\rangle - \sum_{ij} \lambda_{ij}(\langle\phi_i|\phi_j\rangle - \delta_{ij}) \\ &= \sum_i \langle\phi_i|\hat{h}|\phi_i\rangle + \frac{1}{2} \sum_{ij} \langle\phi_i\phi_j|\hat{u}|\phi_i\phi_j - \phi_j\phi_i\rangle - \sum_{ij} \lambda_{ij}(\langle\phi_i|\phi_j\rangle - \delta_{ij}). \end{aligned} \quad (4.4)$$

The constraints can always be treated separately, $\partial\mathcal{L}/\partial\lambda_{ij} \langle\phi_i|\phi_j\rangle - \delta_{ij}$, as this demand will be fulfilled by finding that the solutions ϕ_i are orthonormal.

In order to find the optimum of the Lagrangian in (Equation 4.4), we choose a $k \in \{1, \dots, N\}$ and compute the directional derivative of ϕ_k^* , by varying this single particle function and leaving all others fixed,

$$\delta\phi_k = \epsilon\eta, \quad \delta\phi_l = 0, k \neq l, \quad (4.5)$$

where ϵ is some small number, and η is a normalized single-particle function. We define a function representing this variation,

$$f(\epsilon) = \mathcal{L}(\phi_1, \dots, \phi_k + \epsilon\eta, \dots, \phi_N, \lambda), \quad (4.6)$$

expanded to first order in ϵ ,

$$f(\epsilon) = f(0) + \epsilon f'(0) + \mathcal{O}(\epsilon^2). \quad (4.7)$$

For an optimum we must have

$$f'(0) = 0, \quad \forall \eta, \quad (4.8)$$

which means that the directional derivative of \mathcal{L} at $\{\phi_i\}_{i=1}^N$, in the direction η vanishes.

We compute the Taylor expansion of the varied Lagrangian (Equation 4.6),

$$\begin{aligned} f(\epsilon) &= \sum_i \langle \phi_i + \delta_{ki}\epsilon\eta | \hat{h} | \phi_i \rangle + \frac{1}{2} \sum_{ij} \langle (\phi_i + \delta_{ki}\epsilon\eta)(\phi_j + \delta_{kj}\epsilon\eta) | \hat{u} | \phi_i\phi_j - \phi_j\phi_i \rangle \\ &\quad - \sum_{ij} \lambda_{ij} (\langle \phi_i + \delta_{ik}\epsilon\eta | \phi_j \rangle - \delta_{ij}) + \mathcal{O}(\epsilon^2) \end{aligned} \quad (4.9)$$

$$\begin{aligned} &= \sum_i \langle \phi_i | \hat{h} | \phi_i \rangle + \frac{1}{2} \sum_i j \langle \phi_i\phi_j | \hat{u} | \phi_i\phi_j - \phi_j\phi_i \rangle + \epsilon \langle \eta | \hat{h} | \phi_k \rangle \\ &\quad + \frac{1}{2} \sum_{ij} \langle \phi_i \delta_{kj}\epsilon\eta | \hat{u} | \phi_i\phi_j - \phi_j\phi_i \rangle \\ &\quad + \frac{1}{2} \sum_{ij} \langle \delta_{ki}\epsilon\eta\phi_j | \hat{u} | \phi_i\phi_j - \phi_j\phi_i \rangle \end{aligned} \quad (4.10)$$

$$\begin{aligned} &\quad - \sum_{ij} \lambda_{ij} (\langle \phi_i | \phi_j \rangle - \delta_{ij}) - \sum_{ij} \lambda_{ij} (\langle \delta_{ik}\epsilon\eta | \phi_j \rangle - \delta_{ij}) + \mathcal{O}(\epsilon^2) \\ &= \sum_i \langle \phi_i | \hat{h} | \phi_i \rangle + \frac{1}{2} \sum_i j \langle \phi_i\phi_j | \hat{u} | \phi_i\phi_j - \phi_j\phi_i \rangle + \epsilon \langle \eta | \hat{h} | \phi_k \rangle - \sum_{ij} \lambda_{ij} (\langle \phi_i | \phi_j \rangle - \delta_{ij}) \\ &\quad + \frac{1}{2} \epsilon \sum_i \langle \phi_i\eta | \hat{u} | \phi_i\phi_k \rangle - \frac{1}{2} \epsilon \sum_i \langle \phi_i\eta | \hat{u} | \phi_k\phi_i \rangle \\ &\quad + \frac{1}{2} \epsilon \sum_j \langle \eta\phi_j | \hat{u} | \phi_k\phi_j \rangle - \frac{1}{2} \epsilon \sum_j \langle \eta\phi_j | \hat{u} | \phi_j\phi_k \rangle \\ &\quad - \epsilon \sum_j \lambda_{jk} \langle \eta | \phi_j \rangle + \mathcal{O}(\epsilon^2) \end{aligned} \quad (4.11)$$

$$\begin{aligned} &= \sum_i \langle \phi_i | \hat{h} | \phi_i \rangle + \frac{1}{2} \sum_i j \langle \phi_i\phi_j | \hat{u} | \phi_i\phi_j - \phi_j\phi_i \rangle - \sum_{ij} \lambda_{ij} (\langle \phi_i | \phi_j \rangle - \delta_{ij}) \\ &\quad + \epsilon \langle \eta | \hat{h} | \phi_k \rangle + \epsilon \sum_i \langle \eta\phi_i | \hat{u} | \phi_k\phi_i \rangle - \epsilon \sum_i \langle \eta\phi_i | \hat{u} | \phi_i\phi_k \rangle \\ &\quad - \epsilon \sum_j \lambda_{jk} \langle \eta | \phi_j \rangle + \mathcal{O}(\epsilon^2). \end{aligned} \quad (4.12)$$

Notice that the zeroth term, represented by the first line in Equation 4.12, is simply the original Lagrangian in Equation 4.4. We equate all the first-order terms to zero,

$$\langle \eta | \hat{h} | \phi_k \rangle + \sum_i \langle \eta \phi_i | \hat{u} | \phi_k \phi_i \rangle - \sum_i \langle \eta \phi_i | \hat{u} | \phi_i \phi_k \rangle - \sum_i \lambda_{ik} \langle \eta | \phi_i \rangle = 0. \quad (4.13)$$

This must be valid for any choice η , meaning

$$\hat{h} | \phi_k \rangle + \sum_i \langle \cdot | \phi_i | \hat{u} | \phi_k \phi_i \rangle - \sum_i \langle \cdot | \phi_i | \hat{u} | \phi_i \phi_k \rangle - \sum_i \lambda_{ik} | \phi_i \rangle = 0, \quad (4.14)$$

where $\langle \cdot | \hat{u} | \phi_2 \phi_3 \rangle$ is interpreted as an integral over only the second particle in the matrix element. We define,

$$\hat{v}_{\text{HF}} = \hat{v}_{\text{direct}} + \hat{v}_{\text{exchange}} = \sum_i \langle \cdot | \phi_i | \hat{u} | \phi_k \phi_i \rangle - \sum_i \langle \cdot | \phi_i | \hat{u} | \phi_i \phi_k \rangle \quad (4.15)$$

$$\hat{f} = \hat{h} + \hat{v}_{\text{HF}}, \quad (4.16)$$

Where Equation 4.16 is the Fock operator. We can now rewrite Equation 4.14 to

$$\hat{f}(\phi_1, \dots, \phi_N) | \phi_i \rangle = \sum_j \lambda_{ij} | \phi_j \rangle, \quad (4.17)$$

which is a set of linear equations, one equation for each single-particle function ϕ_i , we call the non-canonical Hartree-Fock equations.

It so happens that the Slater determinant $|\Phi\rangle$ is invariant under unitary transformation of the single particle functions. Consider a rotation of the single-particle functions,

$$\tilde{\phi}_k = \sum_j C_k^j \phi_j, \quad (4.18)$$

where C is a unitary matrix. We choose a particular unitary transformation C , rotating the single particle functions in a certain manner so that $\lambda = CEC^\dagger$, where $E_{jk} = \delta_{jk}\epsilon_k$ are the elements of a diagonal matrix (the eigenvalues of λ). This provides us with a new set of eigenvalue equations,

$$\hat{f}(\tilde{\phi}_1, \dots, \tilde{\phi}_N) | \tilde{\phi}_i \rangle = \epsilon_i | \tilde{\phi}_i \rangle, \quad (4.19)$$

which are the canonical Hartree-Fock equations. From now on we will stick with these equations and suppress the tilde notations.

4.2 The Roothan-Hall Equations

In order to solve the Hartree-Fock equations (Equation 4.19) we discretise the equations in terms of a finite, fixed basis $\{\chi_p\}_{p=1}^L$ size L . It is not a necessity for this basis to be orthonormal, and we therefore define the overlap matrix,

$$S_\beta^\alpha \equiv \langle \chi_\alpha | \chi_\beta \rangle. \quad (4.20)$$

The Hartree-Fock single-particle functions are expanded in this basis,

$$|\phi_p\rangle = \sum_{\alpha} C_p^{\alpha} |\chi_{\alpha}\rangle, \quad (4.21)$$

where C is not necessarily unitary, because the basis is not necessarily orthogonal. However, we do have $C^{\dagger}SC = 1$.

We insert the expansion from Equation 4.21 into the expression for the canonical Hartree-Fock equations from Equation 4.19,

$$\hat{f} \sum_{\alpha} C_p^{\alpha} |\chi_{\alpha}\rangle = \epsilon_p \sum_{\alpha} C_p^{\alpha} |\chi_{\alpha}\rangle. \quad (4.22)$$

Then we left project with an arbitrary function from our new basis,

$$\langle \chi_{\beta} | \hat{f} \sum_{\alpha} C_p^{\alpha} |\chi_{\alpha}\rangle = \epsilon_{\alpha} \langle \chi_{\beta} | \chi_{\alpha} \rangle \sum_r C_p^{\alpha} \\ \sum_{\alpha} f_{\alpha}^{\beta} C_p^{\alpha} = \epsilon_p \sum_{\alpha} S_{\alpha}^{\beta} C_p^{\alpha} \quad (4.23)$$

$$F(D)C = SC\epsilon. \quad (4.24)$$

where $D = CC^{\dagger}$ is the density matrix. Equation 4.24 is a matrix equation called the Roothaan-Hall equations.

Elaborating on the computation of the Fock matrix element,

$$f_{\beta}^{\alpha} = \langle \chi_{\alpha} | \hat{f} | \chi_{\beta} \rangle = \langle \chi_{\alpha} | \hat{h} | \chi_{\beta} \rangle + \langle \chi_{\alpha} | \hat{v}_{\text{direct}} | \chi_{\beta} \rangle - \langle \chi_{\alpha} | \hat{v}_{\text{exchange}} | \chi_{\beta} \rangle, \quad (4.25)$$

where

$$\langle \chi_{\alpha} | \hat{v}_{\text{direct}} | \chi_p \rangle = \sum_j \langle \chi_{\alpha} \phi_j | \hat{u} | \chi_p \phi_j \rangle = \sum_{\beta' \alpha' j} C_j^{\alpha'} (C_{\beta'}^j)^* \langle \chi_{\alpha} \chi_{\alpha'} | \hat{u} | \chi_p \chi_{\beta'} \rangle \\ = \sum_{\beta' \alpha'} D_{\beta'}^{\alpha'} \langle \chi_{\alpha} \chi_{\alpha'} | \hat{u} | \chi_p \chi_{\beta'} \rangle \quad (4.26)$$

$$\langle \chi_{\alpha} | \hat{v}_{\text{exchange}} | \chi_p \rangle = \sum_j \langle \chi_{\alpha} \phi_j | \hat{u} | \phi_j \chi_p \rangle = \sum_{\beta' \alpha' j} C_j^{\alpha'} (C_{\beta'}^j)^* \langle \chi_{\alpha} \chi_{\alpha'} | \hat{u} | \chi_{\beta'} \chi_p \rangle \\ = \sum_{\beta' \alpha'} D_{\beta'}^{\alpha'} \langle \chi_{\alpha} \chi_{\alpha'} | \hat{u} | \chi_{\beta'} \chi_p \rangle, \quad (4.27)$$

gives,

$$f_{\beta}^{\alpha} = \langle \chi_{\alpha} | \hat{h} | \chi_{\beta} \rangle + \sum_{\beta' \alpha'} D_{\beta'}^{\alpha'} (\langle \chi_{\alpha} \chi_{\alpha'} | \hat{u} | \chi_{\beta} \chi_{\beta'} \rangle - \langle \chi_{\alpha} \chi_{\alpha'} | \hat{u} | \chi_{\beta'} \chi_{\beta} \rangle), \quad (4.28)$$

which is the matrix element of the Fock operator.

The benefit of the Roothan-Hall equations (Equation 4.21), is that they are represented by matrices, and therefore easy to implement on a computer. The Roothan-Hall equations are solved iteratively, starting from an initial guess for C . This guess can be used to compute the density matrix, $D^{(k)} = C^{(k)}(C^{(k)})^{\dagger}$, where k denotes the k th

iteration. The density matrix is used to compute the Fock matrix. This provides us with a general eigenvalue problem, from which a new C and ϵ can be found. This formula is then repeated until the iterations converge. At this point we say that we have reached self-consistency in the mean field, and this method is usually called the method of self-consistent field (SCF) iterations.

4.3 Restricted Hartree-Fock Theory

Consider N electrons confined in a potential. To begin with we will assume that these are non-interacting, and can therefore be described by the one-body part of the Hamiltonian, only

$$\hat{h}(\mathbf{r}) = \hat{t}(\mathbf{r}) + \hat{v}(\mathbf{r}), \quad (4.29)$$

where \hat{v} is the potential set up by an atomic nucleus, or some other confining force. The one-body operator \hat{h} does not couple to electron spin, so the spin-orbitals or single-particle eigenfunctions of \hat{h} separate,

$$\phi_P(\mathbf{r}, \sigma) = \varphi_p(\mathbf{r})\chi_\alpha(\sigma), \quad (4.30)$$

where $P = (p, \alpha)$ is the combined spin- and spatial index and $\alpha = \pm 1/2$ is the value of the projection of the electron spin along the z -axis. The spin index/coordinate can only take values $\sigma \pm 1$, and we employ orthonormal spinorbitals, $\langle \chi_\alpha | \chi_\beta \rangle = \delta_{\alpha\beta}$.

We restrict the orbitals to have the same spatial wavefunction for spin up and spin down, and we consider only closed-shell configurations. This means that our molecular wavefunctions, in the form of a Slater determinant, can only have an even number of N electrons, with all electrons paired in such a manner that there are two spin values for each of the $n = N/2$ spatial orbitals. The N -electron ground state of \hat{h} is given by the first N eigenfunctions $\phi_{(p,\sigma)}$ occupied,

$$|\Phi\rangle = |\phi_{1,+}\phi_{1,-}\dots\phi_{\frac{N}{2},+}\phi_{\frac{N}{2},-}\rangle, \quad (4.31)$$

commonly also written as

$$|\Phi\rangle_{\text{RHF}} = |\varphi_1\bar{\varphi}_1\dots\varphi_{N/2}\bar{\varphi}_{N/2}\rangle. \quad (4.32)$$

The reasoning behind this restriction is that one would assume, for many systems, that the exact wavefunction has the same kind of structure. This is a good approximation for almost all electronic systems in nature. We therefore do not optimise all the N single-particle functions freely, but assume that they form sets of doubly occupied spatial orbitals. Matrix elements can now be computed more easily on the restricted form,

$$\langle \phi_{(p,\alpha)} | \hat{h} | \phi_{(q,\beta)} \rangle = \langle \chi_\alpha | \chi_\beta \rangle \int d\mathbf{r} \varphi_p(\mathbf{r})^* \hat{h} \varphi_q(\mathbf{r}). \quad (4.33)$$

And similarly for two-body operators,

$$\langle \phi_{p\alpha} \phi_{q\beta} | \hat{u} | \phi_{r\gamma} \phi_{s\delta} \rangle = \langle \chi_\alpha | \chi_\gamma \rangle \langle \chi_\beta | \chi_\delta \rangle \int \int d\mathbf{r}_1 d\mathbf{r}_2 \varphi_p(\mathbf{r}_1) \varphi_q(\mathbf{r}_2) \hat{u}(\mathbf{r}_1 \mathbf{r}_2) \varphi_r(\mathbf{r}_1) \varphi_s(\mathbf{r}_2). \quad (4.34)$$

Now we will find the special form of the Fock operator in restricted Hartree-Fock theory. First we insert the wavefunction restriction into the Hartree-Fock equation

$$\begin{aligned}\hat{f}\phi_I(\mathbf{r}, \sigma) &= \epsilon_i\phi_I(\mathbf{r}, \sigma) \\ \hat{f}\varphi_i(\mathbf{r})\chi_\alpha(\sigma) &= \epsilon_i\varphi_i(\mathbf{r})\chi_\alpha(\sigma).\end{aligned}\quad (4.35)$$

Here we have joined the spatial- and spin indices with a capital letter $I = (i, \alpha)$. We left multiply with χ_α^* , suppress indices for brevity and integrate over spin,

$$\langle \chi_\alpha | \hat{f} | \varphi_i \chi_\alpha \rangle = \langle \chi_\alpha | \hat{f} | \phi_{I=(i,\alpha)} \rangle = \epsilon_i \varphi_i. \quad (4.36)$$

Next we insert the Fock operator,

$$\hat{f} = \hat{h} + \sum_i \langle \cdot \varphi_i | \hat{u} | \cdot \varphi_i \rangle_{AS}.$$

This special notation $\langle \cdot \varphi_1 | \hat{u} | \cdot \varphi_2 \rangle$ means that we integrate over the second orbital in the matrix element only. After insertion we get

$$\begin{aligned}\langle \chi_\alpha | \hat{h} | \chi_\alpha \rangle \varphi_i + \sum_J \langle \chi_\alpha \phi_J | \hat{u} | \phi_I \phi_J \rangle_{AS} &= \epsilon_i \varphi_i \\ \hat{h} \varphi_i + \sum_J \langle \chi_\alpha \phi_J | \hat{u} | \phi_I \phi_J \rangle - \sum_J \langle \chi_\alpha \phi_J | \hat{u} | \phi_J \phi_I \rangle &= \epsilon_i \varphi_i.\end{aligned}\quad (4.37)$$

Because we have a closed-shell system, the sum over occupied spinorbitals include an equal sum over spin up and spin down functions so that

$$\sum_J^N = \sum_\beta \sum_j^{n/2}.$$

We next insert this into our eigenvalue equation and split the single-particle functions into separate spin- and spatial orbitals,

$$\begin{aligned}\hat{h} \varphi_i + \sum_\beta \sum_j^{n/2} \langle \chi_\alpha \varphi_j \chi_\beta | \hat{u} | \varphi_i \chi_\alpha \varphi_j \chi_\beta \rangle - \sum_\beta \sum_j^{n/2} \langle \chi_\alpha \varphi_j \chi_\beta | \hat{u} | \varphi_j \chi_\beta \varphi_i \chi_\alpha \rangle \\ = \hat{h} \varphi_i + 2 \sum_j^{n/2} \langle \cdot \varphi_j | \hat{u} | \varphi_i \varphi_j \rangle + \sum_j^{n/2} \langle \cdot \varphi_j | \hat{u} | \varphi_j \varphi_i \rangle = \epsilon_i \varphi_i.\end{aligned}\quad (4.38)$$

We now have the form of the Fock operator within the restricted Hartree-Fock theory,

$$\begin{aligned}\hat{f} &= \hat{h} + \sum_i^{n/2} \langle \cdot \varphi_i | (2\hat{u} - \hat{P}_{12}) | \cdot \varphi_i \rangle \\ &= \hat{h} + 2 \sum_i^{n/2} \int d\mathbf{r}_2 \varphi_i^*(\mathbf{r}_2) \hat{u} \varphi_i(\mathbf{r}_2) - \sum_i^{n/2} \int d\mathbf{r}_2 \varphi_i^*(\mathbf{r}_2) \hat{u} \varphi_j(\mathbf{r}_2)\end{aligned}\quad (4.39)$$

The Hartree-Fock energy also has a special form in the restricted Hartree-Fock domain,

$$\begin{aligned}
\langle \Phi | \hat{H} | \Phi \rangle &= \sum_P \langle \phi_P | \hat{h} | \phi_P \rangle + \frac{1}{2} \sum_P \sum_Q \langle \phi_P \phi_Q | \hat{u} | \phi_P \phi_Q \rangle_{\text{AS}} \\
&= \sum_{\alpha} \sum_p^{n/2} \langle \phi_{(p,\alpha)} | \hat{h} | \phi_{(p,\alpha)} \rangle \\
&\quad + \sum_{\alpha} \sum_p^{n/2} \sum_{\beta} \sum_q^{n/2} \langle \phi_{(p,\alpha)} \phi_{(q,\beta)} | \hat{u} (\langle \phi_{(p,\alpha)} \phi_{(q,\beta)} \rangle - \langle \phi_{(q,\beta)} \phi_{(p,\alpha)} \rangle) \\
&= 2 \sum_p^{n/2} \langle \varphi_p | \hat{h} | \varphi_q \rangle + 2 \sum_{pq}^{n/2} \langle \varphi_p \varphi_q | \hat{u} | \varphi_p \varphi_q \rangle - \sum_{pq}^{n/2} \langle \varphi_p \varphi_q | \hat{u} | \varphi_p \varphi_q \rangle.
\end{aligned} \tag{4.40}$$

4.4 Unrestricted Hartree-Fock Theory

The restricted Hartree-Fock model is often a good enough approximation, but under some circumstances it will fail to provide a good result. The unrestricted Hartree-Fock model is an intermediate between the general Hartree-Fock model and the restricted Hartree-Fock model. Compared with the restricted Hartree-Fock single-particle wavefunction form, what we do in unrestricted form is somewhat obvious - we now allow the spins to be different,

$$\phi_P(\mathbf{r}, \sigma) = \varphi_p^{\alpha}(\mathbf{r}) \chi_{\alpha}(\sigma), \tag{4.41}$$

where we have given the spatial orbitals a spin-index as well. As before, a capital index is the combined spatial- and spin index $P = (p, \alpha)$, where $P \in [1, L]$, $p \in [1, L/2]$ and $\alpha = \pm 1/2$. Like before, we require the states to be orthonormal

$$\langle \phi_P | \phi_Q \rangle = \langle \varphi_p^{\alpha} | \varphi_q^{\beta} \rangle \langle \chi_{\alpha} | \chi_{\beta} \rangle = \delta_{PQ}. \tag{4.42}$$

We can write a general unrestricted Hartree-Fock state as

$$|\Phi\rangle_{\text{UHF}} = |\varphi_1^{1/2} \varphi_1^{-1/2} \varphi_2^{1/2} \varphi_2^{-1/2} \dots \varphi_{L/2}^{1/2} \varphi_{L/2}^{-1/2}\rangle = |\phi_1 \phi_2 \phi_3 \phi_4 \dots \phi_{L-1} \phi_L\rangle. \tag{4.43}$$

In order to find an expression for the Fock operator we insert the wavefunction into the canonical Hartree-Fock equation,

$$\hat{f} \phi_P = \epsilon_p \phi_P, \rightarrow \hat{f} \varphi_p^{\alpha} \chi_{\alpha} = \epsilon_p \varphi_p^{\alpha} \chi_{\alpha}. \tag{4.44}$$

Now we left multiply by χ_{α}^* and integrate over spin,

$$\langle \chi_{\alpha} | \hat{f} | \varphi_p^{\alpha} \chi_{\alpha} \rangle = \langle \chi_{\alpha} | \epsilon_p | \varphi_p^{\alpha} \chi_{\alpha} \rangle \tag{4.45}$$

$$\hat{f}^{\alpha} \varphi_p^{\alpha} = \left[\int d\sigma_1 \chi_{\alpha}(\sigma_1)^* \hat{f}(\mathbf{r}, \sigma_1) \chi_{\alpha}(\sigma_1) \right] \varphi_p^{\alpha} = \epsilon_p \varphi_p^{\alpha}. \tag{4.46}$$

We now have what is called the spatial unrestricted Hartree-Fock equations. Inserting for the canonical Fock operator yields the following left-hand side

$$\begin{aligned}
\hat{f}^\alpha \varphi_p^\alpha &= \hat{h} \varphi_p^\alpha + \sum_Q^L \langle \chi_\alpha \phi_Q | \hat{u} | \varphi_p^\alpha \chi_\alpha \phi_Q \rangle q - \sum_Q^L \langle \chi_\alpha \phi_Q | \hat{u} | \phi_Q \varphi_p^\alpha \chi_\alpha \rangle \\
&= \hat{h} \varphi_p^\alpha + \sum_\beta \sum_q^{L/2} \langle \chi_\alpha \varphi_q^\beta \chi_\beta | \hat{u} | \varphi_p^\alpha \chi_\alpha \varphi_q^\beta \chi_\beta \rangle \\
&\quad - \sum_\beta \sum_q^{L/2} \langle \chi_\alpha \varphi_q^\beta \chi_\beta | \hat{u} | \varphi_q^\beta \chi_\beta \varphi_p^\alpha \chi_\alpha \rangle \\
&= \hat{h} \varphi_p^\alpha + \sum_\beta \sum_q^{L/2} \langle \cdot \varphi_q^\beta | \hat{u} | \cdot \varphi_q^\beta \rangle \varphi_p^\alpha - \sum_q^{L/2} \langle \cdot \varphi_q^\alpha | \hat{u} | \cdot \varphi_p^\alpha \rangle \varphi_q^\beta.
\end{aligned} \tag{4.47}$$

This means that we get the following form for the spatial Fock operators in unrestricted Hartree-Fock

$$\hat{f}^\uparrow = \hat{h} + \sum_p^{L/2} [\hat{v}_{\text{Coulomb}}^\uparrow - \hat{v}_{\text{exchange}}^\uparrow] + \sum_p^{L/2} \hat{v}_{\text{Coulomb}}^\downarrow, \tag{4.48}$$

$$\hat{f}^\downarrow = \hat{h} + \sum_p^{L/2} [\hat{v}_{\text{Coulomb}}^\downarrow - \hat{v}_{\text{exchange}}^\downarrow] + \sum_p^{L/2} \hat{v}_{\text{Coulomb}}^\uparrow. \tag{4.49}$$

From the definition of the two spatial Fock operators in Equation 4.48 and Equation 4.49, we see that the two integro-differential eigenvalue equations that arises from inserting \hat{f}^\uparrow and \hat{f}^\downarrow into the canonical Hartree-Fock equation,

$$\hat{f}^\uparrow \varphi_p^\uparrow = \epsilon_p^\uparrow \varphi_p^\uparrow, \tag{4.50}$$

$$\hat{f}^\downarrow \varphi_p^\downarrow = \epsilon_p^\downarrow \varphi_p^\downarrow, \tag{4.51}$$

are coupled and cannot be solved independently. The spin-up orbitals depend on the occupied spin-down orbitals and vice versa. This means that the two equations must be solved by a simultaneous iterative process.

We can also derive an equation for the unrestricted Hartree-Fock energy,

$$\begin{aligned}
E_{UHF} &= \langle \Phi_{UHF} | \hat{H} | \Phi_{UHF} \rangle \\
&= \sum_\alpha \sum_p^{L/2} \langle \varphi_p^\alpha \chi_\alpha | \hat{h} | \varphi_p^\alpha \chi_\alpha \rangle + \sum_\alpha \sum_p^{L/2} \sum_\beta \sum_q^{L/2} \langle \varphi_p^\alpha \chi_\alpha \varphi_q^\beta \chi_\beta | \hat{u} | \varphi_p^\alpha \chi_\alpha \varphi_q^\beta \chi_\beta \rangle_{\text{AS}} \\
&= \sum_\alpha \sum_{pq}^{L/2} \langle \varphi_p^\alpha | \hat{h} | \varphi_p^\alpha \rangle + \sum_{\alpha\beta} \sum_q^{L/2} \langle \varphi_p^\alpha \varphi_q^\beta | \hat{u} | \varphi_p^\alpha \varphi_q^\beta \rangle - \sum_\alpha \sum_{pq}^{L/2} \langle \varphi_p^\alpha \varphi_q^\alpha | \hat{u} | \varphi_q^\alpha \varphi_p^\alpha \rangle.
\end{aligned} \tag{4.52}$$

If we were to expand the unrestricted Hartree-Fock equations, Equation 4.50 and Equation 4.51, in a basis like we did in section 4.2, we would get the Pople-Nesbet-Berthier equations [52, 53].

4.5 Time-Dependent Hartree-Fock

This section follows closely the narrative of Hochstuhl *et al.* [54]. Deriving the time-dependent Hartree-Fock equations starts, of course, with the time-dependent Schrödinger equation,

$$i\hbar \frac{\partial}{\partial t} |\Phi(t)\rangle = \hat{H}(t) |\Phi(t)\rangle, \quad (4.53)$$

where the Hamiltonian is

$$\hat{H}(t) = \hat{h}(t) + \hat{u}(t). \quad (4.54)$$

This is the same Hamiltonian that we started with in this chapter (see Equation 4.1), except for the introduction of a time-dependence. We start by multiplying from the left with the reference Slater determinant $\langle\Phi|$. The right-hand side of the Schrödinger equation becomes the familiar Hartree-Fock energy,

$$\langle\Phi|\hat{H}|\Phi\rangle = \sum_p \langle\phi_p|\hat{h}|\phi_p\rangle + \frac{1}{2} \sum_{pq} \langle\phi_p\phi_q|\hat{u}|\phi_p\phi_q\rangle_{AS}. \quad (4.55)$$

The left-hand side, is more interesting,

$$\langle\Phi|\frac{\partial}{\partial t}|\Phi\rangle = \sum_p \langle\phi_p|\frac{\partial}{\partial t}|\phi_p\rangle, \quad (4.56)$$

which we will deal with in due time, but before doing so we need to introduce functional derivatives and the functional derivatives of various matrix elements. First, the one-body matrix elements,

$$\frac{\delta}{\delta\phi_r^*} \sum_p \langle\phi_p|\hat{h}|\phi_p\rangle = \sum_p \frac{\delta}{\delta\phi_r^*} \int dr \phi_p^* \hat{h} \phi_p = \sum_p \delta_{pr} \hat{\phi} = \hat{h} |\phi_r\rangle. \quad (4.57)$$

Second, the matrix elements of the time-derivative,

$$\frac{\delta}{\delta\phi_r^*} \sum_p \langle\phi_p|\frac{\partial}{\partial t}|\phi_p\rangle = \frac{\partial}{\partial t} |\phi_r\rangle, \quad (4.58)$$

which is so similar to the one-body computation that the result is simply written down, instead of computing the result explicitly. Lastly, we have the two-body matrix elements,

$$\begin{aligned} & \frac{\delta}{\delta\phi_r^*} \sum_{pq} \langle\phi_p\phi_q|\hat{u}|\phi_p\phi_q\rangle_{AS} \\ &= \frac{\delta}{\delta\phi_r^*(r_1)} \sum_{pq} \int dr_1 dr_2 \phi_p^*(r_1) \phi_q^*(r_2) \hat{u} [\phi_p(r_1)\phi_q(r_2) - \phi_q(r_1)\phi_p(r_2)] \\ &= \sum_{pq} \delta_{pq} \int dr_2 \phi_q^*(r_2) \hat{u} [\phi_p(r_1)\phi_q(r_2) - \phi_q(r_1)\phi_p(r_2)] = \sum_q \langle\cdot\phi_q|\hat{u}|\phi_r\phi_q\rangle_{AS}. \end{aligned} \quad (4.59)$$

Now we want to vary the reference state to find the optimal one, applying the so-called time-dependent variational principle[35],

$$\langle \delta\Phi | (\hat{H} - i\hbar \frac{\partial}{\partial t}) |\Phi \rangle = 0, \quad (4.60)$$

which we want to minimise under the requirement of orthonormal single-particle functions in time,

$$\langle \phi_p(t) | \phi_q(t) \rangle = \delta_{pq}. \quad (4.61)$$

Such an optimization problem under a constraint begs the formulation of a Lagrangian. We have then

$$\mathcal{L}(\Phi, \lambda_{pq}) = \langle \Phi | (\hat{H} - i\hbar \frac{\partial}{\partial t}) |\Phi \rangle - \sum_{pq} \lambda_{pq} (\langle \phi_p | \phi_q \rangle - \delta_{pq}). \quad (4.62)$$

We find a stationary point of this Lagrangian functional, by variation of the single-particle functions so that

$$\frac{\delta \mathcal{L}}{\delta \phi_r^*} = 0, \quad \forall r. \quad (4.63)$$

This is where we will make use of the functional derivatives we computed before,

$$\frac{\delta \mathcal{L}}{\delta \phi_r^*} = \hat{h} |\phi_r\rangle + \sum_q \langle \cdot \phi_q | \hat{u} | \phi_r \phi_q \rangle_{AS} - i\hbar \frac{\partial}{\partial t} |\phi_r\rangle - \sum_q \lambda_{rq} |\phi_r\rangle = 0. \quad (4.64)$$

Now we want to solve for the Langrange multiplier, we do this by left-projection of the functional derivative above with $\langle \phi_s |$ and move the resulting multiplier λ_{sq} to the left, and all other terms to the right. We get the following expression for the Langrange multiplier,

$$\lambda_{sq} = \langle \phi_s | \hat{h} | \phi_r \rangle + \langle \phi_s \phi_q | \hat{u} | \phi_r \phi_q \rangle_{AS} - i\hbar \langle \phi_s | \frac{\partial}{\partial t} | \phi_r \rangle \quad (4.65)$$

We insert this expression for the Langrange multiplier into Equation 4.64 which results in,

$$\hat{P} \left[\hat{h} |\phi_r\rangle + \sum_q \langle \cdot \phi_q | \hat{u} | \phi_r \phi_q \rangle_{AS} - i\hbar \frac{\partial}{\partial t} |\phi_r\rangle \right] = 0, \quad (4.66)$$

where we have introduced the projection operator \hat{P} ,

$$\hat{P} = \hat{1} - \sum_p |\phi_p\rangle \langle \phi_p|. \quad (4.67)$$

Rearranging Equation 4.66 yields

$$i\hbar \hat{P} \frac{\partial}{\partial t} |\phi_r\rangle = \hat{P} \left[\hat{h} |\phi_r\rangle + \langle \cdot \phi_q | \hat{u} | \cdot \phi_q \rangle \right] |\phi_r\rangle_{AS} = \hat{P} \hat{f} |\phi_r\rangle, \quad (4.68)$$

where we see that Fock operator has appeared. This equation is an integro-differential equation, as the projection operator \hat{P} appear on both sides of the equality sign, and a solution can be difficult to find. Because the time-dependent Hartree-Fock wavefunction

is invariant under unitary transformation, we can obtain equations that are numerically more appropriate, by applying a unitary transformation $\hat{Q}(t)$ which satisfies

$$i\hbar \langle \phi_p | \frac{\partial}{\partial t} | \phi_q \rangle \equiv \langle \phi_p | \hat{Q}(t) | \phi_q \rangle. \quad (4.69)$$

It turns out that a reasonable choice for $\hat{Q}(t)$ is $\hat{f}(t)$, in which case Equation 4.68 becomes

$$i\hbar \frac{\partial}{\partial t} | \phi_p(t) \rangle = \hat{f}(t) | \phi_p(t) \rangle, \quad (4.70)$$

where we have explicitly written out the time-dependence. This is the time-dependent Hartree-Fock equation.

Now we pick a specific, finite and static basis $\{\chi_p\}_{p=1}^L$ and expand the Hartree-Fock single-particle functions in this basis,

$$| \phi_p(t) \rangle = \sum_{\alpha} C_p^{\alpha}(t) | \chi_{\alpha} \rangle. \quad (4.71)$$

Notice that the basis set is indeed static, with no time-dependence, only the coefficients of the expansions $U_p^{\alpha}(t)$ evolve in time. We insert the expansion into Equation 4.70,

$$i\hbar \frac{\partial}{\partial t} \sum_{\alpha} C_p^{\alpha} | \chi_{\alpha} \rangle = \hat{f}(t) \sum_{\alpha} C_p^{\alpha} | \chi_{\alpha} \rangle. \quad (4.72)$$

We left-project this equation with $\langle \chi_{\beta} |$,

$$\begin{aligned} i\hbar \frac{\partial}{\partial t} \sum_{\alpha} C_p^{\alpha}(t) \langle \chi_{\beta} | \chi_{\alpha} \rangle &= \sum_{\alpha} C_p^{\alpha}(t) \langle \chi_{\beta} | \hat{f}(t) | \chi_{\alpha} \rangle \\ &\rightarrow i\hbar \sum_{\alpha} \dot{C}_p^{\alpha} S_{\alpha}^{\beta} = \sum_{\alpha} C_p^{\alpha} \hat{f}_{\alpha}^{\beta}(t), \end{aligned} \quad (4.73)$$

which can be written as a matrix equation,

$$i\hbar \mathbf{S} \dot{\mathbf{C}}(t) = \mathbf{F}(t) \mathbf{C}(t). \quad (4.74)$$

We have derived the time-dependent Hartree-Fock equations, in the form of a matrix equation in Equation 4.74. The time-dependent Hartree-Fock equations are a set of elegant equations of motion that dictate the time-development of the system by simple propagation of the Hartree-Fock coefficients. Moreover, we have come to the realisation that it is necessary to compute the Hartree-Fock self-consistent field iterations only once, and after that we can treat Equation 4.74 as set of ordinary differential equations, which can be solved numerically without great effort. The only consideration one must make is to update the Fock matrix at each time step.

Chapter 5

Perturbation Theory

Perturbation theory is a very powerful method and a generic method applicable to all matrix problems. Additionally, perturbation theory is relatively cheap in terms of computing time, especially compared with coupled cluster theory. The method provides a different route to the solution of the Schrödinger equation, by approaching the exact solution systematically, based on an order-by-order expansion of the energy and wavefunction. Therefore, perturbation theory is often used to improve the results from other computational schemes. What is more, the exponential form of the wavefunction in coupled cluster theory stems from the non-degenerate Rayleigh-Schrödinger perturbation theory (RSPT) expansion.

5.1 Formal perturbation theory

We split the Hamiltonian into a known part and a perturbed part,

$$\hat{H} = \hat{H}_0 + \hat{V}. \quad (5.1)$$

Sometimes it is convenient to write

$$\hat{H} = \hat{H}_0 + \lambda \hat{V}, \quad (5.2)$$

where we have included an "order parameter" λ . This parameter is used to categorise the contributions of different orders. The exact solution is given by

$$\begin{aligned} \hat{H}\Psi_n &= E_n\Psi_n \\ (\hat{H}_0 + \hat{V})\Psi_n &= E_n\Psi_n, \quad \Psi_n = \Phi_n + \chi_n, \end{aligned} \quad (5.3)$$

while the solvable and simple zero order problem is given by

$$\hat{H}_0\Phi_n = E_n^{(0)}\Phi_n. \quad (5.4)$$

The set $\{\Phi_n\}$ is assumed to be an orthonormal basis for the Hilbert space. The exact wavefunction Ψ_n is split into a zero-order part Φ_n and the perturbative part χ_n .

By projecting Equation 5.3 with $\langle \Phi_0 |$ we get

$$\begin{aligned} \langle \Phi_n | \hat{H}_0 | \Psi_n \rangle + \langle \Phi_n | \hat{V} | \Psi_n \rangle &= E_n \langle \Phi_n | \Psi_n \rangle \\ \rightarrow E_n &= \langle \Phi_n | \hat{H} | \Psi_n \rangle \\ \rightarrow \Delta E_n &= E_n - E_n^0 = \langle \Phi_n | \hat{V} | \Psi_n \rangle \end{aligned} \quad (5.5)$$

where we have used that

$$\langle \Phi_m | \Phi_n \rangle = \delta_{mn}, \quad (5.6)$$

$$\langle \Psi_n | \Phi_n \rangle = \langle \Phi_n + \chi_n | \Phi_n \rangle = 1, \quad (5.7)$$

$$\langle \Psi_n | \Psi_n \rangle = 1 + \langle \chi_n | \chi_n \rangle. \quad (5.8)$$

This is called the intermediate normalisation assumption.

5.1.1 Energy- and Wavefunction Expansion

To proceed further we expand the wavefunction and energy in the order parameter λ from Equation 5.2,

$$\begin{aligned} \Psi_n &= \Phi_n + \chi_n = \Psi_n^{(0)} + \lambda \Psi_n^{(1)} + \lambda^2 \Psi_n^{(2)} + \dots \quad (\Psi_n^{(0)} \equiv \Phi_n) \\ E_n &= E_n^{(0)} + \Delta E_n = E_n^{(0)} + \lambda E_n^{(1)} + \lambda^2 E_n^{(2)} + \dots \end{aligned} \quad (5.9)$$

We insert these expansions into the Schrödinger equation,

$$\begin{aligned} (\hat{H} - E_n) \Psi_n &= 0 \\ (\hat{H}_0 + \lambda \hat{V}) \Psi_n &= 0, \end{aligned} \quad (5.10)$$

resulting in

$$(\hat{H}_0 + \lambda \hat{V} - E_n^{(0)} - \lambda E_n^{(1)} - \lambda^2 E_n^{(2)} - \dots)(\Psi_n^{(0)} + \lambda \Psi_n^{(1)} + \lambda \Psi_n^{(2)} + \dots) = 0. \quad (5.11)$$

We gather the coefficients of different powers of λ and obtain

$$(\hat{H}_0 - E_n^{(0)}) \Psi_n^{(0)} = 0 \quad (5.12)$$

$$(\hat{H}_0 - E_n^{(0)}) \Psi_n^{(1)} = (E_n^{(1)} - \hat{V}) \Psi_n^{(0)} \quad (5.13)$$

$$(\hat{H}_0 - E_n^{(0)}) \Psi_n^{(2)} = (E_n^{(1)} - \hat{V}) \Psi_n^{(1)} + E_n^{(2)} \Psi_n^{(0)} \quad (5.14)$$

...

$$(\hat{H}_0 - E_n^{(0)}) \Psi_n^{(m)} = (E_n^{(1)} - \hat{V}) \Psi_n^{(m-1)} + \sum_{l=0}^{m-2} E_n^{(m-l)} \Psi_n^{(l)}, \quad (5.15)$$

where the last line gives a general m th-order equation. This equation can be simplified somewhat,

$$(E_n^{(0)} - \hat{H}_0) \Psi_n^{(m)} = \hat{V} \Psi_n^{(m-1)} - \sum_{l=0}^{m-1} E_n^{(m-l)} \Psi_n^{(l)}. \quad (5.16)$$

By applying $\langle \Phi_n |$ to each of the equations, we get expressions for $E_n^{(m)}$. For λ^1 (Equation 5.13) we get,

$$\begin{aligned} \langle \Phi_n | \hat{H}_0 - E_n^{(0)} | \Psi_n^{(1)} \rangle &= \langle \Phi_n | E_n^{(1)} - \hat{V} | \Phi_n \rangle \\ \langle (\hat{H}_0 - E_n^{(0)}) \Phi_n | \Psi_n^{(1)} \rangle &= \langle \Phi_n | E_n^{(1)} - \hat{V} | \Phi_n \rangle \\ \rightarrow E_n^{(1)} &= \langle \Phi_n | \hat{V} | \Phi_n \rangle = \hat{V}_{nn}. \end{aligned} \quad (5.17)$$

Since we have an expression for $E_n^{(1)}$, we can solve the equation for $\Psi_n^{(1)}$, by also requiring the intermediate normalisation condition $\langle \Phi_n | \Psi_n^{(1)} \rangle = 0$. For the general m th-order expression (Equation 5.15) we have,

$$\begin{aligned} \langle \Phi_n | E_e^0 - \hat{H}_0 | \Psi_n^{(m)} \rangle &= \langle \Phi_n | \hat{V} | \Psi_n^{(m-1)} \rangle - \sum_{l=0}^{m-1} E_n^{(m-l)} \langle \Phi_n | \Psi_n^{(l)} \rangle \\ E_n^{(m)} &= \langle \Phi_n^{(m)} | = \langle \Phi_n | \hat{V} | \Psi_n^{(m-1)} \rangle. \end{aligned} \quad (5.18)$$

In principle, we can obtain every next-order energy contribution $E_n^{(m)}$ from the previous-order wavefunctions $\Psi_n^{(m-1)}$ and then solve for $\Psi_n^{(m)}$.

5.1.2 Projection Operators

We define the projection operators, \hat{P} and \hat{Q} , in terms of the zero-order wavefunctions,

$$\begin{aligned} \hat{P} &= |\Phi_0\rangle\langle\Phi_0| \\ \hat{Q} &= \hat{1} - \hat{P} = \sum_{i=1}^N |\Phi_i\rangle\langle\Phi_i|. \end{aligned} \quad (5.19)$$

The projection operators have the following convenient properties,

$$\begin{aligned} \hat{P}^2 &= |\Phi_0\rangle\langle\Phi_0|\Phi_0\rangle\langle\Phi_0| = |\Phi_0\rangle\langle\Phi_0| = \hat{P} \\ \hat{Q}^2 &= (1 - \hat{P})^2 = \hat{1} - \hat{P} - \hat{P} + \hat{P} = \hat{1} - \hat{P} = \hat{Q} \\ \hat{P}\hat{Q} &= \hat{Q}\hat{P} = 0 \\ [\hat{P}, \hat{H}_0] &= [\hat{Q}, \hat{H}_0] = 0 \end{aligned} \quad (5.20)$$

If we write the wavefunction as a linear expansion in terms of Φ_i ,

$$\Phi = \sum_i a_i \Phi_i, \quad (5.21)$$

acting on it with the projection operators yields

$$\hat{P}\Psi = \sum_i a_i |\Phi_0\rangle\langle\Phi_0|\Phi_i\rangle = \sum_i a_i |\Phi_0\rangle\delta_{0i} = a_0 \Phi_0. \quad (5.22)$$

For sake of specificity, the operator \hat{P} will extract Φ_0 from Ψ , while \hat{Q} annihilates Φ_0 ,

$$\hat{Q}\Psi = (\hat{1} - \hat{P})\Psi = \Psi - a_0\Phi_0 = \sum_{i=1}^N a_i\Phi_i, \quad (5.23)$$

meaning we can write

$$\Psi = \hat{P}\Psi + \hat{Q}\Psi. \quad (5.24)$$

5.1.3 The Resolvent

Now follows what some considers a more elegant derivation of the perturbation equations, including the introduction of the *resolvent* of the unperturbed part of the Hamiltonian \hat{H}_0 .

Starting from a rearrangement of the Schrödinger equation,

$$\begin{aligned} (\hat{H}_0 + \hat{V})\Psi &= E\Psi, \\ \rightarrow -\hat{H}_0\Phi &= (\hat{V} - E)\Psi, \end{aligned} \quad (5.25)$$

we introduce a seemingly arbitrary parameter ζ , the purpose of which will be apparent later. This parameter is introduced by adding $\zeta\Phi$ to both sides,

$$(\zeta - \hat{H}_0)\Phi = (\hat{V} - E + \zeta)\Phi. \quad (5.26)$$

Next, we apply \hat{Q} to both sides,

$$\hat{Q}(\zeta - \hat{H}_0)\Psi = \hat{Q}(\hat{V} - E + \zeta)\Psi. \quad (5.27)$$

The right-hand side of this expression can be rewritten as,

$$\begin{aligned} \hat{Q}(\zeta - \hat{H}_0)\Psi &= \hat{Q}^2(\zeta - \hat{H}_0) = \hat{Q}(\zeta - \hat{H}_0)\hat{Q}\Psi \\ &= \sum_{i \neq 0} \sum_{j \neq 0} |\Phi_i\rangle \langle \Phi_i| \zeta - \hat{H}_0 |\Phi_j\rangle \langle \Phi_j|, \end{aligned} \quad (5.28)$$

Equation 5.27 is now

$$\hat{Q}(\zeta - \hat{H}_0)\hat{Q}\Psi = \hat{Q}(\hat{V} - E + \zeta)\Psi. \quad (5.29)$$

By restricting to choice of ζ , so they do not coincide with the eigenvalues of \hat{H}_0 in \hat{Q} -space, i.e. $\{\Phi_i | i \neq 0\}$, we ensure that the inverse of $\hat{Q}(\zeta - \hat{H}_0)\hat{Q}$ exists. This inverse is the *resolvent* of \hat{H}_0 ,

$$\hat{R}_0(\zeta) = \frac{\hat{Q}}{\zeta - \hat{H}_0} \equiv \sum_{i \neq 0} \sum_{j \neq 0} |\Phi_i\rangle \langle \Phi_i| (\zeta - \hat{H}_0)^{-1} |\Phi_j\rangle \langle \Phi_j|. \quad (5.30)$$

The resolvent simplifies in the diagonal case to

$$\hat{R}_0(\zeta) = \sum_{i \neq 0} |\Phi_i\rangle \langle \Phi_i| (\zeta - E_j^{(0)})^{-1} |\Phi_j\rangle \langle \Phi_j| = \sum_{i \neq 0} \frac{|\Phi_i\rangle \langle \Phi_i|}{(\zeta - E_i^{(0)})}. \quad (5.31)$$

We can prove that $\hat{R}_0(\zeta)$ is the inverse of $\hat{Q}(\zeta - \hat{H}_0)\hat{Q}$ in \hat{Q} -space,

$$\begin{aligned}
& \frac{\hat{Q}}{\zeta - \hat{H}_0} \hat{Q}(\zeta - \hat{H}_0)\hat{Q} \\
&= \left(\sum_{i,j \neq 0} |\Phi_i\rangle \langle \Phi_i| (\zeta - \hat{H}_0)^{-1} |\Phi_j\rangle \langle \Phi_j| \right) \left(\sum_{k,l \neq 0} |\Phi_k\rangle \langle \Phi_k| (\zeta - \hat{H}_0) |\Phi_l\rangle \langle \Phi_l| \right) \\
&= \sum_{i,l \neq 0} |\Phi_i\rangle \langle \Phi_i| (\zeta - \hat{H}_0)^{-1} \left(\sum_{j \neq 0} |\Phi_j\rangle \langle \Phi_j| \right) (\zeta - \hat{H}_0) |\Phi_l\rangle \langle \Phi_l| \\
&= \sum_{i,l \neq 0} |\Phi_i\rangle \langle \Phi_i| (\zeta - \hat{H}_0)^{-1} (1 - |\Phi_0\rangle \langle \Phi_0|) (\zeta - \hat{H}_0) |\Phi_l\rangle \langle \Phi_l| \\
&= \sum_{i \neq 0} |\Phi_i\rangle \langle \Phi_i| = \hat{Q}.
\end{aligned} \tag{5.32}$$

Applying the resolvent to both sides of Equation 5.29,

$$\begin{aligned}
& \hat{Q}\Psi = \hat{R}_0(\zeta)(\hat{V} - E + \zeta)\Psi \\
& \rightarrow \Psi = \Phi_0 + \hat{R}_0(\zeta)(\hat{V} - E + \zeta)\Psi,
\end{aligned} \tag{5.33}$$

which can be interpreted as a recursive relation for Ψ . Inserting the expression for Ψ into itself repeatedly, yields

$$\Psi = \sum_{m=0}^{\infty} [\hat{R}_0(\zeta)(\hat{V}) - E + \zeta]^m \Phi_0. \tag{5.34}$$

We can find an expression for the perturbative energy correction by left-projecting this expression with $\langle \Phi_0 | \hat{V}$,

$$\Delta E = \langle \Phi_0 | \hat{V} | \Psi \rangle = \sum_{m=0}^{\infty} \langle \Phi_0 | [\hat{R}_0(\zeta)(\hat{V} - E + \zeta)]^m | \Phi_0 \rangle. \tag{5.35}$$

The problem with these equations is that E , which is unknown, appears on the right-hand side. One would also wonder what to do with ζ . There are two common choices for ζ that give rise to two important theories,

$$\begin{aligned}
& \zeta = E \leftarrow \text{Brillouin-Wigner Perturbation} \\
& \zeta = E_0^{(0)} \rightarrow -E + \zeta = -\Delta E \leftarrow \text{Rayleigh-Schrödinger Perturbation.}
\end{aligned}$$

5.2 Brillouin-Wigner Perturbation Theory

By setting $\zeta = E$ in Equation 5.34 and Equation 5.35 we get Brilloun-Wigner perturbation theory[55, 56]. The wavefunction- and energy expression becomes the following,

$$\Psi = \sum_{m=0}^{\infty} [\hat{R}_0(E)\hat{V}]^m \Phi_0 \tag{5.36}$$

$$\Delta E = \sum_{m=0}^{\infty} \langle \Phi_0 | \hat{V} [\hat{R}_0(E) \hat{V}]^m | \Phi_0 \rangle. \quad (5.37)$$

Moreover, the resolvent is given by

$$\hat{R}_0 = \sum_i \frac{|\Phi_i\rangle\langle\Phi_i|}{E - E_i^{(0)}}. \quad (5.38)$$

As we can see, these equations are still implicit, i.e. E appears on the right-hand side. In order to compute corrections in the energy and wavefunctions estimates, we need an estimate for E . A common estimate for the first-order energy is $E_0^{(0)} + \langle \Phi_0 | \hat{V} | \Phi_0 \rangle$. From this we can continue computing the second-order energy,

$$\begin{aligned} E^{(2)} &= \langle \Phi_0 | \hat{V} \hat{R}_0(E) \hat{V} | \Phi_0 \rangle \\ &= \sum_i \frac{\langle \Phi_0 | \hat{V} | \Phi_i \rangle \langle \Phi_i | \hat{V} | \Phi_0 \rangle}{E - E_i^{(0)}} \\ &= \sum_i \frac{V_{0i} V_{i0}}{E - E_i^{(0)}}. \end{aligned} \quad (5.39)$$

Similiarly for the third-order energy,

$$E^{(3)} = \sum_{ij} \frac{V_{0i} V_{ij} V_{j0}}{(E - E_i^{(0)})(E - E_j^{(0)})}. \quad (5.40)$$

These expressions are somewhat simple, but Brilloun-Wigner is plagued by a fundamental problem as it does not provide a true order-by-order expansion of the energy. This is due to the systematically prevalent presence of the infinite-order E -term in the right-hand sides of the equations. Related to this problem, is the lack of extensivity if the perturbation is truncated at any finite order. See Shavitt & Bartlett[20] for a derivation of this non-extensivity of finite-order Brilloun-Wigner perturbation theory. For this reason, we move on to Rayleigh-Schrödinger perturbation theory.

5.3 Rayleigh-Schrödinger Perturbation Theory

By setting $\zeta = E_0^{(0)}$ in Equation 5.34 and Equation 5.35 we get Rayleigh-Schrödinger perturbation theory[57, 58]. This parametrisation means that $\zeta - E = -\Delta E$, which gives us

$$\Psi = \sum_{m=0}^{\infty} \left[\hat{R}_0(E_0^{(0)}) (\hat{V} - \Delta E) \right]^m \Phi_0 \quad (5.41)$$

$$\Delta E = \sum_{m=0}^{\infty} \langle \Phi_0 | \hat{V} \left[\hat{R}_0(E_0^{(0)}) (\hat{V} - \Delta E) \right]^m | \Phi_0 \rangle, \quad (5.42)$$

where the resolvent becomes

$$\hat{R}_0(E_0^{(0)}) = \sum_i \frac{|\Phi_i\rangle\langle\Phi_i|}{E^{(0)} - E_i^{(0)}}. \quad (5.43)$$

The keen reader will have noticed that these expressions are lacking the unknown E , but we still have an expression for ΔE in the right-hand side of the expressions.

The first-order correction in energy is simply

$$E^{(1)} = \langle \Phi_0 | \hat{V} | \Phi_0 \rangle. \quad (5.44)$$

For the second order energy correction, $E^{(2)}$ we need the first-order wavefunction correction,

$$\Psi^{(1)} = \hat{R}_0 \hat{V} \Phi_0. \quad (5.45)$$

Notice that the ΔE -term to the right disappears as $\hat{R}_0 \Delta_E |\Phi_0\rangle = \Delta_E \hat{R}_0 |\Phi_0\rangle = 0$. This gives us

$$E^{(2)} = \langle \Phi_0 | \hat{V} \hat{R}_0 \hat{V} | \Phi_0 \rangle = \sum_i \frac{|\langle \Phi_0 | \hat{V} | \Phi_i \rangle|^2}{E^{(0)} - E_i^{(0)}}. \quad (5.46)$$

For the third-order energy correction we need the second-order wavefunction correction,

$$\Psi^{(2)} = \hat{R}_0 (\hat{V} - \Delta E) \hat{R} \hat{V} \Phi_0 = \hat{R}_0 (\hat{V} - \langle \Phi_0 | \hat{V} | \Phi_0 \rangle) \hat{R} \hat{V} \Phi_0, \quad (5.47)$$

where we have started to treat the stepwise expansions as a recursive relation, by inserting the first-order energy corrections for ΔE . Generally, we can write this recursive relation as

$$E^{(n)} = \left\langle \Psi_k \middle| \hat{V} \right| \Psi_k^{(n-1)} \rangle, \quad (5.48)$$

$$\Psi^n = \hat{R}_0 \hat{V} \Psi^{(n-1)} - \sum_{j=1}^{n-1} E^{(n-j)} \Psi^{(j)}. \quad (5.49)$$

The third order-energy correction becomes

$$\begin{aligned} E^{(3)} &= \langle \Phi_0 | \hat{V} \hat{R}_0 [\hat{V} - \langle \Phi_0 | \hat{V} | \Phi_0 \rangle] | \Phi_0 \rangle \\ &= \langle \Phi_0 | \hat{V} \hat{R} \hat{V} \hat{R} \hat{V} | \Phi_0 \rangle - \langle \Phi_0 | \hat{V} \hat{R}^2 \hat{V} | \Phi_0 \rangle \end{aligned} \quad (5.50)$$

We should now notice that a pattern has arisen in the energy terms, albeit a bit complicated one. There will always be a leading term,

$$E^{(n)} = \langle \Phi_0 | \hat{V} \hat{R} \hat{V} \hat{R} \dots \hat{V} | \Phi_0 \rangle, \quad (5.51)$$

with n factors \hat{V} and $n-1$ factors \hat{R} . But then we will have terms that are on the form

$$E^{(j)} \langle \Psi^{(n-1)} | \Psi^{(n-j)} \rangle = E^{(j)} \langle \Phi_0 | \hat{V} \mathcal{M}(\hat{R}, \hat{V}) \hat{V} | \Phi_0 \rangle, \quad (5.52)$$

where $\mathcal{M}(\hat{R}, \hat{V})$ is the *monomial* of in total $n-j-2$ operators \hat{V} and \hat{R} 's, in some order. The terms can be systematically generated from the leading energy term by a procedure called *bracketing*.

The bracketing procedure can be quickly summarised as follows. The n th order energy $E^{(n)}$ can be written as the leading term plus terms generated by inserting some brackets $\langle \rangle$ around one or more \hat{V} s, except for the outer ones, in *any* possible way, in *any* number. These terms may also be nested. The bracket represents an expectation

value with Ψ . The sign of each term is $(-1)^j$, where j is the number of brackets in the term. For example, for $n = 4$ we have four possibilities,

$$\langle \Phi_0 | \hat{V} \hat{R}_0 \langle \hat{V} \rangle \hat{R}_0 \hat{V} \hat{R}_0 \hat{V} | \Phi_0 \rangle = - \langle \Phi_0 | \hat{V} | \Phi_0 \rangle \langle \Phi_0 | \hat{V} \hat{R}_0^2 \hat{V} \hat{R}_0 \hat{V} | \Phi_0 \rangle \quad (5.53)$$

$$\langle \Phi_0 | \hat{V} \hat{R}_0 \hat{V} \hat{R}_0 \langle \hat{V} \rangle \hat{R}_0 \hat{V} | \Phi_0 \rangle = - \langle \Phi_0 | \hat{V} | \Phi_0 \rangle \langle \Phi_0 | \hat{V} \hat{R}_0 \hat{V} \hat{R}_0^2 \hat{V} | \Phi_0 \rangle \quad (5.54)$$

$$\langle \Phi_0 | \hat{V} \hat{R}_0 \langle \hat{V} \rangle \hat{R}_0 \langle \hat{V} \rangle \hat{R}_0 \hat{V} | \Phi_0 \rangle = \langle \Phi_0 | \hat{V} | \Phi_0 \rangle^2 \langle \Phi_0 | \hat{V} \hat{R}_0^3 \hat{V} | \Phi_0 \rangle \quad (5.55)$$

$$\langle \Phi_0 | \hat{V} \hat{R}_0 \langle \hat{V} \hat{R}_0 \hat{V} \rangle \hat{R}_0 \hat{V} | \Phi_0 \rangle = - \langle \Phi_0 | \hat{V} \hat{R}_0 \hat{V} | \Phi_0 \rangle \langle \Phi_0 | \hat{V} \hat{R}_0^2 \hat{V} | \Phi_0 \rangle. \quad (5.56)$$

For higher order energies, we would see brackets within brackets, leading to an increasing growth rate in the number of terms.

We will end our discussion of many-body perturbation theory presently. In closing, one should take notice of the special form the second term in $E^{(3)}$ (Equation 5.50) takes. These kinds of terms, called *unlinked* terms, becomes more and more prevalent as the series expansion continues. This is apparent from the fourth-order energy term derived from the bracketing technique above. A very powerful theorem called the *linked-diagram theorem*, derived by Goldstone [22], states that the energy and the wavefunctions can be expressed as a sum of *linked* terms only (!), because all the unlinked diagrams in a Rayleigh-Schrödinger perturbation series cancels against the renormalisation terms¹. Proving the linked-diagram theorem requires a herculean effort, and we will refrain from doing so. The entirety of chapter 6 in Shavitt & Bartlett [20] is devoted to a proof of the linked-diagram theorem. What we will take with us is that the linked-diagram theorem forms the foundation for the coupled cluster “ansatz” wavefunction, which we will introduce at the very beginning of the next chapter.

¹Additional sums in the wavefunction expression involving lower-order energies in RSPT, see Equation 5.49

Chapter 6

Coupled Cluster

In the late 1950s Fritz Coester constructed a rigorous formal solution of the bound state Schrödinger equation as a set of single particle wave functions [23]. He wanted to find an expression for the wave operator Ω , which transforms a zero-order wavefunction to the exact wave function,

$$\Psi = \Omega \Phi_0. \quad (6.1)$$

From Coester's solutions it would become apparent that the Rayleigh-Schrödinger perturbation expansions of the energy does not contain matrix elements representing the products of so-called unlinked diagram. In other words, one form of Ω is given a "linked-diagram expansion",

$$\Omega |\Phi_0\rangle = |\Phi_0\rangle = \sum_{k=1}^{\infty} \left((\hat{R}_0 \hat{V})^k |\Phi_0\rangle \right)_L. \quad (6.2)$$

This is further underlined in discussions by Hubbard [59] and Hugenholtz [60].

Conveniently, Ω may be written quite generally as

$$\Omega = e^{\hat{T}}, \quad \Psi = e^{\hat{T}} \Phi_0. \quad (6.3)$$

This exponential form is known as the Coupled Cluster ansatz, even though it is much more than a simple guess for the form of the exact wavefunction. To underline this point we quote Herman Kümmel: "Strange as it may be, in spite of the many successes of the coupled cluster method there is still a widespread belief that the underlying exponential structure is something artificial, accidental or an approximation only. This is why I want to make it clear that this feature is extremely natural - even necessary - on a very fundamental level, not necessarily connected with many-body theory" [61].

Throughout the 1950s and early 1960s, Coester and Kümmel developed the coupled cluster method together and proposed using the exponential-form wave operator as a relation between the shell-model state and the correct state vector for nuclear matter [24]. At the time, the method proved to be too computationally intensive. Specifically, the hard core potentials of nuclear physics leave no freedom in truncating the set of coupled cluster equations. However, the method was picked up by Jiří Čížek who in 1966 reformulated the method for studies of electron correlations in atoms and molecules

[62]. Further development by Josef Paldus made the coupled cluster method one of the most prevalent methods in quantum chemistry. Together with Isaiah Shavitt, Čížek and Paldus did the first *ab initio* computations with the method, which they called the coupled-pair many-electron-theory (MET) [63], as it can be interpreted as the perturbative variant of the many-electron-theory of Sinanoğlu [64]. See Löwdin [65] for a thorough historical development of the treatment of the electron correleation problem.

6.1 The Cluster Operator

Having established the form of the coupled cluster wavefunction as

$$|\Psi\rangle = e^{\hat{T}} |\Phi_0\rangle, \quad (6.4)$$

we now take a closer look at the cluster operator, which is divided into sub-operators

$$\hat{T} = \hat{T}_1 + \hat{T}_2 + \hat{T}_3 + \dots, \quad (6.5)$$

where the one-, two- and three-body operators are defined,

$$\hat{T}_1 = \sum_{ai} t_i^a \{ \hat{a}^\dagger \hat{i} \} \quad (6.6)$$

$$\hat{T}_2 = \frac{1}{(2!)^2} \sum_{ijab} t_{ij}^{ab} \{ \hat{a}^\dagger \hat{i} \hat{b}^\dagger \hat{j} \} \quad (6.7)$$

$$\hat{T}_3 = \frac{1}{(3!)^2} \sum_{ijkabc} \{ \hat{a}^\dagger \hat{i} \hat{b}^\dagger \hat{j} \hat{c}^\dagger \hat{k} \}, \quad (6.8)$$

where the coefficients $t_{ijk\dots}^{abc\dots}$ are commonly referred to as the coupled cluster *amplitudes*, and are coefficients to be determined. The strings of operators are automatically normal-ordered. The general m -body cluster operator is given by

$$\hat{T}_m = \frac{1}{(m!)^2} \sum_{ij\dots ab\dots} t_{ij\dots}^{ab\dots} \{ \hat{a}^\dagger \hat{i} \hat{b}^\dagger \hat{j} \dots \}, \quad (6.9)$$

which produces an m -fold excitation. It is not necessary to include cluster-operators up to an infinite-fold excitation. Logically, the maximum excitation order is dictated by the number of electrons in the system n , such that $n \geq m$. Any higher-order excitation operator would eventually annihilate an unoccupied orbital, resulting in a zero-contribution. The prefactor $1/(m!)^2$ accounts for the redundancy created by unrestricted summations, as a permutation of any of the m hole or m particle indices will not produce a distinct contribution. Indeed, we have for example that

$$\hat{a}^\dagger \hat{i} \hat{b}^\dagger \hat{j} = -\hat{a}^\dagger \hat{j} \hat{b}^\dagger \hat{i} = -\hat{b}^\dagger \hat{i} \hat{a}^\dagger \hat{j} = \hat{b}^\dagger \hat{j} \hat{a}^\dagger \hat{i}, \quad (6.10)$$

and therefore we must also have that

$$t_{ij}^{ab} = -t_{ji}^{ab} = -t_{ij}^{ba} = t_{ji}^{ba}. \quad (6.11)$$

Hence, the $(2!)^2 = 4$ contributions of two hole indices, ab , and two particle indices, ij , will produce four equal terms, which is offset by the prefactor $1/4$.

The exponential wave operator $e^{\hat{T}}$ may be expanded as a Taylor series,

$$e^{\hat{T}} = 1 + \hat{T} + \frac{1}{2!}\hat{T}^2 + \frac{1}{3!}\hat{T}^3 + \dots \quad (6.12)$$

By including only single- and double excitations, $\hat{T}_{\text{CCSD}} = \hat{T}_1 + \hat{T}_2$, this expression becomes

$$e^{\hat{T}_{\text{CCSD}}} = 1 + \hat{T}_1 + \hat{T}_2 + \frac{1}{2}\hat{T}_1^2 + \hat{T}_1\hat{T}_2 + \frac{1}{2}\hat{T}_2^2 + \frac{1}{3!}\hat{T}_1^3 + \frac{1}{2}\hat{T}_1^2\hat{T}_2 + \frac{1}{2}\hat{T}_1\hat{T}_2^2 + \frac{1}{3!}\hat{T}_2^3 + \dots \quad (6.13)$$

Contributions to the wave function containing only a single cluster operator, \hat{T}_m , are called connected cluster contributions, while those containing products of cluster operators, $\hat{T}_{m_1}^\alpha \hat{T}_{m_2}^\beta$, are called disconnected cluster contributions.

This inclusion of only single- and double excitations is called “Coupled Cluster Singles Doubles”, elucidating the subscript CCSD [66]. The most common approximation in coupled cluster theory is the CCSD model. Here, the operator \hat{T}_2 describes the important electron-pair interaction and the \hat{T}_1 operator carries out the orbital relaxations induced by the field set up by electron-pair interactions.

Importance of different parts of the cluster operator

The most important contribution to the wave-function in quantum chemistry is undoubtedly \hat{T}_2 , because of the two-electron nature of the Hamiltonian. It describes the most important interaction of quantum chemistry, the electron-pair interaction. The inclusion of \hat{T}_1 and its products are relatively insensitive to the choice of basis set, as the operators $e^{\hat{T}_1}$ has the effect of transforming the reference state $|\Phi_0\rangle$ to another Slater determinant. This is known as Thouless theorem [67]. With very high electron-density, the three-particle operator \hat{T}_3 becomes important. Higher-order terms are usually of less and decreasing importance, but they can be of concern in special situations. For instance, the four-particle operator \hat{T}_4 is very important in nuclear physics. See for instance Helgaker *et al.* [16] or Shavitt & Bartlett [20] for further discussions on this topic.

6.2 Coupled-Cluster Doubles

As a good starting point for understanding the coupled cluster scheme and especially where the coupled-cluster equations come from, we now constrain the cluster operator to

$$\hat{T}_{\text{CCD}} = \hat{T}_2, \quad (6.14)$$

and derive the coupled cluster equations for this case. The CCD wave function includes all connected and disconnected clusters involving \hat{T}_2 only,

$$\Psi_{\text{CCD}} = e^{\hat{T}_2} = \Phi_0 + \hat{T}_2\Phi_0 + \frac{1}{2}\hat{T}_2^2\Phi_0 + \frac{1}{3!}\hat{T}_2^3\Phi_0 + \dots \quad (6.15)$$

There are several methods with which to arrive at the coupled-cluster equations. Here we will give an example derivation of how to derive the coupled cluster doubles equations, using the “algebraic method”, employing second quantisation and Wick’s theorem. As an alternative, in section B.3, we use the configuration-space technique and the Slater-Condon rules (section B.2). A third way is with the aid of diagrams, which is done in Shavitt and Bartlett [20], for instance. Instead of deriving coupled cluster equations by hand it is often convenient to do so with the aid of a symbolic calculator. For higher-order schemes we have used python’s SymPy library.

In this derivation we make great use of second quantisation formalism and Wick’s theorem. We start with the normal-ordered Hamiltonian,

$$\begin{aligned}\hat{H}_N &= \hat{F}_N + \hat{W}_N \\ &= \sum_{pq} f_{pq} \{\hat{p}^\dagger \hat{q}\} + \frac{1}{4} \sum_{pqrs} u_{rs}^{pq} \{\hat{p}^\dagger \hat{q}^\dagger \hat{s} \hat{r}\}.\end{aligned}\quad (6.16)$$

First we want to find an expression for the energy,

$$\Delta E_{\text{CCD}} = \langle 0 | \hat{H}_N (1 + \hat{T}^2) | 0 \rangle = \langle 0 | \hat{H}_N \hat{T}_2 | 0 \rangle, \quad (6.17)$$

where only the vacuum expectation value of the product of the Hamiltonian and the doubles cluster operators give contributions, because the vacuum expectation value of the Hamiltonian is zero. Inserting for the operators we get

$$\Delta E_{\text{CCD}} = \sum_{\substack{i>j \\ a>b}} \langle 0 | \left[\sum_{pq} f_{pq} \{\hat{p}^\dagger \hat{q}\} + \frac{1}{4} \sum_{pqrs} u_{rs}^{pq} \{\hat{p}^\dagger \hat{q}^\dagger \hat{s} \hat{r}\} \right] \{\hat{a}^\dagger \hat{b}^\dagger \hat{j} \hat{i}\} | 0 \rangle t_{ij}^{ab}. \quad (6.18)$$

Here the one-particle part will vanish as there are no ways one can contract all the operators in this term without using an internal contraction in the normal-ordered product. It is also useful to convert the first sum to an unrestricted sum,

$$\Delta E_{\text{CCD}} = \frac{1}{16} \sum_{ijab} \sum_{pqrs} u_{rs}^{pq} \langle 0 | \{\hat{p}^\dagger \hat{q}^\dagger \hat{s} \hat{r}\} \{\hat{a}^\dagger \hat{b}^\dagger \hat{j} \hat{i}\} | 0 \rangle t_{ij}^{ab}. \quad (6.19)$$

We contract the operators in the normal-ordered products using Wick’s theorem,

$$\begin{aligned}&\langle 0 | \{\hat{p}^\dagger \hat{q}^\dagger \hat{s} \hat{r}\} \{\hat{a}^\dagger \hat{b}^\dagger \hat{j} \hat{i}\} + \{\hat{p}^\dagger \hat{q}^\dagger \hat{s} \hat{r}\} \{\hat{a}^\dagger \hat{b}^\dagger \hat{j} \hat{i}\} \\ &+ \{\hat{p}^\dagger \hat{q}^\dagger \hat{s} \hat{r}\} \{\hat{a}^\dagger \hat{b}^\dagger \hat{j} \hat{i}\} + \{\hat{p}^\dagger \hat{q}^\dagger \hat{s} \hat{r}\} \{\hat{a}^\dagger \hat{b}^\dagger \hat{j} \hat{i}\} | 0 \rangle\end{aligned}\quad (6.20)$$

$$\begin{aligned}&= \delta_{pi} \delta_{qj} \delta_{sb} \delta_{ra} - \delta_{pi} \delta_{qj} \delta_{sa} \delta_{rb} \\ &- \delta_{pj} \delta_{qi} \delta_{sb} \delta_{ra} + \delta_{pj} \delta_{qi} \delta_{sa} \delta_{rn}.\end{aligned}\quad (6.21)$$

All these products of delta functions give us a reduction in the sums and the CCD energy becomes,

$$\Delta E_{\text{CCD}} = \frac{1}{4} \sum_{ijab} u_{ab}^{ij} t_{ij}^{ab}. \quad (6.22)$$

The natural next step is to find the amplitude equations,

$$\langle \Phi_{ij}^{ab} | \hat{H}_N \left(1 + \hat{T}_2 + \frac{1}{2} \hat{T}^2 \right) | 0 \rangle = \Delta E_{CCCD} t_{ij}^{ab}. \quad (6.23)$$

We compute this expression in steps, starting with the lone normal-ordred Hamiltonian,

$$\langle \Phi_{ij}^{ab} | \hat{H}_N | 0 \rangle = \frac{1}{4} \sum_{pqrs} \langle 0 | \{ \hat{a} \hat{b} \hat{j}^\dagger \hat{i}^\dagger \} \{ \hat{p}^\dagger \hat{q}^\dagger \hat{s} \hat{r} \} | 0 \rangle u_{rs}^{pq}, \quad (6.24)$$

here we also have to compute a few contractions. Using Wick's theorem we obtain,

$$\langle 0 | \{ \hat{i}^\dagger \hat{j}^\dagger \hat{b} \hat{a} \} \{ \hat{p}^\dagger \hat{q}^\dagger \hat{s} \hat{r} \} + \{ \hat{i}^\dagger \hat{j}^\dagger \hat{b} \hat{a} \} \{ \hat{p}^\dagger \hat{q}^\dagger \hat{s} \hat{r} \} \quad (6.25)$$

$$+ \{ \hat{i}^\dagger \hat{j}^\dagger \hat{b} \hat{a} \} \{ \hat{p}^\dagger \hat{q}^\dagger \hat{s} \hat{r} \} + \{ \hat{i}^\dagger \hat{j}^\dagger \hat{b} \hat{a} \} \{ \hat{p}^\dagger \hat{q}^\dagger \hat{s} \hat{r} \} | 0 \rangle \\ = \delta_{ir} \delta_{js} \delta_{bq} \delta_{ap} - \delta_{ir} \delta_{js} \delta_{bp} \delta_{aq} \\ - \delta_{is} \delta_{jr} \delta_{bq} \delta_{ap} + \delta_{is} \delta_{jr} \delta_{bp} \delta_{aq}. \quad (6.26)$$

This will leave us with a similar expression as the one in the energy equation,

$$\langle \Phi_{ij}^{ab} | \hat{H}_N | 0 \rangle = u_{ij}^{ab}. \quad (6.27)$$

Now for the linear terms,

$$\begin{aligned} \langle \phi_{ij}^{ab} | \hat{H}_N \hat{T}_2 | 0 \rangle &= \sum_{\substack{k>l \\ c>d}} \langle \Phi_{ij}^{an} | \hat{H}_N \{ \hat{c}^\dagger \hat{d}^\dagger \hat{l} \hat{k} \} | 0 \rangle t_{kl}^{cd} \\ &= \frac{1}{4} \sum_{klcd} \left\langle \Phi_{ij}^{ab} \right| \hat{F}_N + \hat{W}_N \left| \Phi_{kl}^{cd} \right\rangle t_{kl}^{cd}. \end{aligned} \quad (6.28)$$

Starting with the first term we obtain,

$$\begin{aligned} L_1 &= \frac{1}{4} \sum_{klcd} \left\langle \Phi_{ij}^{ab} \right| \hat{F}_N \left| \Phi_{kl}^{cd} \right\rangle t_{kl}^{cd} \\ &= \frac{1}{4} \sum_{klcd} \sum_{pq} f_{pq} \left\langle \Phi_{ij}^{ab} \right| \{ \hat{p}^\dagger \hat{q} \} \left| \Phi_{kl}^{cd} \right\rangle t_{kl}^{cd} \\ &= \frac{1}{4} \sum_{klcd} \sum_{pq} f_{pq} \langle 0 | \{ \hat{i}^\dagger \hat{j}^\dagger \hat{b} \hat{a} \} \{ \hat{p}^\dagger \hat{q} \} \{ \hat{c}^\dagger \hat{d}^\dagger \hat{l} \hat{k} \} | 0 \rangle t_{kl}^{cd}. \end{aligned} \quad (6.29)$$

The product of normal-ordered operators must be contracted in such a way that three and three operators in the first and last operator strings are contracted with one another, and the two operators in the middle string are contracted with one operator in the last and first operator string. This provides us with a total of $4 \times 4 = 16$ possible contractions. Here are the first four contractions,

$$\begin{aligned} &\{ \hat{i}^\dagger \hat{j}^\dagger \hat{b} \hat{a} \} \{ \hat{p}^\dagger \hat{q} \} \{ \hat{c}^\dagger \hat{d}^\dagger \hat{l} \hat{k} \} + \{ \hat{i}^\dagger \hat{j}^\dagger \hat{b} \hat{a} \} \{ \hat{p}^\dagger \hat{q} \} \{ \hat{c}^\dagger \hat{d}^\dagger \hat{l} \hat{k} \} \\ &+ \{ \hat{i}^\dagger \hat{j}^\dagger \hat{b} \hat{a} \} \{ \hat{p}^\dagger \hat{q} \} \{ \hat{c}^\dagger \hat{d}^\dagger \hat{l} \hat{k} \} + \{ \hat{i}^\dagger \hat{j}^\dagger \hat{b} \hat{a} \} \{ \hat{p}^\dagger \hat{q} \} \{ \hat{c}^\dagger \hat{d}^\dagger \hat{l} \hat{k} \} \end{aligned} \quad (6.30)$$

$$= \delta_{ik}\delta_{jl}\delta_{bd}\delta_{ap}\delta_{cq} + \delta_{ik}\delta_{jl}\delta_{ac}\delta_{bp}\delta_{dq} \\ - \delta_{ik}\delta_{jq}\delta_{bd}\delta_{ac}\delta_{pl} - \delta_{iq}\delta_{pk}\delta_{jl}\delta_{bd}\delta_{ac}. \quad (6.31)$$

The last twelve contractions will be equivalent to these four, and thus we get rid of the $\frac{1}{4}$ -prefactor from Equation 6.29, yielding

$$L_1 = \sum_c (f_{bc}t_{ij}^{ac} - f_{ac}t_{ij}^{bc}) + \sum_k (f_{ik}t_{jk}^{ab} - f_{jk}t_{ik}^{ab}). \quad (6.32)$$

Proceeding to the second linear term,

$$\begin{aligned} L_2 &= \frac{1}{4} \sum_{klcd} \langle \Phi_{ij}^{ab} | \hat{u} | \Phi_{kl}^{cd} \rangle t_{kl}^{cd} \\ &= \frac{1}{16} \sum_{pqrs} \sum_{klcd} u_{rs}^{pq} \langle 0 | \{\hat{j}^\dagger \hat{b}^\dagger \hat{a}\} \{\hat{p}^\dagger \hat{q}^\dagger \hat{s} \hat{r}\} \{\hat{c}^\dagger \hat{d}^\dagger \hat{k} \hat{l}\} | 0 \rangle t_{kl}^{cd} \end{aligned} \quad (6.33)$$

Here there are many possible ways to contract the operator strings. Then it is convenient to label the different kinds of contractions. We divide the types of contractions into three groups, for which we choose the labels a , b and c . The a -terms consist of two hole-hole contractions, the b -terms consist of two particle-particle contractions and the c -terms consist of one particle-hole contraction and one hole-particle contraction,

$$\begin{aligned} L_{2a} &= \frac{1}{8} \sum_{pqrs} \sum_{klcd} u_{rs}^{pq} \langle 0 | \{\hat{i}^\dagger \hat{j}^\dagger \hat{b} \hat{a}\} \{\hat{p}^\dagger \hat{q}^\dagger \hat{s} \hat{r}\} \{\hat{c}^\dagger \hat{d}^\dagger \hat{k} \hat{l}\} | 0 \rangle t_{kl}^{cd} \\ &= \frac{1}{8} \sum_{pqrs} \sum_{cd} u_{rs}^{pq} \langle 0 | \{\hat{b} \hat{a}\} \{\hat{p}^\dagger \hat{q}^\dagger \hat{s} \hat{r}\} \{\hat{c}^\dagger \hat{d}^\dagger\} | 0 \rangle t_{kl}^{cd} \end{aligned} \quad (6.34)$$

$$\begin{aligned} L_{2b} &= \frac{1}{8} \sum_{pqrs} \sum_{klcd} u_{rs}^{pq} \langle 0 | \{\hat{i}^\dagger \hat{j}^\dagger \hat{b} \hat{a}\} \{\hat{p}^\dagger \hat{q}^\dagger \hat{s} \hat{r}\} \{\hat{c}^\dagger \hat{d}^\dagger \hat{l} \hat{k}\} | 0 \rangle t_{kl}^{cd} \\ &= \frac{1}{8} \sum_{pqrs} \sum_{kl} u_{rs}^{pq} \langle 0 | \{\hat{i}^\dagger \hat{j}^\dagger\} \{\hat{p}^\dagger \hat{q}^\dagger \hat{s} \hat{r}\} \{\hat{l} \hat{k}\} | 0 \rangle t_{kl}^{cd} \end{aligned} \quad (6.35)$$

$$\begin{aligned} L_{2c} &= \frac{1}{4} \sum_{pqrs} \sum_{klcd} u_{rs}^{pq} \langle 0 | \{\hat{i}^\dagger \hat{j}^\dagger \hat{b} \hat{a}\} \{\hat{p}^\dagger \hat{q}^\dagger \hat{s} \hat{r}\} \{\hat{c}^\dagger \hat{d}^\dagger \hat{l} \hat{k}\} \\ &\quad + \{\hat{i}^\dagger \hat{j}^\dagger \hat{b} \hat{a}\} \{\hat{p}^\dagger \hat{q}^\dagger \hat{s} \hat{r}\} \{\hat{c}^\dagger \hat{d}^\dagger \hat{l} \hat{k}\} \\ &\quad + \{\hat{i}^\dagger \hat{j}^\dagger \hat{b} \hat{a}\} \{\hat{p}^\dagger \hat{q}^\dagger \hat{s} \hat{r}\} \{\hat{c}^\dagger \hat{d}^\dagger \hat{l} \hat{k}\} \\ &\quad + \{\hat{i}^\dagger \hat{j}^\dagger \hat{b} \hat{a}\} \{\hat{p}^\dagger \hat{q}^\dagger \hat{s} \hat{r}\} \{\hat{c}^\dagger \hat{d}^\dagger \hat{l} \hat{k}\} | 0 \rangle t_{kl}^{cd} \end{aligned} \quad (6.36)$$

$$\begin{aligned} &= \frac{1}{4} \sum_{pqrs} \sum_{kc} u_{rs}^{pq} \langle 0 | \{\hat{i}^\dagger \hat{a}\} \{\hat{p}^\dagger \hat{q}^\dagger \hat{s} \hat{r}\} \{\hat{c}^\dagger \hat{k}\} \\ &\quad - \{\hat{j}^\dagger \hat{a}\} \{\hat{p}^\dagger \hat{q}^\dagger \hat{s} \hat{r}\} \{\hat{c}^\dagger \hat{k}\} \\ &\quad - \{\hat{i}^\dagger \hat{b}\} \{\hat{p}^\dagger \hat{q}^\dagger \hat{s} \hat{r}\} \{\hat{c}^\dagger \hat{k}\} \\ &\quad + \{\hat{j}^\dagger \hat{b}\} \{\hat{p}^\dagger \hat{q}^\dagger \hat{s} \hat{r}\} \{\hat{c}^\dagger \hat{k}\} | 0 \rangle. \end{aligned}$$

The vacuum expectation value in L_{2a} can be evaluated as,

$$\begin{aligned} & \langle 0 | \{\hat{b}\hat{a}\} \{\hat{p}^\dagger \hat{q}^\dagger \hat{s}\hat{r}\} \{\hat{c}^\dagger \hat{d}^\dagger\} + \{\hat{b}\hat{a}\} \{\hat{p}^\dagger \hat{q}^\dagger \hat{s}\hat{r}\} \{\hat{c}^\dagger \hat{d}^\dagger\} \\ & + \{\hat{b}\hat{a}\} \{\hat{p}^\dagger \hat{q}^\dagger \hat{s}\hat{r}\} \{\hat{c}^\dagger \hat{d}^\dagger\} + \{\hat{b}\hat{a}\} \{\hat{p}^\dagger \hat{q}^\dagger \hat{s}\hat{r}\} \{\hat{c}^\dagger \hat{d}^\dagger\} | 0 \rangle \end{aligned} \quad (6.37)$$

$$\begin{aligned} & = -\delta_{bq}\delta_{ap}\delta_{sd}\delta_{rc} - \delta_{bq}\delta_{ap}\delta_{sc}\delta_{rd} \\ & - \delta_{aq}\delta_{bp}\delta_{sd}\delta_{rc} + \delta_{aq}\delta_{bp}\delta_{sc}\delta_{rd}. \end{aligned} \quad (6.38)$$

Inserting this result into the original expression and substituting similar indices yields,

$$L_{2a} = \frac{1}{2} \sum_{cd} u_{cd}^{ab} t_{ij}^{cd}. \quad (6.39)$$

A very similar computation yields the following result for the next linear term,

$$L_{2b} = \frac{1}{2} \sum_{kl} u_{ij}^{kl} t_{kl}^{ab}. \quad (6.40)$$

The last linear term is somewhat different, however,

$$L_{2c} = - \sum_k c \left(u_{cj}^{bk} t_{ik}^{ac} - u_{ci}^{bk} t_{jk}^{ac} - u_{cj}^{ak} t_{ik}^{bc} + u_{ci}^{ak} t_{jk}^{bc} \right) \quad (6.41)$$

Finally, we have only the quadratic term to deal with,

$$Q = \frac{1}{8} \sum_{pqrs} \sum_{\substack{k>l \\ c>d}} \sum_{\substack{m>n \\ e>f}} u_{rs}^{pq} \langle 0 | \{\hat{i}^\dagger \hat{j}^\dagger \hat{b}\hat{a}\} \{\hat{p}^\dagger \hat{q}^\dagger \hat{s}\hat{r}\} \{\hat{c}^\dagger \hat{d}^\dagger \hat{l}\hat{k}\} \{\hat{e}^\dagger \hat{f}^\dagger \hat{n}\hat{m}\} | 0 \rangle t_{kl}^{dc} t_{mn}^{ef}. \quad (6.42)$$

In this expression there are no non-zero contractions between the third and fourth normal-ordered operator string. We therefore need to contract operators in the first normal-ordered string with operators either in the third or four string, and the operator in the second string with the rest.

We start by contracting all operators in the first normal-ordered string with all the operators in the fourth normal-ordered string,

$$\begin{aligned} & \frac{1}{8} \sum_{pqrs} \sum_{\substack{k>l \\ c>d}} \sum_{\substack{m>n \\ e>f}} u_{rs}^{pq} \langle 0 | \{\hat{i}^\dagger \hat{j}^\dagger \hat{b}\hat{a}\} \{\hat{p}^\dagger \hat{q}^\dagger \hat{s}\hat{r}\} \{\hat{c}^\dagger \hat{d}^\dagger \hat{l}\hat{k}\} \{\hat{e}^\dagger \hat{f}^\dagger \hat{n}\hat{m}\} | 0 \rangle t_{kl}^{cd} t_{mn}^{ef} \\ & = \frac{1}{8} \sum_{pqrs} \sum_{\substack{k>l \\ c>d}} u_{rs}^{pq} \langle 0 | \{\hat{p}^\dagger \hat{q}^\dagger \hat{s}\hat{r}\} \{\hat{c}^\dagger \hat{d}^\dagger \hat{l}\hat{k}\} | 0 \rangle t_{kl}^{cd} t_{ij}^{ab}. \end{aligned} \quad (6.43)$$

There are four possible ways to contract this last term, resulting in

$$\frac{1}{2} \sum_{\substack{k>l \\ c>d}} u_{cd}^{kl} t_{kl}^{cd} t_{ij}^{ab}. \quad (6.44)$$

We get the same result by contracting the four operators in the first string with the four operators in the third string, cancelling the factor $\frac{1}{2}$, eventually yielding a result equal to $\Delta E_{CCD} t_{ij}^{ab}$.

There are four reasonable groups into which to sort the permutations of contractions that remain in Equation 6.42.

- a the two hole operators in the first string are contracted with either the third or fourth operator string. The remaining two particle operators are contracted with the fourth or third operator string, respectively;
- b one hole operator and one particle operator in the first string are contracted with operators in the third or fourth string, the remaining two operators in the first string are contracted with operators in the fourth or third string, respectively;
- c two particle operators and one hole operator from the first string are contracted with operators in the third string, the last hole operator is contracted with an operator in the fourth string, or vice versa;
- d one particle operator and two hole operators are contracted with operators in the third string and the last particle operator with an operator in the fourth string, or vice versa.

The results for group *a* are arguably the least complicated to compute, there are two types of contractions that yield the same result, cancelling a factor $\frac{1}{2}$. Making the sums unrestricted then adds a factor $\frac{1}{4}$,

$$\begin{aligned} Q_a &= \frac{1}{16} \sum_{pqrs} \sum_{klcd} u_{rs}^{pq} \langle 0 | \{ \hat{p}^\dagger \hat{q}^\dagger \hat{s} \hat{r} \} \{ \hat{l} \hat{k} \} \{ \hat{c}^\dagger \hat{d}^\dagger \} | 0 \rangle t_{ij}^{cd} t_{kl}^{ab} \\ &= \frac{1}{4} \sum_{klcd} u_{rs}^{kl} t_{ij}^{cd} t_{kl}^{ab}. \end{aligned} \quad (6.45)$$

For group *b* we have many more possible contractions. There are four ways to contract \hat{i} and \hat{a} with operators in the third string, and four ways to contract \hat{j} and \hat{b} with operators in the fourth string, for a total of 16 possible contractions. These contractions can be exchanged in four possible ways leading to a total of 64 choices. The final result becomes,

$$\begin{aligned} Q_b &= \frac{1}{4} \sum_{pqrs} \sum_{klcd} u_{rs}^{pq} \langle 0 | \{ \hat{p}^\dagger \hat{q}^\dagger \hat{s} \hat{r} \} \{ \hat{c}^\dagger \hat{k} \} \{ \hat{d}^\dagger \hat{l} \} | 0 \rangle (t_{ik}^{ac} t_{jl}^{bd} - t_{ik}^{bc} t_{jl}^{ad}) \\ &= \sum_{klcd} u_{cd}^{kl} (t_{ik}^{ac} t_{jl}^{bd} - t_{ik}^{bc} t_{jl}^{ad}) = \sum_{klcd} u_{cd}^{kl} (t_{ik}^{ac} t_{jl}^{bd} - t_{ik}^{bd} t_{jl}^{ac}) \end{aligned} \quad (6.46)$$

The sets of terms for group *c* and group *d* can each be generated in two distinct ways, dependent on the choice of the tree operators from the first operator string ($\hat{i}^\dagger \hat{a} \hat{b}$ or $\hat{j}^\dagger \hat{a} \hat{b}$ for *c* and $\hat{i}^\dagger \hat{j}^\dagger \hat{a}$ or $\hat{i}^\dagger \hat{j}^\dagger \hat{b}$ for *d*). In each case there are 16 possibilities; the three operators from the first string can be contracted with operators in both the third or fourth string in four ways and the remaining operators can then be contracted in two

ways. All these possibilities lead to equivalent results. For example, here is the first Q_c term,

$$\begin{aligned} & \frac{1}{8} \sum_{pqrs} \sum_{klcd} \sum_{mnef} u_{rs}^{pq} \langle 0 | \{\hat{i}^\dagger \hat{j}^\dagger \hat{b} \hat{a}\} \{\hat{c}^\dagger \hat{d}^\dagger \hat{l} \hat{k}\} \{\hat{c}^\dagger \hat{d}^\dagger \hat{l} \hat{k}\} \{\hat{e}^\dagger \hat{f}^\dagger \hat{n} \hat{m}\} | 0 \rangle t_{kl}^{cd} t_{mn}^{ef} \\ &= -\frac{1}{8} \sum_{pqrs} \sum_{klcd} u_{rs}^{pq} \langle 0 | \{\hat{p}^\dagger \hat{q}^\dagger \hat{s} \hat{r}\} \{\hat{c}^\dagger \hat{d}^\dagger \hat{k}\} \{\hat{l}\} | 0 \rangle t_{kj}^{cd} t_{li}^{ab} | 0 \rangle \end{aligned} \quad (6.47)$$

The remaining operators in this expression can be contracted in four ways,

$$\langle 0 | \{\hat{p}^\dagger \hat{q}^\dagger \hat{s} \hat{r}\} \{\hat{c}^\dagger \hat{d}^\dagger \hat{k}\} \{\hat{l}\} + \{\hat{p}^\dagger \hat{q}^\dagger \hat{s} \hat{r}\} \{\hat{c}^\dagger \hat{d}^\dagger \hat{k}\} \{\hat{l}\} \quad (6.48)$$

$$+ \{\hat{p}^\dagger \hat{q}^\dagger \hat{s} \hat{r}\} \{\hat{c}^\dagger \hat{d}^\dagger \hat{k}\} \{\hat{l}\} + \{\hat{p}^\dagger \hat{q}^\dagger \hat{s} \hat{r}\} \{\hat{c}^\dagger \hat{d}^\dagger \hat{k}\} \{\hat{l}\} | 0 \rangle \quad (6.49)$$

$$= \delta_{pl} \delta_{qk} \delta_{rd} \delta_{sc} - \delta_{pk} \delta_{ql} \delta_{rd} \delta_{sc} - \delta_{pl} \delta_{qk} \delta_{rc} \delta_{sd} + \delta_{pk} \delta_{ql} \delta_{rc} \delta_{sd}$$

Some algebraic exertion will eventually lead to,

$$-\frac{1}{2} \sum_{klcd} u_{cd}^{kl} t_{ik}^{ab} t_{jl}^{cd}. \quad (6.50)$$

A similar computation provides the second Q_c term,

$$-\frac{1}{2} \sum_{klcd} u_{cd}^{kl} t_{ik}^{cd} t_{jl}^{ab}. \quad (6.51)$$

These two terms give us,

$$Q_c = -\frac{1}{2} \sum_{klcd} u_{cd}^{kl} (t_{ik}^{ab} t_{jl}^{cd} - t_{ik}^{cd} t_{jl}^{ab}) \quad (6.52)$$

Treating the group d terms gives,

$$Q_d = \frac{1}{2} \sum_{klcd} u_{cd}^{kl} (t_{ij}^{ac} t_{kl}^{bd} - t_{ij}^{bd} t_{kl}^{ac}). \quad (6.53)$$

Collecting all terms yields the complete Coupled Cluster Doubles (CCD) amplitude equation,

$$\begin{aligned} & u_{ij}^{ab} + f_c^b t_{ij}^{ac} P(ab) - f_j^k t_{ik}^{ab} P(ij) + \frac{1}{4} t_{ij}^{cd} t_{mn}^{ab} u_{cd}^{mn} + \frac{1}{2} t_{ij}^{cd} u_{cd}^{ab} \\ &+ \frac{1}{2} t_{jm}^{cd} t_{in}^{ab} u_{cd}^{mn} P(ij) - \frac{1}{2} t_{nm}^{ac} t_{ij}^{bd} u_{cd}^{mn} P(ab) + t_{im}^{ac} t_{jn}^{bd} u_{cd}^{mn} P(ij) \\ &+ t_{im}^{ac} u_{jc}^{bm} P(ab) P(ij) + \frac{1}{2} t_{mn}^{ab} u_{ij}^{mn} = 0, \end{aligned} \quad (6.54)$$

where we have introduced exchange operators $P(ab)$ and $P(ij)$ which interchanges two particles with indices a, b and i, j , respectively. Here we have also removed the summation signs for simplicity, and taken advantage of the Einstein notation [68], where summation over equal indices is implied.

6.3 The Coupled Cluster Equations

In general there is a more useful and compact approach that can be used to derive the coupled cluster equations, compared to the lengthy derivation of the CCD equations above. We start by inserting the coupled cluster wavefunction into the time-independent Schrödinger equation,

$$\hat{H}_N e^{\hat{T}} |\Phi_0\rangle = \Delta E e^{\hat{T}} |\Phi_0\rangle. \quad (6.55)$$

In order to find an expression for the energy and amplitude equations one could try to left-project with $\langle\Phi_0|$. This would propel us in the same direction as in the previous section. Instead, we multiply from the left with $e^{-\hat{T}}$ first, and then left-project with $\langle\Phi_0|$,

$$\begin{aligned} \langle\Phi_0| e^{-\hat{T}} \hat{H}_N e^{\hat{T}} |\Phi_0\rangle &= \langle\Phi_0| e^{-\hat{T}} \Delta E e^{\hat{T}} |\Phi_0\rangle \\ &\rightarrow \langle\Phi_0| e^{-\hat{T}} \hat{H}_N e^{\hat{T}} |\Phi_0\rangle = \Delta E. \end{aligned} \quad (6.56)$$

Left-projecting with an excited state, $\langle\Phi_{ij\dots}^{ab\dots}|$ will give us an expression for the corresponding amplitude $t_{ij\dots}^{ab\dots}$,

$$\langle\Phi_{ij\dots}^{ab\dots}| e^{-\hat{T}} \hat{H}_N e^{\hat{T}} |\Phi_0\rangle = 0. \quad (6.57)$$

Now we have obtained a *non-Hermitian*¹, similarity-transformed Hamiltonian,

$$\mathcal{H} = e^{-\hat{T}} \hat{H}_N e^{\hat{T}}, \quad (6.58)$$

which has $|\Phi_0\rangle$ as right eigenfunction and E as the corresponding eigenvalue. Importantly, a similarity-transformation will not change the eigenvalue spectrum of the operator. This holds for any operator or matrix, and is easy to show.

Consider some matrix A , and the matrix C which is a square, non-singular matrix of the same order as A . We say that the matrices A and $C^{-1}AC$ are *similar*, and $C^{-1}AC$ is the *similarity transformation* of A . If (λ, \mathbf{x}) is an eigenvalue-eigenvector pair of A , then $(\lambda, C^{-1}\mathbf{x})$ is the eigenvalue-eigenvector pair for $C^{-1}AC$,

$$(C^{-1}AC)C^{-1}\mathbf{x} = C^{-1}A\mathbf{x} = \lambda C^{-1}\mathbf{x}. \quad (6.59)$$

Thus, we have shown that the eigenvalue spectrum of an operator is unchanged by a similarity transformation.

A benefit of the similarity-transformed Hamiltonians that we will take advantage of, is that we can write the operators more explicitly by applying the Baker-Campbell-

¹We will show later that this non-Hermiticity is somewhat problematic.

Hausdorff expansion [69–71],

$$\begin{aligned}
e^{-\hat{B}} \hat{A} e^{\hat{B}} &= (1 - \hat{B} + \frac{1}{2}\hat{B}^2 - \frac{1}{3!} + \dots) \hat{A} (1 + \hat{B} + \frac{1}{2} + \frac{1}{3!}\hat{B}^3 + \dots) \\
&= \hat{A} + (\hat{A}\hat{B} - \hat{B}\hat{A}) + \frac{1}{2}(\hat{A}\hat{B}^2 + 2\hat{B}\hat{A}\hat{B} + \hat{B}^2\hat{A}) \\
&\quad + \frac{1}{3!}(\hat{A}\hat{B}^3 - 3\hat{B}\hat{A}\hat{B}^2 + 3\hat{B}^2\hat{A}\hat{B} - \hat{B}^3\hat{A}) + \dots \\
&= \hat{A} + [\hat{A}, \hat{B}] + \frac{1}{2}\{(\hat{A}\hat{B} - \hat{B}\hat{A})\hat{B} - \hat{B}(\hat{A}\hat{B} - \hat{B}\hat{A})\} \\
&\quad + \frac{1}{3!}\{[(\hat{A}\hat{B} - \hat{B}\hat{A})\hat{B} - \hat{B}(\hat{A}\hat{B} - \hat{B}\hat{A})]\hat{B} \\
&\quad - \hat{B}[(\hat{A}\hat{B} - \hat{B}\hat{A})\hat{B} - \hat{B}(\hat{A}\hat{B} - \hat{B}\hat{A})]\} + \dots \\
&= \hat{A} + [\hat{A}, \hat{B}] + \frac{1}{2}[[\hat{A}, \hat{B}], \hat{B}] + \frac{1}{3!}[[[\hat{A}, \hat{B}], \hat{B}], \hat{B}] + \dots
\end{aligned} \tag{6.60}$$

Applying the Baker-Campbell-Hausdorff expansion to the similarity-transformed Hamiltonians yields

$$\begin{aligned}
\mathcal{H} = e^{-\hat{T}} \hat{H}_N e^{\hat{T}} &= \hat{H}_N + [\hat{H}_N, \hat{T}] + \frac{1}{2}[[\hat{H}_N, \hat{T}], \hat{T}] + \frac{1}{3!}[[[\hat{H}_N, \hat{T}], \hat{T}], \hat{T}] \\
&\quad + \frac{1}{4!}[[[[\hat{H}_N, \hat{T}], \hat{T}], \hat{T}], \hat{T}].
\end{aligned} \tag{6.61}$$

Notice the absence of an “and so on”-operator (...) in this expression. The Baker-Campbell-Hausdorff expansion for the electronic Hamiltonian, containing at most two-particle interactions, will terminate with the four-fold commutator. We will show this presently.

By applying the generalised Wick’s theorem to the Baker-Campbell-Hausdorff expansion of the Hamiltonian in Equation 6.61, we will be confronted with a vast simplification. Applying the generalised Wick’s theorem to a commutator gives the following

$$[\hat{A}, \hat{B}] = \hat{A}\hat{B} - \hat{B}\hat{A} = \{\hat{A}\hat{B}\} + \overline{\{\hat{A}\hat{B}\}} - \{\hat{B}\hat{A}\} - \overline{\{\hat{B}\hat{A}\}}, \tag{6.62}$$

where \hat{A} and \hat{B} are normal-ordered operators, each with an even number of creation- and annihilation operators². In this expression $\{\}$ denotes a normal-ordering of the operators inside the braces and $\{\hat{A}\hat{B}\}$ represents a sum of all normal-ordered products of operators in which there are one or more contractions between creation or annihilation operators in \hat{A} and those in \hat{B} . We must also have that

$$\{\hat{A}\hat{B}\} = \{\hat{B}\hat{A}\}, \tag{6.63}$$

since the two operators both contain an even number of creation- and annihilation operators. This means that what remains of Equation 6.62 is simply

$$[\hat{A}, \hat{B}] = \{\hat{A}\hat{B}\} - \overline{\{\hat{A}\hat{B}\}}. \tag{6.64}$$

²It is not a coincidence that both the normal-ordered Hamiltonian \hat{H}_N and the cluster operator \hat{T} satisfy these conditions

The general m -fold cluster operator T_m contains some number of creation operators $\hat{a}^\dagger, \hat{b}^\dagger \dots$ and hole operators \hat{i}, \hat{j}, \dots , and the only possible non-zero contractions are $\hat{a}\hat{b}^\dagger = \delta_{ab}$ and $\hat{i}\hat{j}^\dagger = \delta_{ij}$. Moreover, since the different cluster operators commute, no nonzero contractions exist between different \hat{T}_m operators. Ergo, in the nested commutators from Equation 6.61, we only see surviving terms between the Hamiltonian \hat{H}_N and one or more of the cluster operators \hat{T}_m . This accounts for the natural truncation at the four-fold commutator. In fact, we can rewrite the Baker-Campbell-Hausdorff-expanded similarity-transformed Hamiltonian as

$$\mathcal{H} = e^{-\hat{T}} \hat{H}_N e^{\hat{T}} = \hat{H}_N + \hat{H}_N \overline{\hat{T}} + \frac{1}{2!} \hat{H}_N \overline{\hat{T}} \overline{\hat{T}} + \frac{1}{3!} \hat{H}_N \overline{\hat{T}} \overline{\hat{T}} \overline{\hat{T}} + \frac{1}{4!} \hat{H}_N \overline{\hat{T}} \overline{\hat{T}} \overline{\hat{T}} \overline{\hat{T}}, \quad (6.65)$$

where the notation combining a contraction line and a horizontal bar indicates a sum over all terms in which the Hamiltonian \hat{H}_N is connected by at least one contraction with each of the following cluster operators \hat{T} .

Disconnected clusters on the form $\hat{T}_m \hat{T}_n$, which can be found in the coupled cluster wavefunction are not present in the Baker-Campbell-Hausdorff expansion of the similarity-transformed Hamiltonian. This is true also for the coupled cluster amplitude equations, which may be written

$$\langle \Phi_0 | e^{-\hat{T}} \hat{H}_N e^{\hat{T}} | \Phi_0 \rangle = \langle \Phi_0 | \hat{H}_N e^{\hat{T}} | \Phi_0 \rangle_C = \Delta E \quad (6.66)$$

$$\langle \Phi_{ij\dots}^{ab\dots} | e^{-\hat{T}} \hat{H}_N e^{\hat{T}} | \Phi_0 \rangle = \langle \Phi_{ij\dots}^{ab\dots} | \hat{H}_N e^{\hat{T}} | \Phi_0 \rangle_C = 0, \quad (6.67)$$

where the inclusion of only connected terms is underlined.

The Coupled Cluster Singles Doubles (CCSD) equations take the form

$$\langle \Phi_0 | \hat{H}_N \left(\hat{T}_1 + \frac{1}{2} \hat{T}_1^2 + \hat{T}_2 \right) | \Phi_0 \rangle_C = \Delta E \quad (6.68)$$

$$\langle \Phi_i^a | \hat{H}_N \left(1 + \hat{T}_1 + \frac{1}{2} \hat{T}_1^2 + \frac{1}{3!} \hat{T}_1^3 + \hat{T}_1 \hat{T}_2 + \hat{T}_2 \right) | \Phi_0 \rangle_C = 0 \quad (6.69)$$

$$\langle \Phi_{ij}^{ab} | \hat{H}_N \left(1 + \hat{T}_1 + \frac{1}{2} \hat{T}_1^2 + \frac{1}{3!} \hat{T}_1^3 + \frac{1}{4!} \hat{T}_1^4 + \hat{T}_2 + \frac{1}{2} \hat{T}_2^2 + \hat{T}_1 \hat{T}_2 + \frac{1}{2} \hat{T}_1^2 \hat{T}_2 \right) | \Phi_0 \rangle_C = 0. \quad (6.70)$$

For Coupled Cluster Singles Doubles Triples (CCSDT), the energy expression is the same, while the amplitude equations take the form

$$\langle \Phi_i^a | \hat{H}_N \left(1 + \hat{T}_1 + \frac{1}{2} \hat{T}_1^2 + \frac{1}{3!} \hat{T}_1^3 + \hat{T}_1 \hat{T}_2 + \hat{T}_2 + \hat{T}_3 \right) | \Phi_0 \rangle_C = 0 \quad (6.71)$$

$$\begin{aligned} \langle \Phi_{ij}^{ab} | \hat{H}_N \left(1 + \hat{T}_1 + \frac{1}{2} \hat{T}_1^2 + \frac{1}{3!} \hat{T}_1^3 + \frac{1}{4!} \hat{T}_1^4 + \hat{T}_2 + \frac{1}{2} \hat{T}_2^2 + \hat{T}_1 \hat{T}_2 + \frac{1}{2} \hat{T}_1^2 \hat{T}_2 + \hat{T}_3 + \hat{T}_1 \hat{T}_3 \right) | \Phi_0 \rangle_C = 0 \end{aligned} \quad (6.72)$$

$$\begin{aligned} \langle \Phi_{ijk}^{abc} | \hat{H}_N \left(\hat{T}_2 + \hat{T}_3 + \frac{1}{2} \hat{T}_2^2 + \hat{T}_1 \hat{T}_2 + \hat{T}_2 \hat{T}_3 + \hat{T}_1 \hat{T}_3 + \frac{1}{2} \hat{T}_1 \hat{T}_2 + \frac{1}{2} \hat{T}_1 \hat{T}_2^2 + \frac{1}{2} \hat{T}_1^2 \hat{T}_3 + \frac{1}{3!} \hat{T}_1^3 \hat{T}_2 \right) | \Phi_0 \rangle_C = 0 \end{aligned} \quad (6.73)$$

The Coupled Cluster Singles Doubles (CCSD) amplitude equations, fully written out are provided in section B.4.

6.4 A Variational Formulation of Coupled Cluster

In the following section we follow the narrative of Kvaal [72] closely.

The Coupled Cluster method is very successful in computing energies, but computing other expectations values has been a problem. For instance we see that the way we compute the coupled cluster energy,

$$E_{\text{CC}} = \langle \Phi | e^{-\hat{T}} \hat{H} e^{\hat{T}} | \Phi \rangle, \quad (6.74)$$

is not the same as one would compute the energy of the system variationally,

$$\langle \hat{H} \rangle_{\text{var}} = \frac{\langle \Psi | \hat{H} | \Psi \rangle}{\langle \Psi | \Psi \rangle} = \frac{\langle \Phi | e^{\hat{T}^\dagger} \hat{H} e^{\hat{T}} | \Phi \rangle}{\langle \Phi | e^{\hat{T}^\dagger} e^{\hat{T}} | \Phi \rangle}. \quad (6.75)$$

Moreover, the similarity transformed operators are not Hermitian. This can be showed by inference

$$\hat{T}_1^\dagger = \left(\sum_{ia} t_i^a \hat{a}^\dagger \hat{i} \right)^\dagger \sum_{ia} (t_i^a)^* \hat{i}^\dagger \hat{a} \neq \hat{T}_1, \quad (6.76)$$

from which it follows that

$$(e^{-\hat{T}} \hat{H} e^{\hat{T}})^\dagger = (e^{\hat{T}})^\dagger \hat{H} (e^{-\hat{T}})^\dagger = e^{\hat{T}^\dagger} \hat{H} e^{-\hat{T}^\dagger} \neq e^{-\hat{T}} \hat{H} e^{\hat{T}}. \quad (6.77)$$

Variational computations as in Equation 6.75 have been attempted by Cizek [62] and Fink [73]. Regrettably, the coupled cluster exponential wavefunction is not a variationally optimal wavefunction, as it give rise to series expansions in the numerator and denominator in the expression for the variational expectation value. For a general operator \hat{O} , we have

$$\begin{aligned} \langle \hat{O} \rangle_{\text{var}} &= \frac{\langle \Psi | \hat{O} | \Psi \rangle}{\langle \Psi | \Psi \rangle} = \frac{\langle \Phi | e^{\hat{T}^\dagger} \hat{O} e^{\hat{T}} | \Phi \rangle}{\langle \Phi | e^{\hat{T}^\dagger} e^{\hat{T}} | \Phi \rangle} \\ &= \frac{\langle \Phi | [1 + \hat{T}^\dagger + \frac{1}{2!}(\hat{T}^\dagger)^2 + \frac{1}{3!}(\hat{T}^\dagger)^3 + \dots] \hat{O} [1 + \hat{T} + \frac{1}{2!}\hat{T}^2 + \frac{1}{3!}\hat{T}^3 + \dots] | \Phi \rangle}{\langle \Phi | [1 + \hat{T}^\dagger + \frac{1}{2!}(\hat{T}^\dagger)^2 + \frac{1}{3!}(\hat{T}^\dagger)^3 + \dots] [1 + \hat{T} + \frac{1}{2!}\hat{T}^2 + \frac{1}{3!}\hat{T}^3 + \dots] | \Phi \rangle}. \end{aligned} \quad (6.78)$$

In contrast with the expansions of the coupled cluster amplitude equations, which truncate naturally after products of four \hat{T} operators, the expansions for $e^{\hat{T}^\dagger}$ and $e^{\hat{T}}$ terminates only if the total excitation level represented by a product of \hat{T} operators exceeds the number of electrons in the wavefunctions. This means that the number of terms and the computational effort required to compute expectation values in this way are usually very high.

An idea is to simply use a similar expression to the coupled cluster energy expression

$$\langle O \rangle_{\text{Goldstone}} = \langle \Phi | e^{-\hat{T}} \hat{O} e^{\hat{T}} | \Phi \rangle. \quad (6.79)$$

The problem with this expression, as well as with Equation 6.78, is that none of them conform with the Hellmann-Feynman theorem and the problem remains, the coupled cluster energy is arrived at non-variationally, and is therefore non-stationary.

6.4.1 The Hellmann-Feynman Theorem

The Hellmann-Feynman[74] theorem relates the first order change the total energy with respect to a parameter to the first order change of the Hamiltonian with respect to the same parameters,

$$\frac{dE}{d\alpha} \Big|_{\alpha=0} = \frac{\partial}{\partial t} \langle \Psi_\alpha | \hat{H} | \Psi_\alpha \rangle, \quad (6.80)$$

where Ψ is the exact state, variationally determined from the Hamiltonian of the system, and $\Psi_\alpha = N(\Psi + \alpha\delta\Psi)$ is a variation of this state, implicitly dependent on the parameter α .

Proof of the Hellmann-Feynman theorem

Using the following conditions,

$$\hat{H}_\lambda |\psi_\lambda\rangle = E_\lambda |\psi_\lambda\rangle \quad (6.81)$$

$$\langle \psi_\lambda | \psi_\lambda \rangle = 1, \quad (6.82)$$

we prove

$$\frac{\partial E_\lambda}{\partial \lambda} = \langle \psi_\lambda | \frac{\partial \hat{H}}{\partial \lambda} | \psi_\lambda \rangle. \quad (6.83)$$

Now,

$$E_\lambda = \langle \psi_\lambda | \hat{H} | \psi_\lambda \rangle = \int \psi_\lambda \hat{H} \psi_\lambda^* dr \quad (6.84)$$

whence,

$$\begin{aligned} \frac{\partial E_\lambda}{\partial \lambda} &= \int \psi_\lambda \frac{\hat{H}}{\partial \lambda} \psi_\lambda^* dr + \int \frac{\psi_\lambda}{\partial \lambda} \hat{H} \psi_\lambda^* dr + \int \psi_\lambda \hat{H} \frac{\psi_\lambda^*}{\partial \lambda} dr \\ &= \int \psi_\lambda \frac{\hat{H}}{\partial \lambda} \psi_\lambda^* dr + E_\lambda \int \frac{\psi_\lambda}{\partial \lambda} \psi_\lambda^* dr + E_\lambda \int \psi_\lambda \frac{\psi_\lambda^*}{\partial \lambda} dr \\ &= \int \psi_\lambda \frac{\hat{H}}{\partial \lambda} \psi_\lambda^* dr + E_\lambda \frac{\partial}{\partial \lambda} \langle \psi_\lambda | \psi_\lambda \rangle = \langle \psi_\lambda | \frac{\partial \hat{H}}{\partial \lambda} | \psi_\lambda \rangle. \end{aligned} \quad (6.85)$$

By treating an observable of the system as a perturbation of the Hamiltonian,

$$\hat{H}'(\alpha) = \hat{H} + \alpha \hat{V},$$

the Hellman-Feynman theorem provides us with a way to evaluate the expected value of this observable if we have the exact wavefunction and energy,

$$\frac{dE}{d\alpha} \Big|_{\alpha=0} = \frac{\partial}{\partial \alpha} \langle \Psi_\alpha | \hat{H} + \alpha \hat{O} | \Psi_\alpha \rangle = \langle \hat{O} \rangle. \quad (6.86)$$

The problem with some computational techniques, like the coupled cluster method, is that the final energy is not variationally determined (non-stationary), and we cannot invoke the Hellmann-Feynman theorem to simplify computations of molecular properties. At first, it would appear that one would have to resort to a more cumbersome

computation, like the expansion of cluster operators above (Equation 6.78). But fortunately, there exists a way to reformulate the energy function of a non-variational wavefunction in such a way that the energy is stationary with respect to the variables of the new formulation.

Consider an energy that depends on two sets of parameters. The parameter α which describes a perturbation and the parameters λ which describe the wavefunction. The optimal energy $E(\alpha)$ is obtained by an optimised set of parameters λ^* , which are inserted into the energy function

$$E(\alpha) = E(\alpha, \lambda^*), \quad (6.87)$$

the values for α and λ^* are obtained as the solution to some set of equations

$$\mathbf{f}(\alpha, \lambda^*) = 0 \quad \forall \alpha, \quad (6.88)$$

For *variational* wavefunctions, this condition corresponds to the stationarity requirement,

$$\frac{\partial E_{\text{var}}(\alpha, \lambda)}{\partial \lambda} \Big|_{(\lambda=\lambda^*)} = 0 \quad \forall \alpha, \quad (6.89)$$

but not for *non-variational* wavefunctions. Writing out this derivative yields,

$$\frac{dE(\alpha)}{d\alpha} = \frac{dE(\alpha, \lambda)}{d\alpha} \Big|_{(\lambda=\lambda^*)} = \frac{\partial E(\alpha, \lambda)}{\partial \alpha} \Big|_{(\lambda=\lambda^*)} + \frac{\partial E(\alpha, \lambda)}{\partial \lambda} \Big|_{(\lambda=\lambda^*)} \cdot \frac{\partial \lambda}{\partial \alpha} \Big|_{(\lambda=\lambda^*)}. \quad (6.90)$$

For a variational wavefunction, the last term will vanish due to the stationarity condition in Equation 6.89. This would leave us with

$$\frac{dE_{\text{var}}(\alpha)}{d\alpha} = \frac{\partial E(\alpha, \lambda)}{\partial \alpha} \Big|_{(\lambda=\lambda^*)}, \quad (6.91)$$

i.e. that the total derivative corresponds to the partial derivative. This means that if the variational energy corresponds to an expectation value $E_{\text{var}}(\alpha, \lambda) = \langle \lambda | \hat{H}(\alpha) | \lambda \rangle$, and the perturbed system is described by the Hamiltonian $\hat{H}(\alpha) = \hat{H} + \alpha \hat{V}$, we recover the presumed expression

$$\frac{dE(\alpha, \lambda)}{d\alpha} \Big|_{(\alpha=0)}, \quad (6.92)$$

in accordance with first-order perturbation theory and the Hellmann-Feynmann theorem.

But if we look at nonvariational energies, Equation 6.90, will not simplify to just the partial derivative, since the stationarity condition does not hold. What we do is replace the now nonvariational function $E(\alpha, \lambda)$ by a new function $L(\alpha, \lambda, \bar{\lambda})$ with a stationary point $(\lambda^*, \bar{\lambda}^*)$ that satisfies the nonvariational condition Equation 6.88, and whose values at this point correspond to the optimal energy. Indeed, we apply Lagrange's method of undetermined multipliers, by regarding the energy $E(\alpha, \lambda)$ as an *unconstrained* optimisation problem, but subject to the constraints of the variational parameters λ , which satisfy Equation 4.17;

$$L(\alpha, \lambda, \bar{\lambda}) = E(\alpha, \lambda) + \bar{\lambda} \cdot \mathbf{f}(\alpha, \lambda). \quad (6.93)$$

A necessary condition for the optimum Lagrange multipliers $\bar{\lambda}^*$ to be unique is that the Jacobian of \mathbf{f} , $\mathcal{J} \equiv \partial \mathbf{f}(\alpha, \lambda) / \partial \lambda$ is non-singular and invertible.

6.4.2 The Lagrangian Formulation of Coupled Cluster

As we outlined in the previous section, the solution to making the coupled cluster theory into a variational theory is to find a set of equations which are zero for a set of parameters (Equation 6.88). These parameters should in turn provide the optimal energy by insertion into the expression for energy. Luckily, Helgaker and Jørgensen [32, 75] had the insight to realise that we are already given such a set of parameters and equations in the formulation of coupled cluster, namely the amplitudes and the amplitude equations respectively. The Hellmann-Feynman theorem will be baked into the very definition of such an expectation value functional,

$$\langle \hat{O} \rangle_{\text{H-F}} = \mathcal{L}_O(\alpha^*, \lambda^*, \bar{\lambda}^*) = E(\alpha^*, \lambda^*, \bar{\lambda}^*) + \bar{\lambda}^* \cdot \mathbf{f}(\alpha^*, \lambda^*). \quad (6.94)$$

This equation is essentially a restatement of Equation 6.93, with the optimal parameters.

More specifically, we simplify the notation in some measure and state the coupled cluster energy Lagrangian,

$$\mathcal{L}_{\hat{H}}(t, \lambda) = \langle \Phi | e^{-\hat{T}} \hat{H} e^{\hat{T}} | \Phi \rangle + \sum_{\mu} \lambda_{\mu} \langle \Phi | X_{\mu}^{\dagger} e^{-\hat{T}} \hat{H} e^{\hat{T}} | \Phi \rangle = \langle \Phi | (1 + \Lambda) e^{-\hat{T}} \hat{H} e^{\hat{T}} | \Phi \rangle, \quad (6.95)$$

where we have introduced $\Lambda = \sum_{\mu} X_{\mu}^{\dagger}$. Here, X_{μ}^{\dagger} is a general relaxation operator, for instance $\hat{X}_1^{\dagger} = \{\hat{i}\hat{a}^{\dagger}\}$. The sum of relaxation operators, Λ , written out is

$$\Lambda = \sum_{ia} \lambda_a^i \hat{i}^{\dagger} \hat{a} + \frac{1}{2!^2} \sum_{ijab} \lambda_{ab}^{ij} \hat{i}^{\dagger} \hat{a} \hat{j}^{\dagger} \hat{a} + \dots \quad (6.96)$$

In section B.5 we have provided the Coupled Cluster Singles Doubles (CCSD) Lagrangian written out fully.

The coupled cluster Lagrangian in Equation 6.95 can be rewritten with the use of density operators,

$$\mathcal{L}_{\hat{H}}(t, \lambda) = \text{tr}\{\hat{H}\hat{\rho}\}, \quad \hat{\rho} = e^{\hat{T}} |\Phi\rangle\langle\Phi| (1 + \Lambda) e^{-\hat{T}}, \quad (6.97)$$

in a pure state description. We check to see if the attributes of the density operator endures,

$$\begin{aligned} \hat{\rho}^2 &= e^{\hat{T}} |\Phi\rangle\langle\Phi| (1 + \Lambda) e^{-\hat{T}} e^{\hat{T}} |\Phi\rangle\langle\Phi| (1 + \Lambda) e^{-\hat{T}} \\ &= e^{\hat{T}} |\Phi\rangle\langle\Phi| (1 + \Lambda) e^{-\hat{T}} + e^{\hat{T}} |\Phi\rangle \underbrace{\langle\Phi| \Lambda | \Phi\rangle}_{0} \langle\Phi| e^{-\hat{T}} = \hat{\rho} \\ \text{Tr}\{\hat{\rho}\} &= \sum_p \langle \phi_p | e^{\hat{T}} |\Phi\rangle\langle\Phi| (1 + \Lambda) e^{-\hat{T}} | \phi_p \rangle = 1 \\ (\hat{\rho})^{\dagger} &= e^{-\hat{T}^{\dagger}} (1 + \Lambda^{\dagger}) |\Phi\rangle\langle\Phi| e^{\hat{T}^{\dagger}} \neq \hat{\rho}. \end{aligned}$$

We see that another problem has presented itself, as the density operator is non-Hermitian. This leads us to the *bivariational*, Hellmann-Feynman conforming framework developed by Arponen [33].

6.4.3 The Bivariational Principle

Arponen approached the coupled cluster problem by employing a very general form of the variational principle called the bivariational principle. Letting \hat{H} , be a (possibly non-Hermitian) operator over Hilbert space \mathcal{H} , the bivariational expectation functional is defined by

$$\mathcal{E}_{\hat{H}} : \mathcal{H}' \times \mathcal{H} \rightarrow \mathbb{C}, \quad \mathcal{E}_{\hat{H}}(\tilde{\Psi}, \Psi) = \frac{\langle \tilde{\Psi} | \hat{H} | \Psi \rangle}{\langle \tilde{\Psi} | \Psi \rangle} = \frac{\text{tr}\{\hat{H}\hat{\rho}\}}{\text{tr}\{\rho\}}. \quad (6.98)$$

The main difference from the traditional and usual variational principle is that $\langle \tilde{\Psi} |$ and $| \Psi \rangle$ are treated as independent elements of the Hilbert space, and $\hat{\rho} = |\Psi\rangle\langle\tilde{\Psi}|$. Since the Hamiltonian \hat{H} is Hermitian, $\langle \tilde{\Psi} |$ and $| \Psi \rangle$ can be treated independently in the derivations of stationary conditions. However, we must have that $\langle \tilde{\Psi} |$ and $| \Psi \rangle$ are left- and right eigenvalues of the Hamiltonian, with the same eigenvalue

$$\hat{H} | \Psi \rangle = E | \Psi \rangle, \quad \langle \tilde{\Psi} | \hat{H} = \langle \tilde{\Psi} | E. \quad (6.99)$$

We also have that $E = \mathcal{E}_{\hat{H}}(\tilde{\Psi}, \Psi)$ is the value at the stationary point.

We transition to coupled cluster theory by inserting the coupled cluster exponential wave functions, $|\Phi\rangle = e^{\hat{T}}|\Phi\rangle$ and $\langle\tilde{\Psi}| = \langle\Phi|e^{\tilde{T}}$, where $\tilde{T} = \tilde{t}X^\dagger$ are some general relaxation operator. The bivariational functional becomes

$$\mathcal{E}_{\hat{H}} = \frac{\langle\Phi|e^{\hat{T}}\hat{H}e^{\hat{T}}|\Phi\rangle}{\langle\Phi|e^{\tilde{T}}e^{\hat{T}}|\Phi\rangle} \quad (6.100)$$

Varying this functional over all untruncated excitation and relaxation operators, \hat{T} and \tilde{T} , is the foundation of variational coupled cluster theory [76], which is equivalent to full configuration interaction within the given single-particle basis set.

Now we wish to show that Arponen's framework corresponds to that of Helgaker and Jørgensen [32]. We simplify the expression by performing a variable change $(\hat{T}, \tilde{T}) \rightarrow (\hat{T}, \hat{S})$, where S is a new relaxation operator. We start by introducing

$$\langle\omega| = \frac{\langle\tilde{\Psi}|e^{\hat{T}}}{\langle\tilde{\Psi}|\Psi\rangle}, \quad (6.101)$$

which satisfies $\langle\omega|\Phi\rangle = 1$, implying that there must exist an operator $\hat{S} = sX^\dagger$, such that $\langle\omega| = \langle\Phi|e^{\hat{S}}$. Then we can write,

$$\frac{\langle\tilde{\Psi}|e^{\hat{T}}}{\langle\tilde{\Psi}|\Psi\rangle} = \langle\Psi|e^{\hat{S}}, \rightarrow \langle\tilde{\Psi}| = \langle\tilde{\Psi}|\Psi\rangle\langle\Phi|e^{\hat{S}}e^{-\hat{T}}. \quad (6.102)$$

This enables us to rewrite the bivariational principle (Equation 6.100) as

$$\mathcal{E}_{\hat{H}} = \langle\Phi|e^{\hat{S}}e^{-\hat{T}}\hat{H}e^{\hat{T}}|\Phi\rangle, \quad (6.103)$$

which is an exact functional if \hat{T} and \hat{S} are not truncated. Comparing this expression to the coupled cluster Lagrangian in Equation 6.95, we can only conclude that the basis

change has revealed that $e^{\hat{S}} = 1 + \Lambda$. Truthfully, we have strong indication that the coupled cluster bivariational functional (Equation 6.100) is the same as the the coupled cluster Lagrangian (Equation 6.95)³.

First-order conditions of the coupled cluster energy Lagrangian in Equation 6.95 give us a new set of amplitude equations,

$$\frac{\partial}{\partial \lambda_\mu} \mathcal{L}(t, \lambda) = \langle \Phi_{X_\mu} | e^{-\hat{T}} \hat{H} e^{\hat{T}} | \Phi \rangle = 0 \quad (6.104)$$

$$\frac{\partial}{\partial t_\mu} \mathcal{L}(t, \lambda) = \langle \Phi | (1 + \Lambda) e^{-\hat{T}} [\hat{H}, X_\mu] e^{\hat{T}} | \Phi \rangle = 0. \quad (6.105)$$

Under constrained optimisation all partial derivatives vanish at the same point,

$$\left. \frac{\partial \mathcal{L}}{\partial \lambda_\mu} \right|_{t=t^*} = 0, \quad \left. \frac{\partial \mathcal{L}}{\partial t_\mu} \right|_{(t,\lambda)=(t^*,\lambda^*)} = 0, \quad \forall X_\mu. \quad (6.106)$$

What we have arrived at are amplitude equations both for the “bra part” and the “ket part” of the problem, which we refer to as the λ amplitude equations (Equation 6.104) and the τ amplitude equations (Equation 6.105), respectively. Notice that the τ amplitude equations only depend on τ , whilst the λ equations depend both on τ and λ . This means that the τ amplitude equations are solved iteratively first, and then the λ amplitudes are solved similarly. The full equations are given in section B.4.

The benefit of going through the exercise of reformulating the coupled cluster framework entirely is that it is now possible to define operators,

$$\rho_p^q = \langle \tilde{\Psi} | c_p^\dagger c_q | \Psi \rangle \quad (6.107)$$

$$\rho_{pr}^{qs} = \langle \tilde{\Psi} | c_p^\dagger c_q^\dagger c_s c_r | \Psi \rangle, \quad (6.108)$$

which we can use to compute expectation values of operators, $\langle \hat{A} \rangle = \text{tr} \{ \rho \hat{A} \}$. Here, \hat{A} is a general one- and two-body operator,

$$\hat{A} = a_q^p c_p^\dagger c_q + \frac{1}{4} a_{qs}^{pr} c_p^\dagger c_q^\dagger c_s c_r. \quad (6.109)$$

Then we have,

$$\langle \hat{A} \rangle = \langle \tilde{\Psi} | \hat{A} | \Psi \rangle = a_q^p \langle \tilde{\Psi} | c_p^\dagger | \Psi \rangle + \frac{1}{4} a_{qs}^{pr} \langle \tilde{\Psi} | c_p^\dagger c_q^\dagger c_s c_r | \Psi \rangle = a_q^p \rho_p^q + \frac{1}{4} a_{qs}^{pr} \rho_{pr}^{qs}. \quad (6.110)$$

6.5 Generalisation in Time

Here, we will outline a derivation of the orbital-adaptive time-dependent coupled cluster method, a generalisation in time for the coupled cluster method put forth by Kvaal[1]. The method inherits both size-extensivity and size-consistency from the coupled cluster method and is a hierarchy of approximations to the multi-configurational time-dependent Hartree method for fermions.

³Pruning the expression in Equation 6.103 to only include single and double excitations will yield Arponen’s *extended coupled cluster* (ECC) method[77]. This method has seen little use due to its complexity.

We now define a time-dependent generalisation of the bivariational principle (Equation 6.98). This is similar to the usual time-dependent action functional and the time-dependent Schrödinger equation can be recovered from it,

$$\mathcal{S}[\Psi'(\cdot), \Psi(\cdot)] = \int_0^T dt \frac{\langle \Psi'(t) | \left(i\hbar \frac{\partial}{\partial t} - \hat{H} \right) | \Psi(t) \rangle}{\langle \Psi'(t) | \Psi(t) \rangle}. \quad (6.111)$$

Functionals like these are quite common throughout the literature on quantum mechanics, appearing as early as in Dirac[35]. The integral of the functional depends on all history for the system in question. By applying the principle of least action, requiring that the functional is stationary, $\delta\mathcal{S} = 0$, under all variations of $\langle \Psi' |$ and $|\Psi\rangle$ and vanishing in the endpoints $t = 0$ and $t = T$, gives us the following conditions

$$i\hbar \frac{\partial}{\partial t} |\Psi(t)\rangle = \hat{H} |\Psi(t)\rangle \quad -i\hbar \frac{\partial}{\partial t} \langle \Psi'| = \langle \Psi' | \hat{H}.$$

By a specific parametrisation of $\langle \Psi' |$, such that $\langle \Psi' | \Psi \rangle = 1$ we have indeed recovered the familiar time-dependent Schrödinger euqation.

Instead of venturing down this path, we will presuppose that it is possible that $\langle \Psi' | \Psi \rangle \neq 1$. Indeed, that $\langle \Psi' |$ and $|\Psi\rangle$ are independent. This means we must enact Arponen's [33] Hellmann-Feynman conforming bivariational principle, where the energy expectation functial is given by

$$\mathcal{E}_{\hat{H}}(\tau', \tau, \Phi', \Phi) = \frac{\langle \Phi' | e^{\hat{T}' \hat{H} e^{\hat{H}}} | \Phi \rangle}{\langle \Phi' | e^{\hat{T}' e^{\hat{T}}} | \Phi \rangle}. \quad (6.112)$$

We perform a variable change $(T', T) \rightarrow (\lambda, T)$, similarly to the section above, and introduce

$$\langle \tilde{\Psi} | = \frac{\langle \Psi' |}{\langle \Psi' | \Psi \rangle} = \langle \tilde{\Phi} | (1 + \Lambda) e^{\hat{T}}, \quad (6.113)$$

Where Λ is the same as in Equation 6.96. The bivariational energy expectation functional in Equation 6.112 now becomes

$$\mathcal{E}_{\hat{H}}(\lambda, \tau, \tilde{\Phi}, \Phi) = \langle \tilde{\Phi} | (\hat{1} + \lambda) e^{-\hat{T} \hat{H} e^{\hat{T}}} | \Phi \rangle. \quad (6.114)$$

Disregarding the difference in $\tilde{\Phi}$ and Φ , this expression is the same as the coupled cluster expectation functional in Equation 6.103, where the interpretation is that the λ s are Lagrange multipliers for a constrained energy minimisation problem. This is not the interpretation here, as the λ -part of the problem is seen as equally important.

We are now assuming biorthogonality in orbitals, $\langle \tilde{\phi}_p | \phi_q \rangle = \delta_{pq}$, but independence of bra and ket states otherwise. For a full Slater determinant state consisting of these orbitals, we have

$$\langle \tilde{\phi}_{p_1} \dots \tilde{\phi}_{p_n} | \phi_{q_1} \dots \phi_{q_n} \rangle = \delta_{p_1 q_1} \dots \delta_{p_N q_N}. \quad (6.115)$$

The second quantised operators asscoiated with these Slater determinants are defined through

$$|\phi_{q_1} \dots \phi_{q_n}\rangle \equiv c_{p_1}^\dagger \dots c_{p_N}^\dagger | \rangle \quad \langle \tilde{\phi}_{p_1} \dots \tilde{\phi}_{p_n}| = \langle | \tilde{c}_{q_N} \dots \tilde{c}_{q_1}. \quad (6.116)$$

These creation- and annihilation operators can furthermore be defined by,

$$c_p^\dagger = \int \phi_p(\mathbf{x}) \Psi^\dagger(\mathbf{x}) d\mathbf{x} \quad \tilde{c}_p = \int \tilde{\phi}_p(\mathbf{x}) \Psi(\mathbf{x}) d\mathbf{x}, \quad (6.117)$$

where Ψ^\dagger and Ψ are field creation- and annihilation operators. This particular definition may seem like an unnecessary and stringent tangent, but its purpose is to underline the dependence of the cluster operator \hat{T} not only on the amplitudes τ , but also on the orbitals. This is an important point to emphasise, in “ordinary” coupled cluster theory, one thinks of the amplitudes as the only unknowns while keeping the orbitals fixed and the dependence on τ are one-to-one. This becomes very important when one computes derivatives with respect to time of the cluster operators \hat{T} . Furthermore, the second quantised operators are subject to the anticommutator relation,

$$\{ \tilde{c}_p, c_q^\dagger \} \equiv \tilde{c}_p c_q^\dagger + c_q^\dagger \tilde{c}_p \stackrel{!}{=} \langle \tilde{\phi}_p | \phi_q \rangle = \delta_{pq}. \quad (6.118)$$

The time dependent action (-like) functional (Equation 6.111) defining the Schrödinger dynamics becomes,

$$\begin{aligned} \mathcal{S}[\lambda, \tau, \tilde{\Phi}, \Phi] &= \int_0^T \left\langle \tilde{\Phi} \left| (1 + \Lambda) e^{-\hat{T}} \left(\frac{\partial}{\partial t} - \hat{H} \right) e^{\hat{T}} \right| \Phi \right\rangle dt \\ &= \int_0^T i\hbar \left\langle \tilde{\Phi} \left| (1 + \Lambda) e^{-\hat{T}} \frac{\partial}{\partial t} e^{\hat{T}} \right| \Phi \right\rangle dt - \mathcal{E}_{\hat{H}}(\lambda, \tau, \tilde{\Phi}, \Phi). \end{aligned} \quad (6.119)$$

Herein, it is necessary to compute $\frac{\partial}{\partial t} |\Psi\rangle = \frac{\partial}{\partial t} e^{\hat{T}} |\Phi\rangle$. In order to accomplish this we introduce the expansion,

$$|\Psi\rangle = \Pi |\Psi\rangle = |\Phi\rangle + \sum_\mu A^\mu |\Phi_\mu\rangle, \quad A^\mu = A^\mu(\tau) = \langle \tilde{\Phi}^\mu | e^{\hat{T}} | \Phi \rangle \quad (6.120)$$

Here we write Φ as the reference Slater determinant and Φ_μ are all the other excited Slater determinant. The coefficients A^μ do not depend explicitly on the orbitals, only on the amplitudes τ . It is important to note that this summation is not truncated, regardless of the truncation of the cluster amplitudes at some excitation level τ^μ . To further the matter, we have introduced a projection operator,

$$\Pi \equiv |\Phi\rangle\langle\tilde{\Phi}| + \sum_\mu |\Phi_\mu\rangle\langle\tilde{\Phi}^\mu|. \quad (6.121)$$

The projection operator has the following properties,

$$\begin{aligned} \Pi |\Psi\rangle &= |\Psi\rangle, \quad \langle \Psi' | \Phi = \langle \Psi' |, \\ \langle \Psi' | \hat{H} | \Psi \rangle &= \langle \Psi' | \Pi \hat{H} \Pi | \Psi \rangle, \quad \Pi^\dagger \neq \Pi \end{aligned} \quad (6.122)$$

and unless orbitals are complete we have $\Pi \hat{H} \Pi \neq \hat{H}$.

Now we compute the time derivative of a Slater determinant,

$$\begin{aligned} \frac{\partial}{\partial t} c_{p_1}^\dagger c_{p_2}^\dagger \dots c_{p_N}^\dagger | \rangle &= \dot{c}_{p_1}^\dagger c_{p_2}^\dagger \dots c_{p_N}^\dagger | \rangle + c_{p_1}^\dagger \dot{c}_{p_2}^\dagger \dots c_{p_N}^\dagger | \rangle + \dots \\ &= \left(\sum_q \dot{c}_q^\dagger \tilde{c}_q \right) c_{p_1}^\dagger c_{p_2}^\dagger \dots c_{p_N}^\dagger | \rangle = \hat{D} c_{p_1}^\dagger c_{p_2}^\dagger \dots c_{p_N}^\dagger | \rangle, \end{aligned}$$

where we have defined the operator \hat{D} by

$$\hat{D} = \sum_q \dot{c}_q^\dagger \tilde{c}_q, \quad (6.123)$$

which depends explicitly on orbitals, unlike \hat{H} . The derivative of the exact wavefunction becomes,

$$\begin{aligned} \frac{\partial}{\partial t} |\Psi\rangle &= \sum_\mu \left(\frac{\partial}{\partial t} A^\mu(\tau) \right) |\Phi_\mu\rangle + \hat{D} |\Phi\rangle + \sum_\mu A^\mu(\tau) \hat{D} |\Phi_\mu\rangle \\ &= \left(\sum_\nu \dot{\tau}^\nu \frac{\partial}{\partial \tau^\nu} + \hat{D} \right) |\Psi\rangle = \left(\sum_\nu \dot{\tau}^\nu X_\nu + \hat{D} \right) |\Psi\rangle. \end{aligned} \quad (6.124)$$

The time-derivative part of the functional (Equation 6.119) integrand becomes,

$$\begin{aligned} i\hbar \langle \tilde{\Phi} | (1 + \Lambda) e^{-\hat{T}} \frac{\partial}{\partial t} e^{\hat{T}} | \Phi \rangle \\ = i\hbar \langle \tilde{\Phi} | \left(1 + \sum_\mu \lambda_\mu \tilde{X}^\mu \right) e^{-\hat{T}} \left(\sum_\nu \dot{\tau}^\nu X_\nu + \hat{D} \right) e^{\hat{T}} | \Phi \rangle \\ = i\hbar \sum_\mu \lambda_\mu \dot{\tau}^\mu + i\hbar \langle \tilde{\Phi} | (1 + \Lambda) e^{-\hat{T}} \Pi \hat{D} \Pi e^{\hat{T}} | \Phi \rangle, \end{aligned} \quad (6.125)$$

where the projected operator $\Pi \hat{D} \Pi$ is given by

$$\Pi \hat{D} \Pi = \hat{D}_0 \equiv \sum_{pq} \langle \tilde{\phi}_p | \dot{\phi}_q \rangle c_p^\dagger \tilde{c}_q. \quad (6.126)$$

Finally we obtain a new expression for the functional in Equation 6.119

$$\mathcal{S}[\lambda, \tau, \tilde{\Phi}, \Phi] = \sum_0^T i\hbar \sum_\mu \lambda_\mu \dot{\tau}^\mu - \mathcal{E}_{\hat{H}-i\hbar\hat{D}_0}[\lambda, \tau, \tilde{\Phi}, \Phi] dt \quad (6.127)$$

$$= \int_0^T i\hbar \lambda_\mu \dot{\tau}^\mu + \rho_p^q (h_q^p - i\hbar \eta_q^p) + \frac{1}{4} \rho_{pr}^{qs} u_{qs}^{pr} dt, \quad (6.128)$$

where

$$\rho_p^q = \rho_p^q(\lambda, \tau) \equiv \langle \tilde{\Phi} | (1 + \Lambda) e^{-\hat{T}} c_p^\dagger \tilde{c}_q e^{\hat{T}} | \Phi \rangle, \quad (6.129)$$

$$\rho_{pr}^{qs} = \rho_{pr}^{qs}(\lambda, \tau) \equiv \langle \tilde{\Phi} | (1 + \Lambda) e^{-\hat{T}} c_p^\dagger c_r^\dagger \tilde{c}_s \tilde{c}_q e^{\hat{T}} | \Phi \rangle, \quad (6.130)$$

$$h_q^p = h_q^p(\tilde{\Phi}, \Phi) \equiv \langle \tilde{\phi}_p | \hat{h} | \varphi_q \rangle, \quad (6.131)$$

$$\eta_q^p = \eta_q^p(\tilde{\Phi}, \Phi) \equiv \langle \tilde{\phi}_p | \dot{\varphi}_q \rangle, \quad (6.132)$$

$$u_{qs}^{pr} = u_{qs}^{pr}(\tilde{\Phi}, \Phi) \equiv \langle \tilde{\phi}_p \tilde{\varphi}_r | (\hat{u} - \hat{P}_{12}) | \phi_q \varphi_s \rangle. \quad (6.133)$$

We introduced the Einstein summation convention over repeated indices of opposite vertical placement in Equation 6.128.

6.5.1 Equations of Motion

The time has now come to apply the principle of least action to the orbital-adaptive coupled cluster functional from Equation 6.127 in order to find the equations of motion. First we keep τ^ν constant and vary λ_μ ,

$$\delta\mathcal{S}[\lambda, \tau] = \int_0^T i\hbar\delta\lambda_\mu\dot{\tau}^\nu - \frac{\partial\mathcal{E}_{\hat{H}-i\hbar\hat{D}_0}}{\partial\lambda_\mu}\delta\lambda_\mu dt = 0. \quad (6.134)$$

We see that the stationary condition is

$$i\hbar\dot{\tau}^\mu = \frac{\partial}{\partial\lambda_\mu}\mathcal{E}_{\hat{H}-i\hbar\hat{D}_0}[\lambda, \tau, \tilde{\Phi}, \Phi] = \langle\tilde{\Phi}_\mu|e^{-\hat{T}}(\hat{H} - i\hbar\hat{D}_0)e^{\hat{T}}|\Phi\rangle, \quad (6.135)$$

which is also the equation of motion, dictating the time-development of τ . Next, we hold λ_μ fixed and vary τ^ν ,

$$\delta\mathcal{S}[\lambda, \tau] = \int_0^T i\hbar\lambda_\nu\delta\dot{\tau}^\nu - \frac{\partial\mathcal{E}_{\hat{H}-i\hbar\hat{D}_0}}{\partial\tau^\nu}dt. \quad (6.136)$$

through integration by parts we see that the first term becomes,

$$i\hbar\int_0^T \lambda_\nu\delta\dot{\tau}^\nu = i\hbar\lambda_\nu\delta\tau^\nu - i\hbar\int_0^T \dot{\lambda}_\nu\delta\tau^\nu dt,$$

yielding

$$\delta\mathcal{S}[\lambda, \tau] = \int_0^T \delta\tau^\nu \left(-i\hbar\dot{\lambda}_\nu - \frac{\partial\mathcal{E}_{\hat{H}-i\hbar\hat{D}_0}}{\partial\tau^\nu} \right). \quad (6.137)$$

Here the stationary condition is

$$-i\hbar\dot{\lambda}_\nu = \frac{\partial}{\partial\tau^\nu}\mathcal{E}_{\hat{H}-i\hbar\hat{D}_0}[\lambda, \tau, \tilde{\Phi}, \Phi] = \langle\tilde{\Phi}|(1 + \Lambda)e^{-\hat{T}}[\hat{H} - i\hbar\hat{D}_0, X_\mu]e^{\hat{T}}|\Phi\rangle. \quad (6.138)$$

Equation 6.135 and Equation 6.138 together make up the orbital-adaptive coupled cluster (OACC) amplitude equations of motion.

We will return to the OACC equations of motion shortly, but first we consider a special situation where the operator $\hat{D}_0 \equiv \sum_{pq} \langle\tilde{\phi}_p|\tilde{\phi}_q\rangle c_p^\dagger \tilde{c}_q$, equates to zero. This is the same as keeping the orbitals static over time. The resulting equations of motions are

$$i\hbar\dot{\tau}^\mu = \frac{\partial}{\partial\lambda_\mu}\mathcal{E}_{\hat{H}}[\lambda, \tau, \tilde{\Phi}, \Phi] = \langle\tilde{\Phi}_\mu|e^{-\hat{T}}\hat{H}e^{\hat{T}}|\Phi\rangle \quad (6.139)$$

$$-i\hbar\dot{\lambda}_\nu = \frac{\partial}{\partial\tau^\nu}\mathcal{E}_{\hat{H}}[\lambda, \tau, \tilde{\Phi}, \Phi] = \langle\tilde{\Phi}|(1 + \Lambda)e^{-\hat{T}}[\hat{H}, X_\mu]e^{\hat{T}}|\Phi\rangle. \quad (6.140)$$

We call these equations the time-dependent coupled cluster (TDCC) amplitude equations. Setting the left-hand side of Equation 6.139 and Equation 6.140 to zero will give a set of non-linear equations that can be solved in order to find initial amplitudes ($\lambda^{(0)}$, $\tau^{(0)}$). These equations are the same as Equation 6.104 and Equation 6.105.

Returning to the orbital-adaptive scheme, the OATDCC equations (Equation 6.135 and Equation 6.138) have parametric redundancies that we need to address briefly⁴. The parametric redundancies exist in the sense that when one derives equations of motion for $(\tau, \lambda, \tilde{\Phi}, \Phi) = (\tau^\mu, \lambda_\mu, \tilde{\phi}_p, \phi_q)$, under the stationary condition $\delta\mathcal{S} = 0$, for a given pair of coupled cluster wavefunctions $(\langle \tilde{\Psi} |, |\Psi\rangle) \in \mathcal{M}$, there are many choices for the amplitudes and orbitals that would give this same wavefunction pair. It is therefore necessary to define a transformation as a many-to-one mapping from this collection of points $(\lambda, \tau, \tilde{\Phi}, \Phi) \in \mathcal{N}$ to the wavefunction pair on $(\langle \tilde{\Psi} |, |\Psi\rangle) \in \mathcal{M}$,

$$f : \mathcal{N} \rightarrow \mathcal{M}. \quad (6.141)$$

As circumstances would have it, the simplest of such transformations corresponds to a rotation that eliminates the singles amplitudes τ_i^a . This is the same ansatz employed in orbital-optimised- or Brueckner coupled cluster theory (see box). Additionally, including λ_a^i after this rotation would leave the equations of motions overdetermined. The presence of \hat{T}_1 is compensated by the freely varying orbitals, but this does not hold for Λ_1 , which gives more parameters in the $\langle \tilde{\Psi} |$ than in $|\Psi\rangle$. As such, we set all single amplitudes, τ_i^a and λ_a^i equal to zero.

Orbital-optimised and Bruecker coupled cluster theories [78, 79]

In standard coupled cluster theory including single excitations,

$$e^{\hat{T}_1} = \exp \left\{ \sum_{ai} \tau_i^a c_a^\dagger c_i \right\}, \quad (6.142)$$

we determine a set of non-zero single-excitation amplitudes τ_i^a together with any higher-excitation amplitudes. An alternative parametrisation of the singles manifold in Equation 6.142 is the orthogonal orbital-rotation operator

$$e^{-\kappa} = \exp \left\{ - \sum_{ai} \kappa_a i (c_a^\dagger c_i - c_i^\dagger c_a) \right\} \quad (6.143)$$

This is a rephrasing of Thouless' theorem[67]. We may therefore use

$$|\Psi_{\text{OCC}}\rangle = e^{-\kappa} e^{\hat{T}_{\text{O}}} |\Phi\rangle \quad (6.144)$$

as a wavefunction ansatz instead. Here,

$$\hat{T}_{\text{O}} = \hat{T}_2 + \hat{T}_3 + \dots \quad (6.145)$$

In orbital-adaptive time-dependent coupled cluster theory such a gauge condition corresponds to considering orbital time derivatives of the form

$$\langle \dot{\phi}_q \rangle = (P + Q) \langle \dot{\phi}_q \rangle = \sum_p |\phi_p\rangle \langle \tilde{\phi}_p | \dot{\phi}_q \rangle + Q \langle \dot{\phi}_q \rangle = \sum_p \eta_q^p + Q \langle \dot{\phi}_q \rangle \quad (6.146)$$

⁴A thorough decription of this matter can be found in the supplementary to Kvaal's articl on OATDCC[1]

$$\langle \dot{\tilde{\phi}}_p | = \left\langle \dot{\tilde{\phi}}_p \right| (P + Q) = \sum_q \left\langle \dot{\tilde{\phi}}_p \right| \phi_q \rangle \left\langle \tilde{\phi}_q \right| + \left\langle \dot{\tilde{\phi}}_p \right| Q = - \sum_q \eta_q^p \left\langle \tilde{\phi}_q \right| + \left\langle \dot{\tilde{\phi}}_p \right| Q, \quad (6.147)$$

with $\eta_j^i = \eta_b^a = 0$, $\eta_q^p = \langle \tilde{\phi}_p | \dot{\phi}_q \rangle = -\langle \dot{\tilde{\phi}}_p | \phi_q \rangle$. Here we have defined the projection operators P and Q , where $P = \Phi \tilde{\Phi} = \sum_p |\phi_p\rangle\langle\phi_p|$ projects onto the single-particle space defined by the orbitals, and $Q = 1 - P$ projects onto everything else.

We can write down the equations of motions just for the nonzero P -components η_i^a and η_a^i of the orbital derivatives,

$$i\hbar \sum_{bj} A_{aj}^{ib} \eta_b^j = \sum_p \rho_p^i h_a^p - \sum_q \rho_a^q h_q^i + \frac{1}{2} \left[\sum_{qrs} \rho_{pr}^{is} u_{as}^{pr} - \sum_{rqs} \rho_{ar}^{qs} u_{qs}^{ir} \right] \quad (6.148)$$

$$-i\hbar \sum_{bj} A_{bi}^{ja} \eta_j^b = \sum_p \rho_p^a h_i^p - \sum_q \rho_i^q h_q^a + \frac{1}{2} \left[\sum_{prs} \rho_{ps}^{as} u_{is}^{pr} - \sum_{rqs} \rho_{ir}^{qs} u_{qs}^{ar} \right] + i\hbar \hat{\rho}_i^a, \quad (6.149)$$

where the matrix elements A_{aj}^{ib} are defined by,

$$A_{aj}^{ib} \equiv \left\langle \tilde{\Psi} \right| [c_j^\dagger \tilde{c}_b, c_a^\dagger \tilde{c}_i] \left| \Psi \right\rangle = \delta_a^b \rho_j^i - \delta_j^i \rho_a^b. \quad (6.150)$$

The Q -part of the orbital derivatives are,

$$i\hbar \sum_q \rho_p^q Q \frac{\partial}{\partial t} |\phi_q\rangle = \sum_q \rho_p^q Q h |\phi_q\rangle + \sum_{qrs} \rho_{pr}^{qs} Q W_s^r |\phi_q\rangle, \quad \forall p \quad (6.151)$$

$$-i\hbar \sum_p \rho_p^q \left(\frac{\partial}{\partial t} \left\langle \tilde{\phi}_p \right| \right) Q = \sum_p \rho_p^q \left\langle \tilde{\phi}_p \right| h Q + \sum_{prs} \rho_{pr}^{qs} \left\langle \tilde{\phi}_p \right| W_s^r Q, \quad \forall q, \quad (6.152)$$

where the mean-field operators W_s^r are defined by

$$W_s^r |\psi\rangle \equiv \langle \cdot \tilde{\phi}_r | u | \psi \phi_s \rangle. \quad (6.153)$$

The logical next step is to write down the equations of motion for the lowest truncated form of OATDCC available to us, namely OATDCCD. In addition to the orbitals Φ and $\tilde{\Phi}$, the only parameters of the exact wavefunction are the amplitudes $\tau = \tau_{ij}^{ab}$ and $\lambda = \lambda_{ab}^{ij}$. The OATDCCD amplitude equations read

$$i\hbar \dot{\tau}_{ij}^{ab} = \frac{\partial}{\partial \lambda_{ab}^{ij}} \mathcal{E}_H[\lambda, \tau, \tilde{\Phi}, \Phi] = \left\langle \tilde{\phi}_{ij}^{ab} \right| e^{-\hat{T}} \hat{H} e^{\hat{T}} \left| \phi \right\rangle \quad (6.154)$$

$$-i\hbar \dot{\lambda}_{ab}^{ij} = \frac{\partial}{\partial \tau_{ij}^{ab}} \mathcal{E}[\lambda, \tau, \tilde{\Phi}, \Phi] = \left\langle \tilde{\phi} \right| (1 + \Lambda) e^{-\hat{T}} [\hat{H}, X_{ab}^{ij}] e^{\hat{T}} \left| \phi \right\rangle. \quad (6.155)$$

The P -space orbitals read

$$i\hbar \sum_{bj} A_{aj}^{ib} \eta_b^j = \sum_j \rho_j^i h_a^j - \sum_b \rho_a^b h_b^i + \frac{1}{2} \left[\sum_{prs} \rho_{pr}^{is} u_{as}^{pr} - \sum_{rqs} \rho_{ar}^{qs} U_{qs}^{ir} \right], \quad (6.156)$$

$$-i\hbar \sum_{bj} A_{bi}^{ja} \eta_j^b = \sum_b \rho_b^a h_i^b - \sum_j \rho_i^j h_j^a + \frac{1}{2} \left[\sum_{prs} \rho_{pr}^{as} u_{is}^{pr} - \sum_{rqs} \rho_{ir}^{qs} U_{qs}^{ar} \right] \quad (6.157)$$

and the Q -space orbitals read

$$i\hbar \sum_q \rho_p^q Q \frac{\partial}{\partial t} |\phi_q\rangle = \sum_q \rho_q^p Q h |\phi_q\rangle + \sum_{qrs} \rho_{pr}^{qs} Q W_s^r |\phi_q\rangle, \quad (6.158)$$

$$-i\hbar \sum_p \rho_p^q \left(\frac{\partial}{\partial t} \langle \tilde{\phi}_q | \right) Q = \sum_p \rho_p^q |\phi_q\rangle Q h + \sum_{prs} \rho_{pr}^{qs} \langle \phi_q | W_s^r Q. \quad (6.159)$$

Notice that the τ and λ OATDCCD equations (Equation 6.154 and Equation 6.155) are the same equations as those used in standard TDCCCD (Equation 6.139 and Equation 6.140), because the operator \hat{D}_0 is eliminated due to $\rho_i^a = \rho_a^i = 0$. Because the operators \hat{D}_0 disappears from Equation 6.154 and Equation 6.155, the right-hand sides can be evaluated independently of equations 6.156, 6.157, 6.158, 6.159. In order to compute $\dot{\tilde{\Phi}}$ and $\dot{\Phi}$, η must be solved for in addition to $Q |\dot{\phi}_q\rangle$ and $\langle \dot{\phi}_p | Q$, according to Equation 6.146 and Equation 6.147.

Part III

Implementation

Chapter 7

Quantum Systems

In order to study a quantum system on the computer it is necessary to make a distinction for what defines the system, and one must therefore undergo the mathematical procedure of constructing a finite basis sets that defines the system in question. Here we present the `quantum_systems` python module, mainly designed to provide basis sets for one- and two-dimensional quantum dots.

For the one-dimensional quantum dot we provide a wide selection of different potentials. This is possible due to the relative computational ease associated with the model. As for the two-dimensional systems we have implemented each confining potential in separate classes including the regular harmonic quantum dot, a double quantum dot, as well as a quantum dot affected by a homogenous, static magnetic field.

In order to achieve maximum usability, the `quantum_systems` module includes a class for constructing custom systems, using basis sets imported from somewhere else, or basis sets defined by the user. We have written functions that interface with popular quantum chemistry packages PySCF[3] and Psi4[4], allowing the user to easily construct basis sets representing all kinds of systems of interest in quantum chemistry, like atoms and molecules.

What is more, the `quantum_systems` module also contains an implementation of a plane wave or homogenous electron gas basis set, sometimes called the jellium model¹. However, this implementation exists mainly as a curiosity at the time of writing. In the future it can potentially be developed into something more useful, as the electron gas can serve as a first approximation to a metal or a semi-conductor.

A complete diagrammatic class hierarchy of the `quantum_systems` module is shown in `???`. This class hierarchy also illustrates how the `quantum_systems` module fits into and works with the `coupled_cluster` module, to be presented in the next chapter.

The `quantum_system` module can be installed from github with `pip` by the following command,

```
pip install git+https://github.com/Schoyen/quantum-systems.git
```

The same task can of course be accomplished by more commands,

```
git clone https://github.com/Schoyen/quantum-systems.git
```

¹See for instance Ch. 10 in Gross and Heinonen [80]

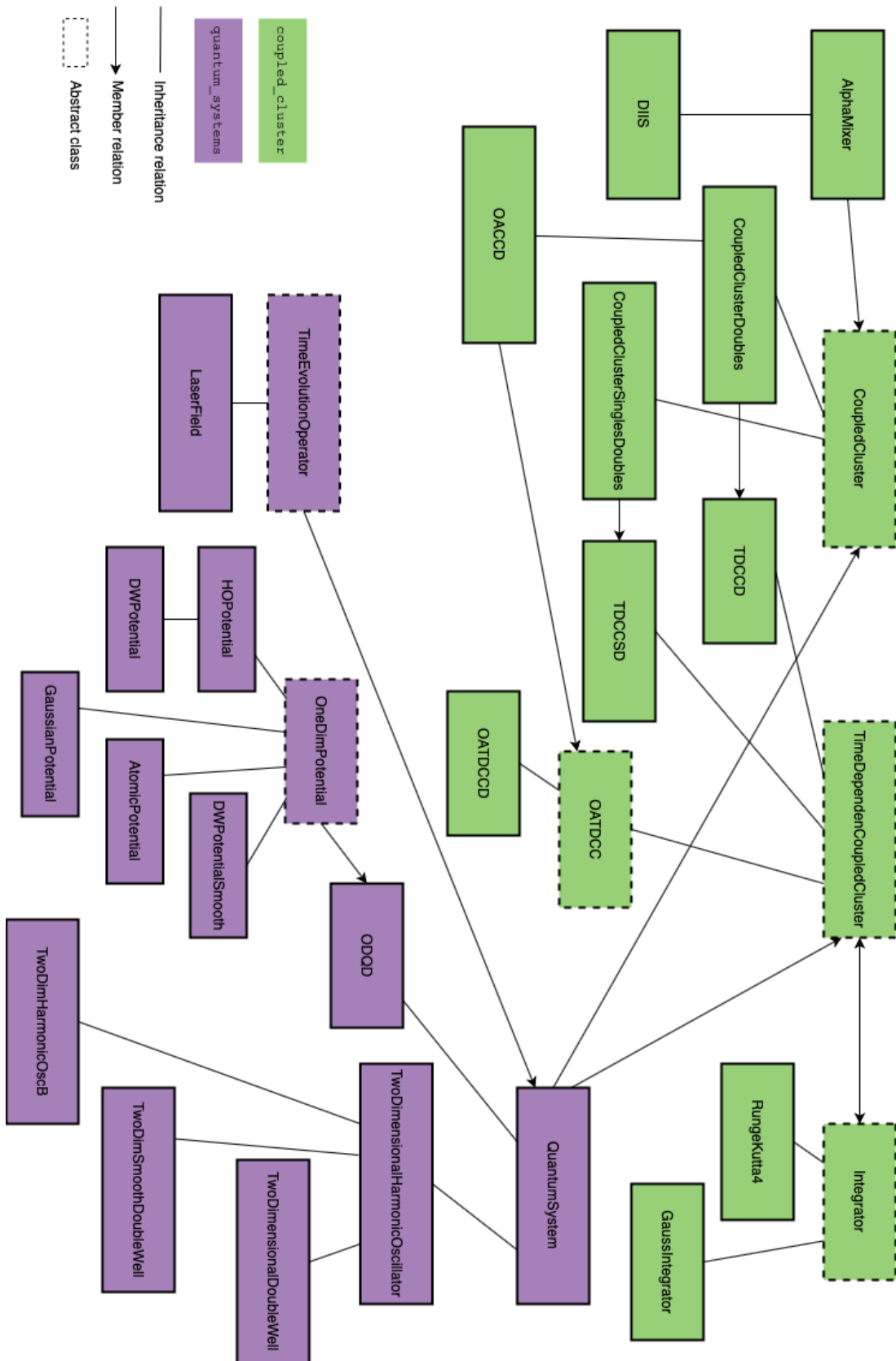


Figure 7.1: Class hierarchy of the two Python modules, `coupled_cluster` and `quantum_systems`.

```
cd quantum-systems
pip install .
```

It can be useful to install the module to a separate environment. We have made this possible through `conda`,

```
conda environment create -f environment.yml
conda activate quantum-systems
```

7.1 Quantum System Abstract Base Class

Here we present the abstract base class that every system class in the `quantum_systems` module is built upon. This base class forms the foundation of any quantum system, in order to make a system specification work together with solver from the `coupled_cluster` module presented in the next chapter. The base class is named `QuantumSystem`.

Many of the methods necessary to set up a quantum system can be abstracted away, which is most of the motivation for constructing a parent class that all other quantum system classes can inherit from. Examples of such functionality is setting up the Fock matrix. The one- and two-body operators are necessary to set up for a specific system, but the Fock matrix computations can be abstracted away to the superclass.

In the `QuantumSystem` abstract base class we have included a method that changes the basis of the system according to the coefficient matrices \mathbf{C} and $\tilde{\mathbf{C}}$, the `change_basis(...)` method. This method will be useful later, especially when computing the basis for the double well system. In the time-dependent coupled cluster scheme with adaptive orbitals, this method becomes particularly useful.

A similar method `change_to_hf_basis()` is also implemented in the `QuantumSystems` class. This changes the system basis to a basis based on the coefficient matrix found from the Roothan-Hall equations,

$$FC = SC\epsilon, \quad (7.1)$$

which are thoroughly discussed in section 4.2. The basis transformation is performed by multiplication with the coefficient matrix,

$$|\phi_p\rangle = C_p^\alpha |\chi_\alpha\rangle, \quad (7.2)$$

where we go from a (naïve) basis $|\chi_\alpha\rangle$, to the much better Hartree-Fock basis $|\phi_p\rangle$. The basis would be better suited to represent the system because it already constitutes an approximate ground state solution. The improvement in ground state energies by using the Hartree-Fock basis is well documented[81, 82].

The principal method that needs to be implemented in a subclass of `QuantumSystem` is `setup_system()`, including special considerations for dipole computations. These factors will be discussed for each specific system we have implemented in the following sections.

```
class quantum_systems.QuantumSystem (n, l, n_up=None, np=None)
```

Abstract base class defining the common methods used by all different quantum systems.

Parameters:

- n** (*int*) Number of electrons
- l** (*int*) Number of spinorbitals
- n_up** (*int, default=None*) Number of spin-up spinorbitals
- np** (*module*) Matrix library, i.e. numpy, cupy etc.

Attributes:

- h** One-body matrix **Type** *np.array*
- f** Fock matrix **Type** *np.array*
- u** Two-body matrix **Type** *np.array*
- s** Overlap matrix of spinorbitals **Type** *np.array*
- spf** Single-particle functions **Type** *np.array*
- spf_bra** Conjugated single-particle functions **Type** *np.array*

Methods:

- setup_system()**
Method must be implemented by subclasses.
- change_basis(*c, c_tilde=None*)**
Changes basis of system according to coefficient matrices **C** and **tilde C**.
- change_to_hf_basis(*args, verbose=False **kwargs)**
Changes basis of system to Hartree-Fock basis.
- set_time_evolution_operator(*time_evolution_operator*)**
Setter for time-evolution operator.

Parameters:

- time_evolution_operator** (*TimeEvolutionOperator*)

7.2 Quantum Dots

In reality, quantum dots are nanometre-sized structures made of semiconductor materials. Theoretically, quantum dots are easy to model with the harmonic oscillator potential and in practice they are relatively easy to manufacture in a laboratory. This doubly theoretical-experimental benefit has made quantum dots a popular area of study. Moreover so because of their wide area of applications.

The possible applications of quantum dots are many. Coupled single-electron quantum dots could potentially be used as hardware elements in quantum computers [83]; quantum dots also promise to increase the efficiency of photovoltaic solar cells; and they have already found use in cellular imaging in biology. Reimann and Manninen [84] has written a thorough review on quantum dots, covering their varied types of fabrication, theoretical methods common in their study and several applications.

We find that the study of quantum dot systems is warranted because of their great usefulness. What is more, it is relatively easy to approximate such systems theoretically and numerically. Several classes have been implemented in the `quantum_systems` module that constructs basis sets modelling quantum dots in both one and two dimensions. Most of these basis sets model *bound* systems with the characteristics of infinite quantum wells.

7.2.1 One Dimension

The one-dimensional quantum harmonic oscillator is perhaps one of the simplest of all quantum mechanical models. It is studied thoroughly in every introductory quantum mechanics course. This is with good reason because the system is analytically easy to manage, and because any arbitrary potential can be approximated by a harmonic oscillator as long as the oscillations are small enough. One must bear in mind that the harmonic oscillator potential, sometimes also called the parabolic potential, is one of many potentials that one can use in a quantum dot system.

We have implemented the one-dimensional quantum dot in a class `ODQD`, which is a subclass of the `QuantumSystems` class. We will now go through some of the intricacies necessary to compute the basis set contained in the `ODQD` class. Not much is needed, only a matrix representation of the one-body operator \hat{h} and the two-body operator \hat{u} . In addition we need the single-particle functions, which are the eigenfunctions of \hat{h} .

The one-body part of the Hamiltonian for the one-dimensional quantum dot is,

$$\hat{h} = \hat{t} + \hat{v} = \frac{\hat{p}^2}{2m} + \frac{1}{2}m\omega^2\hat{x}^2, \quad (7.3)$$

where the potential, $\hat{v} = \frac{1}{2}m\omega^2\hat{x}^2$, forms the well known harmonic potential, making this example implementation a harmonic quantum dot. In a general one-dimensional system, this potential could readily be exchanged for something else. For instance that of the *double well*,

$$\hat{v} = \frac{1}{2}m\omega^2 \left(\hat{x}^2 + \frac{1}{4}l^2 - l|\hat{x}| \right), \quad (7.4)$$

where l is the width of a barrier in the middle of the parabolic potential. We have implemented several other potentials, which we summarise in section 7.2.1.

In atomic units we can set $\hbar = m = 1$. Substituting into the momentum operator, $\hat{p} = -i\hbar(\hat{\partial}/\partial x)$, this gives us

$$\hat{h} = -\frac{1}{2} \frac{\partial^2}{\partial x^2} + \hat{v}. \quad (7.5)$$

The second-order derivative can be approximated by the central difference formula for some function $f(x)$, yielding

$$f''(x) = \frac{f(x + dx) - 2f(x) + f(x - dx)}{dx^2}, \quad (7.6)$$

for some small dx . This means that we approximate the Hamilton operator of the

system (Equation 7.5) by a matrix,

$$h_q^p = \begin{pmatrix} 1/dx^2 + v_1 & -1/2dx^2 & & \cdots \\ -1/2dx^2 & 1/dx^2 + v_2 & -1/2dx^2 & \cdots \\ \ddots & -1/2dx^2 & 1/dx^2 + v_3 & -1/2dx^2 & \ddots \\ & \ddots & \ddots & \ddots & \ddots \\ \ddots & & -1/2dx^2 & 1/dx^2 + v_{n-1} & -1/2dx^2 \\ & & & \ddots & -1/2dx^2 & 1/dx^2 + v_n \end{pmatrix}, \quad (7.7)$$

and we have thus transformed the time-independent Schrödinger equation

$$\hat{h} |\phi\rangle = \epsilon |\phi\rangle, \quad (7.8)$$

into a matrix equation which constitutes a better representation on a computer. Here n is the number of points used to numerically represent the wavefunction and Hamiltonian matrix representation. This is done with some generic eigenvalue solver, for instance `numpy.linalg.eigh(...)`. The eigenfunctions $|\phi\rangle$ provide the foundation for the single-particle functions we need.

Since we would like to model interactions between particles we need something more than just a numerical representation of the one-body operator. We therefore need to compute Coulomb integrals. The Coulomb integral matrix elements u_{rs}^{pq} is computed in several steps, starting with an “inner intergral” over all all space and two and two single-particle functions,

$$u_s^q = \int \phi_q(x_1) \frac{\alpha}{(x_1 - x_2)^2 + a^2} \phi_s(x_2) dx, \quad (7.9)$$

where α is the interaction strength parameter and a is called the shielding parameter and is necessary for this integral to be calculable, as it avoids singular values in the integrand at $x_1 = x_2$. Numerically, this part is divided into two functions in our python implementation,

```
def _shielded_coulomb(x_1, x_2, alpha, a):
    return alpha / np.sqrt((x_1 - x_2) ** 2 + a ** 2)

def _compute_inner_integral(spf, l, num_grid_points, grid, alpha, a):
    inner_integral = np.zeros((l, l, num_grid_points), dtype=np.complex128)

    for q in range(l):
        for s in range(l):
            for i in range(num_grid_points):
                inner_integral[q, s, i] = _trapz(
                    spf[q]
                    * _shielded_coulomb(grid[i], grid, alpha, a)
                    * spf[s],
```

```
    grid)

return inner_integral
```

The inner orbital is subsequently used in the computation of the orbital integral,

$$u_{rs}^{pq} = \int \phi_p u_s^q \phi_r dx, \quad (7.10)$$

which is implemented numerically as follows,

```
def _compute_orbital_integrals(spf, l, inner_integral, grid):
    u = np.zeros((l, l, l, l), dtype=np.complex128)

    for p in range(l):
        for q in range(l):
            for r in range(l):
                for s in range(l):
                    u[p, q, r, s] = _trapz(
                        spf[p] * inner_integral[q, s] * spf[r], grid)

    return u
```

Each integral is solved by the trapezoidal scheme, which approximates the integral by

$$\int_x^{x+\Delta x} f(x) dx \approx \Delta x \frac{f(x + \Delta x) - f(x)}{2}. \quad (7.11)$$

Needless to say, computing the Coulomb integrals is one of the more intensive tasks, and we therefore make great use of one the fly compilation from the `numba` [31] module for Python.

One-dimensional potentials

We provide several one-dimensional potential classes (Table 7.1) that can be passed to the `setup_system(Potential)` method in the `ODQD` class. All these potentials are implemented as subclasses of the abstract base class `OneDimPotential`. The only thing necessary for an inheriting class to implement is the primitive `__call__` method which takes position on the grid, x , as argument, and must return the value of the potential at that point x .

The parabolic harmonic oscillator potential, which we have made most use of and which is discussed above is implemented as follows,

```
class HOPotential(OneDimPotential):
    def __init__(self, omega):
        self.omega = omega

    def __call__(self, x):
        return 0.5 * self.omega ** 2 * x ** 2
```

```
class quantum_systems.ODQD
    (n, l, grid_length, num_grid_points, a=0.25, alpha=1.0)

Create One-Dimensional Quantum Dot basis set.

Parameters
    n(int) Number of electrons
    l(int) Number of spinorbitals
    grid_length(int, float) Space over which to construct wavefunction.
    num_grid_points(int, float) Number of points for construction of wavefunction.
    a(float, default 0.25) Coulomb screening parameter.
    alpha(float, default 1.0) Coulomb strength parameter.

Attributes
    h One-body matrix Type np.array
    f Fock matrix Type np.array
    u Two-body matrix Type np.array

Methods
    setup_system(Potential=None)
        Must be called in order to compute basis functions. The method will revert to regular harmonic oscillator potential with  $\omega = 0.25$  if no potential has been provided. Optional potentials include one-dimensional double well potentials.
    construct_dipole_moment()
        Constructs dipole moment. This method is called by setup_system(). Necessary when constructing custom systems with time development.
```

Table 7.1: One-dimensional potential classes in `quantum_systems`.

DWPotential	$\frac{1}{2}\omega^2 (x^2 + \frac{1}{4}l^2 - l x)$
DWPotentialSmooth	$\frac{1}{2a^2} (x + \frac{a}{2})^2 (x - \frac{a}{2})^2$
GaussianPotential	$Ae^{-\frac{(x-\mu)^2}{2\sigma^2}}$
AtomicPotential	$-\frac{Z_a}{\sqrt{x^2+c}}$

7.2.2 Two Dimensions

The one-body part of the Hamiltonian for a two-dimensional quantum dots is almost identical to the one-body part for a one-dimensional quantum dot. In cartesian coordinates we merely include a second coordinate y in the potential as well as an x , but because we have analytical expressions for the Coulomb integrals in polar coordinates[85], we write the one-body operator in polar coordinates as well,

$$\hat{h} = \frac{\hat{p}^2}{2m} + \frac{1}{2}m\omega^2\hat{r}^2 = -\frac{\hbar^2}{2m}\left(\frac{\partial^2}{\partial r^2} + \frac{1}{r}\frac{\partial}{\partial r} + \frac{1}{r^2}\frac{\partial^2}{\partial\theta^2}\right) + \frac{1}{2}m\omega^2\hat{r}^2. \quad (7.12)$$

The wavefunctions for a two-dimensional harmonic oscillator can be written using the spherical harmonics,

$$\phi(r, \theta) = N_{nm}R_{nm}(r)Y_m(\theta) = N_{nm}(ar)^{|m|}L_n^{|m|}(a^2r^2)e^{-a^2r^2/2}e^{im\theta}, \quad (7.13)$$

where $a = \sqrt{m\omega/\hbar}$ si the Bohr radius, $L_n^{|m|}$ is the associated Laguerre polynomials, n and m are the principal and the azimuthal quantum numbers respectively², and N_{nm} is a normalisation factor given by,

$$N_{nm} = a\sqrt{\frac{n!}{\pi(n+|m|)!}}. \quad (7.14)$$

The energy eigenvalues of a two-dimensional harmonic oscillator is given by

$$\epsilon_{nm} = \hbar\omega(2n + |m| + 1). \quad (7.15)$$

It is very beneficial that such a nice expression exists, because the one-body matrix elements of a harmonic oscillator is simply,

$$\langle\phi_p|\hat{h}|\phi_q\rangle = \hat{h}_q^p = \epsilon_p\delta_q^p. \quad (7.16)$$

These matrix elements encompass both the kinetic energy operator matrix element and potential energy matrix element. If we deal with completely non-interacting particles not much more would be needed. We see, however, that this form of one-body matrix elements necessitate a mapping from the general coordinates p, q , as used above, and the quantum numbers n, m .

This functionality $(n, m) \mapsto p$ is achieved by the following python function

```
def get_index_p(n, m):
    num_shells = 2 * n + abs(m) + 1

    previous_shell = 0
    for i in range(1, num_shells):
        previous_shell += i
```

²There is usually another quantum number called the magnetic quantum number. Because of our restriction to two dimensions, this quantum number does not appear. In three dimensions we would usually denote the azimuthal quantum number by l and the magnetic quantum number by m or m_l . A fourth quantum number is the spin projection quantum number commonly written m_s .

```
class quantum_systems.TwoDimensionalHarmonicOscillator
    (n, l, radius_length, num_grid_points, omega=0.25, mass=1)
```

Create Two-Dimensional Quantum Dot basis set.

Parameters

- n(int)** Number of electrons
- l(int)** Number of spinorbitals
- grid_length(int or float)** Space over which to construct wavefunction.
- num_grid_points(int or float)** Number of points for construction of wavefunction.
- omega(float, default 0.25)** Angular frequency of harmonic oscillator potential.
- mass(int or float, default 1.0)** Mass of electrons. Atomic units is used as default.

Attributes

- h** One-body matrix **Type** np.array
- f** Fock matrix **Type** np.array
- u** Two-body matrix **Type** np.array

Methods

- setup_system()**
Must be called in order to compute basis functions.
- construct_dipole_moment()**
Constructs dipole moment. This method is called by **setup_system()**.

```
current_shell = previous_shell + num_shells

if m == 0:
    if n == 0:
        return 0

    p = previous_shell + (current_shell - previous_shell) // 2

    return p

elif m < 0:
    return previous_shell + n

else:
    return current_shell - (n + 1)
```

It will also be necessary to map back $p \mapsto (n, m)$,

```
def get_indices_nm(p):
```

```

n, m = 0, 0
previous_shell = 0
current_shell = 1
shell_counter = 1

while current_shell <= p:
    shell_counter += 1
    previous_shell = current_shell
    current_shell = previous_shell + shell_counter

middle = (current_shell - previous_shell) / 2 + previous_shell

if (current_shell - previous_shell) & 0x1 == 1 and abs(
    p - math.floor(middle)
) < 1e-8:
    n = shell_counter // 2
    m = 0

return n, m

if p < middle:
    n = p - previous_shell
    m = -((shell_counter - 1) - 2 * n)

else:
    n = (current_shell - 1) - p
    m = (shell_counter - 1) - 2 * n

return n, m

```

An important difference between the one-dimensional quantum dot and a two-dimensional quantum dot is that in the latter we have energy degeneracies of the eigenstates, as shown in Figure 7.2. In this figure we have included a spin-up and a spin-down state for each n, m -state. This spin feature is not in any way included in Equation 7.13, but we may represent the spin condition by including it in the orthonormality conditions of the wavefunctions,

$$\langle n_1 m_1 \sigma_1 | n_2 m_2 \sigma_2 \rangle = \delta_{n_1 n_2} \delta_{m_1 m_2} \delta_{\sigma_1 \sigma_2}, \quad (7.17)$$

where σ is the spin.

Because the electrons we will be studying are interacting, we need two-body matrix elements u_{rs}^{pq} as well. The analytical formula for the Coulomb interaction integrals,

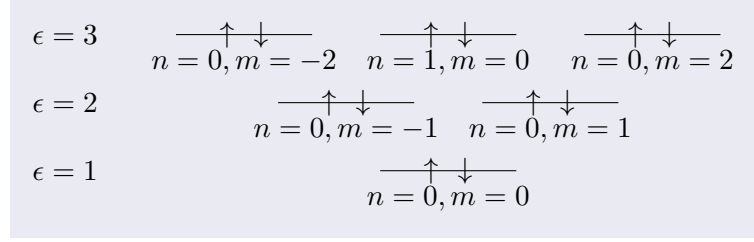


Figure 7.2: The lowest three energy levels in the two-dimensional quantum dot. Each arrow represents a spin up or a spin down state with the quantum numbers n and m as listed below. This pattern goes on indefinitely with the addition of one bar (two oscillators) per level.

provided by Anisimovas and Matulis [85] is

$$\begin{aligned} \langle \phi_1 \phi_2 | \hat{u} | \phi_3 \phi_4 \rangle = & \delta_{s_1, s_4} \delta_{s_2, s_3} \delta_{m_1 + m_2, m_3 + m_4} \left[\prod_{i=1}^4 \frac{n_i!}{(|m_i| + n_i)} \right]^{1/2} \sum_{(4)j=0}^n \frac{(-1)^{j_1+j_2+j_3+j_4}}{j_1! j_2! j_3! j_4!} \\ & \times \left[\prod_{i=1}^n \binom{n_i + |m_i|}{n_i + j_i} \right] \frac{1}{2^{(G+1)/2}} \sum_{(4)l=0}^{\gamma} (-1)^{\gamma_2 + \gamma_3 - l_2 - l_3} \\ & \times \delta_{l_1 + l_2, l_3 + l_4} \left[\prod_{i=1}^4 \binom{\gamma_i}{l_i} \right] \Gamma\left(1 + \frac{L}{2}\right) \Gamma\left(\frac{G - L + 1}{2}\right). \end{aligned} \quad (7.18)$$

The symbols j_i are integer summation indices (regular indices) running from 0 to n_i . The symbols γ_i stand for numbers,

$$\begin{aligned} \gamma_1 &= j_1 + j_4 + (|m_1| + m_1)/2 + (|m_4| - m_4)/2 \\ \gamma_4 &= j_1 + j_4 + (|m_1| - m_1)/2 + (|m_4| + m_4)/2 \end{aligned}$$

γ_2 and γ_3 can be obtained by replacing indices $1 \rightarrow 2$ and $4 \rightarrow 3$. Moreover,

$$\sum_{(4)j=0}^n = \sum_{j_1=0}^{n_1} \sum_{j_2=0}^{n_2} \sum_{j_3=0}^{n_3} \sum_{j_4=0}^{n_4}, \quad G = \sum_i \gamma_i, \quad L = \sum_i l_i$$

For the implementation of this expression for the purpose of computing the two-dimensional quantum dot Coulomb integral matrix elements, we refer the reader to section C.1.

Dipole Moments

For our implementation of time dependent Hamiltonians, outlined below, we make use of a dipole approximation of an electric field. For this reason it is necessary to compute dipole moments. The transitions rules of quantum mechanics stem from evaluating matrix elements of this kind,

$$\mathbf{d}_q^p = \langle \phi_p | \hat{\mathbf{r}} | \phi_q \rangle = \hat{i} \langle \phi_p | \hat{x} | \phi_q \rangle + \hat{j} \langle \phi_p | \hat{y} | \phi_q \rangle, \quad (7.19)$$

where ϕ_p, ϕ_q are single-particle functions, on the type in Equation 7.13. As we will be representing the two-dimensional quantum dots in polar coordinates, we can rewrite this to,

$$\mathbf{d}_q^p = \hat{i} \langle \phi_p | \hat{r} \cos \hat{\theta} | \phi_q \rangle = \hat{j} \langle \phi_p | \hat{r} \sin \hat{\theta} | \phi_q \rangle. \quad (7.20)$$

The integrals we need to compute are

$$\langle \phi_p | r \cos \theta | \phi_q \rangle = N_{nm}^* N_{nm} \int_0^\infty r^2 R_{nm}^*(r) R_{nm}(r) dr \int_0^{2\pi} \cos \theta Y_m^*(\theta) Y_m(\theta) d\theta \quad (7.21)$$

$$\langle \phi_p | r \sin \theta | \phi_q \rangle = N_{nm}^* N_{nm} \int_0^\infty r^2 R_{nm}^*(r) R_{nm}(r) dr \int_0^{2\pi} \sin \theta Y_m^*(\theta) Y_m(\theta) d\theta. \quad (7.22)$$

The radially dependent integrals are the most difficult to compute, and we compute this symbolically with `sympy`. For the angular integrals, we can find analytical expressions that can be evaluated quickly,

$$\int_0^{2\pi} \cos \theta e^{i\bar{m}\theta} = \frac{e^{i\bar{m}\theta}}{1 - \bar{m}^2} (\sin \theta - i\bar{m} \cos \theta) \Big|_0^{2\pi}, \quad (7.23)$$

where $\bar{m} = (m_q - m_p) \in \mathbb{Z}$. We see that the integral evaluates to 0 for all possible values of \bar{m} except for $\bar{m} = \pm 1$. This special case warrants further investigation,

$$\int_0^{2\pi} \cos \theta e^{i\theta} d\theta = \int_0^{2\pi} \cos^2 \theta + i \cos \theta \sin \theta d\theta = \frac{1}{2} \sin \theta \cos \theta + \frac{\theta}{2} + \frac{i}{2} \sin^2 \theta \Big|_0^{2\pi} = \pi. \quad (7.24)$$

Similarly,

$$\begin{aligned} \int_0^{2\pi} \sin \theta e^{i\bar{m}\theta} d\theta &= \frac{e^{i\bar{m}\theta}}{1 - \bar{m}^2} (i\bar{m} \sin \theta - \cos \theta) \Big|_0^{2\pi} = 0 \quad \forall \bar{m} \in \mathbb{Z} \neq 1 \\ \int_0^{2\pi} \sin \theta e^{i\theta} d\theta &= \int_0^{2\pi} \cos \theta \sin \theta + i \sin^2 \theta d\theta = \frac{1}{2} \sin \theta - \frac{i}{2} \sin \theta \cos \theta + i \frac{\theta}{2} \Big|_0^{2\pi} = i\pi \end{aligned} \quad (7.25)$$

This is a very nice result, as it conforms with the selection rule related to the azimuthal quantum number m .

7.2.3 Two-Dimensional Double Well

The extension from a single two-dimensional quantum dot to a double quantum dot is a relatively straight-forward procedure, as it is a mere perturbation of the regular single dot. There are at least two ways to implement the potential of a double well in two dimensions. One method is to add a fourth-degree polynomial potential along one cartesian axis, resulting in a smooth “bump” dividing the two potential wells. We have opted for another method, with the an absolute value function resulting in a sharp edge. The potential reads as follows,

$$\hat{h} = \frac{\hat{p}}{2m} + \frac{1}{2} m \omega^2 \hat{r}^2 + \frac{1}{2} m \omega^2 \left(\frac{1}{4} l^2 - l |\hat{x}| \right), \quad (7.26)$$

```
class quantum_systems.TwoDimensionalDoubleWell
    (n, l, radius_length, num_grid_points, barrier_strength=1.0, l_ho_factor=1.0,
     omega=0.25, mass=1)
```

Create Two-Dimensional Quantum Dot with double well potential, i.e. the Double Dot. This class inherits from **TwoDimensionalHarmonicOscillator**.

Parameters

- n(int)** Number of electrons
- l(int)** Number of spinorbitals
- grid_length(int or float)** Space over which to construct wavefunction.
- num_grid_points(int or float)** Number of points for wavefunction.
- barrier_strength(float, default 1.0)** Barrier strength in double well potential.
- l_ho_factor(float, default 1.0)** Normal HO vs double well basis function.
- omega(float, default 0.25)** Angular frequency of harmonic oscillator potential.
- mass(int or float, default 1.0)** Mass of electrons. Atomic units is used as default.

Attributes

- h** One-body matrix **Type** np.array
- f** Fock matrix **Type** np.array
- u** Two-body matrix **Type** np.array

Methods

setup_system(axis=0)

Must be called in order to compute basis functions. Parameter *axis* decides to which axis the well barrier is aligned. $(0, 1) = (x, y)$.

where l is the “strength” of the barrier between the wells. We can readily see what makes the barrier so acute, namely the absolute value of the position operator, $|\hat{x}|^3$.

In Equation 7.26, we immediately recognise the first two terms as the normal quantum dot. This is beneficial, as we can reuse single-particle functions from Equation 7.13. This means that the one-body matrix elements are simply,

$$\begin{aligned} h_q^p &= \epsilon_p \delta_q^p + \frac{1}{2} m \omega^2 \langle \phi_p | \frac{1}{4} l^2 - l |\hat{x}| |\phi_q \rangle \\ &= \epsilon_p \delta_q^p + \frac{1}{8} m \omega^2 l^2 \delta_q^p - \frac{1}{2} m \omega^2 l \langle \phi_p | \hat{x} | \phi_q \rangle. \end{aligned} \quad (7.27)$$

We see from the first two terms a perturbation in the diagonal matrix elements, i.e.

$$\epsilon_p^{\text{DW}} = \epsilon_p + \frac{1}{8} m \omega^2 l^2, \quad (7.28)$$

and that we need only compute the matrix elements of the position operator. Because we are still working with polar coordinates, we make the necessary transformation, and

³Here we might as well have used the position operator \hat{y} , which would have resulted in an equivalent potential, rotated ninety degrees.

the integral becomes

$$\langle \phi_p | |\hat{x}| | \phi_q \rangle = \int_0^\infty \int_0^{2\pi} \phi_{n_p m_p}^*(r, \theta) r^2 |\cos \theta| \phi_{n_q m_q}(r, \theta) dr d\theta \quad (7.29)$$

We see that the wavefunctions ϕ_{nm} are the same as for the unperturbed two-dimensional quantum dot, and this directs us to the same kind of integrals as for the dipole calculations above. The radial integral is cumbersome, and therefore left for a symbolic solver, but for the angular integral we have,

$$\begin{aligned} \int_0^{2\pi} |\cos \theta| e^{i\bar{m}\theta} d\theta &= \int_0^\pi \cos \theta e^{-i\bar{m}\theta} d\theta - \int_\pi^{2\pi} \cos \theta e^{-i\bar{m}\theta} d\theta \\ &= \int_0^\pi (\cos(\theta\bar{m}) - i \sin(\theta\bar{m})) \cos \theta \\ &\quad - \int_\pi^{2\pi} (\cos(\theta\bar{m}) - i \sin(\theta\bar{m})) \cos \theta \\ &= \left[\frac{e^{-\bar{m}\theta}}{(1 - \bar{m}^2)} (\sin \theta - i\bar{m} \cos \theta) \right]_0^\pi \\ &\quad - \left[\frac{e^{-\bar{m}\theta}}{(1 - \bar{m}^2)} (\sin \theta - i\bar{m} \cos \theta) \right]_\pi^{2\pi} \\ &= \frac{2i\bar{m}}{1 - \bar{m}^2} (e^{-i\pi\bar{m}} + 1) = \frac{4i\bar{m}}{1 - \bar{m}^2}, \quad \bar{m} = 2k, \quad \forall k \in \mathbb{Z}. \end{aligned} \quad (7.30)$$

where $\bar{m} = (m_q - m_p) \in \mathbb{Z}$. We see that this expression is not defined for $\bar{m} = 1$, but inserting for this value in the integral will yield zero as a result. In fact, we see that the integral will evaluate to zero for each odd value of \bar{m} . If the barrier was aligned in the other direction, along the y -axis, a similar computation can be performed for $\sin \theta$ instead of $\cos \theta$.

Since the particles are interacting in the same way as before, there is no need to compute a special version of the Coulomb integral matrix elements for the double well. We do, however, need to transform the single-particle functions and two-body elements from the regular harmonic oscillator basis to an approximate basis for the double-well problem. This can be done via diagonalisation of the one-body Hamiltonian in order to find a matrix of coefficients \mathbf{C} , that performs this basis change,

$$|\phi_q\rangle_{\text{DW}} = \sum_p C_p |\phi_p\rangle_{\text{HO}}, \quad (7.31)$$

which can be inserted into an eigenvalue equation for the one-body operator,

$$\begin{aligned} \hat{h} |\psi_q\rangle_{\text{DW}} &= \epsilon_q |\psi_q\rangle_{\text{DW}} \\ \sum_p \hat{h} C_p |\phi_p\rangle &= \sum_p \epsilon_p C_{pq} |\phi_p\rangle. \end{aligned} \quad (7.32)$$

Assuming that the eigenvalues ϵ_q are eigenvalues for the double well single-particle

functions, we project onto the regular harmonic oscillator basis,

$$\begin{aligned} \sum_p \langle \phi_r | \hat{h} | \phi_p \rangle &= \sum_p C_{pr} \epsilon_p \langle \phi_r | \phi_p \rangle \\ \sum_p h_{pr} C_{pr} &= C_{pr} \epsilon_p \\ \mathbf{hC} &= \mathbf{C}\epsilon \end{aligned} \tag{7.33}$$

This is an eigenvalue equation we can solve in order to obtain the coefficient matrix which transforms from the one basis to the other. This transformation can subsequently be applied to the two-body operator,

$$\langle \psi_\alpha \psi_\beta | \hat{u} | \psi_\gamma \psi_\delta \rangle = C_\alpha^{p*} C_\beta^{p*} \langle \phi_p \phi_q | \hat{u} | \phi_r \phi_s \rangle C_\gamma^r C_\delta^s, \tag{7.34}$$

where summation over same indices is assumed.

7.2.4 Two-Dimensional Magnetic Quantum dots

Extending the two-dimensional quantum dot to be under the influence of a static, transverse magnetic field is only a matter of adding constant terms to the one-body operators. We are now considering a system with the following one-body hamiltonian, where an angular momentum term is added,

$$\hat{h} = \frac{\hat{p}^2}{2m} + \frac{1}{2}m\Omega^2 \hat{r}^2 + \frac{\omega_c}{2} \hat{L}_z, \tag{7.35}$$

where $\Omega = \sqrt{\omega_0^2 + \frac{\omega_c^2}{4}}$ and ω_c is the parameter dictating the strength of the magnetic field, the *Larmor frequency*. We see that this Hamiltonian is the same as the normal two-dimensional quantum dot one-body Hamiltonian (Equation 7.12) for $\omega_c = 0$ as $\Omega \rightarrow \omega_0$. Conversely, if the magnetic field is infinitely strong we see that $\Omega \rightarrow \omega_c/2$ and Equation 7.35 becomes the one-body hamiltonian of a free electron in a transverse magnetic field.

The single-particle functions in Equation 7.13, with the adjusted Bohr radius $a = \sqrt{m\Omega/\hbar}$, are also eigenfunctions of the angular momentum L_z . The corresponding energy eigenvalues are simply

$$\epsilon_{nm} = \hbar\Omega(2n + |m| + 1) - \frac{\hbar\omega_c}{2}m. \tag{7.36}$$

We see immediately that the energy undergoes a general shift due to the new Ω which is dependent on ω_c , but also that the energy shift of a particular state is dependent on the sign of the azimuthal quantum number m . These factors will give different degeneracies, as illustrated in Figure 7.3. Such a plot of single-particle particle energies are sometimes referred to as the Fock-Darwin spectrum [86, 87]. With these new degeneracies that are dependent on the Larmor frequency ω_c , comes the challenge of sorting the one-body matrix elements correctly, and ensuring that we keep a closed-shell structure.

Notice in Figure 7.3, that there are lengthy intervals of b -field strength where there is no degeneracy in the eigenenergies. Conversely, for certain specific field strengths

```
class quantum_systems.TwoDimHarmonicOscB
    (n, l, radius_length, num_grid_points, omega_0=1.0, mass=1, omega_c=0)
```

Create Two-Dimensional Quantum Dot with constant homogenous magnetic field.
This class inherits from `TwoDimensionalHarmonicOscillator`.

Parameters

- `n(int)` Number of electrons
- `l(int)` Number of spinorbitals
- `grid_length(int or float)` Space over which to construct wavefunction.
- `num_grid_points(int or float)` Number of points for wavefunction.
- `omega_0(float, default 1.0)` Part of harmonic osc. not dep. on magnetic field.
- `mass(int or float, default 1.0)` Mass of electrons. Atomic units is used as default.
- `omega_c(float, default 0)` Larmor frequency.

Attributes

- `h` One-body matrix **Type** np.array
- `f` Fock matrix **Type** np.array
- `u` Two-body matrix **Type** np.array

Methods

- `setup_system()`
Must be called in order to compute basis functions.
- `construct_dipole_moment()`
Constructs dipole moment. This method is called by `setup_system()`.

there are very interesting shell structures with diverse energies and new degeneracies. Such accidental bunching occurs for $\omega_c/\omega = 1/\sqrt{2}, 2/\sqrt{3}, 3/2, 4/\sqrt{5} \dots$. We also see from figure Figure 7.3 that for an infinitely strong magnetic field as $\omega_c/\omega \rightarrow \infty$, in the free particle limit, that the energy levels form a sequence of so-called Landau bands.

As for the computation of the basis set, not much needs to be added in the computation than the extra energy to the diagonal part of the one-body matrix elements h_q^p , as everything else is the same, including the two-body Coulomb integrals. But, as we have already mentioned and displayed in Figure 7.3, for increasing strength of the magnetic field, the eigenenergies as function of ω_c eventually cross over one another. The magnetic field has the effect of decreasing the energy of a state with $m > 0$ and increasing the energy of a state with $m < 0$. This means that it is necessary to sort the eigenvalues after they have been computed.

7.3 Constructing a Custom System

We have constructed a subclass of the `QuantumSystem` base class called `CustomSystem` with the intent of interfacing with other quantum chemistry libraries. This interfacing allows us to extract basis sets for other systems, like atoms and molecules, that will

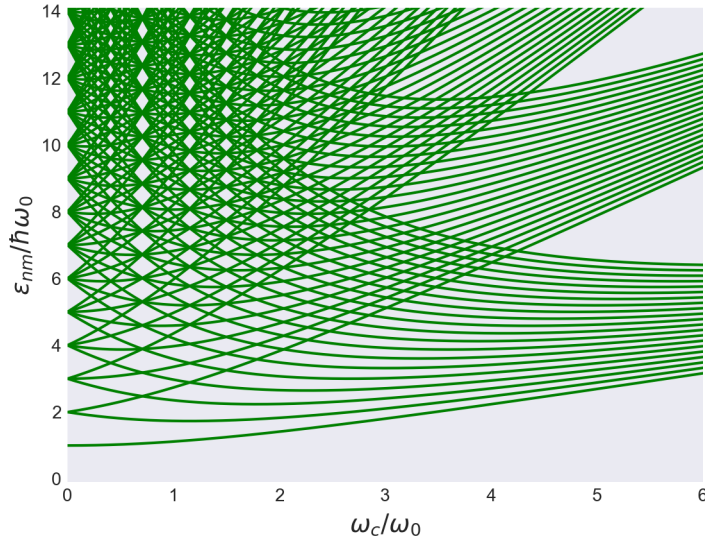


Figure 7.3: A few of the lowest eigenvalues ϵ_{nm} for a two-dimensional quantum dot for transverse magnetic field of increasing strength. This plot of the single-particle energies form the Fock-Darwin spectrum. Some states for very high values of m are omitted to make the formation of Landau bands in strong fields more visible.

function with the coupled cluster solvers we have implemented.

The function of the member methods in the `CustomSystem` class should be evident from their names. One can set the one-body matrix elements with `set_h(h, add_spin)`, set dipole matrix with `set_dipole_moment(dipole_moment, add_spin)` and so on. How one would go about getting these structures is somewhat non-trivial, at least for someone not used to using quantum chemistry libraries. We have therefore added functions to the `quantum_systems` module that do just that. The functions

```
quantum_systems.custom_system.construct_psi4_system() and
quantum_systems.custom_system.construct_pyscf_system()
```

extracts the one-body matrix, Coulomb intergrals, dipole moment, overlap matrix and nuclear repulsion from Psi4[4] and PySCF[3], respectively. The functions are provided in full in section C.2 and section C.3. We have picked Psi4 and PySCF to interface with as they seem to be widely used in the quantum chemistry community. Psi4 has 354 stars and 235 forks, while PySCF has 308 stars and 175 forks on GitHub. Arguably this can be considered widely popular considering the specificity of the topic.

7.4 Time Evolution

In order to compute the time-development of a quantum system, we add a time-dependent term to the Hamiltonian that describes the system. The class `TimeEvolutionOperator` is an abstract base class, which defines components necessary to make such

```
class quantum_systems.CustomSystem
```

Constructs custom quantum system, where a uses can add matrix elements for other sources. The purpose of this class is to allow usage of quantum many-body solvers that function with *quantum_systems* module using other sources basis sets.

Methods:

`set_h(h, add_spin=False)`

Add one-body matrix elements, i.e. matrix elements from non-interacting part of Hamiltonian.

Parameters:

`h (np.array)` One-body matrix

`add_spin (bool)` Enforces spin orthogonality

`set_u(u, add_spin=False, anti_symmetrize=False)`

Add two-body matrix elements, i.e. matrix elements from interacting part of Hamiltonian.

Parameters:

`u (np.array)` Two-body matrix

`add_spin (bool)` Enforces spin orthogonality

`anti_symmetrize (bool)` Anti-symmetrises two-body matrix

`set_s(u, add_spin=False)`

Add overlap matrix

Parameters:

`s (np.array)` Overlap matrix

`add_spin (bool)` Enforces spin orthogonality

`set_dipole_moment(dipole_moment, add_spin=False)`

Add dipole moment, i.e. transition matrix.

Parameters:

`dipole_moment (np.array)` Dipole moment

`add_spin (bool)` Enforces spin orthogonality

`set_spf(spf, add_spin=False)`

Add single-particle functions, i.e. eigenfunctions of non-interacting part of Hamiltonian.

Parameters:

`spf (np.array)` Single-particle functions

`add_spin (bool)` Enforces spin orthogonality

`set_nuclear_repulsion_energy (set_nuclear_repulsion_energy)`

Add nuclear repulsion energy. For atoms and molecules.

Parameters:

`nuclear_repulsion_energy (float)` Nuclear reulsion energy

```
class quantum_systems.LaserField (laser_pulse, polarization_vector=None)
```

Implementation of laser field. Needs time-dependent *callable* to function properly.

Attributes:

`is_one_body_operator` Always `True` Type `Bool`

Methods:

`h_t(current_time)`

Computes one-body operator as a sum of the one-body operator of the system and product of `laser_pulse` parameter at current time, `polarization_vector` parameter and `dipole_moment` attribute of system.

time-dependent operators. A time-dependent operator usually applies solely the one- or two-body part of the Hamiltonian, and more often just the non-interacting one-body operator. For this reason we have implemented abstract attributes in the `TimeEvolutionOperator` which will make it possible for the time-dependent coupled cluster solver to determine what parts of the Hamiltonian is necessary to update for each time step.

A common time evolution operator used in the study is a dipole approximation of a laser field. We have implemented a class `LaserField`, which makes a simulation of such a field possible. This is a relatively simple time evolution operator, as it only affects the one-body part of the Hamiltonian, i.e. the non-interacting part. Consequently, the `LaserField` class only needs to switch the `is_one_body_operator` to `True` and implement the method `h_t(current_time)`. The time-dependent pulse, incorporating the shape and frequency of the laser is passed as a parameter to the class. This can be any callable type. The polarisation of the field is also passed to the class as a simple static vector, meaning that as of now the class only allows for linear polarisation. The electric field in the dipole approximation typically reads

$$\mathbf{E}(t) = \epsilon \mathbf{E}_0(t) \cos(\omega t), \quad (7.37)$$

where ϵ is the polarisation vector, $\mathbf{E}_0(t)$ defines a time-dependent envelope of the laser pulse, the cosine term makes sure the laser pulse is a waveform and ω is the angular frequency of the laser light.

```
class quantum_systems.TimeEvolutionOperator
```

Abstract base class for time evolution operator

Attributes:

is_one_body_operator

Property used to determine if the time-evolution operator only applies to the one-body part of the Hamiltonian.

Type *bool*

is_two_body_operator

Property used to determine if the time-evolution operator only applies to the two-body part of the Hamiltonian.

Type *bool*

Methods:

set_system(*system*)

Internal function used to set callback system. This is done in the *QuantumSystem* class and allows the user to specify the time-evolution operator parameters when setting the operator.

Parameters:

system (*QuantumSystem*) System the time-evolution operator is applied to.

h_t(*current_time*)

Function computing the one-body part of the Hamiltonian for a specified time.

Parameters:

current_time (*float*) One-body operator evaluated at specified time.

Returns: One-body operator.

Return type: np.array

u_t(*current_time*)

Function computing the two-body part of the Hamiltonian for a specified time.

Parameters:

current_time (*float*) Two-body operator evaluated at specified time.

Returns: Two-body operator.

Return type: np.array

Chapter 8

Coupled Cluster

The main product of this study is manifested in the `coupled_cluster` module for Python. This module is designed to fit together with the `quantum_systems` module described in the previous chapter. We have tried to make this module easy to extend, resulting in a framework where every solver scheme inherits from an abstract parent class that specifies what must be implemented in order to make a supplemental solver class operational in conjunction with the rest of the framework.

As a beginning to this project, which we hope will continue to grow and be used, we have implemented several different ground state solver classes, and several time-dependent solver classes. In order of increasing sophistication and elegance, we have a ground state- and a time-dependent solver for both the coupled cluster method with double excitations (CCD), the coupled cluster method with singles- and double excitations (CCSD), and for the orbital-adaptive coupled cluster method with double excitations (OACCD). The time-dependent solvers within a particular category are dependent on its ground state counterpart, but the ground state solvers can be used independently.

A complete diagrammatic class hierarchy of the `coupled_cluster` module can be found in Figure 8.1. This class hierarchy also illustrates how the `coupled_cluster` module fits into and works with the `quantum_systems` module. This figure is the same figure as the one shown in Figure 7.1, but inserting the class diagram here as well should make this chapter easier to read.

The `coupled_cluster` module can be installed from github via `pip` by the following command,

```
pip install git+https://github.com/Schoyen/coupled-cluster.git
```

If one prefers, the same task can be accomplished by the following commands,

```
git clone https://github.com/Schoyen/coupled-cluster.git
cd coupled-cluster
pip install .
```

We have supplied environment specifications for `conda`, with requirement specifications for the convenience of the user. Assuming the git repository is cloned properly,

```
conda environment create -f environment.yml
```

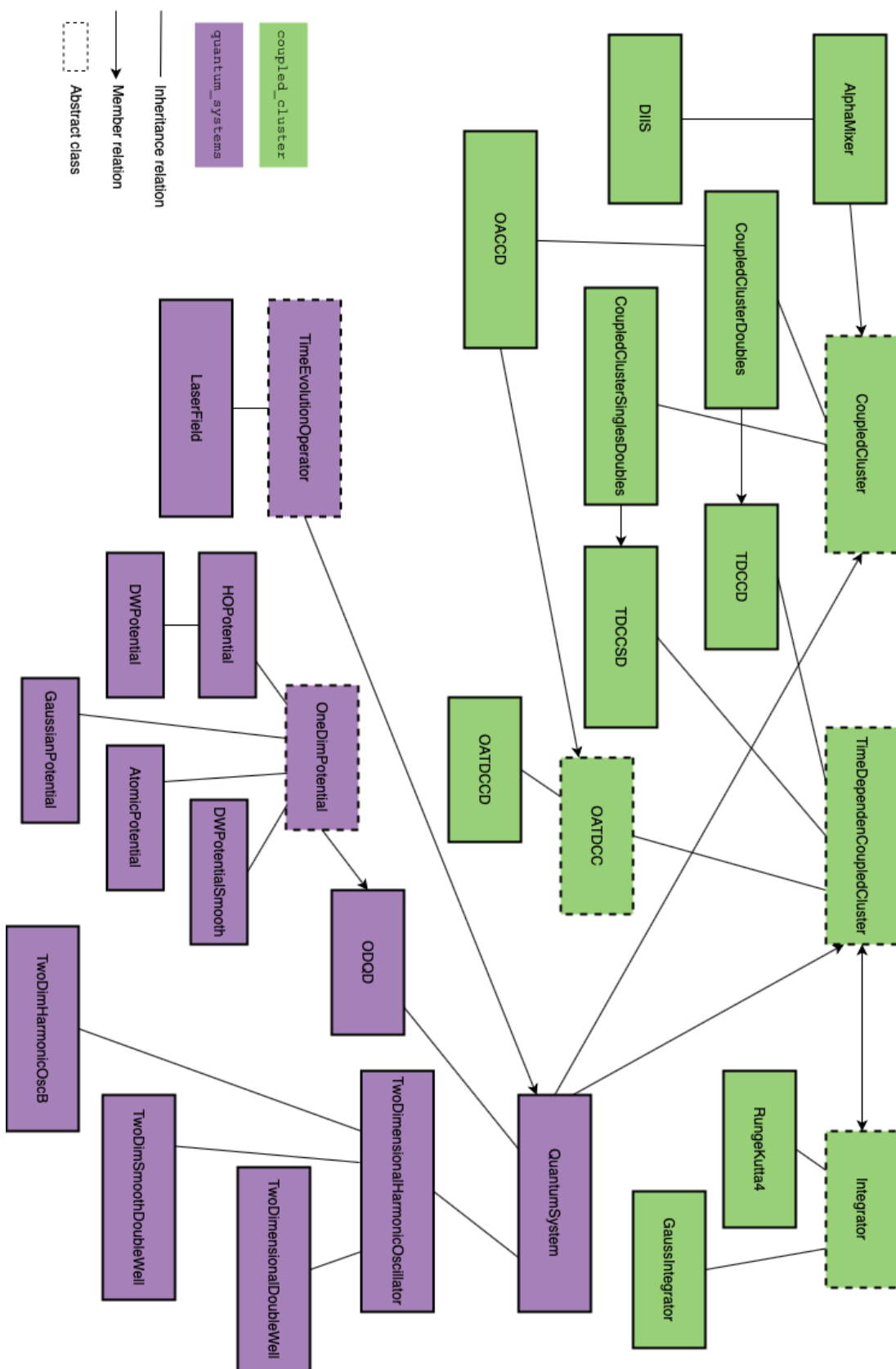


Figure 8.1: Class hierarchy of the two Python modules, `coupled_cluster` and `quantum_systems`.

Activate the environment with,

```
conda activate cc
```

Full documentation of this module, which we hope will be kept up to date with any future revisions can be found at www.coupled-cluster.com.

8.1 Ground State Computations

Before any development in time can be performed, we need to arrive at configurations of systems that we can be somewhat certain exist in nature. This makes the implementation of ground state solvers necessary. We have implemented several ground state solvers; the `CoupledClusterDoubles` and `CoupledClusterSinglesDoubles` are based on the theoretical framework from the Lagrangian formulation of Coupled Cluster theory (see subsection 6.4.2), while `OATDCCD` is a ground state version of an orbital-adaptive ground state coupled cluster solver with double excitations. Moreover, we constructed a data structure for the amplitudes in the `AmplitudeContainer` class and we have implemented two “mixer” classes that help with convergences of the ground state solvers, `AlphaMixer` and `DIIS`.

```
class coupled_cluster.cc_helper.AmplitudeContainer (t, l, np)
```

Container for amplitude functions.

Parameters:

- `t(list, tuple, set)` τ amplitudes
- `l(list, tuple, set)` λ amplitudes
- `np(module)` Matrix library, e.g. numpy, cupy etc

Attributes:

- `t` τ amplitudes
- `l` λ amplitudes

Methods:

- `unpack()`
 - Returns:** Amplitudes
 - Return type:** generator
- `asarray()`
 - Returns:** Amplitude vector
 - Return type:** `np.array`

8.1.1 Representation of Amplitudes

The most central structure in any Coupled Cluster solver the way we represent the amplitudes. The amplitudes are what define the true structure of the wavefunction as

a linear combination of single-particle functions contained in the reference state Slater determinant. We have found it beneficial to implement a special container class for the amplitudes, aptly called `AmplitudeContainer`.

The `AmplitudeContainer` class is built as a data structure for the amplitude functions, and comprises all methods and attributes to serve this purpose. This includes overloading of primitive methods of the base python `Object` type.: `__add__` and `__radd__` enables adding a scalar or properly shaped vector to the amplitudes, `__mul__` and `__rmul__` allows for multiplication with scalars and vectors, and `__iter__` is implemented to make the class an iterable. In summary, the `AmplitudeContainer` functions as a fully operational data structure for amplitudes of coupled cluster solver, with both τ and λ amplitudes. The τ -amplitudes are first introduced in 6.1 and the λ -amplitudes are introduced in 6.4.2.

8.1.2 Coupled Cluster Base Class

All ground state solvers within the `coupled_cluster` module are built as sub-classes of the abstract base class `CoupledCluster`. The most important method of this class is the `compute_ground_state()` method. This method in turn calls the `iterate_t_amplitudes()` and `iterate_l_amplitudes()` successively.

As we have outlined in chapter 6, the τ amplitudes are only dependent on τ , while the λ amplitudes are dependent on both τ and λ . Therefore, the τ amplitude equations iterative solver `iterate_t_amplitudes()` is called first, and the λ amplitude equation solver is called second. For illustration, the most important section of the `compute_l_amplitudes()` method is the following

```

for i in range(max_iterations):
    self.compute_l_amplitudes()
    residuals = self.compute_l_residuals()

    if self.verbose:
        print(f"Iteration: {i}\tResiduals (1): {residuals}")

    if all(res < tol for res in residuals):
        break

    assert i < (
        max_iterations - 1
    ), f"The l amplitudes did not converge. Last residual: {residuals}"

```

The equivalent section of code in the `compute_t_amplitudes()` method is nearly identical. The `CoupledCluster` class is supposed to provide a framework for which to implement various coupled cluster ground state solver classes. It therefore has several abstract methods that such subclasses need to implement and overwrite. The most important of these are the methods `compute_t_amplitudes` and `compute_l_amplitudes`, which are supposed to contain the evaluation of amplitude equations for a given coupled cluster truncation and scheme.

```
class coupled_cluster.cc.CoupledCluster
    (system, mixer=<class'coupled_cluster.mix.DIIS'>, verbose=False, np=None)
```

Abstract base class defining a coupled cluster ground state solver class.

Parameters

system(QuantumSystem) A system class from the *quantum_systems* module.
mixer(AlphaMixer, default AlphaMixer) Mixer - Subclass of *AlphaMixer* class.
verbose(bool, default False) Will print results for each iteration if *True*.

Methods

compute_ground_state

```
(t_args=[], t_kwargs={}, I_args=[], I_kwargs={})
```

Computes ground state of system given as parameter. Allows for parameters relating the the τ - and λ amplitudes, for use in inheriting classes.

compute_particle_density()

Computes the one-body density of the system.

Returns: Particle density

Return type: *np.array*

compute_reference_energy()

Computes reference energy

Returns: Reference energy

Return type: *np.array*

get_amplitudes(*get_t_0=False*)

Getter for amplitudes.

Parameters:

get_t_0 (bool, default False) Returns amplitude at $t = 0$ if *True*.

Returns: Amplitudes

Return type: *AmplitudeContainer*

iterate_l_amplitudes (*max_iterations=100, tol=1e-4, **mixer_kwargs*)

Finds solution to λ amplitudes iteratively.

Parameters:

max_iterations (int) The limit of iterations allowed.

tol (float, default $1e^{-4}$) The tolerance for convergence.

iterate_t_amplitudes (*max_iterations=100, tol=1e-4, **mixer_kwargs*)

Finds solution to τ amplitudes iteratively.

Parameters:

max_iterations (int) The limit of iterations allowed.

tol (float, default $1e^{-4}$) The tolerance for convergence.

_get_t_copy Abstract method

_get_l_copy Abstract method

compute_energy Abstract method

compute_one_body_density_matrix Abstract method

compute_t_amplitudes Abstract method

compute_l_amplitudes Abstract method

setup_t_mixer Abstract method

setup_l_mixer Abstract method

compute_t_residuals Abstract method

compute_l_residuals Abstract method

With the hope that the functionality of the rest of the methods in the abstract base class `CoupledCluster` can be inferred from name, and with the goal of brevity we proceed to a study of the simplest ground state coupled cluster solver, namely CCD, implemented in the `CoupledClusterDoubles` class.

8.1.3 Coupled Cluster Doubles

Starting from construction, the `CoupledClusterDoubles` class passes the system, defined through a `QuantumSystem` object to the parent class constructor, along with any keyword arguments, such as turning on verbosity, mixer type and what matrix library to apply. The `QuantumSystem` class will contain all the information necessary to set up the system, i.e. construct a one-body matrix, fock matrix and two-body matrix. These will be used to set up empty arrays for the τ and λ amplitudes. The `compute_initial_guess` is called lastly in the constructor, computing the initial guess of the double-excited amplitudes as

$$\tau^{(0)} = \frac{u_{ij}^{ab}}{D_{ij}^{ab}}, \quad (8.1)$$

where u is the two-body operator and $D_{ij}^{ab} = f_a^a + f_b^b - f_i^i - f_j^j$, where f is the Fock operator.

In the `CoupledClusterDoubles` class specification one would notice that it has implementations of all the abstract methods from the `CoupledCluster` abstract class. The reason for the existence of the class, the `compute_ground_state()` method, is inherited from the parent class, and does the same thing as described above - calling `iterate_t_amplitudes()` and `iterate_l_amplitudes()`. These methods also exist as members of `CoupledClusterDoubles`, but are excluded from the class specification for sake of brevity. It is possible to pass arguments to the the two iterator methods; one list for each iteration method, or as keywords. One can also pass arguments to the mixer through the `compute_ground_state_method()`. An overview of mixing applied to iterative solvers is given in the next section.

The important part of the specific coupled cluster scheme solver is contained in the two methods `compute_t_amplitudes()` and `compute_l_amplitudes()`. These functions evaluate the entire coupled cluster doubles amplitude equations. The computation of each term (diagram) in the amplitude equation is done in separate functions, as calls to `numpy.tensordot()`, for a total of ten terms for the τ amplitude equation in the coupled cluster doubles method including permutation operators:

$$\begin{aligned} 0 = & u_{ij}^{ab} + f_c^b \tau_{ij}^{ac} P(ab) - f_j^k \tau_{ik}^{ab} P(ij) + \frac{1}{4} \tau_{ij}^{ac} \tau_{mn}^{ab} u_{cd}^{mn} + \frac{1}{2} \tau_{ij}^{cd} u_{cd}^{ab} + \frac{1}{2} \tau_{jm}^{cd} \tau_{in}^{ab} u_{cd}^{mn} P(ij) \\ & - \frac{1}{2} \tau_{nm}^{ac} \tau_{ij}^{bd} u_{cd}^{nm} P(ab) + \tau_{im}^{ac} \tau_{jn}^{bd} u_{cd}^{mn} P(ij) + \tau_{im}^{ac} u_{jc}^{bm} P(ab) P(ij) + \frac{1}{2} \tau_{mn}^{ab} u_{ij}^{mn}. \end{aligned} \quad (8.2)$$

The initial guess in equation Equation 8.1 is terms 2 and 3 from Equation 8.2. These terms also form the basis of the iterative scheme, if we move them to the left of the equal sign in Equation 8.2,

$$D_{ij}^{ab} \tau_{ij}^{ab} = g(u, \tau), \quad (8.3)$$

```
class coupled_cluster.cc.CoupledClusterDoubles (system, **kwargs)
```

Implementation of coupled cluster with double excitations ground state solver. Inherits from the `CoupledCluster` abstract base class.

Parameters

`system(QuantumSystem)` A system class from the `quantum_systems` module.

Methods

`compute_ground_state(t_args=[], t_kwargs={}, l_args=[], l_kwargs={})`

Computes CCD ground state of given system.

`compute_initial_guess()` Computes initial guess for amplitudes.

`_get_t_copy()`

Returns: Copy of τ_{ij}^{ab} amplitudes

Return type: `AmplitudeContainer`

`_get_l_copy()`

Returns: Copy of λ_{ab}^{ij} amplitudes

Return type: `AmplitudeContainer`

`compute_t_residuals()`

Returns: Norm of τ_{ij}^{ab} amplitudes

Return type: `float`

`compute_l_residuals()`

Returns: Norm of λ_{ab}^{ij} amplitudes

Return type: `float`

`setup_t_mixer(**kwargs)` Sets up mixer for τ amplitudes

`setup_l_mixer(**kwargs)` Sets up mixer for λ amplitudes

`compute_energy()`

Returns: CCD ground state energy

Return type: `float`

`compute_t_amplitudes()` Computes τ amplitudes

`compute_l_amplitudes()` Computes λ amplitudes

`compute_one_body_density()`

Returns: One-body density matrix

Return type: `np.array`

`compute_two_body_density()`

Returns: Two-body density matrix

Return type: `np.array`

where $g(u, \tau)$ now consists of the rest of the doubles amplitude equation, our recursion relation can be written

$$t^{(k+1)} = \frac{g(u, \tau^{(k)})}{D_{ij}^{ab}}. \quad (8.4)$$

An example of a computation of one term from Equation 8.2 is,

```
def add_d2e_t(u, t, o, v, out, np):
    term = np.tensordot(t, u[o, v, v, o], axes=((1, 3), (2, 0)))
    .transpose(
        0, 2, 1, 3
    )
    term -= term.swapaxes(0, 1)
    term -= term.swapaxes(2, 3)
    out += term
```

which is a function function for computing the D_{2e} diagram¹.

Most of the rest of the methods in the `CoupledClusterDoubles` class are there for the use of other methods, or for extracting observables. We now proceed to the treatment of the logical expansion of the Coupled Cluster Doubles method, where we have included single excitations as well, i.e. the Coupled Cluster Singles Doubles (CCSD) method.

8.1.4 Coupled Cluster Singles Doubles

```
class coupled_cluster.cc.CoupledClusterSinglesDoubles
    (system, include_singles=True, **kwargs)
```

Implementation of coupled cluster with single- and double excitations ground state solver. Inherits from the `CoupledCluster` abstract base class.

Parameters

system(*QuantumSystem*) A system class from the `quantum_systems` module.
include_singles(*bool*, default `True`) Includes single excitations if `True`.

The coupled cluster method with single- and double excitations is now a matter of taking into account the extra computations needed in this scheme, for each method in the abstract base clase `CoupledCluster`. There are indeed many more computations, but the code in this class will structurally be the same as the Coupled Cluster Doubles class. The class specification for `CoupledClusterSinglesDoubles` is therefore given here without specification of the methods as they are exactly the same. For testing purposes, the `CoupledClusterSingelsDoubles` class have the option to only include double excitation at construction. The amplitude equations for the CCSD scheme are found

¹ After the labelling from chapter 6 and Shavitt and Bartlett[20]

by constructing the coupled cluster Lagrangian (Equation 6.95) in `sympy` and differentiating it symbolically. These resulting equations written in full can be found in section B.4.

8.1.5 Orbital-Adaptive Coupled Cluster

The algorithm applied when computing the ground state in the orbital-adaptive sphere is the Non-orthogonal Orbital-optimised Coupled Cluster (NOCC) method, developed by Myhre [2]. The NOCC scheme is shown to converge towards full configuration interaction. Since the `OACCD` class is actually applying NOCC it can be perceived as a misnomer, but as of yet there exist no ground state equivalent of the time-dependent orbital-adaptive coupled cluster (OACC) method. Such a method is in development, and there is strong indication that NOCC would be equivalent to a OACC ground state solver. What is more, in addition to solving some specialised amplitude equations iteratively in a way that is similar to a normal coupled cluster solver, the NOCC method *does* vary the orbitals, and we have therefore opted to call it the Orbital-Adaptive Coupled Cluster (OACC) method.

Our implementation of the NOCC ground state solver is inherited from a code written by Myhre [2] and adapted to our framework. We supply a brief overview of the algorithm here. The starting point for the NOCC model is the bivariational Lagrangian

$$\mathcal{L} = \langle \tilde{\Psi} | \hat{H} | \Psi \rangle = \langle \tilde{\phi} | (1 + \Lambda) e^{-\hat{T}} e^{-\kappa} \hat{H} e^{\kappa} e^{\hat{T}} | \phi \rangle, \quad (8.5)$$

which is very similar to the coupled cluster Lagrangian (Equation 6.95), except for a biorthogonal basis and a transformation of the Hamiltonian, defined as follows

$$\begin{aligned} \hat{c}_p^\dagger &= e^{-\kappa} \hat{c}_p^\dagger e^\kappa, \\ c_p &= e^{-\kappa} \hat{c}_p^\dagger e^\kappa, \\ |\phi\rangle &= e^{-\kappa} |\hat{\phi}\rangle, \end{aligned} \quad (8.6)$$

where the orthogonal reference creation- and annihilation operators are marked with a hat ($\hat{\cdot}$), as is the reference state function. We require that κ is antihermitian,

$$\kappa = \sum_{pq} \kappa_{pq} c_p^\dagger c_q, \quad \kappa^\dagger = -\kappa. \quad (8.7)$$

Moreover, we split κ into excitations and relaxations (up and down),

$$\kappa = \sum_{ai} \kappa_{ai}^u c_a^\dagger \tilde{a}_i + \kappa_{ia}^d c_i^\dagger \tilde{c}_a = \sum_{ai} \kappa_{ai}^u X_{ai} + \kappa_{ia}^d \tilde{X}_{ia}^\dagger. \quad (8.8)$$

As in any many-body formulation that includes a Lagrangian, we would like to compute the first-order conditions of the Lagrangian, in order to derive what would be the Non-orthogonal Orbital-optimised Coupled Cluster (NOCC) equation. The problem with this is that the result would be some extremely lengthy expressions, because κ does not commute with the cluster operators \hat{T} and Λ . Therefore, we express the NOCC equations with an optimized basis where $\kappa = 0$, where a solution would correspond

```
class coupled_cluster.cc.OACCD (system, **kwargs)
```

Implementation of the orbital-adaptive coupled cluster method with double excitation (OACCD). This algorithm require orthonormal basis functions. Based on work by Rolf H. Myhre[2]. Inherits from the **CoupledClusterDoubles** class.

Parameters

system(*QuantumSystem*) A system class from the *quantum_systems* module.

Methods

```
compute_ground_state (max_iterations=100, tol=1e-4,
                      termination_tol=1e-4, tol_factor=0.1, change_system_basis=False,
                      **mixer_kwargs)
```

Computes ground state of system by iterating over κ equations.

Parameters:

max_iterations (*int, default 100*) Maximum number of iterations.

tol (*float, default $1e^{-4}$*) Tolerance of convergence.

termination_tol (*float, default $1e^{-4}$*) Break if tolerance below this.

tol_factor (*float, default 0.1*) Stricter for each κ -iteration.

change_system_basis (*bool, default False*) Changes basis.

```
setup_kappa_mixer (**kwargs) Set up mixer for  $\kappa$  vector iterations.
```

```
compute_kappa_down_rhs (f, u, t_2, l_2, o, v, np)
```

Parameters:

f (*np.array*) Fock matrix.

u (*np.array*) Two-body operator, Coulomb integrals.

t_2 (*np.array*) τ_{ij}^{ab} amplitudes.

l_2 (*np.array*) λ_{ab}^{ij} amplitudes.

o (*Slice*) Occupied orbitals.

v (*Slice*) Virtual orbitals.

np (*Module*) Linear algebra library.

```
compute_kappa_up_rhs (f, u, t_2, l_2, o, v, np)
```

Parameters:

f (*np.array*) Fock matrix.

u (*np.array*) Two-body operator, Coulomb integrals.

t_2 (*np.array*) τ_{ij}^{ab} amplitudes.

l_2 (*np.array*) λ_{ab}^{ij} amplitudes.

o (*Slice*) Occupied orbitals.

v (*Slice*) Virtual orbitals.

np (*Module*) Linear algebra library.

to a stationary point of the Schrödinger equation. This is the same as expanding the exponentials in κ and keeping only zero-order terms. This trick leads to an algorithm which iterates over both orbital transformations and amplitude equations, switching between the two optimiser schemes, until self-consistency.

At a particular stationary point the differential of the Lagrangian (Equation 8.5) must be zero with respect to the four sets of parameters $\{\tau\}$, $\{\lambda\}$, $\{\kappa^u\}$ and $\{\kappa^d\}$, giving us four sets of equations,

$$\frac{\partial \mathcal{L}}{\partial \lambda_{\mu_n}} = \langle \tilde{\phi} | \tilde{X}_{\mu_n} e^{-\hat{T}} \hat{H} e^{\hat{T}} | \phi \rangle, \quad (8.9)$$

$$\frac{\partial \mathcal{L}}{\partial \tau_{\mu_n}} = \langle \tilde{\phi} | (1 + \Lambda) e^{-\hat{T}} [\hat{H}, X_{\mu_n}] e^{\hat{T}} | \phi \rangle, \quad (8.10)$$

$$\frac{\partial \mathcal{L}}{\partial \kappa_{\mu_1}^u} = \langle \tilde{\phi} | (1 + \Lambda) e^{-\hat{T}} [\hat{H}, X_{\mu_1}] e^{\hat{T}} | \phi \rangle, \quad (8.11)$$

$$\frac{\partial \mathcal{L}}{\partial \kappa_{\mu_1}^d} = \langle \tilde{\phi} | (1 + \Lambda) e^{-\hat{T}} [\hat{H}, \tilde{X}_{\mu_1}] e^{\hat{T}} | \phi \rangle. \quad (8.12)$$

The first two equations, Equation 8.9 and Equation 8.10, are the Lagrangian Coupled Cluster stationary points, i.e. the τ amplitude equations and the λ amplitude equations, respectively. The last two equations, Equation 8.11 and Equation 8.12, we call the κ equations. These equations dictate the orbital rotations, and we have provided the full κ equations for doubles excitations in section B.6.

We are now ready to outline the full algorithm of the `compute_ground_state()` in the `OACCD` class. The method iterates over the κ equations, computing the norm of the right-hand side of Equation 8.11, and Equation 8.12 for each step. We call these norms the κ residuals, and we continue this iteration until the κ residuals are low enough, compared to a preset tolerance level. For each κ iteration, we also iterate over the τ and λ doubles amplitude, exactly as in a regular Coupled Cluster ground state computation, but at a less strict tolerance value than we would in the `CoupledClusterDoubles` class. After the iteration over τ and λ has converged, the values for κ^u and κ^d are recalculated, in order to compute the aggregate κ given by Equation 8.8. This aggregate value can then in turn be used to transform the orbitals,

$$h^{(k+1)} = e^{-\kappa} h^{(k)} e^{\kappa},$$

$$(u_{rs}^{pq})^{(k+1)} = (e^{-\kappa})_a^p (e^{-\kappa})_b^q (u_{cd}^{ab})^{(k)} (e^{\kappa})_s^d (e^{\kappa})_r^c,$$

which is used to compute a new Fock operator. The resulting rotation of the orbitals will aid in better convergence towards the ground state.

Specialised Orbital-Adaptive AmplitudeContainer

Because of the nature of the orbital-adaptive coupled cluster scheme, it is no longer sufficient to store just the amplitudes as representation of the exact state. Therefore, we have implemented a subclass of the `AmplitudeContainer` data structure which also contains the coefficient matrices necessary to perform the required orbital transformations.

```
class coupled_cluster.cc_helper.OACCVector (t, I, C, C_tilde np)
```

Container for amplitude functions.

Parameters:

- `t(list, tuple, set)` τ amplitudes
- `I(list, tuple, set)` λ amplitudes
- `C(np.array)` Right-hand side coefficient matrix
- `C_tilde(np.array)` Left-hand side coefficient matrix
- `np(module)` Matrix library, e.g. numpy, cupy etc

Attributes:

- `t` τ amplitudes
- `I` λ amplitudes
- `C` Coefficient matrix **C**
- `C_tilde` Coefficient matrix **Č**

Methods:

- `unpack()`
 - Returns:** Amplitudes and coefficient matrices
 - Return type:** generator
- `asarray()`
 - Returns:** Amplitude vector and coefficient matrices
 - Return type:** `np.array`

Like the `AmplitudeContainer` class, this data structure also implements functionality for addition, multiplications and iteration. The `OACCVector` class adds some components that are very important to the orbital-adaptive Coupled Cluster schemes, namely the coefficient matrices that define the orbital rotations, **C** for the ket-side state vectors and **Č** for the bra-side state vectors. This class would also function as a regular `AmplitudeContainer` by setting the coefficient matrices equation to equal the unity operator.

8.1.6 Mixing of Amplitude Vectors

Iterative many-body methods are prone to convergence problems for certain configurations. This would be doubly important since we have moved to a variational description of coupled cluster theory, where generalisations of the variational theory dictate infinitesimal variations, which is not always feasible to implement. Moreover, an iterative optimisation scheme may not always converge properly at all. Luckily, there are numerous techniques both for controlling and accelerating convergence.

```
class coupled_cluster.mix.AlphaMixer (theta=0.1, np=None)
```

Class defining the α mixer. Computes a superposition of current and new amplitude vector. Also defines base class and methods the new mixer classes must implement.

Parameters

theta(*float, default 0.1*) Mixing parameter. $\theta \in [0, 1]$

np(*Module*) Matrix library to be used, e.g. numpy, cupy.

Methods

```
compute_new_vector (trial_vector, direction_vector error_vector)
```

Computes new trial vector for mixing with full right hand side of amplitude equation.

Parameters:

trial_vector (*np.array*) Initial vector for mixing

direction_vector (*np.array*) Vector to be added to *trial_vector*.

error_vector (*np.array*) Not used in α mixer. Needed in subclasses.

Returns: New mixed vector

Return type: *np.array*

Alpha mixer

The simplest way to “massage” convergence out of the coupled cluster ground state methods is to use a dampening, where one would include a part of the result from the previous iteration, here applied to the τ amplitudes,

$$\bar{\tau}^{(k+1)} = (1 - \theta)\tau^{(k+1)} + \theta\tau^{(k)}, \quad (8.13)$$

where $\tau^{(k+1)}$ is the current result from evaluating the amplitude equations, and $\tau^{(k)}$ is the previous value. Choosing $\theta \in [0, 1]$ will tune how much of the previous amplitude to include in the new state. The idea is to allow for a more gentle transition between the iterations. We have implemented this very simple mixing scheme in the **AlphaMixer** class, which also serves as a base class for further mixer implementations.

The Quasi-Newton method with DIIS acceleration

A more sophisticated method to aid in convergence, and perhaps the most popular, is by performing a direct inversion of the iterative subspace (DIIS). The DIIS method is built to accelerate the quasi-Newton method, and we will outline the quasi-Newton before we examine DIIS, which is explained in Helgaker et al. [16].

The commutator of Fock operator with the cluster operator is generally

$$[\hat{f}, \hat{T}] = \sum_{\mu} D_{\mu} \tau_{\mu} X_{\mu}, \quad (8.14)$$

where ϵ_{μ} is the sum of unoccupied energies minus the sum of all occupied energies, i.e. $D_{ij}^{ab} = \epsilon_a + \epsilon_b - \epsilon_i - \epsilon_j$, τ_{μ} is the amplitude of a particular excitation, and X_{μ} is an

```
class coupled_cluster.mix.DIIS (num_vecs=10, np=None)
```

General vector mixing class to accelerate quasi-Newton method using the direct inversion of iterative space (DIIS) scheme. Inherits from *AlphaMixer*.

Parameters

num_vecs(*float, default 10*) Number of vectors to keep in memory.
np(*Module*) Matrix library to be used, e.g. numpy, cupy.

Methods

compute_new_vector (*trial_vector, direction_vector error_vector*)

Computes new trial vector for mixing with full right hand side of amplitude equation.

Parameters:

trial_vector (*np.array*) Initial vector for mixing
direction_vector (*np.array*) Vector to be added to *trial_vector*.
error_vector (*np.array*) Error vector associated with QN DIIS.

Returns: New mixed vector

Return type: *np.array*

clear_vectors()

Delete all stored vectors.

excitation operator. For CCD Equation 8.14 becomes,

$$[\hat{f}, \hat{T}_2] = D_{ij}^{ab} \tau_{ij}^{ab} c_a^\dagger c_b^\dagger c_i c_j. \quad (8.15)$$

This allows us to write the coupled cluster vector function $\Omega_\mu^{(0)}$, and its Jacobian $\Omega_{\mu\nu}^{(1)}$ of the *n*th iteration in the form

$$\Omega_\mu^{(0)} = D_\mu \tau_\mu^{(n)} + \langle \Phi_\mu | e^{-\hat{T}^{(n)}} \hat{U} e^{\hat{T}^{(n)}} | \Phi_0 \rangle \quad (8.16)$$

$$\Omega_{\mu\nu}^{(1)} = D_\mu \delta_{\mu\nu} + \langle \Phi_\mu | e^{-\hat{T}^{(n)}} [\hat{U}, X^\nu] e^{\hat{T}^{(n)}} | \Phi_0 \rangle \quad (8.17)$$

which are very similar to the coupled cluster energy and amplitude equations, but the matrix element contains just \hat{U} , the fluctuation potential, instead of the entire Hamiltonian $\hat{H} = \hat{F} + \hat{U}$.

The Jacobian consists only of a diagonal part, involving differences of the orbital energies, and a nondiagonal part, containing the fluctuation potential. The trick from Newton's method is to expand the vector functions around the set of amplitudes of the current iteration $\tau^{(n)}$,

$$\Omega(\tau^{(n)} + \Delta\tau) = \Omega^{(0)}(\tau^{(n)}) + \Omega^{(1)}(\tau^{(n)})\Delta\tau + \dots, \quad (8.18)$$

which leads to a recursion relation, neglecting terms that are nonlinear in $\Delta\tau$,

$$\Omega^{(1)}(\tau^{(n)})\Delta\tau^{(n)} = -\Omega^{(0)}(\tau^{(n)}). \quad (8.19)$$

By inserting Equation 8.16 and Equation 8.17 we get the *quasi-Newton* equations for the optimisation of the coupled-cluster wavefunction,

$$\Delta\tau_{\mu}^{(n)} = -\frac{\Omega_{\mu}^{(0)}(\tau^{(n)})}{D_{\mu}} \quad (8.20)$$

The quasi-Newton method is fairly robust, but the convergence may be improved significantly by introducing DIIS.

In the DIIS framework [88], the new amplitudes $\tau^{(n+1)}$ are obtained by a linear interpolation among the previous estimates of the amplitudes,

$$\tau^{(n+1)} = \sum_{k=1}^n w_k (\tau^{(k)} + \Delta\tau^{(k)}), \quad (8.21)$$

where $\Delta\tau^{(k)}$ are obtained from Equation 8.20, and the interpolations weights sum to unity,

$$\sum_{k=1}^n w_k = 1.$$

To determine the DIIS weights, we associate each set of amplitudes $\tau^{(k)}$ with an error vector. We use the scaled vector function $\Delta\tau^{(k)}$ as error vector and determine the interpolation coefficients by minimising the norm of the averaged vector

$$\Delta\tau^{\text{ave}} = \sum_{k=1}^n w_k \Delta\tau^{(k)} \quad (8.22)$$

subject to Equation 8.1.6.

We have implemented the DIIS acceleration of the quasi-Newton method in the class `DIIS`. This class inherits from the `AlphaMixer` class and would function in its place. The `DIIS` class allows one to pick how many vectors to store and compute a linear interpolation of, with a default value of 10 vectors.

8.2 Time Development

We have sought to formulate the time-dependent coupled cluster methods in the abstraction of very general differential equations. By doing this we conform to the mindset of *implement once, apply anywhere*. In any implementation of a time-dependent coupled cluster solver, we consider it as though we are working with a general function $f(u(t), t)$, so that it can be solved by any general solver for a differential equation. The abstract formulation of a differential equation reads

$$u'(t) = f(u(t), t). \quad (8.23)$$

Notice that nearly any equations of motion in physics can be written in this way. Practically, this framework makes it necessary for us to implement the primitive `__call__` method for all coupled cluster solvers, in order to make them into a callable representation of the right-hand side of Equation 8.23.

```
class coupled_cluster.cc.TimeDependentCoupledCluster
(cc, np=None, system, integrator=None **cc_kwargs)
```

Abstract base class defining a time-dependent coupled cluster solver.

Parameters

`cc(CoupledCluster)` Class instance defining the ground state solver.

`system(QuantumSystem)` Class instance defining the system to be solved.

`np(module)` Matrix/linear algebra library to be used, e.g. Numpy, Cupy

`integrator(Integrator)` Integrator class instance, e.g. RK4, GaussIntegrator

Methods

`compute_ground_state(t_args=[], t_kwargs={}, l_args=[], l_kwargs)`

Call on method from `CoupledCluster` class to compute ground state of system.

`compute_particle_density()`

Computes one-body density at time t .

Returns: Particle density

Return type: `np.array`

`rhs_l_amplitudes()`

Abstract function that needs to be implemented as a generator. The generator should return the λ -amplitudes right-hand sides, in order of increasing excitation.

`rhs_t_amplitudes()`

Abstract function that needs to be implemented as a generator. The generator should return the τ -amplitudes right-hand sides, in order of increasing excitation.

`set_initial_conditions(amplitudes=None)`

Set initial condition of system. It is necessary to make a call to this system before computing time-development. Can be called without argument. Will in that case revert to amplitudes of ground state solver.

Parameters:

`amplitudes(AmplitudeContainer)` Amplitudes for initial system configuration.

`solve(time_points, timestep_tol=1e-8)`

Develop given system in time, specified by an array of `time_points`. Integrates equations of motion repeatedly, over all time points.

Parameters:

`time_points (list, np.array)` Time points over which to integrate EOM.

`timestep_tol (float, default 1e-8)` Tolerance in size of steps dt.

Returns: Amplitudes **Return type:** `Generator(AmplitudeContainer)`

`compute_energy()` Abstract function.

`compute_one_body_density_matrix()` Abstract function.

`compute_two_body_density_matrix()` Abstract function.

`compute_time_dependent_overlap()` Abstract function.

`compute_particle_density()` Calls `compute_one_body_density_matrix`.

`update_hamiltonian(current_time, amplitudes)`

Updates Hamiltonian of system in time, constructs new Fock operator.

Similarly to the rest of the `coupled_cluster` module, the portion relating to time development begins with an abstract base class, `TimeDependentCoupledCluster` functioning as an interface for the rest of the classes. At construction, the `TimeDependentCoupledCluster` class is passed an affiliated ground state solver in the form of a `CoupledCluster` object, a `QuantumSystems` object and an `Integrator` object. All these are necessary in order to compute a time-development. The starting point for time development is a system in it's ground state, necessitating the specification of a system and a ground state solver. Inclusion of a `CoupledCluster` object in the `TimeDependentCoupledCluster` class allows one to call the `compute_ground_state()` from this object, and it is included as a wrapper. Several other methods are included from the ground state realm, like the methods for particle density computations. The `__call__` method is implemented in the abstract base class, where the current amplitude in the form as an `AmplitudeContainer` object is passed as an argument together with the current time step. The right hand side of all amplitude equations are evaluated, and new amplitudes are returned. The class is called, i.e. evaluated by an `Integrator`, i.e. the system is developed in time by solving the equations of motion with a numerical integrator. We will consider integrators separately in the next section.

The bare minimum that a time-dependent coupled cluster scheme needs to implement in order to function are the methods `rhs_t_amplitudes()` and `rhs_l_amplitudes()`, which should return the right-hand side of the amplitude equations. These methods should be integrated as generators, to make it possible to iterate over them, and should yield the amplitudes in order of increasing excitation level. Most of the remaining functionality lies in the superclass `TimeDependentCoupledCluster`.

Arguably the most important method in the `TimeDependentCoupledCluster` abstract base class is the `solve(time_steps)` method. For the array of time steps supplied, this method propagates with the integrator member of the class for all amplitudes. This method remains the same for all time-propagation schemes, and is therefore implemented in the base class for inheritance in sub-classes.

The `solve` method in full is

```
def solve(self, time_points, timestep_tol=1e-8):
    n = len(time_points)

    for i in range(n - 1):
        dt = time_points[i + 1] - time_points[i]
        amp_vec = self.integrator.step(
            self._amplitudes.asarray(), time_points[i], dt
        )

        self._amplitudes = type(self._amplitudes).from_array(
            self._amplitudes, amp_vec
        )

    if abs(self.last_timestep - (time_points[i] + dt)) > timestep_tol:
        self.update_hamiltonian(time_points[i] + dt, self._amplitudes)
        self.last_timestep = time_points[i] + dt
```

```
yield self._amplitudes
```

We see that after the integrator is advanced one step in time, returning an amplitude vector. This amplitude object is stored as a member of the class by use of the `from_array()` method from the `AmplitudeContainer` class, after which the Hamiltonian of the system is updated if enough time has passed.

8.2.1 TDCCSD

We have implemented both a time-dependent CCD (TDCCD) solver and a time-dependent CCSD (TDCCSD) solver. For the sake of brevity, we present only the TDCCSD here as their appearance would be nearly identical. The `TDCCSD` class, a subclass of `TimeDependentCoupledCluster`, inherits all methods from this super-class. It accepts the same parameter as the super-class, except the parameter that defines the ground state solver to be used - the `CoupledCluster` class implementation. The ground state solver is already decided by the level of excitation for the computation at hand. All parameters are passed to the constructor in the parent class.

The `solve()` method will have the exact same functionality as in the parent class, but since the `TDCCSD` contains amplitudes and everything else needed to solve the equations of motions in a singles and doubles truncation, it will now yield a `Generator` object containing amplitudes that are developed in time. Any observable can be extracted during an iteration over this `Generator` object. We have implemented several methods that can be useful in extracting information about the state of the time-developed system, for instance `compute_time_dependent_overlap()` which computes the probability of the system being in the ground state, and `compute_energy()` which computes the energy of the system in the current time-dependent state.

The ground state probability, i.e. `compute_time_dependent_overlap()`, is based on a general time-dependent auto-correlation function,

$$A(t', t) \equiv \langle S(t') | S(t) \rangle. \quad (8.24)$$

Because coupled cluster theory is not variational in the usual sense it is necessary to define a general state vector as combination of both $|\Psi\rangle$ and $\langle\tilde{\Psi}|$,

$$|S\rangle = \frac{1}{\sqrt{2}} \begin{pmatrix} |\Psi\rangle \\ \langle\tilde{\Psi}| \end{pmatrix} \quad (8.25)$$

which makes the time-dependent auto-correlation function (Equation 8.24),

$$A(t', t) = \frac{1}{2} \left(\langle\tilde{\Psi}(t')|\Psi(t)\rangle + \langle\Psi(t')|\tilde{\Psi}(t)\rangle \right) \quad (8.26)$$

according to the definitions of the *indefinite* innerproduct by Pedersen and Kvaal [89]. Here we would set $t' = 0$, because we are interested in the ground state overlap, translating to the state before development in time.

```
class coupled_cluster.cc.TDCCSD (*args, **kwargs)
```

Sub-class of **TimeDependentCoupledCluster**. Computes time-development of provided system, employing time-dependent coupled cluster method with single- and double excitations. The orbitals are kept static. This class inherits all methods from the parent class, but includes a few extra.

Parameters

system(*QuantumSystem*) Class instance defining the system to be solved.

np(*module*) Matrix/linear algebra library to be used, e.g. Numpy, Cupy

integrator(*Integrator*) Integrator class instance, e.g. RK4, GaussIntegrator

Methods

rhs_t_0_amplitude(*args, **kwargs)

Evaluates CC energy expression

Returns: CCSD ground state energy.

Return type: *np.array*

rhs_t_amplitudes()

Evaluates τ_i^a and τ_{ij}^{ab} amplitude equations

Returns: τ_i^a , τ_{ij}^{ab}

Return type: *Generator*

rhs_l_amplitudes()

Evaluates λ_a^i and λ_{ab}^{ij} amplitude equations

Returns: λ_a^i , λ_{ab}^{ij}

Return type: *Generator*

compute_energy()

Computes energy at current time step.

Returns: energy

Return type: *float*

compute_particle_density()

Computes one-body density matrix

Returns: One-body density

Return type: *np.array*

compute_time_dependent_overlap()

Computes overlap of current time-developed state with the ground state.

Returns: Probability of ground state **Return type:** *np.array*

solve(*time_points*, *timestep_tol*= $1e^{-8}$)

Develop given system in time, specified by an array of *time_points*. Integrates equations of motion repeatedly, over all time points.

Parameters:

time_points (*list*, *np.array*) Time points over which to integrate EOM.

timestep_tol (*float*, default $1e^{-8}$) Tolerance in size of steps dt.

Returns: Amplitudes **Return type:** *AmplitudeContainer*

Within our truncation to include only single- and double excitations, an inner product of two state vectors, in the normal coupled cluster scheme with static orbitals, can be computed in the following manner

$$\begin{aligned}
 \langle \Psi' | \Psi \rangle &= \langle \Phi | (1 + \Lambda) e^{-\hat{T}'_1} e^{\hat{T}_2} | \Phi \rangle \\
 &= \langle \Phi | (1 + \Lambda_1 + \Lambda_2) (1 - \hat{T}'_1 - \hat{T}'_2 + \frac{1}{2} \hat{T}'_1^2) (1 + \hat{T}_1 + \hat{T}_2 + \frac{1}{2} \hat{T}_1^2) | \Phi \rangle \\
 &= \langle \Phi | \Phi \rangle - \langle \Phi | \Lambda_1 \hat{T}'_1 | \Phi \rangle + \langle \Phi | \Lambda_1 \hat{T}'_1 | \Phi \rangle - \langle \Phi | \Lambda_2 \hat{T}'_1 \hat{T}_1 | \Phi \rangle - \langle \Phi | \Lambda_2 \hat{T}'_2 | \Phi \rangle \\
 &\quad + \langle \Phi | \Lambda_2 \hat{T}_2 | \Phi \rangle + \frac{1}{2} \langle \Phi | \Lambda_2 \hat{T}'_1 \hat{T}'_1 | \Phi \rangle + \frac{1}{2} \langle \Phi | \Lambda_2 \hat{T}_1 \hat{T}_1 | \Phi \rangle,
 \end{aligned} \tag{8.27}$$

where we have ignored terms that would give a zero-contribution. Evaluating the remaining terms can be done with your favourite method. Here is an example using Wick's theorem,

$$\begin{aligned}
 \langle \Phi | \Lambda_2 \hat{T}_2 | \Phi \rangle &= \langle \Phi | \sum_{abij} \frac{1}{4} \lambda_{ab}^{ij} \{ \hat{i}^\dagger \hat{a} \hat{j}^\dagger \hat{b} \} \sum_{cdkl} \frac{1}{4} \tau_{kl}^{cd} \{ \hat{c}^\dagger \hat{k} \hat{d}^\dagger \hat{l} \} | \Phi \rangle \\
 &= \langle \Phi | \sum_{\substack{abcd \\ i j k l}} \frac{1}{16} \lambda_{ab}^{ij} \tau_{kl}^{cd} \{ \hat{i}^\dagger \hat{a} \hat{j}^\dagger \hat{b} \} \{ \hat{c}^\dagger \hat{k} \hat{d}^\dagger \hat{l} \} | \Phi \rangle + \text{three more equivalent contractions} \\
 &= \frac{1}{4} \langle \Phi | \sum_{\substack{abcd \\ i j k l}} \lambda_{ab}^{ij} \tau_{kl}^{cd} \delta_{ac} \delta_{bd} \delta_{ik} \delta_{jl} | \Phi \rangle = \frac{1}{4} \sum_{abij} \lambda_{ab}^{ij} \tau_{ij}^{ab}.
 \end{aligned} \tag{8.28}$$

The entirety of the `compute_time_dependent_overlap_method()` consists of similar computations,

```

def compute_time_dependent_overlap():
    np = self.np
    t_0, t_1, t_2, l_1, l_2 = self._amplitudes.unpack()
    t_1_0, t_2_0 = self.cc.t_1, self.cc.t_2
    l_1_0, l_2_0 = self.cc.l_1, self.cc.l_2

    psi_t_0 = 1
    psi_t_0 += np.einsum("ia, ai ->", l_1, t_1_0)
    psi_t_0 -= np.einsum("ia, ai ->", l_1, t_1)
    psi_t_0 += 0.25 * np.einsum("ijab, abij ->", l_2, t_2_0)
    psi_t_0 -= 0.5 * np.einsum("ijab, aj, bi ->", l_2, t_1_0, t_1_0)
    psi_t_0 -= np.einsum("ijab, ai, bj ->", l_2, t_1, t_1_0)
    psi_t_0 -= 0.5 * np.einsum("ijab, aj, bi ->", l_2, t_1, t_1)
    psi_t_0 -= 0.25 * np.einsum("ijab, abij ->", l_2, t_2)

    psi_0_t = 1
    psi_0_t += np.einsum("ia, ai ->", l_1_0, t_1)
    psi_0_t -= np.einsum("ia, ai ->", l_1_0, t_1_0)
    psi_0_t += 0.25 * np.einsum("ijab, abij ->", l_2_0, t_2)

```

```

psi_0_t -= 0.5 * np.einsum("ijab, aj, bi ->", l_2_0, t_1_0, t_1_0)
psi_0_t -= np.einsum("ijab, ai, bj ->", l_2_0, t_1, t_1_0)
psi_0_t -= 0.5 * np.einsum("ijab, aj, bi ->", l_2_0, t_1, t_1)
psi_0_t -= 0.25 * np.einsum("ijab, abij ->", l_2_0, t_2_0)

auto_corr = 0.5 * (
    psi_t_0 * np.exp(-t_0)
    + (psi_0_t * np.exp(t_0)).conj()
)

return np.abs(auto_corr) ** 2

```

The time-dependent energy in `compute_energy()` is found by evaluation of the coupled cluster Lagrangian (Equation 6.95) at the current time-developed amplitudes.

8.2.2 OATDCCD

In order to move to an orbital-adaptive framework, we have implemented a new abstract base class that includes treatment of orbitals. This class has the modified amplitude container `OACCVector` as a member. Most important differences from the standard time-dependent coupled cluster framework in the way the `__call__` implementation also returns coefficient matrices, how the Hamiltonian is updated for every time step and the inclusion of functions that compute P - and Q -space equations. As we will get into, the Q -space equations will simplify greatly under the assumption of a complete basis, but the P -space equations will differ depending on the excitation level.

```
class coupled_cluster.cc.OATDCCD (*args, **kwargs)
```

Class for computing time-development of provided system, employing orbital-adaptive time-dependent coupled cluster with double excitations. Subclass of abstract class `OATDCC`, which redefines the essential computations for the orbital-adaptive framework. `OATDCC` inherits all methods from `TimeDependentCoupledCluster`, overwriting those that are necessary to overwrite.

Parameters

- `cc(CoupledCluster)` Class instance defining the ground state solver.
- `system(QuantumSystem)` Class instance defining the system to be solved.
- `np(module)` Matrix/linear algebra library to be used, e.g. Numpy, Cupy
- `integrator(Integrator)` Integrator class instance, e.g. RK4, GaussIntegrator

Methods

- `compute_energy()`

Computes energy at current time step.

Returns: energy

Return type: float

Disappearing RHS of Q-space equations.

A necessary addition to an orbital-adaptive time-dependent coupled cluster framework is the computation of P - and Q -space equations. The Q -space equations can be simplified substantially, because almost all the terms disappear for an untruncated basis. We will show this now, starting with Equation 6.158,

$$i\hbar \sum_q \rho_p^q Q \frac{\partial}{\partial t} |\varphi_q\rangle = \sum_q \rho_p^q Q h |\varphi_q\rangle + \sum_{qrs} \rho_{pr}^{qs} Q W_s^r |\varphi_q\rangle. \quad (8.29)$$

Inserting for Q in the second term on the right-hand side gives

$$\sum_{qrs} \rho_{pr}^{qs} Q W_s^r |\varphi_q\rangle = \sum_{qrs} \rho_{pr}^{qs} W_s^r |\varphi_q\rangle - \sum_{qrs} \rho_{pr}^{qs} W_s^r \sum_t |\varphi_t\rangle \langle \tilde{\varphi}_t | \varphi_q\rangle. \quad (8.30)$$

If we assume a complete orthogonal basis, we have

$$\sum_t |\varphi_t\rangle \langle \tilde{\varphi}_t | \varphi_q\rangle = \hat{1},$$

and the term will disappear. Inserting for Q in the first term on the right hand side of the first Q -space equations also yields zero. This means that the first Q -space equations reduce to

$$\begin{aligned} i\hbar \sum_q \rho_p^q Q \frac{\partial}{\partial t} &= 0 \\ i\hbar \sum_q \rho_p^q \frac{\partial}{\partial t} |\varphi_p\rangle &= i\hbar \sum_q \rho_p^q \sum_s |\varphi_s\rangle \langle \tilde{\varphi}_s | \frac{\partial}{\partial t} |\varphi_p\rangle \\ \frac{\partial}{\partial t} |\varphi_p(t)\rangle &= \sum_s |\varphi_s(t)\rangle \langle \tilde{\varphi}_s(t) | \frac{\partial}{\partial t} |\varphi_p(t)\rangle \\ \frac{\partial}{\partial t} C_p^\alpha(t) |\chi_\alpha\rangle &= \sum_s C_s^\alpha(t) |\chi_\alpha\rangle \eta_p^s \\ \dot{C}_p^\alpha &= \sum_s C_s^\alpha \eta_p^s, \end{aligned} \quad (8.31)$$

which we rewrite more nicely using Einstein summation,

$$\dot{\mathbf{C}} = \mathbf{C} \eta_q^p. \quad (8.32)$$

Similarly for the second Q -space equations (Equation 6.159),

$$\dot{\tilde{\mathbf{C}}} = -\eta_q^p \tilde{\mathbf{C}}. \quad (8.33)$$

We see that the Q space equations describe the time propagation of the orbitals through the coefficient matrices \mathbf{C} and $\tilde{\mathbf{C}}$. These equations are valid for all excitation levels of the Orbital-Adaptive Time-Dependent Coupled Cluster (OATDCC) method, and have been implemented in the new abstract class `OATDCC`.

We see that η_q^p is the only thing needed in order to compute the coefficient matrices which dictate the orbital time propagation. We get η_q^p from the P -space equations. Since the P -space equations will be different for each level of sophistication we move onto a treatment of the implementation of the `OATDCCD` class.

P-space equations in OATDCCD

The P-space equations for the Orbital-Adaptive Time-Dependent Coupled Cluster Doubles (OATDCCD) scheme are nothing more than a series of tensor contractions, given by Equation 6.156 and Equation 6.157, restated here.

$$\begin{aligned} i\hbar \sum_{bj} A_{aj}^{ib} \eta_b^j &= \sum_j \rho_j^i h_a^j - \sum_b \rho_a^b h_b^i + \frac{1}{2} \left[\sum_{prs} \rho_{pr}^{is} u_{as}^{pr} - \sum_{rqs} \rho_{ar}^{qs} U_{qs}^{ir} \right], \\ -i\hbar \sum_{bj} A_{bi}^{ja} \eta_b^j &= \sum_b \rho_b^a h_i^b - \sum_j \rho_i^j h_j^a + \frac{1}{2} \left[\sum_{prs} \rho_{pr}^{as} u_{is}^{pr} - \sum_{rqs} \rho_{ir}^{qs} U_{qs}^{ar} \right] \end{aligned}$$

We apply `numpy.linalg.tensorsolve`, in order to find η_i^a and η_b^j , which is the entirety of η_q^p . Now we have everything we need in order to iterate over the OATDCCD equations of motion.

For each iteration, i.e. for each `Integrator.step()` advance, we compute the right hand side of the OATDCCD equations, Equation 6.154 and Equation 6.138, providing us with new amplitudes λ_{ab}^{ij} and τ_{ij}^{ab} . These can be used to compute density matrices, which in turn can be used to find η_q^p from the P -space equations. These will give us the time-development of the orbitals in the form of coefficient matrices \mathbf{C} and $\tilde{\mathbf{C}}$, which are used to update the one- and two-body parts of the Hamiltonian \hat{h} and \hat{u} , respectively.

Problematic Overlap

Notice the absence of a `compute_time_dependent_overlap()` function in the `OATDCCD` class specification. It is unfeasible to compute a time-dependent overlap in an orbital-adaptive scheme, because of the computation increase due to the basis transformations.

Computing the inner product of two state vector at the *same* point in time would be unproblematic, and would result in the same kind of computation as in Equation 8.27. Moreover, in this inner product with static orbitals, many terms evaluate to zero. At two different times, as in a computation of the ground state probability $|\langle \tilde{\Psi}(0)|\Psi(t)\rangle|^2$ this would not be the case, and we need to keep all terms,

$$\begin{aligned} \langle \tilde{\Psi} | \Psi \rangle &= \langle \tilde{\Phi} | (1 + \Lambda) e^{\hat{T}'} e^{\hat{T}} | \Phi \rangle \\ &= \langle \tilde{\Phi} | (1 + \Lambda_2) \left(1 - \hat{T}'_2 + \frac{1}{2} \hat{T}'_2^2 \right) \left(1 + \hat{T}_2 + \frac{1}{2} \hat{T}_2^2 \right) | \Phi \rangle \\ &= \langle \tilde{\Phi} | \Phi \rangle - \langle \tilde{\Phi} | \hat{T}'_2 | \Phi \rangle + \frac{1}{2} \langle \tilde{\Phi} | \hat{T}'_2^2 | \Phi \rangle + \langle \tilde{\Phi} | \Lambda_2 | \Phi \rangle - \langle \tilde{\Phi} | \Lambda_2 \hat{T}'_2 | \Phi \rangle \\ &\quad + \frac{1}{2} \langle \tilde{\Phi} | \Lambda_2 \hat{T}'_2^2 | \Phi \rangle + \langle \tilde{\Phi} | \hat{T}_2 | \Phi \rangle - \langle \tilde{\Phi} | \hat{T}'_2 \hat{T}_2 | \Phi \rangle + \frac{1}{2} \langle \tilde{\Phi} | \hat{T}'_2^2 \hat{T}_2 | \Phi \rangle \\ &\quad + \langle \tilde{\Phi} | \Lambda_2 \hat{T}_2 | \Phi \rangle - \langle \tilde{\Phi} | \Lambda_2 \hat{T}'_2 \hat{T}_2 | \Phi \rangle + \frac{1}{2} \langle \tilde{\Phi} | \Lambda_2 \hat{T}'_2^2 \hat{T}_2 | \Phi \rangle \\ &\quad + \text{six more terms.} \end{aligned} \tag{8.34}$$

With static orbitals, only terms that have the same number of excitations and relaxations would give a contribution to the final result. Now, because the orbitals have

```
class coupled_cluster.integrators.Integrator (np)
```

Abstract integrator parent class. Subclass must implement *step* method **Parameters**

np(*Module*) Matrix library to be used, e.g. numpy, cupy.

Methods

set_rhs (*rhs*)

Setter for right-hand side of problem.

Parameters:

rhs (*callable, int, float*) Right hand side of ODE.

step (*u, t, dt*)

Shell method. Must be implemented by subclass.

evolved in time, we don't have the same orthogonal properties that would cancel the other terms. Because we must include *everything* it becomes unfeasible to compute the time-dependent overlap in the orbital-adaptive scheme. The computation cost would scale at the same level as direct diagonalisation methods does, i.e. Full Configuration Interaction (FCI) schemes.

8.2.3 Integrators and ODE Solvers

Most, if not all, physical systems that evolve in time can be described as set of equations that we call the equations of motion. These can be formulated as a single or a set of ordinary differential equations written on the abstract form

$$u'(t) = f(u(t), t). \quad (8.35)$$

To this particular equation there is an infinite number of solutions, so in order to make the solution unique, we must also specify an initial condition

$$u(0) = U_0. \quad (8.36)$$

Given the right hand side of Equation 8.35, $f(u, t)$ and the initial condition U_0 , our task would be to compute $u(t)$. The simplest equation of motion in physics is Newton's second law,

$$a(t) = \frac{F(t)}{m}, \quad (8.37)$$

which we have reformulated to be on the standard form as Equation 8.35.

In any numerical scheme, the ODE defining our problem will be discretised, such that the initial value problem Equation 8.35 becomes the following

$$u_{n+1} = u_n + h f(u_n, t_n), \quad u(t_0) = u_0, \quad (8.38)$$

where h is some small time step, $t_{n+1} = t_n + h$. We see that the equation(s) at hand is (are) solved in *steps*. The most important method of an implementation of any

```
class coupled_cluster.integrators.RungeKutte4 (np)
    Classical fourth-order Runge-Kutta numerical integrator.

Parameters
    np(Module) Matrix library to be used, e.g. numpy, cupy.

Methods
    set_rhs (rhs)
        Setter for right-hand side of problem.
        Parameters:
            rhs (callable, int, float) Right hand side of ODE.
    step(u, t, dt)
        One integration step
        Parameters:
            u (np.array) Array of equations to be integrated.
            f (float) Current time step.
            dt (float) Time step size.
        Returns: RHS advanced one step,  $u_{n+1}$ .
        Return type: np.array
```

integrator scheme will be the method defining how one would *step* from one point to the next.

We have already derived the equations of motions for several coupled cluster frameworks². Solving these equations in time is done in the same manner as any other equations of motion. The right hand side of these equations is put into practice by implementing `__call__()` for all the time-dependent classes, and the initial condition of the problem is some configuration defined by the amplitudes of the problem. By formulating the time-dependent many-body problem in this way, we can find solutions to the equations of motion by any numerical integrator scheme. For convenience, we have included two integrator implementations in the `coupled_cluster` module - the common fourth order Runge-Kutta method and the symplectic Gauss-Legendre method. Moreover, we have defined an abstract base class `Integrator`, which defines a general integrator for eventual future additons.

The Runge-Kutta Method

The Runge-Kutta methods are a large family of implicit and iterative methods of increasing order. The first-order Runge-Kutta method is the same as the forward Euler method, where a step is defined as follows,

$$u_{n+1} = u_n + hf(u_n, t_n). \quad (8.39)$$

²TDCC:Equation 6.139 and Equation 6.140. OATDCC:Equation 6.135, Equation 6.138

The general step of an explicit n -th order Runge-Kutta method is defined by

$$u_{n+1} = u_n + h \sum_{i=1}^s b_i k_i, \quad (8.40)$$

where

$$\begin{aligned} k_1 &= f(u_n, t_n), \\ k_2 &= f(u_n + h(a_{21}k_1), t_n + c_2h), \\ k_3 &= f(u_n + h(a_{31}k_1 + a_{32}k_2), t_n + c_3h), \\ &\vdots \\ k_s &= f(u_n + h(a_{s1}k_1 + a_{s2}k_2 + \cdots + a_{s,s-1}k_{s-1}), t_n + c_s), \end{aligned} \quad (8.41)$$

where s is the number of stages, and the coefficients a_{ij} (for $j \in [1, i]$ and $i \in \langle j, s \rangle$), b_i (for $b \in [1, s]$) and c_i (for $i \in [2, s]$) defines the particular method. The matrix a_{ij} is called the Runge-Kutta matrix and b_i and c_i are known as the *weights* and *nodes*, respectively. We call the Runge-Kutta method consistent if

$$\sum_{j=1}^{i-1} a_{ij} = c_i, \quad i \in [2, s].$$

We have implemented the fourth-order Runge-Kutta method in the class `RungeKutta4`. This is the most common of the Runge-Kutta method, and is often referred to as simply “the Runge-Kutta method”.

A step of size h in the fourth order Runge-Kutta method is defined by

$$\begin{aligned} u_{n+1} &= u_n + \frac{1}{6}(k_1 + 2k_2 + 2k_3 + k_4), \\ t_{n+1} &= t_n + h, \end{aligned} \quad (8.42)$$

where

$$\begin{aligned} k_1 &= hf(u_n, t_n), \\ k_2 &= hf\left(u_n + \frac{k_1}{2}, t_n + \frac{h}{2}\right), \\ k_3 &= hf\left(u_n + \frac{k_2}{2}, t_n + \frac{h}{2}\right), \\ k_4 &= hf(u_n + k_3, t_n + h), \end{aligned}$$

This is implemented in the `step(u, t, dt)` method as

```
f = self.rhs
K1 = dt * f(u, t)
K2 = dt * f(u + 0.5 * K1, t + 0.5 * dt)
K3 = dt * f(u + 0.5 * K2, t + 0.5 * dt)
K4 = dt * f(u + K3, t + dt)
u_new = u + (1 / 6.0) * (K1 + 2 * K2 + 2 * K3 + K4)
```

```
class coupled_cluster.integrators.GaussIntegrator
    (np, s=2, maxit=20, eps=1e-14)
```

Simple implementation of symplectic Gauss-Legendre integrator of order 4 and 6 ($s = 2$ and $2 = 3$).

Parameters

np (*Module*) Matrix library to be used, e.g. numpy, cupy.
s (*int, default 2*) Order = $2s$. Scheme only implemented for $s \in \{2, 3\}$.
maxit (*int*) Maximum number of iterations.
eps (*float, default 1e⁻⁴*) Convergence tolerance.

Methods

step (*u, t, dt*)

One integration step

Parameters:

u (*np.array*) Array of equations to be integrated.
t (*float*) Current time step.
dt (*float*) Time step size.

Returns: RHS advanced one step, u_{n+1} .

Return type: *np.array*

Symplectic Gauss Integrator

The Runge-Kutta method, as described above, will be unstable for most systems because of its inability to preserve the structure and the energy of the system. It is necessary to apply an integrator which is both structure-preserving and symplectic. We have inherited a code used by Pedersen and Kvaal [89] and have adapted it to our framework. Nevertheless, we give a brief overview of its inner mechanics here.

A quadrature rule is an approximation of the definite integral of a function over an interval $[a, b]$.

The most common family of quadrature rules are derived by defining an equidistant grid of N points on the interval $[a, b]$, where the grid points x_n are given by

$$x_n = a + nh, \quad (8.43)$$

where $h = (b - a)/N$, with index $n \in [0, N]$. A quadrature rule is commonly stated as a weighted sum of function values at specified points.

$$\int_a^b f(x)dx \approx \sum_{i=1}^{(N-1)} h f(x_i).$$

The simplest of such schemes of equidistant points is the *trapezoidal* rule given by

$$\int_a^b f(x)dx = h \left(\frac{1}{2}g(x_0) + f(x_1) + f(x_2) + \dots + f(x_{N-1}) + \frac{1}{2}f(x_N) \right) + \mathcal{O}(h^2). \quad (8.44)$$

A very efficient method consists of repeating the trapezoidal rule and performing it for successive values of h , each having half the size of the previous one. This yields a sequence of approximations to the integral for various values of h can be fitted to a polynomial, and the value for this polynomial for $h = 0$ will yield a very accurate approximation to the exact value. This is called the *Romberg* method.

The n -point Gaussian quadrature rule functions similarly to the family of methods described above, but instead of equidistant points we use the zeros of orthogonal polynomials for the grid points x_n . The first pick of orthogonal polynomials are Legendre polynomials, which are orthogonal on the interval $[-1, 1]$, i.e.,

$$\int_{-1}^1 P_l(x)P_{l'}(x)dx = \delta_{ll'}. \quad (8.45)$$

We also approximate the function f with Legendre polynomials.

The Gauss-Legendre quadrature rule is constructed to yield an exact result for polynomials of degree $2n - 1$ or less. An advantage of the Gauss-Legendre method is that its accuracy is much better than that of other methods using the same number of integration points. In fact, the accuracy of an N -point Gauss-Legendre method is equivalent to that of an equidistant point method using $2N$ points. The resulting Gauss-Legendre quadrature rule can be stated as

$$\int_{-1}^1 f(x)dx = \sum_{n=1}^N w_n f(x_n) + \mathcal{O}(h^{2N}), \quad (8.46)$$

where x_n are the zeroes of the Legendre polynomial P_n , h is $2/N$ and w_n are appropriately chosen weights for the method.

Orthogonal polynomials p_r of degree r and leading coefficient one, satisfy the following recurrence relation,

$$P_{r+1}(x) = (x - a_{r,r})p_r(x) - a_{r,r-1}p_{r-1}(x) \cdots - a_{r,0}p_0(x). \quad (8.47)$$

The three-term recurrence relation can be written as a matrix equation

$$J\tilde{P} = x\tilde{P} - p_n(x) \times \mathbf{e}_n, \quad (8.48)$$

where $\tilde{P} = [p_0(x), p_1(x), \dots, p_{n-1}(x)]^T$, \mathbf{e}_n is the n th standard basis vector and J is the Jacobian matrix,

$$J = \begin{pmatrix} a_0 & 1 & 0 & \dots & & \\ b_1 & a_1 & 1 & 0 & \dots & \\ 0 & b_2 & a_2 & 1 & 0 & \dots \\ 0 & \dots & & & \dots & 0 \\ \dots & 0 & b_{N-2} & a_{N-2} & 1 & \\ & \dots & 0 & n_{N-1} & a_{N-1} & \end{pmatrix} \quad (8.49)$$

The eigenvalues of this matrix will be the nodes x_n , i.e. the zeros of the polynomials up to degree N . If $\phi^{(n)}$ is an eigenvector corresponding to an eigenvalue such an

eigenvalue x_n , the corresponding weight can be found from the first component of this vector

$$w_n = \mu_0 \left(\phi_1^{(n)} \right)^2, \quad (8.50)$$

where

$$\mu_0 = \int_a^b \omega(x) dx$$

and $\omega(x)$ is the weight function. $\omega(x) = 1$ when Legendre polynomials are used in the Gauss quadrature. This efficient way of arriving at weights and nodes is called the Golub-Welsh algorithm [90].

Generally, a quadrature method is not used to compute the solution to ODEs, but we adapt it to a Runge-Kutta solver in the way explained in Pedersen and Kvall [89]. A general implicit s -stage Runge-Kutta method is defined by

$$u_{n+1} = u_n + h \sum_{i=1}^s x_i f(u_n + Z_{ij}, t_n + w_i h), \quad (8.51)$$

$$Z_{in} h \sum_{j=1}^s a_{ij} f(u_n + Z_{jn}, t_n + w_j h). \quad (8.52)$$

This allows us to make an interpolation between each time step t_n and $t_n + h$ by a polynomial of order s and requiring the ODE to be satisfied at the s Gauss-Legendre quadrature points gives a symplectic and reversible integrator of order $2s$. The matrix a_{ij} is computed analytically,

$$a_{ij} = \int_0^{w_j} \ell_j(x) dx, \quad (8.53)$$

where

$$\ell_j(x) = \prod_{k=1, k \neq j}^s \frac{x - w_k}{w_j - w_k}, \quad (8.54)$$

is the j th Lagrange interpolation polynomial. The nonlinear equation Equation 8.52 is solved iteratively for each time step, making the method implicit. These fixed-point iterations are defined by

$$Z_{in}^{(k+1)} = h \sum_{j=1}^s a_{ij} f(u_n + Z_{jn}^{(k)}, t_n + w_j h). \quad (8.55)$$

The initial guess is crucial to the convergence speed of the method. We have employed guess (A) scheme described in section VIII.6.1 of Ref. [91].

For the user of the Gauss integrator, the experience will be much more pleasant than dealing with the derivations of the method, because its operations are the same, as evidenced by the `GaussIntegrator` class specification.

Part IV

Results

Chapter 9

Validation

Here we present a series of reproduced results from the scientific literature as a validation of our computational implementation. We manage to reproduce the instantaneous dipole results from the simulation of the hydrogen molecule in Li *et al.* [92], the time-dependent ground state probability of a quantum dot from Zanghellini *et al.* [93] and the spectrum of Helium from Pedersen and Kvaal [89]. The simulation of the ionisation of beryllium by Miyagi and Madsen [94], serves as an illustration of the advantage of adaptive orbitals versus static orbitals in a time-dependent coupled cluster method. For all time-dependent studies in this chapter we have employed the symplectic `GaussIntegrator` integrator class.

We present all results in Hartree atomic units (abbreviated a.u.). The derivation of these units can be found in subsection 2.3.2.

9.1 Instantaneous dipole in H_2

Li *et al.* [92] employ a time-dependent Hartree-Fock approach in order to study the electronic optical response of molecules in intense fields. To be specific, they model the hydrogen molecule H_2 with a 6-311++G(d,p) basis set¹, subject to an oscillating field of $1.72 \times 10^{13} \text{ W cm}^{-2}$ and 456 nm wavelength. In atomic units, this corresponds to an intensity of $E_{\max} = 0.07 \text{ a.u.}$ and a frequency of $\omega = 0.1 \text{ a.u.}$ They find the time-dependent Hartree-Fock method to be nearly indistinguishable from calculations using the full time-dependent Schrödinger equation. We have managed to replicate the instantaneous dipole results of hydrogen from figure 5 in Li *et al.* [92].

A 6-311++G(d,p) basis set corresponds to a 6-311++Gss basis set in PySCF, and we can extract it from here,

```
molecule = "
    h 0.0 0.0 -0.6948522960236121;
    h 0.0 0.0 0.6948522960236121
"
basis = "6-311++Gss"
```

¹In quantum chemistry, there are several specialised basis sets. For a thorough overview of basis sets, see for instance Jensen [95].

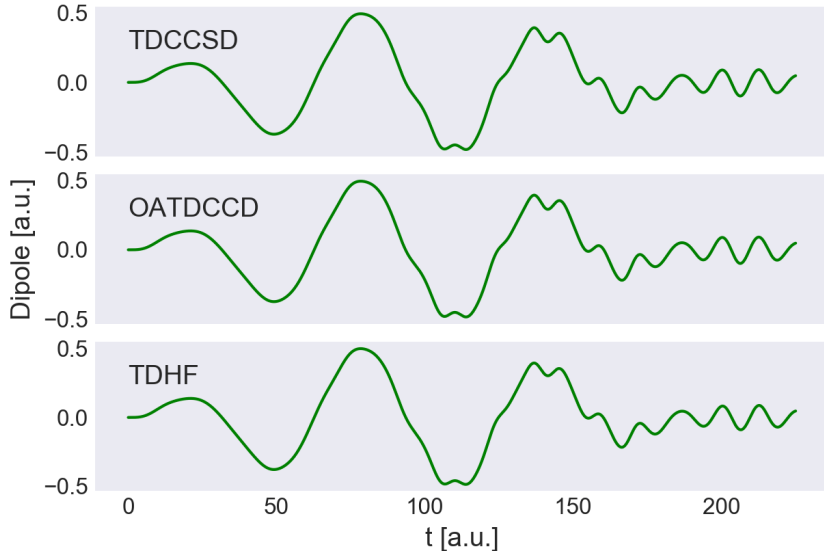


Figure 9.1: Instantaneous dipole for H_2 in an oscillating electric field of intensity $E_{\max} = 0.07$ a.u. and frequency $\omega = 0.1$ a.u., corresponding to 1.72×10^{14} W cm $^{-2}$ and 456 nm, respectively. The 6-311++G(d,p) basis set has been used.

```
system = construct_pyscf_system_ao(molecule, basis=basis)
```

The bond length of the Hydrogen molecule is approximately 0.7354 Å, converted to multiples of the Bohr radius here, the atomic unit for length.

In their simulations Li *et al.* have used a linearly polarised and spatially homogenous external field aligned along the z -axis,

$$\mathbf{e}(t) = \mathbf{E}(t) \sin(\omega t). \quad (9.1)$$

The field envelope $|\mathbf{E}|$ is linearly increased with time to a maximum value $|\mathbf{E}_{\max}|$ at the end of the first cycle and remains at $|\mathbf{E}_{\max}|$ for one cycle and then decreases linearly to zero by the end of the next cycle,

$$\begin{aligned} \mathbf{E}(t) &= (\omega t / 2\pi) \mathbf{E}_{\max} && \text{for } 0 \leq t \leq 2\pi/\omega \\ \mathbf{E}(t) &= \mathbf{E}_{\max} && \text{for } 2\pi/\omega \leq t \leq 4\pi/\omega \\ \mathbf{E}(t) &= (3 - \omega t / 2\pi) \mathbf{E}_{\max} && \text{for } 4\pi/\omega \leq t \leq 6\pi/\omega \\ \mathbf{E}(t) &= 0 && \text{for } t < 0 \text{ and } t > 6\pi/\omega, \end{aligned} \quad (9.2)$$

where the maximum field intensity if 1.72×10^{14} W cm $^{-2}$ ($E_{\max} = 0.07$ a.u.). Li *et al.* also ran a simulation for a lower intensity, but we are concerned only with this relatively more intensive pulse. The entire simulation lasts for $T = 225$ a.u.

The result of our simulation is shown in Figure 9.1, where we have computed the instantaneous dipole $\langle \hat{x}(t) \rangle = \text{tr}\{\rho(t)x\}$ over time using three different methods². The

²The dipole moment normally includes a charge q , i.e., $q \langle \hat{x} \rangle$ but in the atomic units that we use the charge is 1.

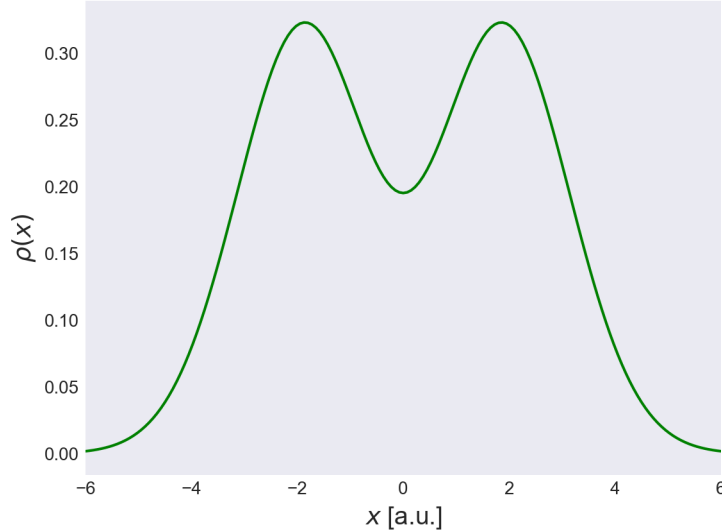


Figure 9.2: Electron density $\rho(x)$ in dimensionless units for the ground state wavefunction of a quantum dot with $n = 2$ electrons and $l = 20$ spin-orbitals in the basis set computed with CCSD. This plot corresponds precisely to figure 1 of Zanghellini *et al.* [93].

time-dependent Hartree-Fock result is shown in the bottom sub-figure, and is exactly the same as figure 4.a from Li *et al.* [92]. For comparison we have computed the result with both of our time-dependent coupled cluster methods. The result of the time-dependent coupled cluster method with single and double excitations are shown in the top subfigure, and the result of the orbital-adaptive coupled cluster method with double excitations are shown in the middle subfigure. We see that there is no perceptible difference between the results of the three methods.

9.2 Ground State Probability in 1D Quantum Dot

Zanghellini *et al.* [93] calculate the time development of a one-dimensional quantum dot with two electrons using the Multi-Configuration Time-Dependent Hartree-Fock method (MCTDHF). This method yields exact results for a very large number of configurations η . This study would provide a proper benchmark for our implementation because the coupled cluster method with singles and doubles excitations (CCSD) is exact for $n = 2$ particles. The harmonic oscillator potential applied in their study had a frequency of $\Omega = 0.25$ a.u., used a strong laser-like field with maximum intensity of $\mathbf{E}_{\max} = 1$ a.u. and a laser frequency of $\omega = 8\Omega = 2$ a.u. The oscillating field is described much more simply than in Li *et al.* [92], using a simple sine function,

$$\mathbf{e}(t) = \mathbf{E} \sin(\omega t), \quad (9.3)$$

where the envelope \mathbf{E} does not vary in time.

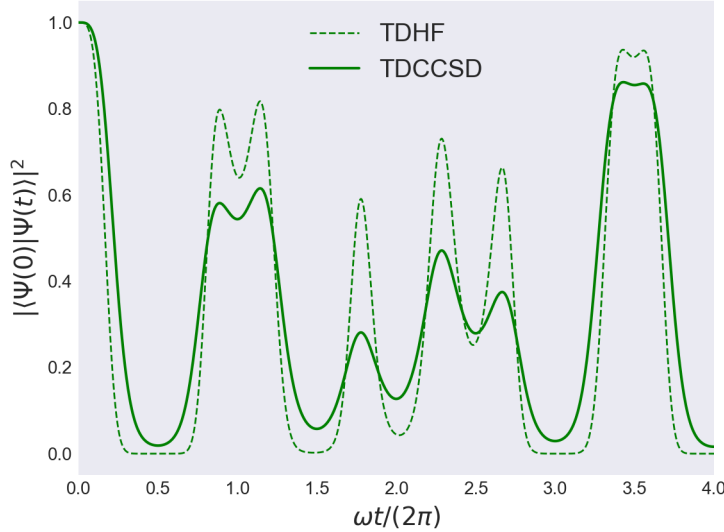


Figure 9.3: Probability of being in the ground state $|\langle \Psi(0) | \Psi(t) \rangle|^2$ using both TDHF and TDCCSD, for a one-dimensional quantum dot with $n = 2$ particles and $l = 20$ spin-orbitals. The ground state probability and the derived frequency units $\omega t / (2\pi)$ are dimensionless. This plot corresponds precisely to figure 2 of Zanghellini *et al.* [93].

Zanghellini *et al.* [93] find that their multi-configurational time-dependent Hartree-Fock scheme converges as the number of configurations is $\eta \geq 15$, up to the resolution of their figures. We are able to reproduce this result precisely by employing the time-dependent coupled cluster method with singles and double excitations (TDCCSD). We have used our own one-dimensional quantum dot class, `ODQD`, with a harmonic potential and $l = 20$ spin-orbitals in the basis set for this simulation.

In Figure 9.2 we see the ground state electron density for the ground state wavefunction computed with CCSD. Zanghellini *et al.* computed the electron density for an increasing number of configurations η using Multi-Configuration Time-Dependent Hartree-Fock (MCTDHF). This figure matches the convergent electron density found by Zanghellini *et al.* as $\eta \rightarrow \infty$, in figure 1 from their article.

Figure 9.3 depicts the probability for the system being in the ground state as a function of time. Here we have included both a time-dependent Hartree-Fock computation, corresponding to a multi-configurational time-dependent Hartree-Fock computation with $\eta = 1$ configurations, and a time-dependent coupled cluster computation with single and double excitations. We see that our coupled cluster scheme corresponds to the multi-configurational Hartree-Fock scheme employed by Zanghellini *et al.* when $\eta \rightarrow \infty$, as Figure 9.3 match figure 2 in Zanghellini *et al.* [93] precisely.

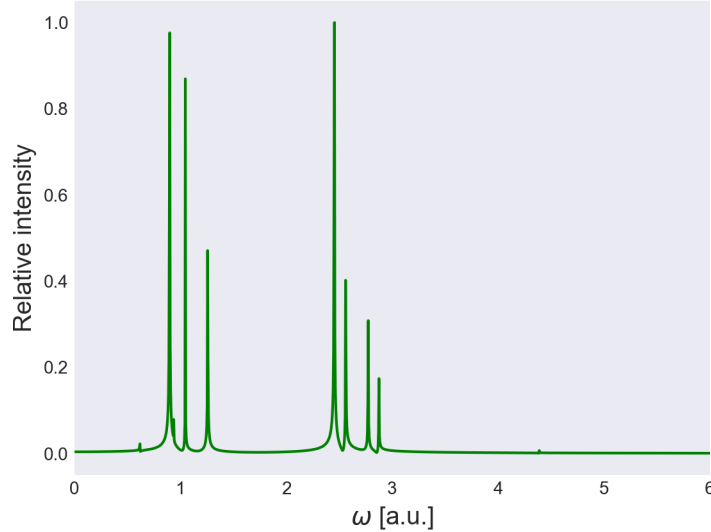


Figure 9.4: Dipole spectrum of helium computed with OATDCCD. The intensity of the spectral lines is in relative dimensionless units. The ground state of the system is excited by an oscillating field with strength $E_{\max} = 10$ a.u. and frequency $\omega = 2.8736$ a.u. for $t_d = 5$ a.u. The system is developed in time for a total of $T = 1500$ a.u. A cc-pVDZ basis set has been used in the simulation.

9.3 Dipole Spectrum of Helium

In their comparison study of symplectic and regular Runge-Kutta type integrators, Pedersen and Kvaal [89] present a dipole spectrum of helium.

The basis set employed by Pedersen and Kvaal is a cc-pVDZ basis set which we extract from Psi4,

```

He = "
  He 0.0 0.0 0.0
  symmetry c1
"
options = {"basis": "cc-pvdz", "scf_type": "pk", "e_convergence": 1e-8}
system = construct_psi4_system(He, options)

```

For hydrogen this basis set amounts to five orbitals in total. See chapter 5 in Jensen [95] for a thorough overview of quantum chemistry basis sets.

In their study Pedersen and Kvaal [89] use an oscillating field with frequency $\omega = 2.8736$ a.u. and maximum intensity $E_{\max} = 10$ a.u. This frequency corresponds to the lowest-lying electric-dipole allowed transition from the ground state of helium. The oscillating field can be described as

$$\mathbf{e}(t) = \mathbf{E}(t) \cos(\omega t), \quad (9.4)$$

with a sinusoidal envelope

$$\mathbf{E}(t) = \epsilon E_{\max} \sin^2 \left(\frac{\pi t}{t_d} \right) H(t_d - t), \quad (9.5)$$

where H is the Heaviside step function designed to return zero when the field has reached its designated halting time t_d . This envelope is similar in behaviour to the one in the study by Li *et al.* [92] - it increases gradually at first, and then gradually decreases.

The oscillating field is only meant to “disturb” the ground state of the atom, as it is quickly switched off at $t_d = 5$. Then the system is allowed to propagate in time for a long period. In our reproduction of the system, we have let the system evolve for a total time $T = 1500$ a.u. For each time step we compute the dipole in the same direction as the polarisation of the oscillating field. The Fourier transform of this signal will then yield the dipole spectrum of the atom. The time-development is performed with the orbital-adaptive time-dependent coupled cluster method with double excitations. The result from this simulation is depicted in Figure 9.4, which is qualitatively equal to figure 7 in Pedersen and Kvaal [89].

9.4 Ionisation of 1D Beryllium

Miyagi and Madsen [94] implement the Time-Dependent Restricted Active Space Self Consistent Field Singles (TD-RASSCF-S) method and compare it with Time-Dependent Configuration Interaction Singles (TDCIS) and the Multi-Configuration Time-Dependent Hartree-Fock (MCTDHF) method. A simulation they perform in this study is the simulation of the ionisation of beryllium. This simulation is performed by applying an oscillating field defined by the following vector potential,

$$\mathbf{A}(t) = \frac{\mathbf{E}_{\max}}{\omega} \sin \left(\frac{\pi t}{T} \right), \quad (9.6)$$

giving the following field

$$\mathbf{e}(t) = -\mathbf{E}_{\max} \sin \left(\frac{\pi t}{T} \right) \left[\frac{2\pi}{T\omega} \cos \left(\frac{\pi t}{T} \right) \sin(\omega t) + \sin \left(\frac{\pi t}{T} \right) \cos(\omega t) \right], \quad (9.7)$$

where $\mathbf{E}_{\max} = \epsilon E_{\max}$, where ϵ is the polarisation vector. We reproduce the one-dimensional beryllium model with our `AtomicPotential` class, which can be passed as a potential to the `ODQD` (one-dimensional quantum dot) class when setting up the system,

```
Z = 4; n = 4; l = 40; c = 1; a = 1; alpha = 1;
potential = AtomicPotential(Z, c)
odbe = ODQD(n, l, grid_length, num_grid_points, a, alpha)
odbe.setup_system(potential=potential)
```

where `Z` are the number of protons, `n` is the number of electrons, `l` is the number of spinorbitals, `c` is the position of the nucleus, `a` is the Coulomb screening parameter and `alpha` is the strength of the Coulomb interaction. We pick a wide grid of 300 a.u., with

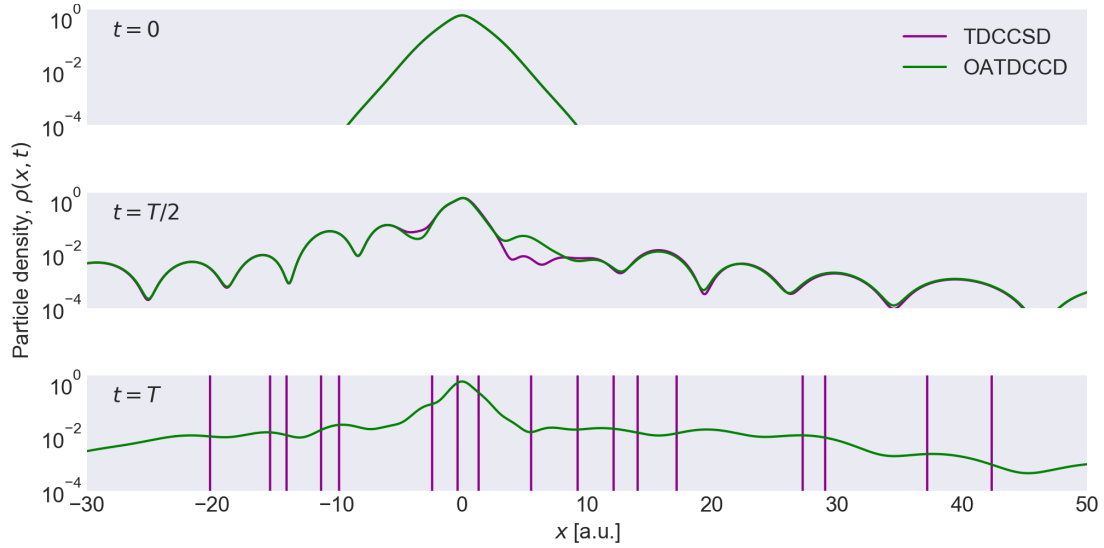


Figure 9.5: Snapshots of the dimensionless electron density $\rho(x, t)$ in the 1D beryllium atom at $t = 0$, $t = T/2$ and T , where $T = 331$ a.u., computed with TDCCSD and OATDCCD.

5001 points, and a time step size of $\Delta t = 0.01$ a.u. The maximum field strength is set to $E_{\max} = 0.0755$ a.u. and the frequency of the laser field is set to $\omega = 0.057$ a.u. This corresponds to a peak intensity of 2.0×10^{14} W cm⁻² and a laser wavelength of 800 nm. The total time of the simulation is $T = 331$ a.u. Both the unit for frequency and time is derived from the Hartree unit for energy E_a , which we derived in subsection 2.3.2. The atomic units for time and frequency are \hbar/E_a and E_a/\hbar , respectively.

The idea behind the simulation is to compute the particle density over time, and see if there is more than a significantly high probability to see an electron very far away from the nucleus. The particle density $\rho(x, t)$ is computed at the very beginning of the simulation, halfway through and at the end of the simulation. We do this both with our time-dependent coupled cluster singles doubles (TDCCSD) method with static orbitals and the orbital-adaptive time-dependent coupled cluster doubles method (OATDCCD). The results of the simulations are shown in Figure 9.5.

In the top subfigure in Figure 9.5 we see the electron density before the system is developed in time, and the two methods are in good agreement. In the middle subfigure the simulation is halfway through its course and the two methods both appear to show the same effects, but with slight discrepancies. In the bottom subfigure, we see that the OATDCCD method is doing fine, but the TDCCSD is absolutely non-sensible, with very high peaks that are periodically greater than 1. We can conclude that propagating orbitals in time enables us to get the same qualitative result as Miyagi & Madsen in figure 4 from their study. Keeping the orbitals static as in the TDCCSD method makes us unable to model the same behaviour. We will delve a bit deeper to try to shed some light on why the TDCCSD method fails.

If we compute the norm of the amplitudes over the course of the simulation for the time-dependent coupled cluster singles doubles (TDCCSD) method, we get the result

shown in Figure 9.6. In essence, the amplitudes in any coupled cluster computation provides a linear combination of orbitals from the reference state $|\Phi_0\rangle$, in order to provide the best representation of the exact state $|\Psi\rangle$. For this reason one would expect the norm of the amplitudes to be relatively low for an exact state $|\Psi\rangle$ that is close to the reference state $|\Phi_0\rangle$. We encounter problems with the static orbitals because we are dealing with a system that moves very far from its initial state. In Figure 9.6 we see that the amplitudes stay within a reasonable magnitude for up to about halfway through the simulation, after which we see the method is struggling greatly to represent the current state with the basis it has been given. In figure Figure 9.7, a plot of the overlap of the current, time-dependent state with the initial ground state helps to underline this point. The inset figure in Figure 9.7 shows the area of the figure with the highest value for the overlap, at a larger scale. We see that the ground state probability reaches values of more than 300, which is most definitely unreasonable, because a probability like this should always be between 0 and 1.

It is difficult to draw a clear conclusion as to when the time-dependent coupled cluster method with static orbitals breaks down and is unfeasible for use. However, we can draw some broader, qualitative strokes towards a diagnosis of the problem. Any coupled cluster method is supposed to provide the best representation of a system's exact wavefunction by picking parts of the basis set contained in the reference state for that system. If the exact wavefunction exists in a very different basis space than the reference state, it stands to reason that it is very difficult, if not impossible to find a mapping between the two. This problem stems from the foundations of the approximative nature of the coupled cluster method as it has a truncated basis set.

Pedersen and Kvaal [89] provide a similar deduction, highlighting there what appears to be a system-dependent upper limit for the strength of the external field. They underline the improvement in the computations by using a symplectic integrator instead of a standard fourth-order Runge-Kutta method. We use the same integrator as the one Pedersen and Kvaal outline. Pedersen and Kvaal argue that a large amplitude norm should make one question the validity of the result. It is difficult to gauge what constitutes a “large” amplitude norm, however.

Lastly with regards to the ionisation study from Miyagi and Madsen [94], we would like to emphasise how well the Orbital-Adaptive Time-Dependent Coupled Cluster Doubles (OATDCCD) method performs. The OATDCCD method manages to replicate the desired results to a significant degree, giving relatively high values for the entire grid of the particle density represented in Figure 9.7. This is normally interpreted as a free particle because one would expect the wavefunction of a free particle to spread out in space as time progresses.

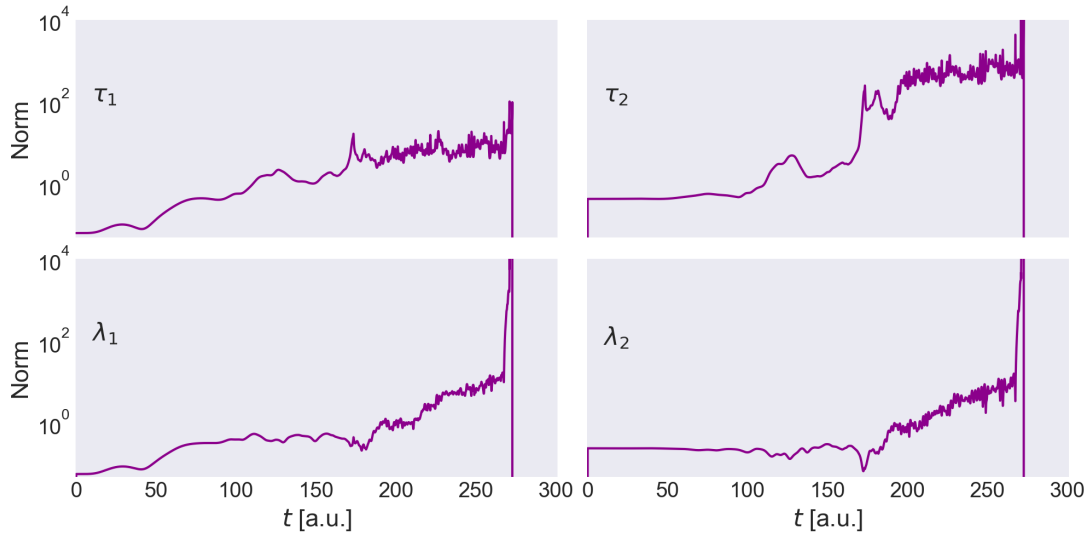


Figure 9.6: Norm of the amplitudes over time in the 1D beryllium atom, computed with TDCCSD. We see unreasonably high amplitude norms.

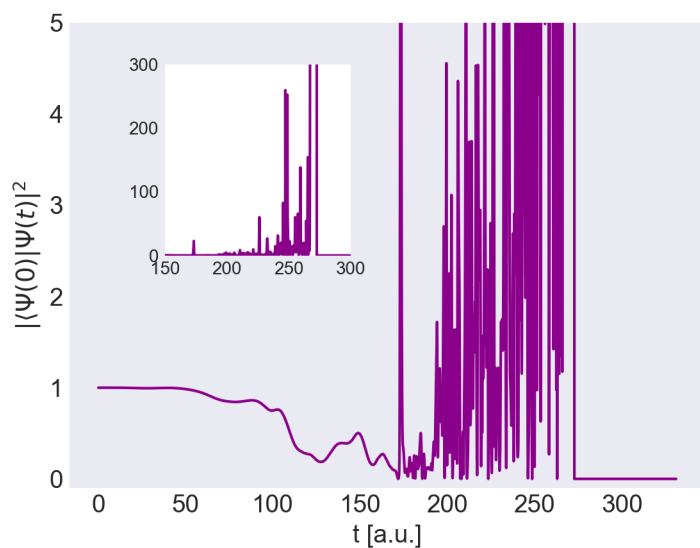


Figure 9.7: Probability of being in the ground state over time $|\langle \Psi(0) | \Psi(t) \rangle|^2$, in dimensionless units, for the 1D beryllium atom, computed with TDCCSD. We see unreasonable probabilities.

Chapter 10

Quantum Dots

Here we present results related to time-dependent simulations of parabolic quantum wells. We have simulated the behaviour of such quantum dots in both one- and two dimensions, producing time dependent energies and ground state probabilities over time as the system is under the influence of oscillating fields. We also present dipole spectra of the one- and two-dimensional quantum dot as well as the two-dimensional double dot and a two-dimensional double dot under the influence of a homogenous, static magnetic field. We find that the *harmonic potential theorem* holds for all simulations.

The *harmonic potential theorem* [5] states that electrons trapped in a parabolic quantum well behave as if they were one large quantum oscillator, instead of a system consisting of many smaller parts. This includes exhibiting only one frequency in the dipole spectrum of the system. If we compute the Fourier transform of the dipole of an n -electron quantum dot with a parabolic potential the result would be one line in the spectrum corresponding to the oscillator frequency of the system. This means that in the dipole approximations, we can not detect many-body effects in a harmonic quantum dot with infrared light.

The harmonic potential theorem generalises to quantum dots under the influence of a magnetic field [96, 97]. The revised theorem states that one would expect to see a shift, both up and down, creating two frequencies Ω_+ and Ω_- in the dipole spectrum. The resulting two frequencies would have a difference equalling the Larmor frequency $\omega_c = \Omega_+ - \Omega_-$.

We present all results in Hartree atomic units (abbreviated a.u.). The derivation of these units can be found in subsection 2.3.2.

10.1 Harmonic Oscillators in One Dimension

For the one-dimensional quantum dot with a harmonic potential we simulate a laser by adding an oscillating field with a sinusoidal envelope, similar to the one in Pedersen and Kvaal [89],

$$\mathbf{e}(t) = \epsilon E_{\max} \sin^2\left(\frac{t\pi}{T}\right) \cos(\omega t). \quad (10.1)$$

We set the period of the envelope equal to the duration of the entire simulation, $T = 20$ a.u., so that we have a field that at first will gradually increase, then de-

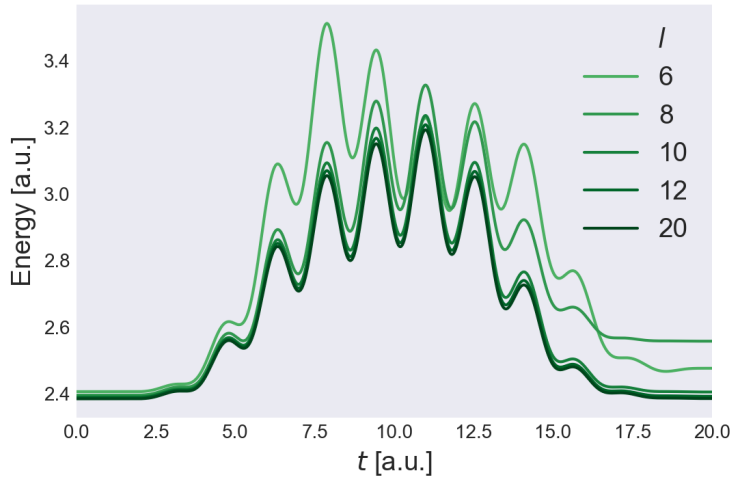


Figure 10.1: Time-dependent energy of a one-dimensional harmonic oscillator with $n = 2$ electrons under the influence of a laser field with maximum intensity $E_{\max} = 1$ a.u. and frequency $\omega = 2$ a.u., for different number of spin-orbitals $l \in \{6, 8, 10, 12, 20\}$. The oscillator frequency of the system is set to $\Omega = 1$ a.u.

crease. The oscillator frequency for all simulations are set to $\Omega = 1$ a.u., and at first we set the frequency of the oscillating field to twice this, $\omega = 2$ a.u. We do this to make sure that we are far from the resonant frequency of the system, and we pick a relatively high laser frequency in order to enforce a more dynamic system. We use the more standard time-dependent coupled cluster singles doubles (TDCCSD) method, for these simulations, with the symplectic Gaussian integrator and a time step of $\Delta t = 0.01$ a.u. The simulations are performed for an increasing number of electrons $n = \{2, 4, 6, 8, 10, 12\}$. We have computed the energy and the time-dependent overlap, i.e. the time-dependent probability of being in the ground state, for each simulation. We repeat the simulations for a wide range of different number of spin-orbitals, in order to find convergent properties of the simulations as the number of spin-orbitals increase.

First we study the time-dependent energy of a quantum dot acted upon by an oscillating field. The result for $n = 2$ electrons is shown in Figure 10.1. We have produced comparative results for other number of particles $n = \{4, 6, 8, 10, 12\}$, which can be found in section A.1. We see an apparent convergence in the time-dependent energy as we increase the number of spin-orbitals in the basis set. For larger systems with more electrons it reasonably becomes necessary to also increase the size of the basis set. As is the tendency with ground state coupled cluster computations for quantum dots[81, 82], the time dependent energy of a quantum dot is decreasing until convergence for increasing basis set size.

We see the same general convergent tendency when computing the time-dependent ground state probability $|\langle \Psi(0) | \Psi(t) \rangle|^2$, shown in Figure 10.2 for $n = 2$ electrons. We see that for a lower number of spin-orbitals, the computation of the overlap with the ground state tends to return a lower value than for a higher number of spin-orbitals.

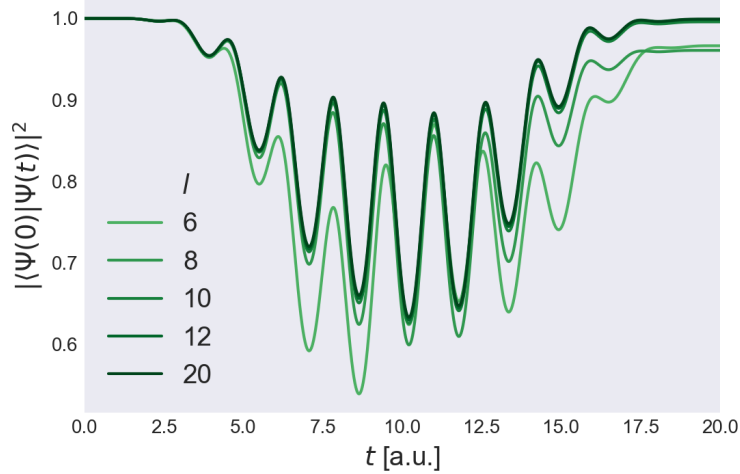


Figure 10.2: Dimensionless probability of being in the ground state $|\langle \Psi(0) | \Psi(t) \rangle|^2$ for a one-dimensional quantum dot with $n = 2$ electrons under the influence of a laser field with maximum intensity $E_{\max} = 1$ a.u. and frequency $\omega = 2$ a.u., for different number of spin-orbitals $l \in \{6, 8, 10, 12, 20\}$. The oscillator frequency of the system is set to $\Omega = 1$ a.u.

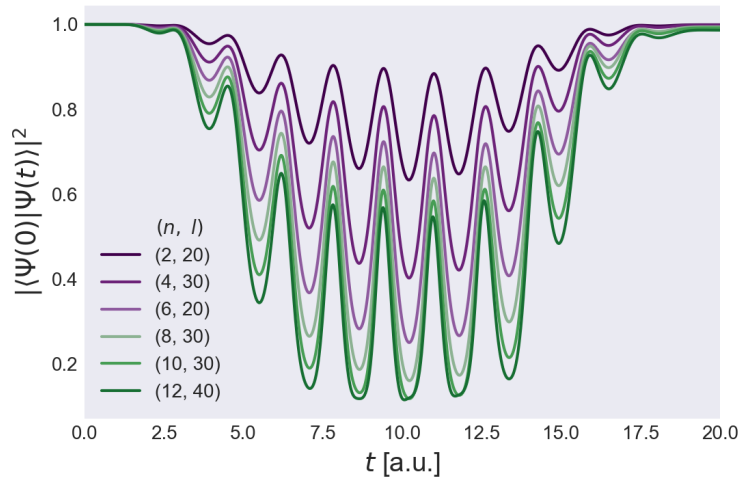


Figure 10.3: Dimensionless probability of being in the ground state for $|\langle \Psi(0) | \Psi(t) \rangle|^2$ for a one-dimensional quantum dot for different number of electrons $n = \{2, 4, 6, 8, 10, 12\}$, with accompanying spin-orbitals $l = \{20, 20, 20, 30, 30, 40\}$. All systems have been subjected to the same oscillating field with maximum intensity $E_{\max} = 2$ a.u. and a frequency of $\omega = 2$ a.u., for a $T = 20$ a.u. time period. The oscillator frequency of each system was $\Omega = 1$ a.u.

Since the ground state probability is a number between zero and one, the results for systems of different number of electrons are comparable. We have produced such a comparison in Figure 10.3. In this figure we have chosen the number of spin-orbitals that would produce a convergent plot for the given system size. The general tendency is that a system with more electrons is less likely to be in the ground state over time than a system with less electrons.

10.1.1 Dipole spectrum

We now turn to a somewhat different kind of simulation. We keep the base system the same, a one-dimensional quantum dot with harmonic potential and oscillator frequency $\Omega = 1$ a.u. We also apply an external oscillating field like in Equation 10.1, which will this time be resonant with the frequency of the oscillator $\omega = \Omega = 1$ a.u., to ensure a population of excited states. In this simulation we set the field to zero at $T_d = 5$ a.u., by the use of a Heaviside function in a similar manner as Pedersen and Kvaal [89] in Equation 9.5. After the field has been switched off we propagate the system in time for a total of $T = 500$ a.u. with a time step $\Delta t = 0.01$ a.u. The same procedure is repeated for systems with $n = \{2, 4, 6, 8, 10, 12\}$ electrons with respective number of spin-orbitals $l = \{20, 20, 20, 30, 30, 40\}$. These systems and basis sizes correspond to the ones used in Figure 10.3. For each time step we collect the dipole moment $\langle \hat{x}(t) \rangle = \text{tr}\{\rho(t)x\}$, and compute the Fourier transform of the entire collected array. The results are presented in Figure 10.4.

We see that the result is in accordance with the harmonic potential theorem, as the simulations have produced dipole spectra that show only one line corresponding to the frequency of the confining potential. Moreover, we see that the relative intensity of the spectra increases with the number of particles.

10.1.2 Resonance Sensitivity

In order to test the response of a quantum dot as the frequency of the oscillating field approaches the oscillator frequency, we have run simulations for a selection of laser frequencies ω with the field described by Equation 10.1. We chose frequencies $\omega \in \{1.0, 1.25, 1.5, 1.75, 2.0\}$ in atomic units, and set the oscillator frequencies of the quantum dot systems to $\Omega = 1$. The laser pulse had a set period of $t_d = 20$ a.u., starting from $t = 0$, while time-development of the system was allowed to continue to $T = 30$ a.u.. The maximum intensity of the oscillating field was lowered to $E_{\max} = 0.25$ a.u., to ensure stability of the simulations.

The results of these simulations are shown for $n = 2$ particles in Figure 10.5 and Figure 10.6, which show the time-dependent energy and the time-dependent ground state probabilities $|\langle \Psi(0) | \Psi(t) \rangle|^2$, respectively.

The results are as expected, but interesting nonetheless. We see that the quantum dots behave very much as a classical driven harmonic oscillator. If the frequency of the driving force, in this case the oscillating field, is far from the resonant frequency of the system the system falls back to the initial position after the force subsides. Only when we get closer to the resonant system do we see an excitation in energy of the system as a whole after the laser field is switched off (Figure 10.5). In the case for the exact resonant

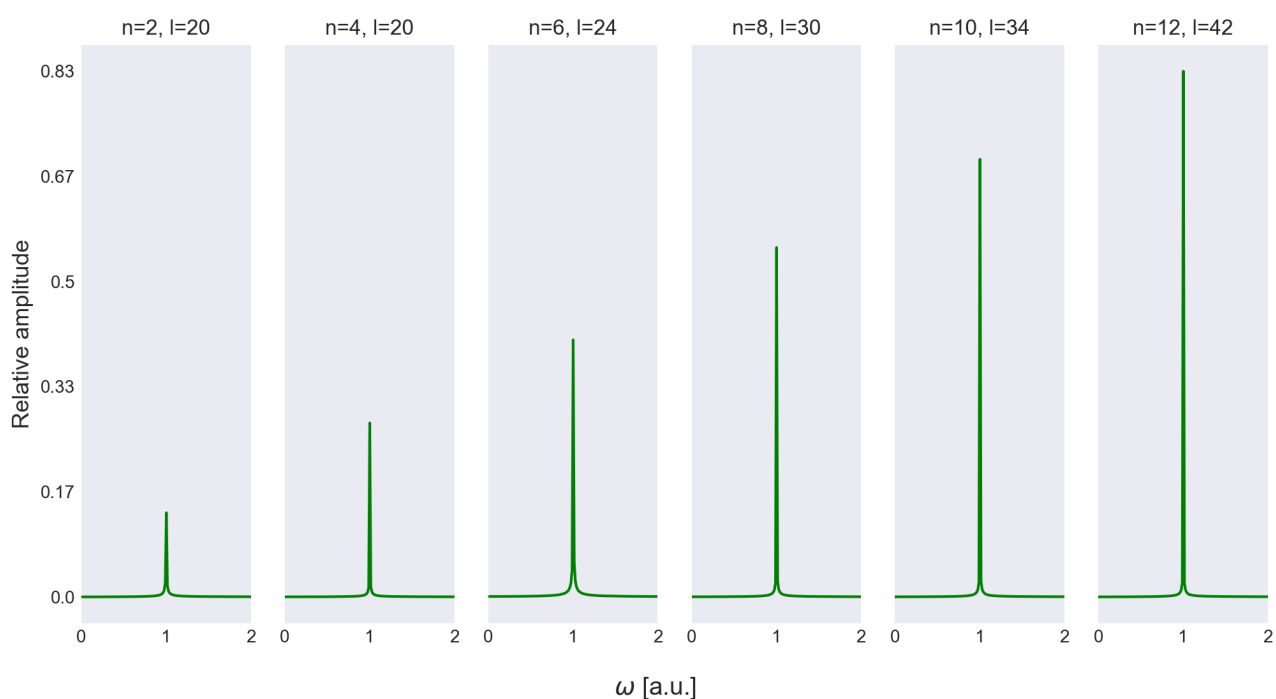


Figure 10.4: Fourier transform of expected value of dipole moment for a one-dimensional quantum dot with different number of electrons $n = \{2, 4, 6, 8, 10\}$ with respective number of spin-orbitals $l = \{20, 20, 24, 30, 34, 42\}$. The intensity of the spectral lines are computed relative to the largest system ($n = 12$), and are dimensionless.

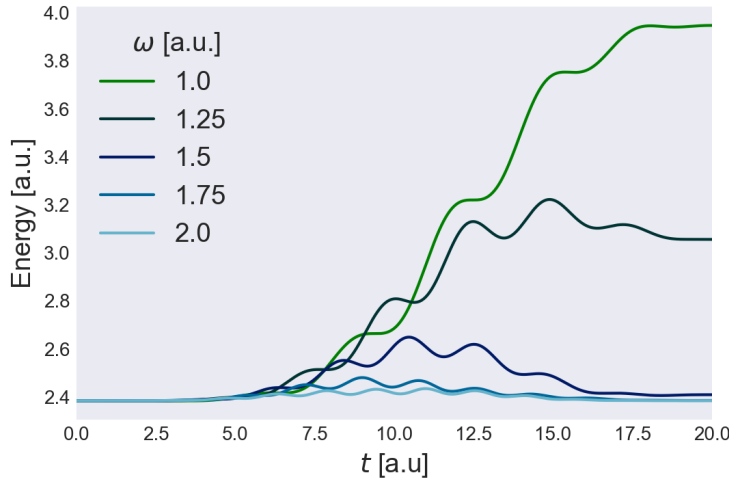


Figure 10.5: Time-dependent energy of a one-dimensional quantum dot with oscillator frequency $\Omega = 1$ a.u. and $n = 2$ electrons. The quantum dot is influenced by an oscillating field of different frequencies $\omega \in \{1.0, 1.25, 1.5, 1.75, 2.0\}$ in atomic units with a maximum intensity of $E_{\max} = 0.25$ a.u.

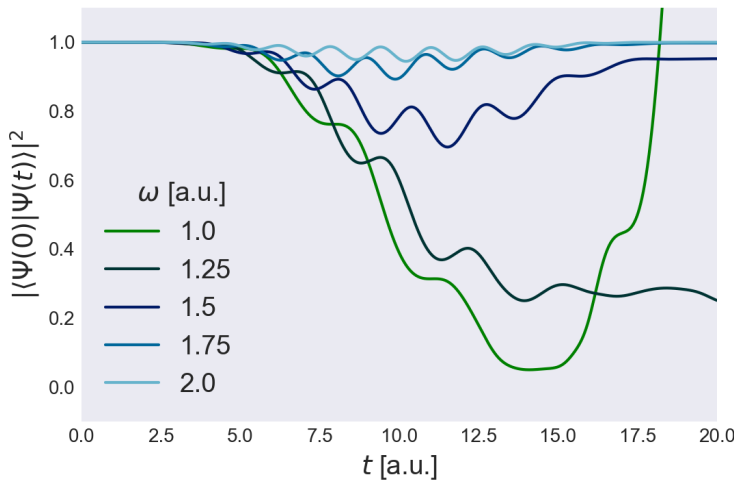


Figure 10.6: Time-dependent ground state probability $|\langle \Psi(0) | \Psi(t) \rangle|^2$ of a one-dimensional quantum dot with oscillator frequency $\Omega = 1$ a.u. and $n = 2$ electrons. The quantum dot is influenced by an oscillating field of different frequencies $\omega \in \{1.0, 1.25, 1.5, 1.75, 2.0\}$ with a maximum intensity of $E_{\max} = 0.25$ a.u.

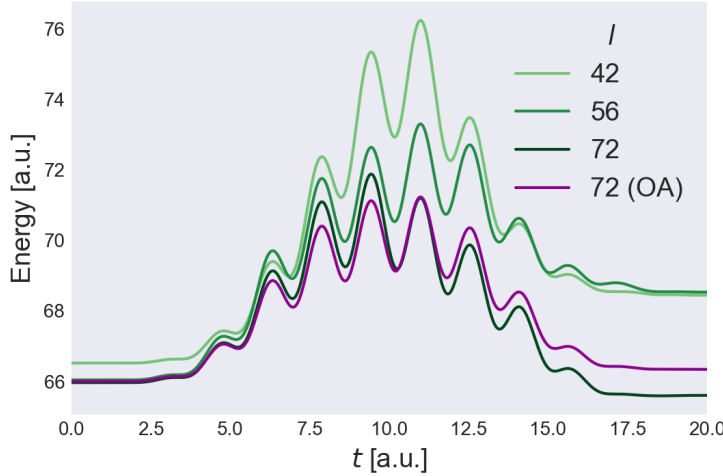


Figure 10.7: Time-dependent energy of a two-dimensional harmonic oscillator with $n = 12$ electrons under the influence of a laser field for different spin-orbitals $l \in \{42, 56, 72\}$.

frequency, such that $\omega = \Omega$, we see that the energy of the system is increased even at the very end of the simulation, when the amplitude of the oscillating field is minuscule. The same effects are apparent when studying the overlap of the time-developed system with the initial ground state in Figure 10.6. Closer to the resonant frequency we see a much lower probability of being in the ground state. For frequencies far away from the resonant frequency we see that the system falls back to the exact ground state or a state close to the ground state.

We have run similar simulations to the one described above, in order to study the resonant properties of a quantum dot, for $n = 4, 6, 8, 10$ electrons in a one-dimensional quantum dots. Figures with the results from these simulations can be found in section A.1. In the ground state probability plots for these simulations, one would notice unreasonable probability values $|\langle \Psi(0) | \Psi(t) \rangle|^2 > 1$. This is an issue we have addressed in the following sections, when reviewing the results of the two-dimensional quantum dot results.

10.2 Two-dimensional Quantum Dot

The two-dimensional quantum dot arguably paints a somewhat more interesting picture than the one-dimensional quantum dot, as we shall see. We construct several harmonic potential systems using the `TwoDimensionalharmonicOscillator` class. Similarly to the one-dimensional case, we simulate a laser by adding an oscillation field of the kind used by Pedersen and Kvaal [89], shown in Equation 10.1. Because we have added a dimension, we must choose a direction of polarisation. This choice is arbitrary because of the symmetry of the quantum dots. We therefore arbitrarily pick the x -direction. Unlike the one-dimensional dot, we are restricted to only a certain selection of systems,

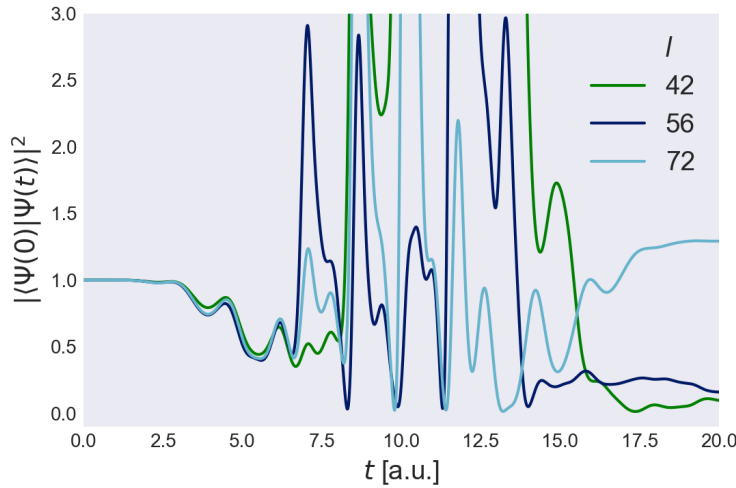


Figure 10.8: Dimensionless ground state probability $|\langle \Psi(0) | \Psi(t) \rangle|^2$ for a two-dimensional quantum dot with $n = 12$ electrons under the influence of a laser field for different number of spin-orbitals $l = \{42, 56, 72\}$.

namely systems of $n \in \{2, 6, 12\}$ electrons, that ensure full shells.

Like in our simulations of a one-dimensional harmonic quantum dot we have at first sought to show that we obtain convergence in the computations by applying an oscillating field far from the resonant frequency of the system. We set the oscillator frequency to $\Omega = 1$ a.u. and the frequency of the electric field to $\omega = 2\Omega = 2$ a.u. We perform a simulation over a period $T = 20$ a.u., for an increasing number of spin-orbitals l . The maximum intensity of the laser field is set to $E_{\max} = 1$ a.u. For these initial computations we use the time-dependent coupled cluster singles doubles (TDCCSD) method with static orbitals. The simulations for two and six electrons show expected results and have therefore been relegated to section A.2, while the results for twelve electrons appear to be on the brink of what the TDCCSD method can handle, within the given basis set size.

The time-dependent energy of a two-dimensional harmonic quantum dot with $n = 12$ electrons under influence of the oscillating field described above is shown in Figure 10.7. In this figure we have run the same simulation for $l \in \{42, 56, 72\}$ spin-orbitals with the time-dependent coupled cluster singles doubles (TDCCSD) method, and we see that only for the very largest of the basis set, we see a behaviour conforming with our expectations. We expect the energy to be close to the ground state energy after the laser-field has died out.

In the same figure (Figure 10.7) we have also included the computed energy over time for the system using the Orbital-Adaptive Time-Dependent Coupled Cluster Doubles (OATDCCD) method and the same number of spin-orbitals. We see that the two methods do not agree completely, and we are prone to trust the OATDCCD method more than the TDCCSD method in this case, because the energy at the end of the simulations is lower than the initial energy for the TDCCSD method.

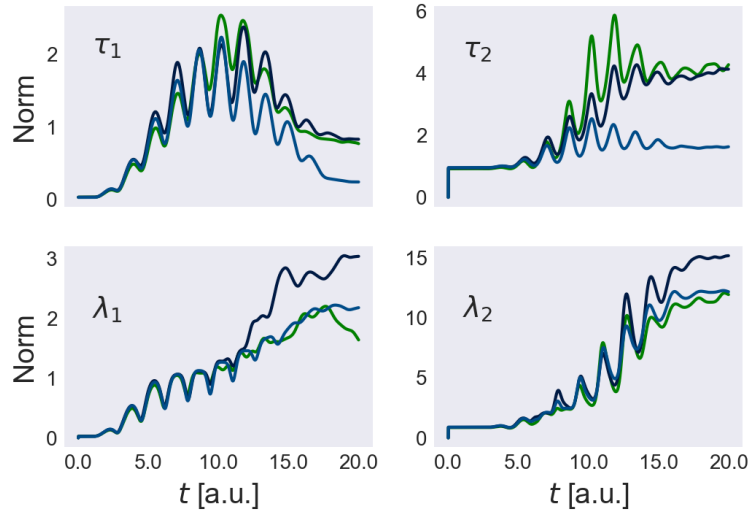


Figure 10.9: Norm of amplitudes, τ_1 , τ_2 , λ_1 and λ_2 (from CCSD, see section B.4) computed with the TDCCSD method in an $n = 12$ electron two-dimensional quantum dot influenced by an oscillating field with frequency $\omega = 2$ a.u., and intensity $E_{\max} = 1$ a.u. The simulation was run for $T = 20$ a.u., for several number of spin-orbitals $l = \{42, 56, 72\}$.

The reason for the problems the TDCCSD method shows are likely caused by the great difference between the exact state $|\Psi\rangle$ and the reference state $|\Phi\rangle$. The coupled cluster method seeks to represent the exact state $|\Psi\rangle$ by a linear combination, determined by the amplitudes, of basis functions in the reference state $|\Phi\rangle$. When the exact state of the system is very far from the reference state, we are not able to approximate it with the basis that is provided. We will outline this problem further as we study the time-dependent ground state probability of the simulation.

The ground state probability of the same simulation with the Time-Dependent Coupled Cluster Singles Doubles (TDDCCSD) method is shown in Figure 10.8. We see immediately that the probability becomes unreasonable at some time step after $t = 6$ a.u. This result is similar to the sort of break-down that occurred for the TDCCSD method in the attempt to replicate the results of Miyagi and Madsen [94] in section 9.4.

The probable cause of the unreasonable ground state probability is the need for the amplitudes of the system to acquire relatively high values, in order to compensate for the inadequateness of the reference state to describe the exact time-dependent state. This is underlined by the norm of the amplitudes, displayed in Figure 10.9. As is apparent, the lambda amplitudes show an upwards trend throughout the simulation. This should be unnecessary because the system would revert back to a state similar to the ground state at the end of the simulation. It appears that some “tipping point” is reached halfway around $t = T/2$ when the instability starts to increase. The τ -amplitudes are more or less well-behaved, at least for the largest basis set, showing some correlation in amplitude with the sinusoidal envelope of the oscillating field.

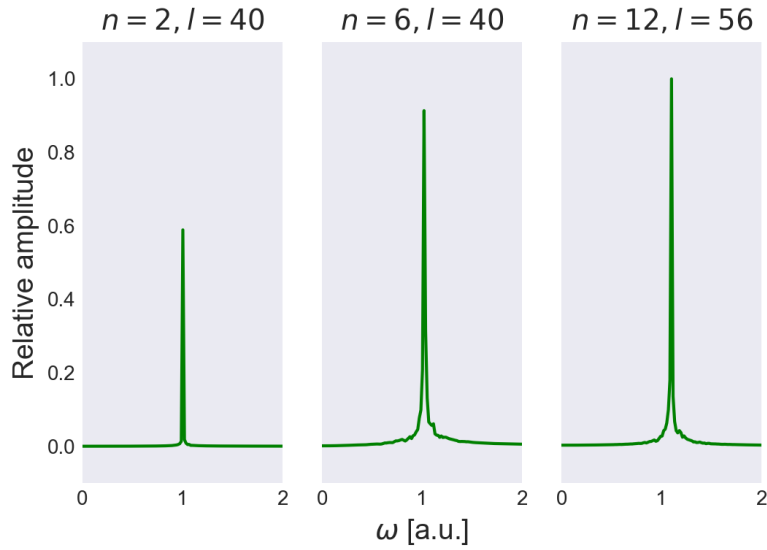


Figure 10.10: Fourier transform of the expected value of the dipole moment for a two-dimensional quantum dot with different number of electrons $n = \{2, 6, 12\}$ and respective number of spin-orbitals $l = \{40, 40, 56\}$. The intensity of the spectra is computed relative to the largest system with $n = 12$ electrons.

We have more trust in the Orbital-Adaptive Time-Dependent Coupled Cluster Doubles (OATDCCD) than the Time-Dependent Coupled Cluster Singles Doubles (TD-CCSD) method for this simulation. By developing the orbitals in time, as well as the amplitudes, we are provided with a continuously improved basis set. It is easier to represent the exact state $|\Psi(t)\rangle$ with a reference state $|\Phi(t)\rangle$ that is refreshed for each time step.

10.2.1 Dipole Spectrum

We have for the two-dimensional quantum dot computed the dipole spectrum for systems of different size, as we did for the one-dimensional quantum dot. We did this for quantum dots with oscillator frequencies $\Omega = 1$ a.u. with $n \in \{2, 6, 12\}$ electrons. We used $l \in \{42, 42, 56\}$ as the number of spin-orbitals for the respective systems. In order to excite and disturb the systems from the initial ground state we applied an oscillating field with a resonant frequency $\omega = \Omega = 1$ a.u. and a somewhat low maximum intensity $E_{\max} = 0.1$ a.u., with a three-step linear envelope as in Equation 9.2. The systems were allowed to develop in time for $T = 500$ a.u. The results of computing the Fourier transform of the dipole $\langle x \rangle(t) = \text{tr}\{\rho(t)x\}$ is depicted in Figure 10.10. In this figure we see that the result is qualitatively in accordance with the harmonic potential theorem - the dipole frequencies of all the systems are the same, with an intensity that increases with the number of particles in the system. For the two larger systems with $n = 6$ and $n = 12$ electrons we see some slight inaccuracies. These are attributable to the time constraint of this study - a simulation with larger number of spin-orbitals would have

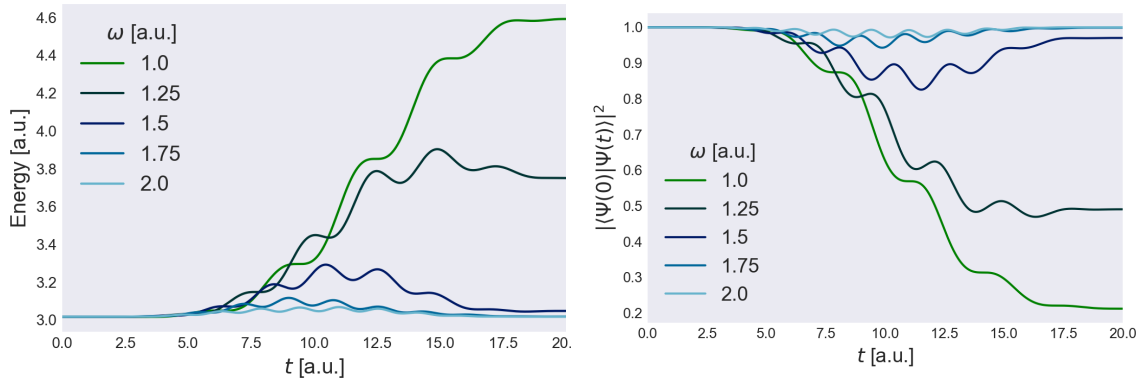


Figure 10.11: Time dependent energy (left) and ground state probability $|\langle \Psi(0) | \Psi(t) \rangle|^2$ (right) for a two-dimensional quantum dot with $n = 2$ electrons. The quantum dot is affected by an oscillating field of different frequencies $\omega \in \{1.0, 1.25, 1.5, 1.75, 2.0\}$ in atomic units with a maximum intensity $E_{\max} = 0.25$ a.u. The confining harmonic potential has frequency $\Omega = 1$ a.u.

remedied these inaccuracies, but would have needed more time to complete.

10.2.2 Resonance Sensitivity

For the two-dimensional quantum dot we have also conducted a resonance sensitivity analysis, similar to the one we performed for the one-dimensional quantum dot. The results for $n = 2$ electrons and $n = 6$ electrons are displayed in Figure 10.11 and Figure 10.12 respectively. The quantum dots in these simulations had an oscillator frequency of $\Omega = 1$ a.u. and were subjected to an oscillating field with a sinusoidal envelope of the type in Equation 10.1 of different frequencies $\omega \in \{1.0, 1.25, 1.5, 1.75, 2.0\}$ in atomic units and a maximum intensity of $E_{\max} = 0.25$ a.u.. The simulations were done with the time-dependent coupled cluster doubles (TDCCSD) method with static orbitals.

As in the one-dimensional analysis we see that the systems are much more prone to excitations as the frequency of the laser field approaches that of the quantum harmonic oscillator. This is apparent both for the energy of the quantum dot systems and the ground state probabilities displayed in the left and right subfigures of Figure 10.11 and Figure 10.12, respectively. In the six-particle case we again see the problems with the TDCCSD method when computing the ground state overlap, as the amplitudes acquire higher and higher values, resulting in probabilities that are unreasonable. In this case we do believe the energy plots to be correct for $\omega \in \{1.5, 1.75, 2.0\}$ in atomic units. We have less trust in the results from the last two simulations where the oscillating field had frequencies $\omega \in \{1.0, 1.25\}$ in atomic units. Here we see the same unreasonable time-dependent ground state probabilities as we did in Figure 10.8, as the TDCCSD method breaks down.

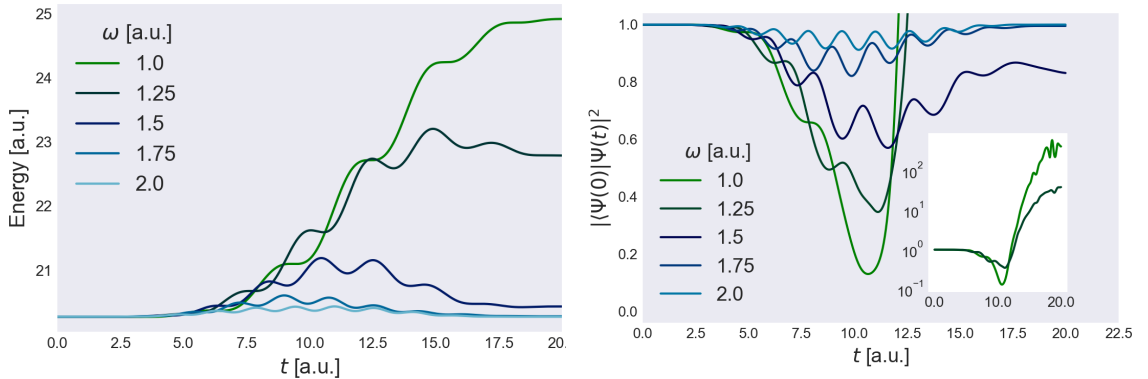


Figure 10.12: Time dependent energy (left) and ground state probability $|\langle \Psi(0) | \Psi(t) \rangle|^2$ (right) for a two-dimensional quantum dot with $n = 6$ electrons. The quantum dot is affected by an oscillating field of different frequencies $\omega \in \{1.0, 1.25, 1.5, 1.75, 2.0\}$ in atomic units with a maximum intensity $E_{\max} = 0.25$ a.u. The confining harmonic potential has frequency $\Omega = 1$ a.u.

10.3 Two-dimensional Double Dot

We have simulated two different two-dimensional double dot systems, one with $n = 2$ electrons and one system with $n = 4$ electrons, using the `TwoDimensionalDoubleWell` class described in subsection 7.2.3. We use $l = 20$ spin-orbitals for the two-electron system and $l = 56$ spin-orbitals for the four-electron system. The class requires two special parameters, `1_ho_factor` and `barrier_strength`. These dimensionless parameters define the number of regular harmonic oscillator functions to which the double well functions are mapped, and the height of the barrier between the wells, respectively. We set the barrier strength to 2 and the harmonic oscillator factor to 2 for both systems. The oscillator frequency of the double dot is set to $\Omega = 1$ a.u. As a visual confirmation of the systems, a one-electron density plot is provided for the $n = 2$ electrons system (left) and the $n = 4$ electron system (right) in Figure 10.13. We see from these density plots that the repulsive Coulomb interaction has a stronger effect for the system with the highest number of electrons.

The double dot is in essence a perturbation of the regular two-dimensional quantum dot, and we are seeking to uncover any many-body effects that such a perturbation could lead to. In order to do this we would like to compute the dipole spectrum of both systems. The time-propagation is done using the orbital-adaptive time-dependent coupled cluster doubles (OATDCCD) method, as it has shown the best stability of our time-dependent methods. Both systems are under the influence of an oscillating field with a linearly decreasing- and increasing envelope of the type used by Li *et al.* [92] (Figure 9.1). We have chosen a frequency of this field that corresponds to the resonant frequency of the first transition energy of the system $\omega = 0.43$ a.u., and an intensity yielding a maximum amplitude $E_{\max} = 0.1$ a.u. The resonant frequency was found by direct diagonalisation of the one-body matrix produced by the system class

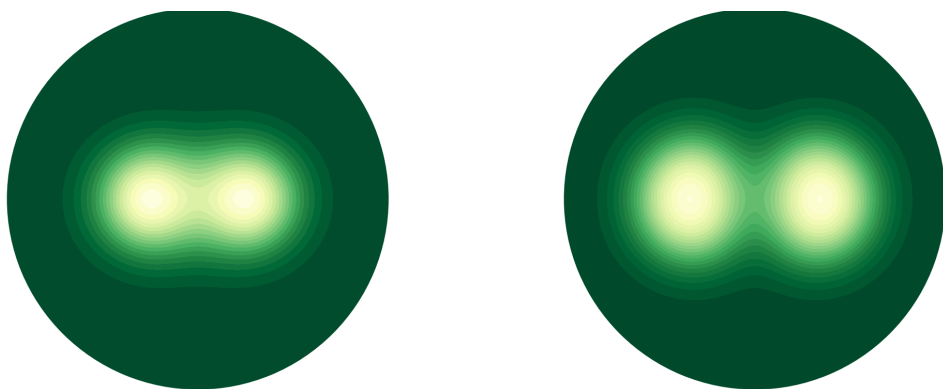


Figure 10.13: Ground state one-electron density for $n = 2$ electrons (left) and $n = 4$ electrons (right) for a double quantum dot. The number of spin-orbitals used in the two systems are $l = 20$ and $l = 56$, respectively. The oscillator frequency of the systems is set to $\Omega = 1$ a.u., with a barrier strength of 2 and a harmonic oscillator mapping ratio of 2.

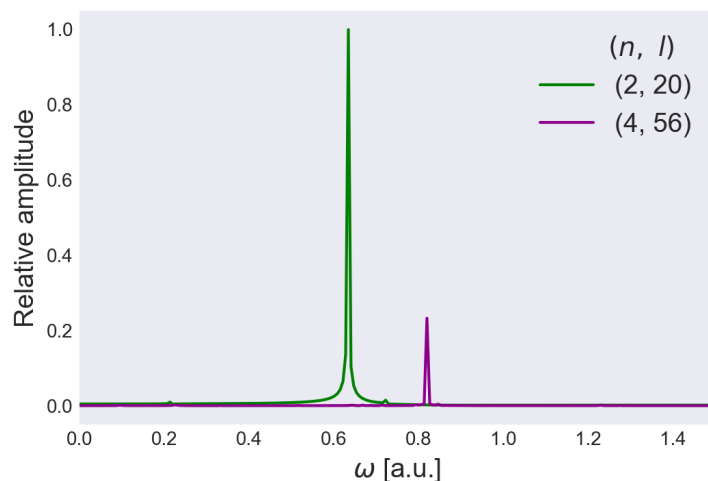


Figure 10.14: Dipole spectrum of two-dimensional double dot system with $n = \{2, 4\}$ electrons and $l = \{20, 56\}$ spin-orbitals. The double well systems have been subject to a laser pulse with frequency $\omega = 0.43$ a.u. and intensity $E_{\max} = 0.1$ a.u. The amplitudes have been computed relative to the highest amplitude value of the two systems.

`TwoDimensionalDoubleWell.`

The system is allowed to develop in time for $T = 100$ a.u. We compute the Fourier transform of the dipole moment $\langle \hat{x}(t) \rangle = \text{tr}\{\rho(t)x\}$, the results of which are shown in Figure 10.14. We immediately see that there is only one frequency apparent in the spectra for each of the systems, meaning that the quantum double dots have a position operator that behaves as if it was the centre of mass of the system. We see that the larger system has a relatively higher dipole frequency compared with the smaller system. We also see that the larger system has lower intensity compared with the smaller system.

This difference in frequency of the two systems may be caused by the increased Coulomb force, which creates a higher effective potential and constrains the electrons more firmly to the wells. The lower intensity of the larger system may also be explained by the same higher-potential effect of the Coulomb force, but can also be attributed to the fact that there is more mass to move with the same intensitity of the external field. We find this decrease in intensity somewhat puzzling, as the same laser field applied to a larger system would yield an increase for the single-well potential.

We may have seen more many-body effects in the form of more spectral lines if we were to increase the intensity of the oscillating laser field, decrease the barrier strength of the double well potential, or both. This may have made it more likely to tunnel through the barrier, i.e. increase transition probabilities of higher energy quantum leaps. With the methods at hand we have had problems with convergence of our solvers for very large field strength, however. We sought to remedy this by implementing a smoother double well potential, but had to abandon this effort due to the time restriction of this thesis.

10.4 Two-dimensional Magnetic Quantum Dot

We start the study of two-dimensional quantum dots under the influence of a magnetic field by defining a system of only one particle and solving the time-dependent Schrödinger equation directly. This is a accomplished by using the `TwoDimHarmonicOscB` class to produce a basis set and dipole elements which is everything we need. All of these items are properties of the class and can be easily extracted. A simple periodic function that simulates an electric field is constructed, as the product of such a time-dependent operator and the interaction define the time propagation. We then use a simple integration scheme, in this case the fourth-order Runge-Kutta method, to propagate the ground state single particle function of the system. Taking care to extract the dipole moment $\langle \hat{x}(t) \rangle = \text{tr}\{\rho(t)x\}$ for every time step, we can compute the discrete Fourier transform of the dipole and compute the frequency spectrum of our system. This procedure is applied to a system completely absent of a magnetic field, and a system under direct influence of a magnetic field. Except for the magnetic field the systems are identical with the same base oscillator frequency $\omega_0 = 1$. It is necessary to define this new variable name due to the effective increase in the confining potential of the system caused by the addition of a magnetic field.

Before going straight to the results, we study the shell structure and allowed transitions of our two systems. The left part of Figure 10.15 presents the shell structure of the regular two-dimensional quantum dot. The states have all been assigned a number for

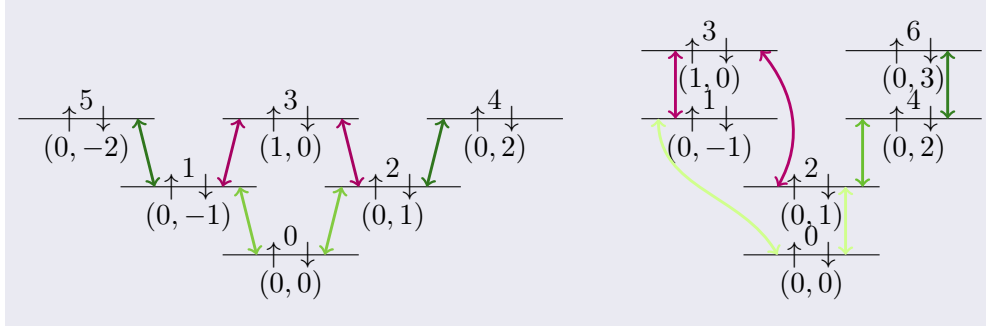


Figure 10.15: Shell structure of six lowest orbitals before (left), and after (right) a magnetic field is applied to a 2D quantum dot.

easier examination. This shell structure is identical to the one presented in Figure 7.2. Additionally, here we have added coloured double arrows to illustrate the allowed transitions in the quantum dot. These transitions can be encountered in the transition matrix for the system, which is reproduced with color coding in the left subfigure of Figure 10.16. Notice that the coloured arrows representing allowed transitions match in colour with the elements of the transition matrix.

When we apply a magnetic field of strength $\omega_c/\omega = \sqrt{2}/2$ we obtain the shell structure represented to the right in Figure 10.15, where the allowed transitions correspond to the transition matrix in the right subfigure in Figure 10.16. The chosen magnetic field strength was not chosen arbitrarily, as these accidental degeneracies occur only rarely as a function of magnetic field strength¹. For succinctness we repeat the function from Equation 7.36 for energy eigenvalues for two-dimensional quantum dot influenced by a magnetic field,

$$\epsilon_{nm} = \hbar\Omega(2n + |m| + 1) - \frac{\hbar\omega_c}{2}m, \quad (10.2)$$

where $\Omega = \sqrt{\omega_0^2 + \frac{\omega_c^2}{4}}$ is the effective frequency of the confining potential, ω_0 is the base frequency of the harmonic oscillator, and ω_c is the Larmor frequency that defines the strength of the magnetic field. Apart from a general shift up in energy by adding a magnetic field, the states with negative azimuthal quantum number m will experience an increase in energy eigenvalue, and vice versa. We see this effect clearly in the new shell structure in Figure 10.15. The states with negative m have indeed undergone a relative shift upwards, whilst the states with positive m have been shifted downwards, relative to the other states. The ground state, labelled 0, remains relatively stationary, the states labelled 2 ($m = 1$) and 4 ($m = 2$) have been shifted downwards and the states labelled 1 ($m = -1$) and 5 ($m = -2$) have been shifted upwards. State number 5 has been shifted upwards in energy so much that it has disappeared from the shell structure, with a new state 6 ($m = 3$) appearing in its place. This is due to our restriction to include only the six lowest-energy orbitals. We see that the possible allowed transitions

¹Hence the term ‘‘accidental’’.

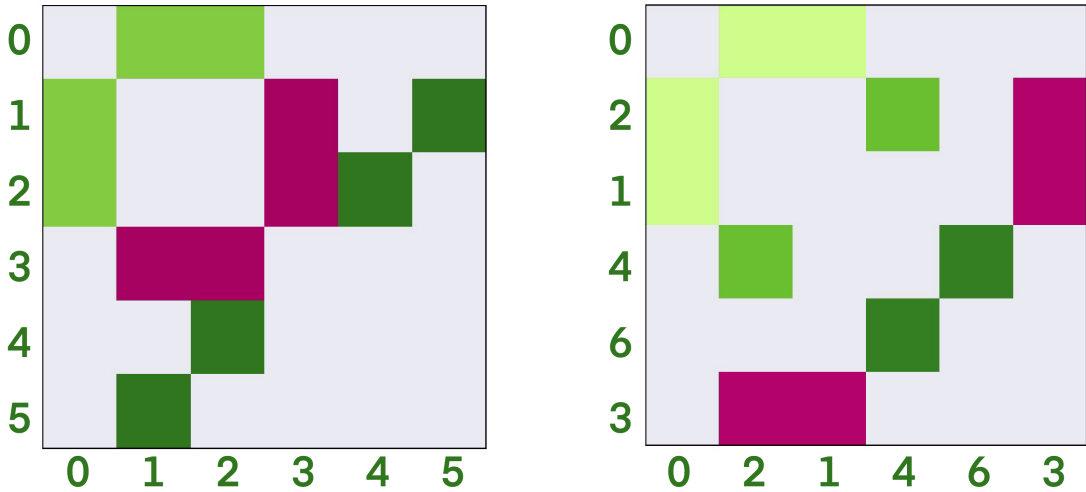


Figure 10.16: Transition matrix for a two-dimensionsal harmonic quantum dot with (left) and without (right) a magnetic field applied. The two systems both have a base oscillator frequency of $\omega_0 = 1$ a.u., while the right figure has a magnetic field applied with Larmor frequency $\omega_c = \sqrt{2}/2$ a.u. The effective confining potential is $\Omega = 1$ a.u. for the system represented in the left figure and $\Omega \approx 1.118$ a.u. for the system represented in the right figure.

remain the same, except for the transition between state 1 and 5, because state 5 has been shifted out of our truncated shell structure. We also see a new possible possible transition between state 4 and state 6.

If we compute the frequency spectrum of the two systems (Figure 10.17) we get a single line for the normal quantum dot. This is expected, as the quantum harmonic oscillator has the same energy difference between each level. However, when we apply a magnetic field and shift the energies of the orbitals in the quantum dot, we see that we get two different energy transitions. This is revealed as two lines in the frequency spectrum in Figure 10.17. This is equivalent to a splitting in transmission spectra of quantum dot arrays under the effect of a magnetic field in experiments [98, 99].

10.4.1 Many-particle Magnetic Quantum Dots

We will now show that the dipole spectrum splitting holds for a quantum dot of several electrons. To do this we conduct several simulations of quantum dots consisting of both $n = 2$ and $n = 4$ electrons. Because of the reordering of quantum degeneracies that occurs by introducing a magnetic field, we will not run into any multi-reference problems for the $n = 4$ electron case.

The quantum dot systems are each excited by a laser pulse with the linearly increasing and decreasing envelope, as defined by Li *et al.* [92], in Equation 9.2. The laser of this oscillating field is set to the same frequency as the system $\omega = \omega_0 = 1$ a.u. and the maximum intensity of the field is $E_{\max} = 0.1$ a.u. The Larmor frequency of the magnetic field that the quantum dots are subjected to is varied, $\omega_c \in \{0.25, 0.5, 0.75, 1.0\}$

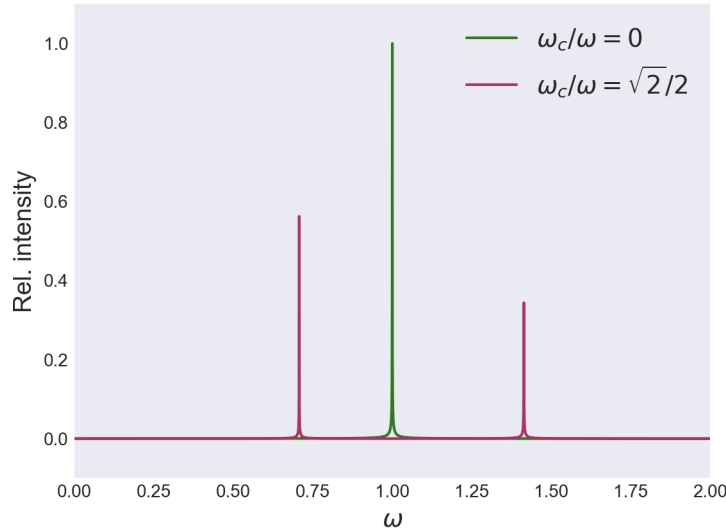


Figure 10.17: Spectrum of a single-electron two-dimensional quantum dot both with and without a magnetic field.

in atomic units. For each of these simulations we compute the Fourier transform of the dipole moment $\langle \hat{x}(t) \rangle = \text{tr}\{\rho(t)\hat{x}\}$, in the same direction as the polarisation of the laser field. In the simulations with $n = 2$ electrons we used $l = 30$ spin-orbitals, and in the simulations with $n = 4$ spin-orbitals we used $l = 56$ spin-orbitals. We let the systems propagate for $T = 1000$ a.u.²

We present some selected results here, for Larmor frequency $\omega_c = 0.25$ for $n = 2$ and $n = 4$ electrons, shown in figure Figure 10.18 and Figure 10.19, respectively. The results for the rest of the different Larmor frequencies are consigned to section A.3. All results of these simulations conform with the harmonic potential theorem. The distance between the two lines of the spectrum is approximately equal to the Larmor frequency. What little error is seen can be attributed to numerical errors, most likely caused by basis set truncations or premature termination of the time-propagation.

²With the notable exception of the $n = 4$ electron simulation for $\omega_c = 0.25$ a.u., which was terminated at $T = 700$ a.u..

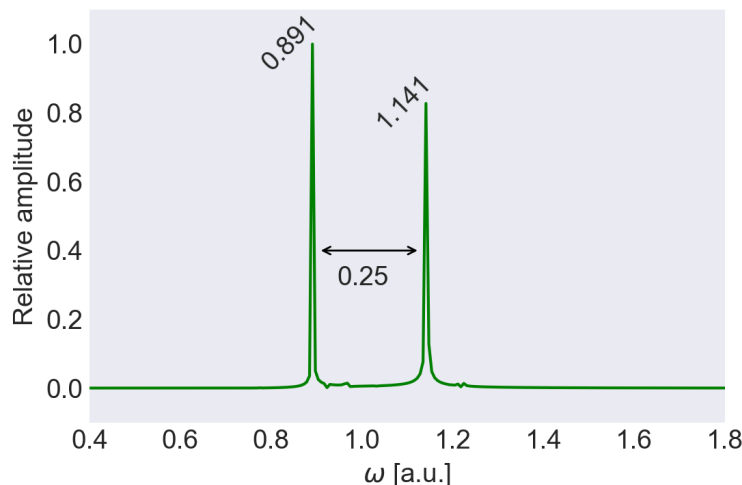


Figure 10.18: Dipole spectrum of a quantum dot with $n = 2$ electrons and base frequency $\omega_0 = 1$, subjected to a magnetic field with Larmor frequency $\omega_c = 0.25$. The system was excited with a laser field with frequency $\omega = 1$ a.u. and intensity $E_{\max} = 0.1$ a.u. for $t_d = 6\pi/\omega$ a.u. then allowed to propagate in time for a total of $T = 1000$ a.u.

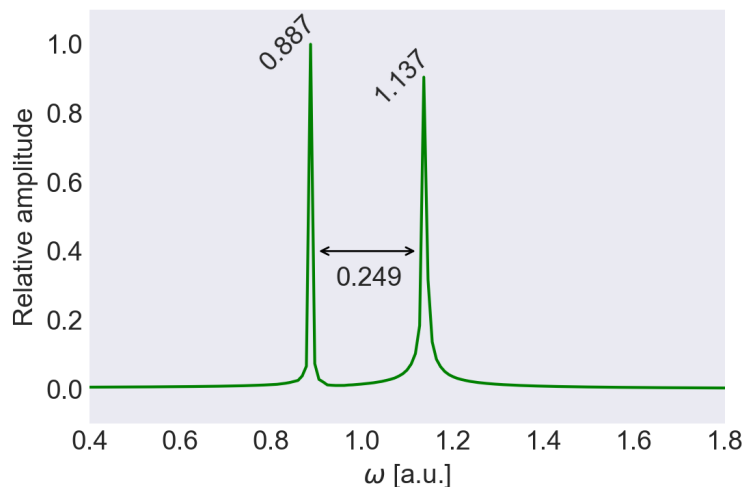


Figure 10.19: Dipole spectrum of a quantum dot with $n = 4$ electrons and base frequency $\omega_0 = 1$, subjected to a magnetic field with the Larmor frequency $\omega_c = 0.25$. The system was excited with a laser field with frequency $\omega = 1$ a.u. and intensity $E_{\max} = 0.1$ a.u. for $t_d = 6\pi/\omega$ a.u. This simulation broke down after a total time of $T \approx 700$ a.u., but the data collected up to this point was sufficient get the desired result.

Part V

Conclusion

Chapter 11

Summary Remarks

The aim of this thesis was to develop and test numerical methods for solving the time-dependent Schrödinger equation. In particular, we wanted to develop the Orbital Adaptive Time-Dependent Coupled Cluster (OATDCC) method introduced by Kvaal [1].

We can with confidence say that this endeavour has been successful. We have implemented both a time-dependent Coupled Cluster Singles Doubles (TDCCSD) solver with static orbitals and an *Orbital Adaptive* Time-Dependent Coupled Cluster Doubles (OATDCCD) solver, as well as several quantum systems and an interface to quantum chemistry software which enables extraction of further basis sets. The resulting product is two modules for python; `quantum_systems` and `coupled_cluster`.

With these methods we have managed to produce many results found in the existing literature on time-dependent ab initio many-body solvers. This includes a reproduction of the instantaneous dipole moment of H_2 from Li *et al.* [92], the time-dependent ground state probability of a one-dimensional quantum dot from Zanghellini *et al.* [93], the dipole spectrum of helium from Pedersen and Kvaal [89] and the ionisation of a one-dimensional model of beryllium from Miyagi and Madsen [94].

We have been able to compute the time-development of a relatively high number of particles, up to $n = 12$ electrons in one- and two-dimensional quantum dots. This stands as a testimony to the capabilities of our implementations. For ever-increasing basis set size we have produced time-dependent results that converge, adding to the confidence in the results. The results relating to quantum dots are in accordance with the results one would expect from theory. Specifically, in both one-dimensional and two-dimensional quantum dots we have shown that the harmonic potential theorem [5] holds - the dipole spectrum of quantum dots consists of only one line consistent with the oscillator frequency in ordinary harmonic quantum dots. For the two-dimensional double dot system, we also see only one spectral line, but a shift in frequency. By adding a homogenous, static magnetic field to the quantum dot, we see a split in the dipole spectrum resulting in two spectral lines at a distance equal to the Larmor frequency of the applied magnetic field, also in agreement with the harmonic potential theorem.

In assessment of the time-dependent coupled cluster method with static orbitals, we found that the solver struggles to correctly represent the current state if the system progresses too far away from the initial reference state. As such the method is not a

method that one can trust blindly, as it returns inaccurate results in these situations. This phenomenon shows most clearly as ground state overlap values that are clearly unreasonable, but also as exceedingly high amplitude values. The orbital-adaptive solver remedies this problem, but has a drawback in that it cannot feasibly produce inner products of two states in time, and therefore is unable to compute time-dependent ground state probabilities.

This study, with the addition of the study by Schøyen [6], has only scratched the surface with regards to the cornucopia of results that our code base is able to produce. The reason for this is for the most part attributed to the time spent in development and the amount in wall clock time necessary to produce the results herein. A challenge with time-dependent studies is the impossibility of true parallelisation, as time step t_n will always depend on t_{n-1} .

11.1 Further Studies

Based on the results we have produced, we think that a comparative study of the method with static orbitals and the one with adaptive orbitals is warranted. One would assume that the two methods yield identical results within a reasonable upper limit in basis set size, but under what conditions do we get close to this limit? We can for instance imagine that the orbital-adaptive scheme yields equivalent results compared to the static-orbital method for a lower number of spin-orbitals, because of the automatic adaption to the current state that an orbital adaption provides. A study is in preparation for publication which seeks to stress-test the orbital-adaptive method [28].

The inclusion of triples amplitudes in order to develop a Time-Dependent Coupled Cluster Singles Doubles Triples (TDCCSDT) algorithm and an Orbital-Adaptive Time-Dependent Coupled Cluster Doubles Triples (OATDCCDT) algororithm would be a logical step to take, and is of great interest. Building an orbital-adaptive method with triples would be a tremendous complication, at least to the orbital equations.

As of now, the apparatus we have manufactured can easily be used to model the time-dependent behaviour of additional systems. In fact, one could even easily argue that the complete investigation of the systems we have implemented ourselves in `quantum_dots` is far from over. We have already begun the implementation of a smoother two-dimensional double well potential, as well as more interesting well potentials such as the double double dot from Nielsen *et al.* [100]. Another idea is the construction of potentials that are not circular-symmetric. That said, we regrettably only had time to study *one* of the *five* potentials we have implemented for the one-dimensional quantum dot. The addition of a three-dimensional quantum dot system would also be essential in any further studies. Here, the integral elements provided by Vorrath and Blümel [101] would be useful.

We would also like to see the addition of more exotic terms to the Hamiltian in the quantum dot systems. We think it would not be too difficult to add spin-operator terms \hat{S}_x , \hat{S}_y , \hat{S}_z , spin-spin coupling terms $\hat{S} \cdot \hat{S}$, and spin-orbit coupling terms \hat{J}^2 , $\hat{L} \cdot \hat{S}$. We believe that these would provide very interesting results and enables us to model richer and more interesting physical effects. We are confident that the mere addition of a \hat{S}_z

operator would enable us to see Zeeman splitting in the dipole spectrum of quantum dots, for instance. Eventually, one could hope to implement much more complicated operators, such as quantum logic gates, with the hope of consequent simulations of quantum gates.

In their seminal article, Loss and DiVincenzo [83] propose an implementation of a universal set of one- and two-quantum-bit gates for quantum computation using the spin states of coupled single-electron quantum dots. The framework that we have built as part of this thesis together with Schøyen, can readily be adjusted to be able to simulate such systems in time.

We should highlight the study of nuclear matter, which was the original area of application for the coupled cluster method, as an area of great interest. With a time-dependent coupled cluster method, as we have built, one could potentially be able to simulate nuclear reactions such as fission and fusion processes, a feat that would be of tremendous value.

In this study we have implemented the dipole approximation of a laser field to function as a time-development operator. Richer physics can be modelled by the implementation of higher order multi-pole terms for such an oscillating laser field. Moving beyond the allowed transitions dictated by the dipole approximation could potentially yield very interesting results.

Currently, an article is in preparation for publication that relies on the software we have developed and the results we have arrived at in this thesis; see Kristiansen *et al.* [102].

Part VI

Appendices

Appendix A

Quantum Dot Results

Here we present supplementary data that completes the results presented in chapter 10 on quantum dot simulations in time. In this appendix we show how the time-dependent coupled cluster method converges for an increasing basis. These simulations are done for quantum dots in both one and two dimensions. Additionally, we provide the results from simulations constructed to show the response of quantum dots subjected to oscillating fields of different frequencies. Lastly, we show how a quantum dot in two dimensions, subject to a magnetic field, leads to a splitting in the dipole spectrum of the system.

A.1 One Dimension

The simulations presented here have been conducted with the Time-Dependent Coupled Cluster Singled Doubles (TDCCSD) method.

Four electrons

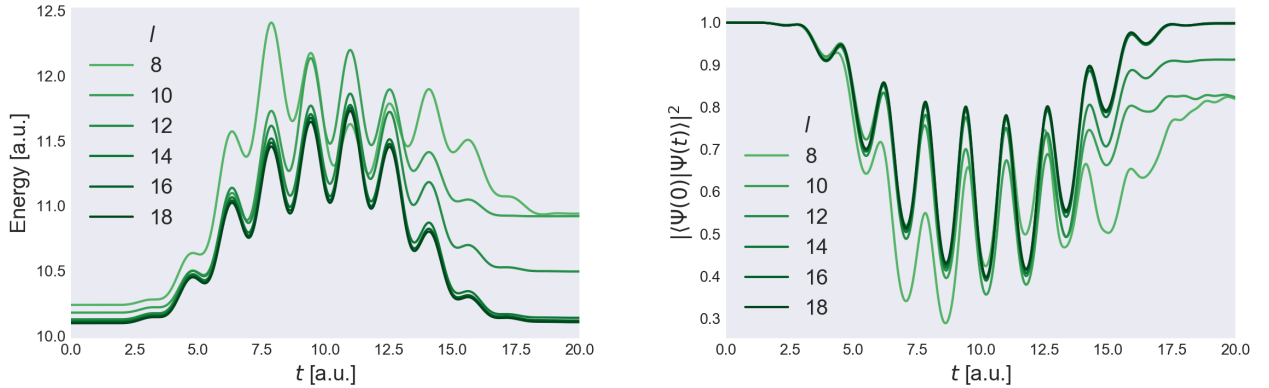


Figure A.1: Time-dependent energy (left) and ground state probability (right) of a one-dimensional harmonic oscillator with $\Omega = 1$ a.u. and $n = 4$ electrons under the influence of a oscillating electric field of frequency $\omega = 2\Omega = 2$ a.u. and field strength $E_{\max} = 1$ a.u., for different number of spin-orbitals $l = \{8, 10, 12, 14, 16, 18\}$.

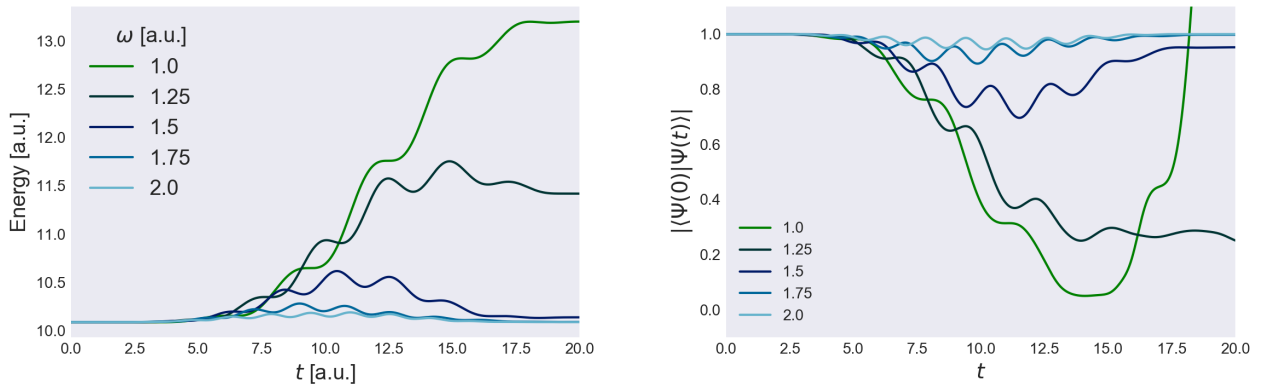


Figure A.2: Time-dependent energy (left) and ground state probability (right) of a one-dimensional harmonic oscillator with $\Omega = 1$ a.u. and $n = 4$ electrons under the influence of a oscillating electric field of different frequencies $\omega \in \{1.0, 1.25, 1.5, 1.75, 2.0\}$ in atomic units with maximum field strength $E_{\max} = 0.25$ a.u. and $l = 30$ spin-orbitals.

Six electrons

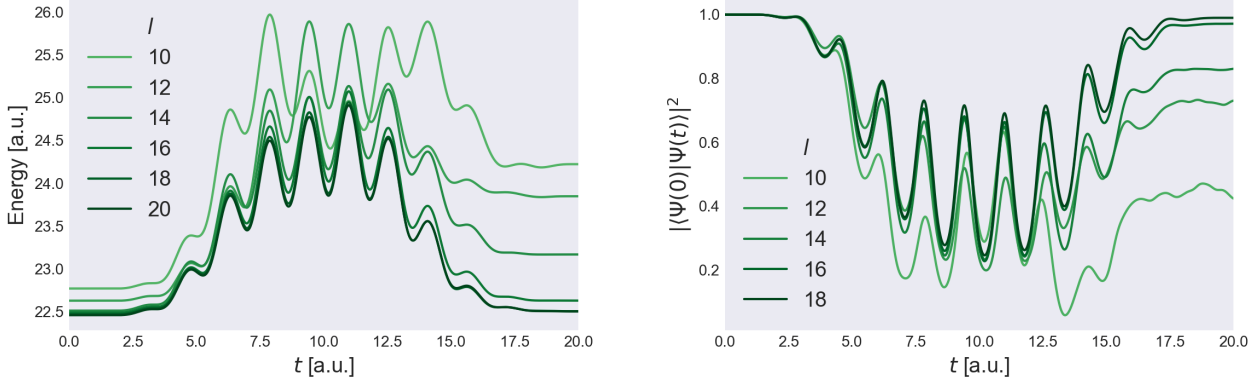


Figure A.3: Time-dependent energy (left) and ground state probability (right) of a one-dimensional harmonic oscillator with $\Omega = 1$ a.u. and $n = 6$ electrons under the influence of a oscillating electric field of frequency $\omega = 2\Omega = 2$ a.u. and field strength $E_{\max} = 1$ a.u., for different number of spin-orbitals $l = \{10, 12, 14, 16, 18, 20\}$.

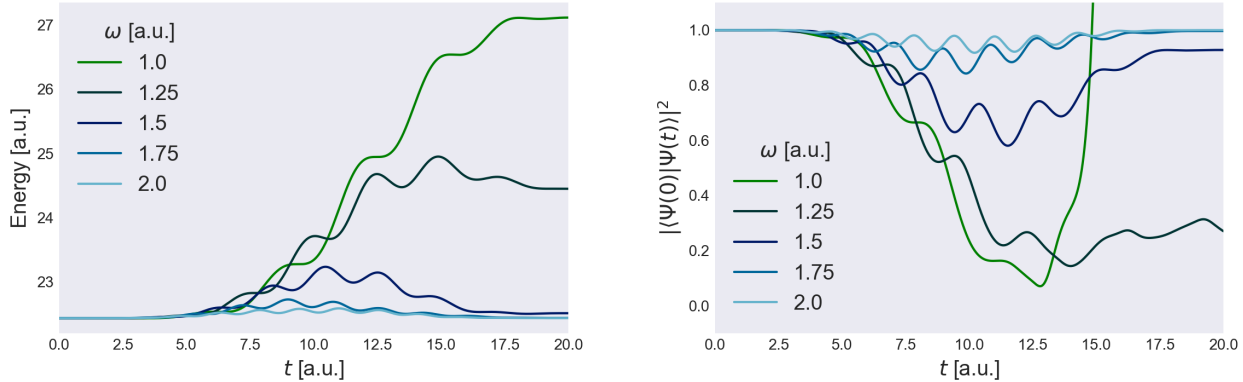


Figure A.4: Time-dependent energy (left) and ground state probability (right) of a one-dimensional harmonic oscillator with $\Omega = 1$ a.u. and $n = 6$ electrons under the influence of a oscillating electric field of different frequencies $\omega \in \{1.0, 1.25, 1.5, 1.75, 2.0\}$ in atomic units with maximum field strength $E_{\max} = 0.25$ a.u. and $l = 30$ spin-orbitals.

Eight electrons

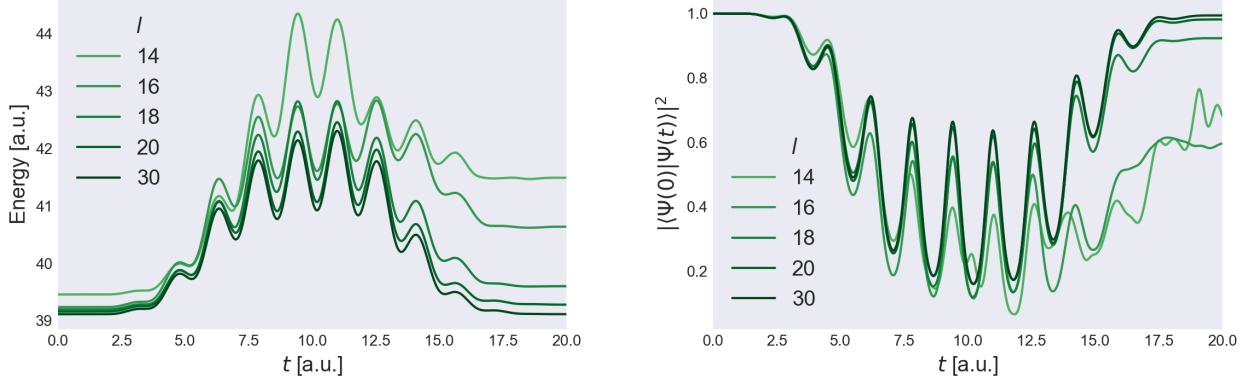


Figure A.5: Time-dependent energy (left) and ground state probability (right) of a one-dimensional harmonic oscillator with $\Omega = 1$ a.u. and $n = 8$ electrons under the influence of a oscillating electric field of frequency $\omega = 2\Omega = 2$ a.u. and field strength $E_{\max} = 1$ a.u., for different number of spin-orbitals $l = \{14, 16, 18, 20, 30\}$.

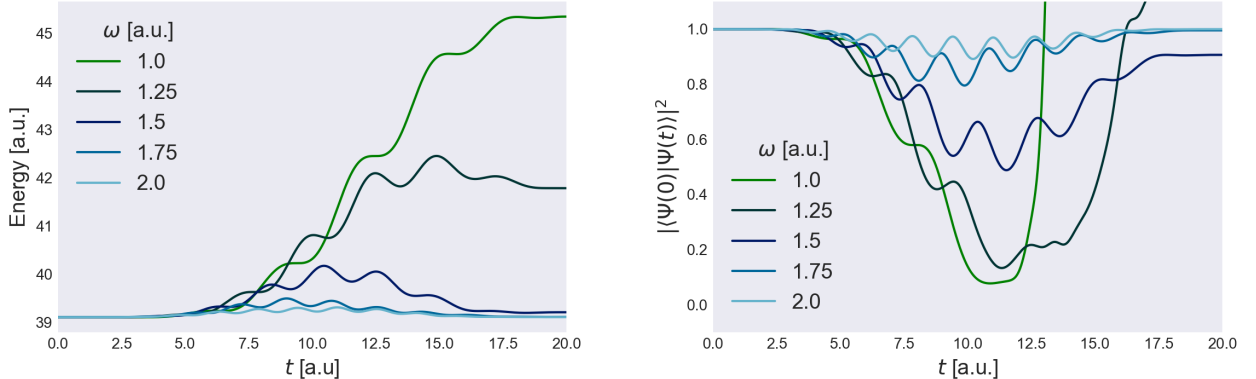


Figure A.6: Time-dependent energy (left) and ground state probability (right) of a one-dimensional harmonic oscillator with $\Omega = 1$ a.u. and $n = 8$ electrons under the influence of a oscillating electric field of different frequencies $\omega \in \{1.0, 1.25, 1.5, 1.75, 2.0\}$ in atomic orbitals with maximum field strength $E_{\max} = 0.25$ a.u. and $l = 36$ spin-orbitals.

Ten electrons

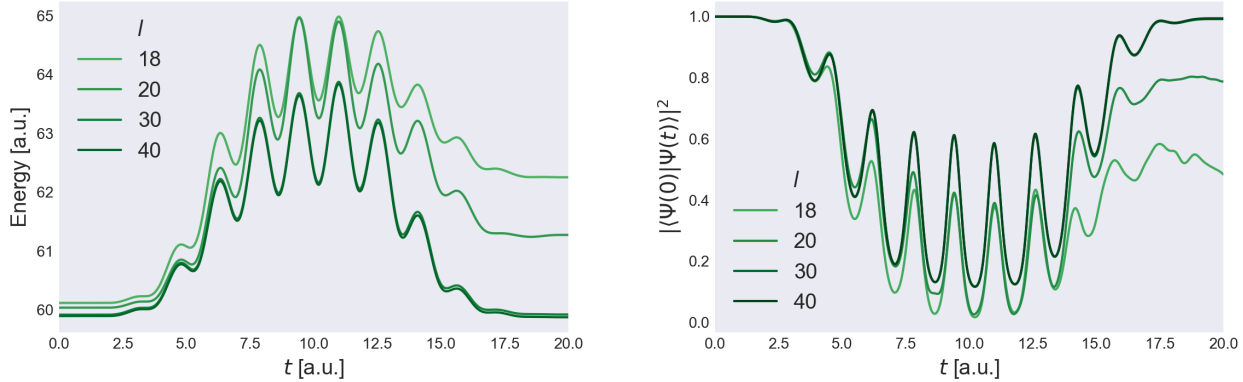


Figure A.7: Time-dependent energy (left) and ground state probability (right) of a one-dimensional harmonic oscillator with $\Omega = 1$ a.u. and $n = 10$ electrons under the influence of a oscillating electric field of frequency $\omega = 2\Omega = 2$ a.u. and field strength $E_{\max} = 1$ a.u., for different number of spin-orbitals $l = \{18, 20, 30, 40\}$.

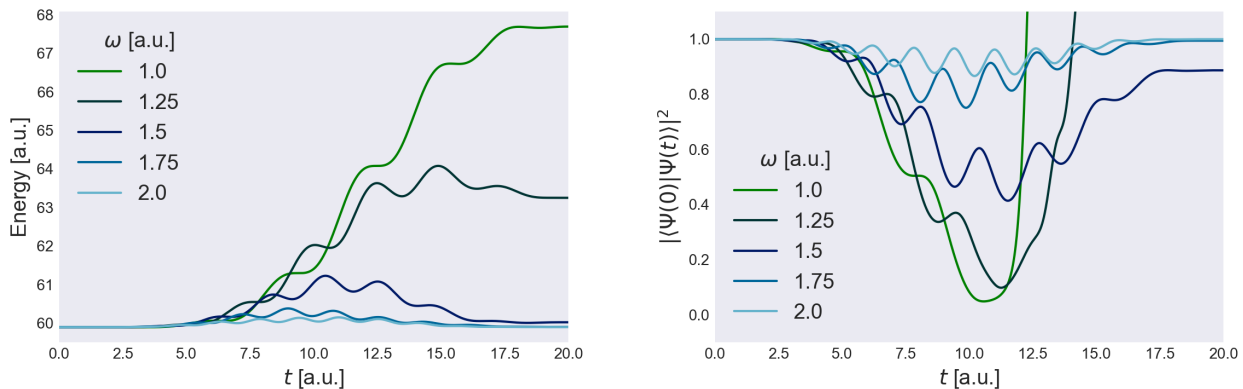


Figure A.8: Time-dependent energy (left) and ground state probability (right) of a one-dimensional harmonic oscillator with $\Omega = 1$ a.u. and $n = 8$ electrons under the influence of a oscillating electric field of different frequencies $\omega \in \{1.0, 1.25, 1.5, 1.75, 2.0\}$ in atomic units with maximum field strength $E_{\max} = 0.25$ a.u. and $l = 40$ spin-orbitals.

Twelve electrons

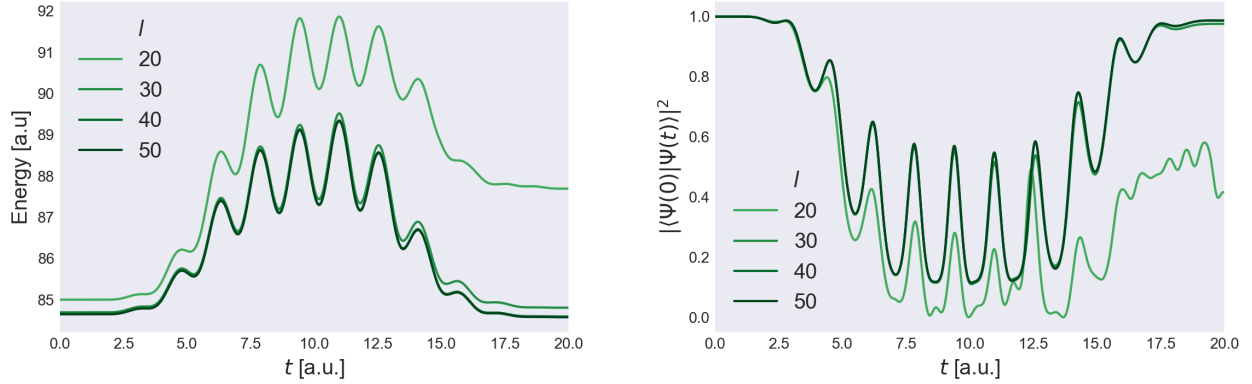


Figure A.9: Time-dependent energy (left) and ground state probability (right) of a one-dimensional harmonic oscillator with $\Omega = 1$ a.u. and $n = 12$ electrons under the influence of a oscillating electric field of frequency $\omega = 2\Omega = 2$ a.u. and field strength $E_{\max} = 1$ a.u., for different number of spin-orbitals $l = \{20, 30, 40, 50\}$.

A.2 Two Dimensions

The simulations presented here have been conducted with the Time-Dependent Coupled Cluster Singled Doubles (TDCCSD) method.

Two electrons

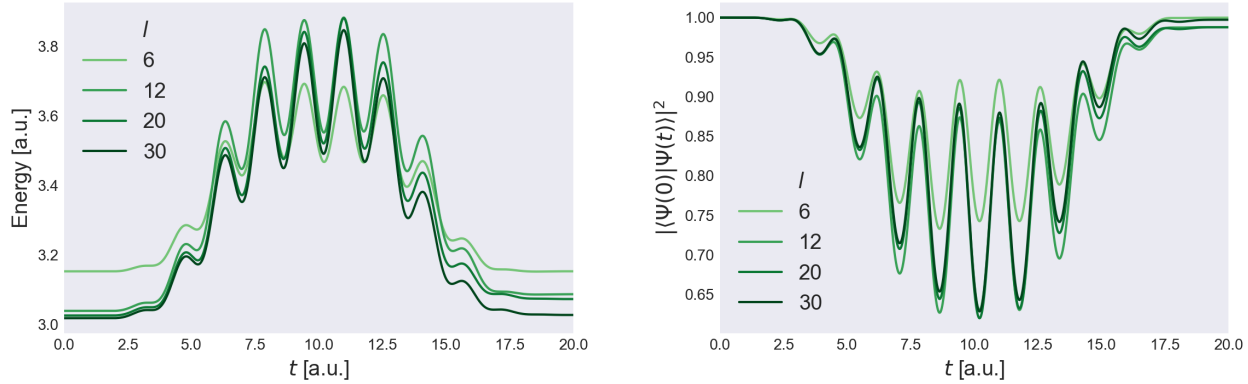


Figure A.10: Time-dependent energy (left) and ground state probability (right) of a two-dimensional harmonic oscillator with $\Omega = 1$ a.u. and $n = 2$ electrons under the influence of a oscillating electric field of frequency $\omega = 2\Omega = 2$ a.u. and field strength $E_{\max} = 1$ a.u., for different number of spin-orbitals $l = \{6, 12, 20, 30\}$.

Six electrons

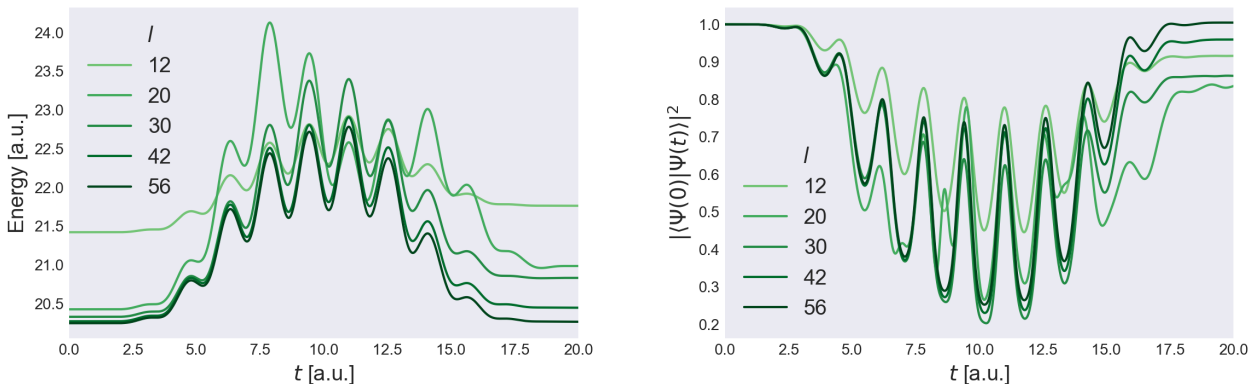


Figure A.11: Time-dependent energy (left) and ground state probability (right) of a two-dimensional harmonic oscillator with $\Omega = 1$ a.u. and $n = 6$ electrons under the influence of a oscillating electric field of frequency $\omega = 2\Omega = 2$ a.u. and field strength $E_{\max} = 1$ a.u., for different number of spin-orbitals $l = \{12, 20, 30, 42, 56\}$.

A.3 Two Dimensions with Magnetic Field

The simulations presented here have been conducted with the Orbital-Adaptive Time-Dependent Coupled Cluster Doubles (OATDCCD) method.

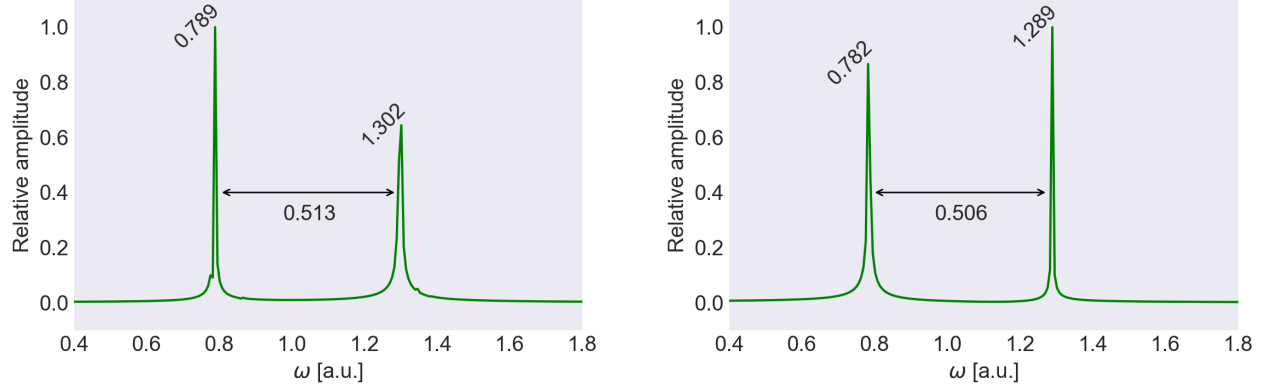


Figure A.12: Dipole spectrum of a quantum dot with $n = 2$ (left), and $n = 4$ electron subjected to a magnetic field with Larmor frequency $\omega_c = 0.50$ a.u.. Both systems have base oscillator frequency $\omega_0 = 1$ a.u. and have been excited with an oscillating field with frequency $\omega = 1$ a.u. and intensity $E_{\max} = 0.1$ a.u.. The oscillating field had a period of $t_d = 6\pi/\omega$ a.u. and the system was developed in time for a total of $T = 1000$ a.u..

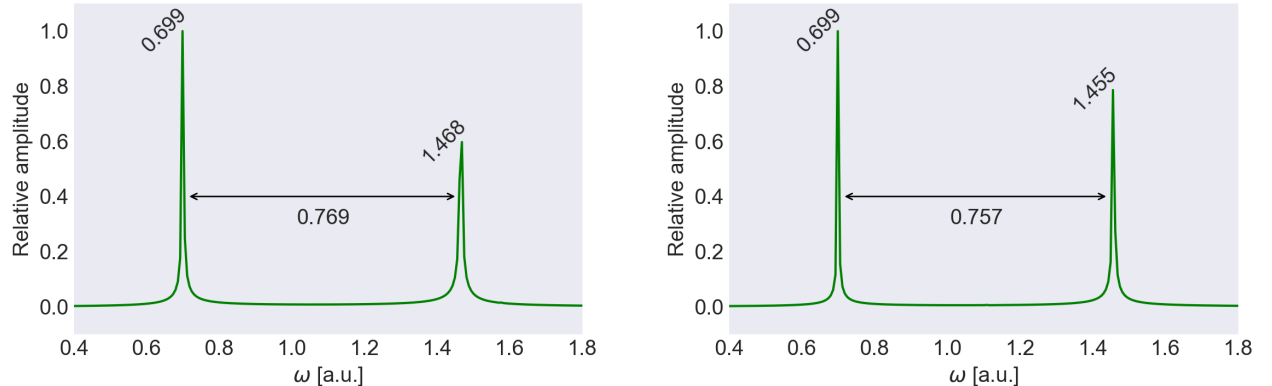


Figure A.13: Dipole spectrum of a quantum dot with $n = 2$ (left), and $n = 4$ electron subjected to a magnetic field with Larmor frequency $\omega_c = 0.75$ a.u.. Both systems have base oscillator frequency $\omega_0 = 1$ a.u. and have been excited with an oscillating field with frequency $\omega = 1$ a.u. and intensity $E_{\max} = 0.1$ a.u.. The oscillating field had a period of $t_d = 6\pi/\omega$ a.u. and the system was developed in time for a total of $T = 1000$ a.u..

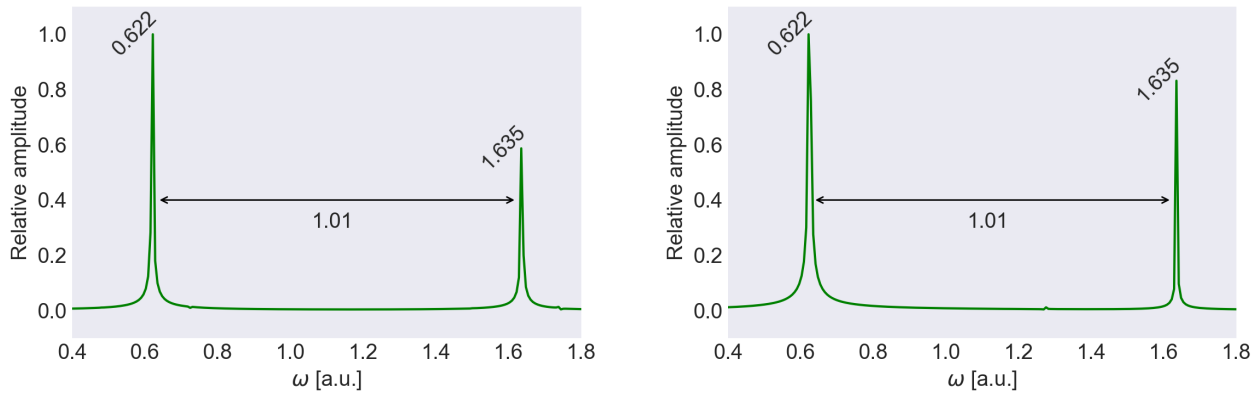


Figure A.14: Dipole spectrum of a quantum dot with $n = 2$ (left), and $n = 4$ electron subjected to a magnetic field with Larmor frequency $\omega_c = 1.0$ a.u.. Both systems have base oscillator frequency $\omega_0 = 1$ a.u. and have been excited with an oscillating field with frequency $\omega = 1$ a.u. and intensity $E_{\max} = 0.1$ a.u.. The oscillating field had a period of $t_d = 6\pi/\omega$ a.u. and the system was developed in time for a total of $T = 1000$ a.u..

Appendix B

Coupled Cluster

Here we present some supplementary material to the coupled cluster method and theory that we did not see fit to include in either chapter 6, on coupled cluster theory, or chapter 8, on the implementation of the coupled cluster methods. Nevertheless, these extra pieces of information that are presented here can be useful. First, we show the relation between a truncated coupled cluster wavefunction and the configuration interaction expansion. Second, we derive the Slater-Condon rules, and third, use them to derive the Coupled Cluster Doubles (CCD) equations. Fourth, we provide the Coupled Cluster Singles Doubles (CCSD) equations, from the Lagrangian formulation, written out in full. Fifth, we provide the CCSD Langrangian functional in its full form. Sixth and last, we provide the κ equations that are used in the Non-orthogonal Orbital-optimised Coupled Cluster (NOCC) scheme.

B.1 CC and CI correspondence

Monkhorst [103] gives a general formula for transferring back and forth between Coupled Cluster (CC) operators \hat{T}_m and Configuration Interaction (CI) operators \hat{C}_m ,

$$\hat{C}_m = \sum_k^m \frac{1}{k!} \sum_{|m_\mu|} \delta(m_1 + m_2 + \dots + m_k, m) \prod_{\mu=1}^k \hat{T}_{m_\mu}, \quad (\text{B.1})$$

where the second sum is over all sets of k m_μ -values that sum up to m . The first four of the terms are,

$$\hat{C}_1 = \hat{T}_1 \quad (\text{B.2})$$

$$\hat{C}_2 = \hat{T}_2 + \frac{1}{2} \hat{T}_1^2 \quad (\text{B.3})$$

$$\hat{C}_3 = \hat{T}_3 + \hat{T}_1 \hat{T}_2 + \frac{1}{3!} \hat{T}_1^3 \quad (\text{B.4})$$

$$\hat{C}_4 = \hat{T}_4 + \frac{1}{2} \hat{T}_2 + \frac{1}{2} \hat{T}_2 \hat{T}_1^2 + \frac{1}{4!} \hat{T}_1^4. \quad (\text{B.5})$$

For the CCSD and CISDTQ wavfunctions we have,

$$|\Psi_{\text{CCSD}}\rangle = \left(1 + \hat{T}_1 + \frac{1}{2} \hat{T}_1^2 + \frac{1}{3!} \hat{T}_1^3 + \hat{T}_2 + \frac{1}{2} \hat{T}_2^2 + \frac{1}{4!} \hat{T}_1^4 + \hat{T}_1 \hat{T}_2 \right) |\Phi_0\rangle \quad (\text{B.6})$$

$$|\Psi_{\text{CISDTQ}}\rangle = \left(1 + \hat{C}_1 + \hat{C}_2 + \hat{C}_3 + \hat{C}_4\right) |\Phi_0\rangle \quad (\text{B.7})$$

which provides us with a relation between the two,

$$|\Psi_{\text{CCSD}}\rangle = |\Psi_{\text{CISDTQ}}\rangle - (\hat{T}_3 + \hat{T}_4) |\Phi_0\rangle. \quad (\text{B.8})$$

Moreover, for a system of $n = 2$ particles, we have that

$$|\Psi_{\text{CCSD}}\rangle = |\Psi_{\text{CISD}}\rangle. \quad (\text{B.9})$$

B.2 Slater-Condon Rules

The Slater-Condon rules are ways to express integrals over operators in terms of single-particle orbitals. Here is an outline of a proof for these rules.

Consider first some Slater determinants,

$$|I\rangle = |i_1 i_2 \dots i_N\rangle = \hat{i}_1^\dagger \hat{i}_2^\dagger \dots \hat{i}_N^\dagger |0\rangle \quad (\text{B.10})$$

$$|J\rangle = |j_1 j_2 \dots j_N\rangle = \hat{j}_1^\dagger \hat{j}_2^\dagger \dots \hat{j}_N^\dagger |0\rangle. \quad (\text{B.11})$$

To get started, we want to compute the inner product $\langle I|J\rangle$ of these two Slater determinants,

$$\langle I|J\rangle = \langle |\hat{i}_N \dots \hat{i}_2 \hat{i}_1 \hat{j}_1^\dagger \hat{j}_2^\dagger \dots \hat{j}_N^\dagger|0\rangle. \quad (\text{B.12})$$

In order to evaluate this expression, we move every annihilation operator \hat{i}_p to the right. Starting with \hat{i}_1 , for instance, we have two possible outcomes. If there is no \hat{j}_q that is the same as \hat{i}_1 we get

$$\langle I|J\rangle = \langle |\hat{i}_N \dots \hat{i}_2 \hat{j}_1^\dagger \hat{j}_2^\dagger \dots \hat{j}_N^\dagger \hat{i}_1|0\rangle (-1)^N = 0, \quad (\text{B.13})$$

because $\hat{i}_1|0\rangle = 0$. The other possibility that may arise is that $\hat{i}_1 = \hat{j}_q$, so that

$$\hat{i}_1 \hat{j}_q^\dagger = \{\hat{i}_1, \hat{j}_q^\dagger\} - \hat{j}_q^\dagger \hat{i}_1 = \delta_{i_1 k_q} - \hat{j}_q^\dagger \hat{i}_1 = 1 - \hat{j}_q^\dagger \hat{i}_1, \quad (\text{B.14})$$

and

$$\langle I|J\rangle = \langle |\hat{i}_N \dots \hat{i}_2 \hat{j}_1^\dagger \hat{j}_2^\dagger \dots \hat{j}_{p-1}^\dagger \hat{j}_{p+1}^\dagger \dots \hat{j}_N^\dagger \hat{i}_1|0\rangle (-1)^{p-1} - 0. \quad (\text{B.15})$$

We continue in this manner, moving all \hat{i} to the right and the final result will be zero if there are any \hat{i}_p without a matching \hat{j}_q or $(-1)^\tau$ if the two operator strings are identical to a permutation τ .

Next, consider a symmetric one-body operator

$$\hat{F} = \sum_{\mu=1}^N \hat{f}_\mu, \quad (\text{B.16})$$

where μ is the identity of the electron on which the identical \hat{f}_μ operate. Computing a matrix element of this one-body operator between two Slater determinants will yield

three possible results,

$$\begin{aligned} \langle I | \hat{F} | J \rangle &= \langle i_1 i_2 \dots i_N | \hat{F} | j_1 j_2 \dots j_N \rangle \\ &= \sum_{\mu} \langle i_1 i_2 \dots i_N | \hat{f}_{\mu} | j_1 j_2 \dots j_N \rangle \\ &= \sum_{\mu} \langle \phi_{i_1} \phi_{i_2} \dots \phi_{i_N} | \hat{f}_{\mu} \sum_{\hat{P}} (-1)^{\sigma(\hat{P})} \left| \hat{P} \phi_{j_1} \phi_{j_2} \dots \phi_{j_N} \right\rangle = \begin{cases} \sum_k \langle i_k | \hat{f} | i_k \rangle (-1)^{\sigma(\hat{P})} & \text{I} \\ \langle i_k | \hat{f} | i'_k \rangle (-1)^{\sigma(\hat{P})} & \text{II} \\ 0 & \text{III} \end{cases} \end{aligned} \quad (\text{B.17})$$

In the last line, the integral is written with spinorbitals instead of Slater determinants. The result will be the first case (I), if the operators needed to construct the Slater determinants are the same, up to a permutation of parity σ associated with the operator \hat{P} needed to permute the product of spinorbitals. If there exists exactly one *noncoincidence* in the string of operators so that $\hat{P} j_1 j_2 \dots j_N = i_1 i_2 \dots i'_k \dots i_N$ where $i_k \neq i'_k$, we get the result in the second case (II). If there are two or more noncoincidences, the result is zero (III).

With second quantisation we might write a one-electron operator differently,

$$\sum_{kl} \langle k | \hat{f} | l \rangle \hat{a}_k^{\dagger} \hat{a}_l = \sum_{kl} f_{kl} \hat{a}_k^{\dagger} \hat{a}_l. \quad (\text{B.18})$$

It is possible to show that the results are the same in this representation. First, consider the case where the two Slater determinants are equal,

$$\begin{aligned} \langle I | \sum_{kl} f_{kl} \hat{a}_k^{\dagger} \hat{a}_l | I \rangle &= \sum_{kl} f_{kl} \langle I | \hat{a}_k^{\dagger} \hat{a}_l | I \rangle \\ &= \sum_{kl} f_{kl} \delta_{kl} n_l(I) = \sum_{k \in I} f_{kk} = \sum_{k=1}^N \langle i_k | \hat{f} | i_k \rangle. \end{aligned} \quad (\text{B.19})$$

Second, we look at the case where we have one noncoincidence, $i_p \neq j_p$,

$$\begin{aligned} \langle I | \sum_{kl} f_{kl} \langle I | \hat{a}_k^{\dagger} \hat{a}_l | J \rangle &= \sum_{kl} f_{kl} \langle I | \hat{a}_k^{\dagger} \hat{a}_l | J \rangle \\ &= \sum_{kl \neq p} f_{kl} \langle I | \hat{a}_k^{\dagger} \hat{a}_l | J \rangle + f_{i_p j_p} \langle I | \hat{i}_p^{\dagger} \hat{j}_p | J \rangle \\ &= 0 + f_{i_p j_p} \langle I' | I' \rangle = \langle \hat{i}_p | \hat{f} | \hat{i}_p \rangle. \end{aligned} \quad (\text{B.20})$$

Lastly, there is no pair of operators $\hat{a}_k^{\dagger} \hat{a}_l$ that will give a non-zero result. Consequently, we see that the second-quantised form of the one-body operator gives the same result.

Similarly, consider a symmetric two-body operator,

$$\hat{G} = \sum_{\mu < \nu}^N \hat{g}_{\mu\nu} = \frac{1}{2} \sum_{\mu \neq \nu}^N \hat{g}_{\mu\nu} = \frac{1}{2} \sum_{ijkl} \langle ij | \hat{g} | kl \rangle \hat{a}_i^{\dagger} \hat{a}_j^{\dagger} \hat{a}_l \hat{a}_k. \quad (\text{B.21})$$

We would like to show that the second-quantized form is correct, and therefore firstly consider the case where the two Slater determinants are equal, i.e. zero noncoincidences;

$$\langle I | \hat{G} | I \rangle = \frac{1}{2} \sum_{ijkl} \langle ij | \hat{G} | kl \rangle \langle I | \hat{a}_i^\dagger \hat{a}_j^\dagger \hat{a}_l \hat{a}_k | I \rangle. \quad (\text{B.22})$$

We must have $k = i_p$ and $l = i_q$ appear in $|I\rangle$, so that

$$\begin{aligned} \langle I | \hat{G} | I \rangle &= \frac{1}{2} \sum_{ij} \langle ij | \hat{g} | i_p i_q \rangle \langle I | \hat{a}^\dagger \hat{a}^\dagger \hat{a}_{i_p} \hat{a}_{i_q} | i_1 i_2 \dots i_p \dots i_q \dots \rangle \\ &= \frac{1}{2} \sum_{ij} \langle ij | \hat{g} | i_p i_q \rangle \langle I | \hat{a}_i^\dagger \hat{a}_j^\dagger | i_1 i_2 \dots \rangle (-1)^{(p-1)+(q-2)}. \end{aligned} \quad (\text{B.23})$$

From this point we have two possibilities for the values of i and j , because the creation operators must put the same values back into the ket,

$$\begin{aligned} \langle i_p i_q | \hat{g} | i_p i_q \rangle \langle I | i_1 i_2 \dots i_p \dots i_q \dots \rangle (-1)^{(p-1)+(q-2)} (-1)^{(p-1)+(q-2)} &\quad (i = i_p, j = i_q); \\ = \langle i_p i_q | \hat{g} | i_p i_q \rangle & \quad (\text{B.24}) \end{aligned}$$

$$\begin{aligned} \langle i_q i_p | \hat{g} | i_p i_q \rangle \langle I | i_1 i_2 \dots i_p \dots i_q \dots \rangle (-1)^{(p-1)+(q-2)} (-1)^{(p-1)+(q-1)} &\quad (i = i_q, j = i_p). \\ = -\langle i_q i_p | \hat{g} | i_p i_q \rangle = -\langle i_p i_q | \hat{g} | i_q i_p \rangle & \quad (\text{B.25}) \end{aligned}$$

By starting in the reverse order, we obtain the same contributions. The total matrix element is therefore,

$$\langle I | \hat{G} | I \rangle = \frac{1}{2} \sum_{i \in I} \sum_{j \in J} (\langle ij | \hat{g} | ij \rangle - \langle ij | \hat{g} | ji \rangle) = \sum_{\substack{i < j \\ i, j \in I}} \langle ij | \hat{g} | ij \rangle_{\text{AS}}. \quad (\text{B.26})$$

Next, we consider a single noncoincidence in $|I\rangle$, $i_p \neq i'_p$,

$$|I\rangle = |i_1 i_2 \dots i_p \dots \rangle, \quad (\text{B.27})$$

$$|I'\rangle = |i_1 i_2 \dots i'_p \dots \rangle. \quad (\text{B.28})$$

We get contributions to $\langle I | \hat{G} | I' \rangle$ from the operator string $\hat{a}_i^\dagger \hat{a}_j^\dagger \hat{a}_l \hat{a}_k$ in the following cases,

$$i = i'_p, k = i_p, j = l = i_q \rightarrow \langle i'_p i_q | i_p i_q \rangle \quad (\text{B.29})$$

$$i = i'_p, l = i_p, j = k = i_q \rightarrow -\langle i'_p i_q | i_q i_p \rangle \quad (\text{B.30})$$

$$j = i'_p, l = i_p, i = k = i_q \rightarrow \langle i_q i'_p | i_q i_p \rangle \quad (\text{B.31})$$

$$j = i'_p, k = i_p, i = l = i_q \rightarrow -\langle i_q i'_p | i_p i_q \rangle, \quad (\text{B.32})$$

where the two first terms are equal to the last terms, respectively. This leaves us with,

$$\langle I' | \hat{G} | I \rangle = 2 \times \frac{1}{2} (\langle i'_p j | \hat{g} | i_p j \rangle - \langle i'_p j | \hat{g} | j i_p \rangle) = \sum_{j \in I} \langle i'_p j | \hat{g} | i_p j \rangle_{\text{AS}}. \quad (\text{B.33})$$

After a while we see a pattern emerges. For two noncoincidences ($i_p \neq i'_p$, $i_q \neq i'_q$) we have,

$$\langle I' | \hat{G} | I \rangle = \langle i'_p i'_q | \hat{g} | i_p i_q \rangle, \quad (\text{B.34})$$

while for three or more noncoincidences,

$$\langle I' | \hat{G} | I \rangle = 0. \quad (\text{B.35})$$

B.3 Configuration space derivation of CCD

We start from the CCD-constrained time-independent Schrödinger equation,

$$\hat{H} \Psi_{\text{CCD}} = E_{\text{CCD}} \Psi_{\text{CCD}}, \quad (\text{B.36})$$

which we left project with the reference state,

$$\begin{aligned} \langle \Phi_0 | \hat{H} | \Psi_{\text{CCD}} \rangle &= \langle \Phi_0 | E_{\text{CCD}} | \Psi_{\text{CCD}} \rangle \\ &\rightarrow E_{\text{CCD}} = \langle \Phi_0 | \hat{H} | \Psi_{\text{CCD}} \rangle, \end{aligned}$$

where we have taken advantage of the intermediate normalisation, $\langle \Phi_0 | \Psi_{\text{CCD}} \rangle = 1$. We then insert the exponential expansion from the coupled cluster ansatz,

$$\begin{aligned} E_{\text{CCD}} &= \langle \Phi_0 | \hat{H}(1 + \hat{T}_2) | \Phi_0 \rangle \\ &= E_{\text{ref}} + \sum_{\substack{i>j \\ a>b}} \langle \Phi_0 | \hat{H} | \Phi_{ij}^{ab} \rangle t_{ij}^{ab} \\ &= E_{\text{ref}} + \sum_{\substack{i>j \\ a>b}} \langle ij | ab \rangle t_{ij}^{ab}. \end{aligned} \quad (\text{B.37})$$

The energy expression will truncate here because no higher-order terms will contribute. It is common to subtract E_{ref} to get,

$$\hat{H}_N \Psi_{\text{CCD}} = \Delta E_{\text{CCD}} \Psi_{\text{CCD}}, \quad (\text{B.38})$$

where $\hat{H}_N = \hat{H} - E_{\text{ref}}$. Here follow the definitions of all the operators we will be dealing with in this derivation,

$$\hat{H}_N = \hat{F} - \hat{U} + \hat{H}_2 - E_{\text{ref}} = \hat{H}_0 + \hat{F}^0 - \hat{U} + \hat{H}_2 - E_{\text{ref}}, \quad (\text{B.39})$$

where,

$$\hat{H}_0 = \hat{F}^d = \sum_{\mu} \hat{f}_{\mu}^d, \quad \langle p | \hat{f}_{\mu}^d | q \rangle = \epsilon_p \delta_{pq} \quad (\text{B.40})$$

$$\hat{F}^0 = \sum_{\mu} \hat{f}_{\mu}^0, \quad \langle p | \hat{f}^0 | q \rangle = (1 - \delta_{pq}) \langle p | \hat{f} | q \rangle \quad (\text{B.41})$$

$$\hat{U} = \sum_{\mu} \hat{u}_{\mu}, \quad \langle p | \hat{u}_{\mu} | q \rangle = \sum_i \langle pi | q i \rangle \quad (\text{B.42})$$

$$\hat{H}_2 = \sum_{\mu>\nu} \frac{1}{r_{\mu\nu}}, \quad E_{\text{ref}} = E_0 + E^{(1)}, \quad (\text{B.43})$$

$$E_0 = \sum_i \epsilon_i, \quad E^{(1)} = -\frac{1}{2} \sum_{ij} \langle ij | ij \rangle. \quad (\text{B.44})$$

In the canonical HF case we have $\hat{F}^0 = 0$ and $\hat{F}^d = \hat{F}$.

In order to compute the energy of the system we need the amplitudes t_{ij}^{ab} . Starting from the modified Schrödinger equation,

$$\hat{H}_N \Psi_{\text{CCD}} = \Delta E_{\text{CCD}} \Psi_{\text{CCD}}. \quad (\text{B.45})$$

We left project with a doubly-excited Slater determinant, and insert for the CC ansatz,

$$\langle \Phi_{ij}^{ab} | \hat{H}_N e^{\hat{T}_2} | \Phi_0 \rangle = \Delta E_{\text{CCD}} \langle \Phi_{ij}^{ab} | e^{\hat{T}_2} | \Phi_0 \rangle \quad (\text{B.46})$$

$$\langle \Phi_{ij}^{ab} | \hat{H}_N \left(1 + \hat{T}_2 + \frac{1}{2} \hat{T}_2^2 \right) | \Phi_0 \rangle = \Delta E_{\text{CCD}} t_{ij}^{ab}. \quad (\text{B.47})$$

Here we have only expanded the exponential function up to the quadratic term. The next term in the series will triple-excite the bra Slater determinant, which will give a zero-contribution according to the Slater-Condon rules, because of two noncoincidences. Next we apply the Slater-Condon rules to the rest of the terms on the right-hand side, starting with just the normal-ordered Hamiltonian,

$$\langle \phi_{ij}^{ab} | \hat{H}_N | \Phi_0 \rangle = \langle ab | ij \rangle, \quad (\text{B.48})$$

where only \hat{H}_2 contributes.

Next we look at the linear term,

$$\begin{aligned} \langle \Phi_{ij}^{ab} | \hat{H}_N \hat{T}_2 | \Phi_0 \rangle &= \sum_{klcd} \left\langle \phi_{ij}^{ab} \middle| \hat{H}_N \middle| \phi_{kl}^{cd} \right\rangle \\ &= \left\langle \Phi_{ij}^{ab} \middle| \hat{H}_0 - E_{\text{ref}} \middle| \Phi_{ij}^{ab} \right\rangle t_{ij}^{ab} + \sum_{\substack{k>l \\ c>d}} \left\langle \Phi_{ij}^{ab} \middle| \hat{F}^0 - \hat{U} \middle| \Phi_{kl}^{cd} \right\rangle t_{kl}^{cd} \\ &\quad + \sum_{\substack{k>l \\ c>l}} \left\langle \Phi_{ij}^{ab} \middle| \hat{H}_2 \middle| \Phi_{kl}^{cd} \right\rangle t_{kl}^{cd} = L_0 + L_1 + L_2. \end{aligned} \quad (\text{B.49})$$

We are going to evaluate these terms one-by-one, starting with L_0 ,

$$\begin{aligned} L_0 &= \left\langle \Phi_{ij}^{ab} \middle| \hat{H}_0 - E_{\text{ref}} \middle| \Phi_{ij}^{ab} \right\rangle = \left\langle \Phi_{ij}^{ab} \middle| \hat{H}_0 - E_0 - E^{(1)} \middle| \Phi_{ij}^{ab} \right\rangle \\ &= \left(-\varepsilon_{ij}^{ab} + \frac{1}{2} \sum_{kl} \langle kl | kl \rangle \right) t_{ij}^{ab}, \end{aligned} \quad (\text{B.50})$$

where $\varepsilon_{ij}^{ab} = \varepsilon_i + \varepsilon_j - \varepsilon_a - \varepsilon_b$.

The next term,

$$L_1 = \sum_{\substack{k>l \\ c>d}} \left\langle \Phi_{ij}^{ab} \middle| \hat{F}^0 - \hat{U} \middle| \Phi_{kl}^{cd} \right\rangle t_{kl}^{cd}, \quad (\text{B.51})$$

yields contributions if at least three of the indices k, l, c, d are equal to the indices i, j, a, b (we want one or zero noncoincidences). All the possible terms are,

$$L_1 = \begin{cases} -\sum_k u_{kk} t_{ij}^{ab} & \text{all indices equal} \\ -\sum_k (f_{jk}^0 - u_{jk}) t_{ik}^{ab} & \text{one hole index unequal} \\ +\sum_k (f_{ik}^0 - u_{ik}) t_{jk}^{ab} & \text{the other hole index unequal} \\ -\sum_c (f_{ac}^0 - u_{ac}) t_{ij}^{bc} & \text{one particle index unequal} \\ +\sum_c (f_{bc}^0 - u_{bc}) t_{ij}^{zc} & \text{the other particle index unequal.} \end{cases} \quad (\text{B.52})$$

For the last linear term,

$$L_2 = \sum_{k>l} \left\langle \Phi_{ij}^{ab} \right| \hat{H}_2 \left| \Phi_{kl}^{cd} \right\rangle t_{kl}^{cd}, \quad (\text{B.53})$$

we require that at least two of the indices k, l, c, d are equal to the indices i, j, a, b , as we can do with at most two noncoincidences in the bra and the ket. For equality in both the hole indices or both the particle indices we have

$$cd = ab \rightarrow \sum_{k>l} \langle ij | kl \rangle t_{kl}^{ab} \quad (\text{B.54})$$

$$kl = ij \rightarrow \sum_{c>d} \langle ab | cd \rangle t_{ij}^{cd}. \quad (\text{B.55})$$

For one equality in both hole and particle index we have

$$-\sum_{kl} (\langle bk | cj \rangle t_{ik}^{ac} - \langle bk | ci \rangle t_{jk}^{ac} - \langle ak | cj \rangle t_{ik}^{bc} - \langle bk | ci \rangle t_{jk}^{ac}), \quad (\text{B.56})$$

where the sign stems from the maximum coincidence permutations as dictated by the Slater-Condon rules. Most of the three- and four equal index terms are accounted for by the expression above, the remaining three-index equality terms are

$$-\sum_{kl} (\langle jl | kl \rangle t_{ik}^{ab} - \langle il | kl \rangle t_{jk}^{ab}) \quad (\text{B.57})$$

$$+\sum_{cl} (\langle bl | cl \rangle t_{ij}^{ac} - \langle al | cl \rangle t_{ij}^{bc}), \quad (\text{B.58})$$

and there is one term for the case where all indices are equal,

$$\sum_{k>l} \langle kl | kl \rangle t_{ij}^{ab} = \frac{1}{2} \sum_{kl} \langle kl | kl \rangle t_{ij}^{ab}. \quad (\text{B.59})$$

These last three- and four-index equality terms are expressible in terms of \hat{u} , and will cancel the first term in L_1 together with the \hat{u} term from L_0 . All terms so far are

the same as in a configuration interaction with doubles excitations (CID) computation. The difference between coupled cluster with doubles (CCD) and CID is the following extra quadratic terms,

$$Q = \frac{1}{2} \left\langle \Phi_{ij}^{ab} \right| \hat{H}_N \hat{T}_2^2 \left| \Phi_0 \right\rangle = \frac{1}{2} \sum_{\substack{k>l \\ c>d}} \sum_{\substack{m>n \\ e>f}} \left\langle \phi_{ij}^{ab} \right| \hat{H}_N \left| \Phi_{klmn}^{cdef} \right\rangle t_{kl}^{cd} t_{mn}^{ef}. \quad (\text{B.60})$$

From this expression we will have a contribution only when four of the indices k, l, m, n, c, d, e, f are equal to i, j, a, b ; and only \hat{H}_2 can contribute. We will find that this becomes,

$$\begin{aligned} Q = & \sum_{\substack{k>l \\ c>d}} \langle kl|cd \rangle [(t_{ij}^{ab} t_{kl}^{cd} + t_{ij}^{cd} t_{kl}^{ab}) - 2(t_{ik}^{ac} t_{jl}^{cd} + t_{ij}^{bd} t_{ij}^{bd}) \\ & - 2(t_{ik}^{ab} t_{jl}^{cd} + t_{ik}^{cd} t_{jl}^{ab}) + 4(t_{ik}^{ac} t_{jl}^{bd} + t_{ik}^{bd} t_{jl}^{ac})]. \end{aligned} \quad (\text{B.61})$$

From Equation B.37 we see that

$$\Delta E_{\text{CCD}} = \sum_{\substack{i>j \\ a>b}} \langle ij|ab \rangle t_{ij}^{ab}, \quad (\text{B.62})$$

and because the indices in Equation B.61 are dummy variables we see that the first term here cancels with the right-hand side of Equation B.47. This leads to,

$$\begin{aligned} \varepsilon_{ij}^{ab} t_{ij}^{ab} = & \langle ab|ij \rangle + \frac{1}{2} \sum_{cd} \langle ab|cd \rangle t_{ij}^{cd} + \frac{1}{2} \sum_{kl} \langle ij|kl \rangle t_{kl}^{ab} \\ & - \sum_{kl} (\langle bk|cj \rangle t_{ik}^{ac} - \langle bk|ci \rangle t_{jk}^{ac} - \langle ak|cj \rangle t_{ik}^{bc} + \langle ak|ci \rangle t_{jk}^{bc}) \\ & - \sum_k \hat{f}_{jk}^0 t_{ik}^{ab} + \sum_k \hat{f}_{ik}^0 t_{jk}^{ab} + \sum_c \hat{f}_{bc}^0 t_{ij}^{ac} - \sum_c \hat{f}_{ac}^0 t_{ij}^{bc} \\ & + \sum_{klcd} \langle kl|cd \rangle \left[\frac{1}{4} t_{ij}^{cd} t_{kl}^{ab} - \frac{1}{2} (t_{ij}^{ac} t_{kl}^{bd} + t_{ij}^{bd} t_{kl}^{ac}) \right. \\ & \left. - \frac{1}{2} (t_{ik}^{ab} t_{jl}^{cd} + t_{ik}^{cd} t_{jl}^{ab}) + (t_{ik}^{ac} t_{jl}^{bd} + t_{ik}^{bd} t_{jl}^{ac}) \right], \end{aligned} \quad (\text{B.63})$$

which is the CCD amplitude equations. This equation contains simultaneous algebraic expressions, contrary to CI. The equations must be solved iteratively, substituting t_{ij}^{ab} obtained in each iteration, into the quadratic terms for the next iteration.

B.4 CCSD Equations

Here we present the Coupled Cluster Singles Doubles (CCSD) equations written out in full. These stem from Equation 6.104 and Equation 6.105 in chapter 6.

Single excited τ -amplitude equation

$$\begin{aligned} f_c^a \tau_{1i}^c + f_c^k \tau_{2ik}^{ac} + \tau_{1k}^c u_{ic}^{ak} + \frac{1}{2} \tau_{2ik}^{cb} u_{cb}^{ak} - f_i^k \tau_{1k}^a - \frac{1}{2} \tau_{2kl}^{ac} u_{ic}^{kl} + \tau_{1k}^c \tau_{1l}^a u_{ic}^{kl} + \tau_{1k}^c \tau_{2il}^{ab} u_{cb}^{kl} \\ - f_c^k \tau_{1i}^c \tau_{1k}^a - \tau_{1k}^c \tau_{1i}^b u_{cb}^{ak} - \frac{1}{2} \tau_{1k}^a \tau_{2il}^{cb} u_{cb}^{kl} - \frac{1}{2} \tau_{1i}^c \tau_{2kl}^{ab} u_{cb}^{kl} - \tau_{1k}^c \tau_{1i}^b \tau_{1l}^a u_{cb}^{kl} + f_i^a = 0 \end{aligned}$$

Double excited τ -amplitude equation

$$\begin{aligned}
& \frac{1}{2}\tau_{2kl}^{ab}u_{ij}^{kl} + \frac{1}{2}\tau_{2ij}^{cd}u_{cd}^{ab} + f_i^k\tau_{2jk}^{ab}P(ij) + \tau_{1k}^a\tau_{1l}^b u_{ij}^{kl} + \tau_{1k}^a u_{ij}^{bk}P(ab) + \tau_{1i}^c\tau_{1j}^d u_{cd}^{ab} \\
& - f_c^a\tau_{2ij}^{bc}P(ab) - \tau_{1i}^c u_{jc}^{ab}P(ij) + \frac{1}{4}\tau_{2ij}^{cd}\tau_{2kl}^{ab}u_{cd}^{kl} + f_c^k\tau_{1k}^a\tau_{2ij}^{bc}P(ab) + f_c^k\tau_{1i}^c\tau_{2jk}^{ab}P(ij) \\
& + \tau_{1k}^c\tau_{2il}^{ab}u_{jc}^{kl}P(ij) + \tau_{2ik}^{ac}\tau_{2jl}^{bd}u_{ca}^{kl}P(ab) + \tau_{2ik}^{ac}u_{jc}^{bk}P(ab)P(ij) + \frac{1}{2}\tau_{1k}^a\tau_{1l}^b\tau_{2ij}^{cd}u_{cd}^{kl} \\
& + \frac{1}{2}\tau_{1k}^a\tau_{2ij}^{cd}u_{cd}^{bk}P(ab) + \frac{1}{2}\tau_{1i}^c\tau_{1j}^d\tau_{2kl}^{ab}u_{cd}^{kl} + \frac{1}{2}\tau_{2jk}^{cd}\tau_{2il}^{ab}u_{cd}^{kl}P(ij) - \tau_{1k}^c\tau_{2ij}^{ad}u_{cd}^{bk}P(ab) \\
& - \frac{1}{2}\tau_{1i}^c\tau_{2kl}^{ab}u_{jc}^{kl}P(ij) - \frac{1}{2}\tau_{2ij}^{ac}\tau_{2kl}^{bd}u_{cd}^{kl}P(ab) + \tau_{1i}^c\tau_{1j}^d\tau_{1k}^a\tau_{1l}^b u_{cd}^{kl} \\
& + \tau_{1i}^c\tau_{1j}^d\tau_{1k}^a u_{cd}^{bk}P(ab) + \tau_{1k}^a\tau_{2il}^{bc}u_{jc}^{kl}P(ab)P(ij) + \tau_{1k}^c\tau_{1l}^a\tau_{2ij}^{bd}u_{cd}^{kl}P(ab) \\
& + \tau_{1k}^c\tau_{1i}^d\tau_{2jl}^{ab}u_{cd}^{kl}P(ij) - \tau_{1i}^c\tau_{1k}^a\tau_{1l}^b u_{jc}^{kl}P(ij) - \tau_{1i}^c\tau_{1k}^a u_{jc}^{bk}P(ab)P(ij) \\
& - \tau_{1i}^c\tau_{2jk}^{ad}u_{cd}^{bk}P(ab)P(ij) - \tau_{1i}^c\tau_{1k}^a\tau_{2jl}^{bd}u_{cd}^{kl}P(ab)P(ij) + u_{ij}^{ab} = 0
\end{aligned}$$

Single excited λ -amplitude equation

$$\begin{aligned}
& f_a^d\lambda_{1d}^i + \lambda_{1d}^l u_{al}^{id} + \tau_{1l}^d u_{ad}^{il} + \frac{1}{2}\lambda_{2de}^{il}u_{al}^{de} - f_l^i\lambda_{1a}^l - \frac{1}{2}\lambda_{2ad}^{lm}u_{lm}^{id} \\
& + \lambda_{1d}^i\tau_{1l}^e u_{ae}^{dl} + \lambda_{1a}^l\tau_{1m}^d u_{dl}^{im} + \lambda_{1d}^l\tau_{1l}^e u_{ae}^{id} + \lambda_{1d}^l\tau_{2lm}^{de}u_{ae}^{im} + \lambda_{2de}^{il}\tau_{1m}^d u_{al}^{em} \\
& + \frac{1}{2}\lambda_{2de}^{il}\tau_{1l}^c u_{ac}^{de} + \frac{1}{2}\lambda_{2ad}^{lm}\tau_{1k}^d u_{lm}^{ik} + \frac{1}{2}\lambda_{2de}^{lm}\tau_{2lm}^{dc}u_{ac}^{ie} - f_d^i\lambda_{1a}^l\tau_{1l}^d \\
& - f_a^l\lambda_{1d}^i\tau_{1l}^d - \lambda_{1d}^l\tau_{1m}^d u_{al}^{im} - \lambda_{2de}^{il}\tau_{2lm}^{dc}u_{ac}^{em} - \lambda_{2ad}^{lm}\tau_{1l}^e u_{em}^{id} \\
& - \lambda_{2ad}^{lm}\tau_{2lk}^{de}u_{em}^{ik} - \frac{1}{2}f_d^i\lambda_{2ae}^{lm}\tau_{2lm}^{de} - \frac{1}{2}f_a^l\lambda_{2de}^{im}\tau_{2lm}^{de} - \frac{1}{2}\lambda_{1d}^i\tau_{2lm}^{de}u_{ae}^{lm} \\
& - \frac{1}{2}\lambda_{1a}^l\tau_{2lm}^{de}u_{de}^{im} - \frac{1}{2}\lambda_{2de}^{lm}\tau_{2lk}^{de}u_{am}^{ik} - \frac{1}{4}\lambda_{2ad}^{lm}\tau_{2lm}^{ec}u_{ec}^{id} + \frac{1}{4}\lambda_{2de}^{il}\tau_{2mk}^{de}u_{al}^{mk} \\
& + \lambda_{2de}^{il}\tau_{1m}^d\tau_{1l}^c u_{ac}^{em} + \lambda_{2ad}^{lm}\tau_{1k}^d\tau_{1l}^e u_{em}^{ik} + \frac{1}{2}\lambda_{2ad}^{lm}\tau_{1m}^e\tau_{1l}^c u_{ec}^{id} \\
& + \frac{1}{2}\lambda_{2de}^{lm}\tau_{1k}^d\tau_{2lm}^{ec}u_{ac}^{ik} + \frac{1}{2}\lambda_{2de}^{lm}\tau_{1l}^c\tau_{2mk}^{de}u_{ac}^{ik} - \lambda_{1d}^i\tau_{1l}^d\tau_{1m}^e u_{ae}^{lm} \\
& - \lambda_{1a}^l\tau_{1l}^d\tau_{1m}^e u_{de}^{im} - \lambda_{1d}^l\tau_{1m}^d\tau_{1l}^e u_{ae}^{im} - \lambda_{2de}^{il}\tau_{1m}^d\tau_{2lk}^{ec}u_{ac}^{mk} \\
& - \lambda_{2ad}^{lm}\tau_{1l}^e\tau_{2mk}^{dc}u_{ec}^{ik} - \frac{1}{2}\lambda_{2de}^{il}\tau_{1k}^d\tau_{1m}^e u_{al}^{mk} - \frac{1}{2}\lambda_{2de}^{il}\tau_{1m}^c\tau_{2lk}^{de}u_{ac}^{mk} \\
& - \frac{1}{2}\lambda_{2ad}^{lm}\tau_{1k}^e\tau_{2lm}^{dc}u_{ec}^{ik} + \frac{1}{4}\lambda_{2de}^{il}\tau_{1l}^c\tau_{2mk}^{de}u_{ac}^{mk} + \frac{1}{4}\lambda_{2ad}^{lm}\tau_{1k}^d\tau_{2lm}^{ec}u_{ec}^{ik} \\
& - \frac{1}{2}\lambda_{2de}^{il}\tau_{1k}^d\tau_{1m}^e\tau_{1l}^c u_{ac}^{mk} - \frac{1}{2}\lambda_{2ad}^{lm}\tau_{1k}^d\tau_{1m}^e\tau_{1l}^c u_{ec}^{ik} + f_a^i = 0
\end{aligned}$$

Double excited λ -amplitude equation

$$\begin{aligned}
& \frac{1}{2}\lambda_{2cd}^{ij}u_{ab}^{cd} + \frac{1}{2}\lambda_{2ab}^{kl}u_{kl}^{ij} + f_k^i\lambda_{2ab}^{jk}P(ij) + \lambda_{1a}^k u_{bk}^{ij}P(ab) + \lambda_{2cd}^{ij}\tau_{1k}^c u_{ab}^{dk} + \lambda_{2ab}^{kl}\tau_{1k}^c u_{cl}^{ij} \\
& - f_a^c\lambda_{2bc}^{ij}P(ab) - \lambda_{1c}^i u_{ab}^{jc}P(ij) + \frac{1}{4}\lambda_{2cd}^{ij}\tau_{2kl}^{cd}u_{ab}^{kl} + \frac{1}{4}\lambda_{2ab}^{kl}\tau_{2kl}^{cd}u_{cd}^{ij} + f_a^i\lambda_{1b}^j P(ab)P(ij)
\end{aligned}$$

$$\begin{aligned}
& + f_c^i \lambda_{2ab}^{jk} \tau_{1k}^c P(ij) + f_a^k \lambda_{2bc}^{ij} \tau_{1k}^c P(ab) + \lambda_1^i \tau_{1k}^c u_{ab}^{jk} P(ij) + \lambda_1^k \tau_{1k}^c u_{bc}^{ij} P(ab) \\
& + \lambda_{2ac}^{ij} \tau_{1k}^d u_{bd}^{ck} P(ab) + \lambda_{2ab}^{ik} \tau_{1l}^c u_{ck}^{jl} P(ij) + \lambda_{2ac}^{ik} u_{bk}^{jc} P(ab) P(ij) - \frac{1}{2} \lambda_{2ac}^{ij} \tau_{2kl}^{cd} u_{bd}^{kl} P(ab) \\
& - \frac{1}{2} \lambda_{2cd}^{ij} \tau_{1l}^c \tau_{1k}^d u_{ab}^{kl} - \frac{1}{2} \lambda_{2ab}^{ik} \tau_{2kl}^{cd} u_{cd}^{jl} P(ij) - \frac{1}{2} \lambda_{2cd}^{ik} \tau_{2kl}^{cd} u_{ab}^{jl} P(ij) \\
& - \frac{1}{2} \lambda_{2ab}^{kl} \tau_{1l}^c \tau_{1k}^d u_{cd}^{ij} - \frac{1}{2} \lambda_{2ac}^{kl} \tau_{2kl}^{cd} u_{bd}^{ij} P(ab) + \lambda_1^i \tau_{1k}^c u_{bc}^{jk} P(ab) P(ij) \\
& + \lambda_{2ac}^{ik} \tau_{1k}^d u_{bd}^{jc} P(ab) P(ij) + \lambda_{2ac}^{ik} \tau_{2kl}^{cd} u_{bd}^{jl} P(ab) P(ij) - \lambda_{2ac}^{ij} \tau_{1k}^c \tau_{1l}^d u_{bd}^{kl} P(ab) \\
& - \lambda_{2ab}^{ik} \tau_{1k}^c \tau_{1l}^d u_{cd}^{jl} P(ij) - \lambda_{2ac}^{ik} \tau_{1l}^c u_{bk}^{jl} P(ab) P(ij) \\
& - \lambda_{2ac}^{ik} \tau_{1l}^c \tau_{1k}^d u_{bd}^{jl} P(ab) P(ij) + u_{ab}^{ij} = 0
\end{aligned}$$

B.5 CCSD Lagrangian

Here we present the Coupled Cluster Singles Doubles (CCSD) Lagrangian, stated in Equation 6.95, written out in full for singles and doubles excitations.

$$\begin{aligned}
\mathcal{L}(\tau, \lambda) = & f_a^a \lambda_a^i + f_a^i \tau_a^a + \frac{1}{4} \lambda_{ab}^{ij} u_{ij}^{ab} + \frac{1}{4} \tau_{ij}^{ab} u_{ab}^{ij} + f_b^a \lambda_a^i \tau_i^b \\
& + f_a^i \lambda_b^j \tau_{ij}^{ab} + \frac{1}{2} f_b^a \lambda_{ac}^{ij} \tau_{ij}^{bc} + \frac{1}{2} \lambda_a^i \tau_{jk}^{ab} u_{bi}^{jk} + \frac{1}{2} \lambda_a^i \tau_{ij}^{bc} u_{bc}^{aj} \\
& + \frac{1}{2} \lambda_{ab}^{ij} \tau_k^a u_{ij}^{bk} + \frac{1}{2} \lambda_{ab}^{ij} \tau_i^c u_{cj}^{ab} - f_i^j \lambda_a^i \tau_j^a - \lambda_a^i \tau_j^b u_{bi}^{aj} \\
& - \lambda_{ab}^{ij} \tau_{ik}^{ac} u_{cj}^{bk} - \frac{1}{2} f_i^j \lambda_{ab}^{ik} \tau_{jk}^{ab} - \frac{1}{2} \tau_j^a \tau_i^b u_{ab}^{ij} + \frac{1}{8} \lambda_{ab}^{ij} \tau_{kl}^{ab} u_{ij}^{kl} \\
& + \frac{1}{8} \lambda_{ab}^{ij} \tau_{ij}^{cd} u_{cd}^{ab} + \lambda_a^i \tau_j^a \tau_k^b u_{bi}^{jk} + \lambda_a^i \tau_j^b \tau_j^c u_{bc}^{aj} + \lambda_a^i \tau_j^b \tau_{ik}^{ac} u_{bc}^{jk} \\
& + \lambda_{ab}^{ij} \tau_k^a \tau_i^c u_{cj}^{bk} - f_a^i \lambda_b^j \tau_j^a \tau_i^b - \lambda_{ab}^{ij} \tau_k^a \tau_{il}^{bc} u_{cj}^{kl} - \lambda_{ab}^{ij} \tau_i^c \tau_{jk}^{ad} u_{cd}^{bk} \\
& - \frac{1}{2} f_a^i \lambda_{bc}^{jk} \tau_j^a \tau_{ik}^{bc} - \frac{1}{2} f_a^i \lambda_{bc}^{jk} \tau_i^b \tau_{jk}^{ac} - \frac{1}{2} \lambda_a^i \tau_j^a \tau_{ik}^{bc} u_{bc}^{jk} - \frac{1}{2} \lambda_a^i \tau_i^b \tau_{jk}^{ac} u_{bc}^{jk} \\
& - \frac{1}{2} \lambda_{ab}^{ij} \tau_k^c \tau_{il}^{ab} u_{cj}^{kl} - \frac{1}{2} \lambda_{ab}^{ij} \tau_k^c \tau_{ij}^{ad} u_{cd}^{bk} - \frac{1}{2} \lambda_{ab}^{ij} \tau_{jk}^{ac} \tau_{il}^{bd} u_{cd}^{kl} \\
& - \frac{1}{4} \lambda_{ab}^{ij} \tau_l^a \tau_k^b u_{ij}^{kl} - \frac{1}{4} \lambda_{ab}^{ij} \tau_j^c \tau_{ij}^d u_{cd}^{ab} - \frac{1}{4} \lambda_{ab}^{ij} \tau_{kl}^{ac} \tau_{ij}^{bd} u_{cd}^{kl} \\
& + \frac{1}{4} \lambda_{ab}^{ij} \tau_k^a \tau_{ij}^{cd} u_{cd}^{bk} + \frac{1}{4} \lambda_{ab}^{ij} \tau_i^c \tau_{kl}^{ab} u_{cj}^{kl} + \frac{1}{8} \lambda_{ab}^{ij} \tau_{il}^{ab} \tau_{jk}^{cd} u_{cd}^{kl} \\
& + \frac{1}{8} \lambda_{ab}^{ij} \tau_{jk}^{ab} \tau_{il}^{cd} u_{cd}^{kl} + \frac{1}{16} \lambda_{ab}^{ij} \tau_{kl}^{ab} \tau_{ij}^{cd} u_{cd}^{kl} - \lambda_a^i \tau_k^a \tau_j^b \tau_i^c u_{bc}^{jk} \\
& - \lambda_{ab}^{ij} \tau_k^a \tau_i^c \tau_{jl}^{bd} u_{cd}^{kl} - \frac{1}{2} \lambda_{ab}^{ij} \tau_k^a \tau_j^c \tau_i^d u_{cd}^{bk} - \frac{1}{2} \lambda_{ab}^{ij} \tau_k^a \tau_l^c \tau_{ij}^{bd} u_{cd}^{kl} \\
& - \frac{1}{2} \lambda_{ab}^{ij} \tau_l^a \tau_k^b \tau_i^c u_{cj}^{kl} - \frac{1}{2} \lambda_{ab}^{ij} \tau_i^c \tau_k^d \tau_{jl}^{ab} u_{cd}^{kl} - \frac{1}{8} \lambda_{ab}^{ij} \tau_l^a \tau_k^b \tau_{ij}^{cd} u_{cd}^{kl} \\
& - \frac{1}{8} \lambda_{ab}^{ij} \tau_j^c \tau_i^d \tau_{kl}^{ab} u_{cd}^{kl} \frac{1}{4} \lambda_{ab}^{ij} \tau_l^a \tau_k^b \tau_j^c \tau_i^d u_{cd}^{kl}.
\end{aligned} \tag{B.64}$$

B.6 Kappa Doubles Equations

Here we present the κ equations from Non-orthogonal Orbital-optimised Coupled Cluster (NOCC), truncated at doubles excitations, written out in full. The expressions here stem from Equation 8.11 and Equation 8.12.

$$\left(\frac{\partial \mathcal{L}}{\partial \kappa_{\mu_1}^u} \right)_a^i = -\frac{1}{2} \lambda_{cd}^{lk} \tau_{mk}^{cd} u_{al}^{im} - \frac{1}{2} \lambda_{cd}^{lk} \tau_{lk}^{ec} u_{ae}^{id} + \frac{1}{2} \lambda_{ac}^{lk} \tau_{lk}^{cd} f_d^i \\ - \lambda_{ac}^{lk} \tau_{mk}^{cd} u_{dl}^{im} - \frac{1}{4} \lambda_{ac}^{lk} \tau_{lk}^{ed} u_{ed}^{ic} - \frac{1}{2} \lambda_{ac}^{lk} u_{lk}^{ic} \\ - \frac{1}{2} \lambda_{cd}^{ik} \tau_{lk}^{cd} f_a^l + \frac{1}{4} \lambda_{cd}^{ik} \tau_{ml}^{cd} u_{ak}^{ml} - \lambda_{cd}^{ik} \tau_{lk}^{ec} u_{ae}^{dl} \\ + \frac{1}{2} \lambda_{cd}^{ik} u_{ak}^{cd} + f_a^i, \quad (\text{B.65})$$

$$\left(\frac{\partial \mathcal{L}}{\partial \kappa_{\mu_1}^d} \right)_i^a = \frac{1}{4} \lambda_{cd}^{lk} \tau_{mk}^{cd} \tau_{il}^{ef} u_{ef}^{am} - \frac{1}{2} \lambda_{cd}^{lk} \tau_{ln}^{ae} \tau_{mk}^{cd} u_{ie}^{mn} + \frac{1}{2} \lambda_{cd}^{lk} \tau_{mk}^{cd} u_{il}^{am} \\ + \frac{1}{8} \lambda_{cd}^{lk} \tau_{lk}^{ae} \tau_{mn}^{cd} u_{ie}^{mn} + \frac{1}{2} \lambda_{cd}^{lk} \tau_{ik}^{cd} f_l^a + \frac{1}{4} \lambda_{cd}^{lk} \tau_{il}^{cd} \tau_{mk}^{ef} u_{ef}^{am} \\ - \frac{1}{8} \lambda_{cd}^{lk} \tau_{im}^{cd} \tau_{lk}^{ef} u_{ef}^{am} - \frac{1}{4} \lambda_{cd}^{lk} \tau_{im}^{cd} u_{lk}^{am} + \frac{1}{2} \lambda_{cd}^{lk} \tau_{lk}^{ec} \tau_{im}^{fd} u_{ef}^{am} \\ + \frac{1}{4} \lambda_{cd}^{lk} \tau_{mn}^{ad} \tau_{lk}^{ec} u_{ie}^{mn} + \frac{1}{4} \lambda_{cd}^{lk} \tau_{lk}^{ec} u_{ie}^{ad} - \lambda_{cd}^{lk} \tau_{mk}^{ec} \tau_{il}^{fd} u_{ef}^{am} \\ - \lambda_{cd}^{lk} \tau_{mk}^{ec} \tau_{ln}^{ad} u_{ie}^{mn} + \frac{1}{4} \lambda_{cd}^{lk} \tau_{lk}^{ad} \tau_{mn}^{ec} u_{ie}^{mn} + \lambda_{cd}^{lk} \tau_{ik}^{ec} u_{el}^{ad} \\ - \frac{1}{2} \lambda_{cd}^{lk} \tau_{lk}^{ac} f_i^d + \lambda_{cd}^{lk} \tau_{mk}^{ac} u_{il}^{dm} + \frac{1}{4} \lambda_{cd}^{lk} \tau_{lk}^{ae} u_{ie}^{cd} \\ - \frac{1}{2} \tau_{ik}^{cd} u_{cd}^{ak} + \frac{1}{2} \tau_{lk}^{ac} u_{ic}^{lk} - f_i^a. \quad (\text{B.66})$$

Appendix C

Code Listings

Here we present a few select code listings that did not fit naturally into the main text, but are quite useful. We provide a python function that computes the analytical values of the Coulomb integral in two dimensions [85]. Moreover, we present two functions that interfaces with and retrieves basis sets from the quantum chemistry libraries Psi4 [4] and PySCF [3].

C.1 2D Coulomb elements

Implementation of two-body matrix elements for the two-dimensional quantum dots [85]. Note that Anisimovas and Matulis uses the convention $\langle ij | \hat{u} | lk \rangle$ which is $\langle ij | \hat{u} | kl \rangle$ in the conventional notation. That is, the last two indices are interchanged.

```
def coulomb_ho(n_i, m_i, n_j, m_j, n_l, m_l, n_k, m_k):
    element = 0

    if m_i + m_j != m_k + m_l:
        return 0

    M_i = 0.5 * (abs(m_i) + m_i)
    dm_i = 0.5 * (abs(m_i) - m_i)
    M_j = 0.5 * (abs(m_j) + m_j)
    dm_j = 0.5 * (abs(m_j) - m_j)
    M_k = 0.5 * (abs(m_k) + m_k)
    dm_k = 0.5 * (abs(m_k) - m_k)
    M_l = 0.5 * (abs(m_l) + m_l)
    dm_l = 0.5 * (abs(m_l) - m_l)

    n = np.array([n_i, n_j, n_k, n_l], dtype=np.int64)
    m = np.array([m_i, m_j, m_k, m_l], dtype=np.int64)
    j = np.array([0, 0, 0, 0], dtype=np.int64)
    l = np.array([0, 0, 0, 0], dtype=np.int64)
    g = np.array([0, 0, 0, 0], dtype=np.int64)
```

```

for j_1 in range(n_i + 1):
    j[0] = j_1
    for j_2 in range(n_j + 1):
        j[1] = j_2
        for j_3 in range(n_k + 1):
            j[2] = j_3
            for j_4 in range(n_l + 1):
                j[3] = j_4

                g[0] = j_1 + j_4 + M_i + dm_l
                g[1] = j_2 + j_3 + M_j + dm_k
                g[2] = j_3 + j_2 + M_k + dm_j
                g[3] = j_4 + j_1 + M_l + dm_i

                G = np.sum(g)
                ratio_1 = log_ratio_1(j)
                prod_2 = log_product_2(n, m, j)
                ratio_2 = log_ratio_2(G)

                temp = 0
                for l_1 in range(g[0] + 1):
                    l[0] = l_1
                    for l_2 in range(g[1] + 1):
                        l[1] = l_2
                        for l_3 in range(g[2] + 1):
                            l[2] = l_3
                            for l_4 in range(g[3] + 1):
                                l[3] = l_4

                                if l_1 + l_2 != l_3 + l_4:
                                    continue

                                L = np.sum(l)

                                temp += (
                                    -2
                                    * (int(g[1]+g[2]-l[1]-l[2]) & 0x1)
                                    + 1)
                                * np.exp(
                                    log_product_3(l, g)
                                    + math.lgamma(1.0 + 0.5 * L)
                                    + math.lgamma(0.5 * (G - L + 1.0)))

                                element += (
                                    (-2 * (int(np.sum(j)) & 0x1) + 1)

```

```

        * np.exp(ratio_1 + prod_2 + ratio_2)
        * temp)

element *= log_product_1(n, m)
return element

```

C.2 Function for constructing system from Psi4

This function extracts a basis set from Psi4 [4], specified by the `molecule` argument. Psi4 also allows for several options in construction of a basis set. Please consult the Psi4 documentation on <https://psicode.org>, for a guide on how to create such a specification. The return object of this function is an instance of the `QuantumSystem` class, specified in chapter 7.

```

def construct_psi4_system(
    molecule, options, np=None, add_spin=True, anti_symmetrize=True
):
    import psi4

    if np is None:
        import numpy as np

    psi4.core.be_quiet()
    psi4.set_options(options)

    mol = psi4.geometry(molecule)
    nuclear_repulsion_energy = mol.nuclear_repulsion_energy()

    wavefunction = psi4.core.Wavefunction.build(
        mol, psi4.core.get_global_option("BASIS")
    )

    molecular_integrals = psi4.core.MintsHelper(wavefunction.basisset())

    kinetic = np.asarray(molecular_integrals.ao_kinetic())
    potential = np.asarray(molecular_integrals.ao_potential())
    h = kinetic + potential

    u = np.asarray(molecular_integrals.ao_eri()).transpose(0, 2, 1, 3)
    overlap = np.asarray(molecular_integrals.ao_overlap())

    n_up = wavefunction.nalpha()
    n_down = wavefunction.nbeta()
    n = n_up + n_down
    l = 2 * wavefunction.nmo()

```

```

dipole_integrals = [
    np.asarray(mu) for mu in molecular_integrals.ao_dipole()
]
dipole_integrals = np.stack(dipole_integrals)

system = CustomSystem(n, l, n_up=n_up, np=np)
system.set_h(h, add_spin=add_spin)
system.set_u(u, add_spin=add_spin, anti_symmetrize=anti_symmetrize)
system.set_s(overlap, add_spin=add_spin)
system.set_dipole_moment(dipole_integrals, add_spin=add_spin)
system.set_nuclear_repulsion_energy(nuclear_repulsion_energy)

return system

```

C.3 Function for constructing system from PySCF

This function extracts a basis set from PySCF [3], specified by the `molecule` and `basis` arguments. Please consult the PySCF documentation on <https://pyscf.github.io>, for a guide on how to create such a specification. The return object of this function is an instance of the `QuantumSystem` class, specified in chapter 7.

```

def construct_pyscf_system(molecule, basis="cc-pvdz", np, verbose=False):
    import pyscf

    if np is None:
        import numpy as np

    # Build molecule in AO-basis
    mol = pyscf.gto.Mole()
    mol.unit = "bohr"
    mol.build(atom=molecule, basis=basis, symmetry=False)
    mol.set_common_origin(np.array([0.0, 0.0, 0.0]))
    nuclear_repulsion_energy = mol.energy_nuc()

    # Perform UHF-calculations to create the MO-basis
    hf = pyscf.scf.UHF(mol)
    ehf = hf.kernel()

    if not hf.converged:
        warnings.warn("UHF calculation did not converge")

    if verbose:
        print(f"UHF energy: {hf.e_tot}")

```

```

# Build the coefficient matrix from the occupied and virtual integrals.
# As we have done a UHF-calculation, we stack the two spin-directions
# on top of each other. That is, instead of using odd or even indices
# for each spin direction, we set up two separate blocks.

C_o = np.hstack(
(
    # Fetch occupied coefficients for both spin-directions
    hf.mo_coeff[0][:, hf.mo_occ[0] > 0],
    hf.mo_coeff[1][:, hf.mo_occ[1] > 0],
)
)

C_v = np.hstack(
(
    # Fetch virtual coefficients for both spin-directions
    hf.mo_coeff[0][:, hf.mo_occ[0] == 0],
    hf.mo_coeff[1][:, hf.mo_occ[1] == 0],
)
)

# Build full coefficient matrix.
C = np.hstack((C_o, C_v))

# Get the number of occupied molecular orbitals
n = C_o.shape[1]
# Fetch the number of molecular orbitals
l = C.shape[1]

# Check that the number of occupied molecular orbitals is correct
assert n == sum(hf.mo_occ[0] > 0) + sum(hf.mo_occ[1] > 0)
# Check that the number of molecular orbitals is twice of that of
# the number of atomic orbitals.
assert l == C.shape[0] * 2

# Note: Should the dipole moments have a negative sign?
dipole_moment = [
    -transform_one_body_elements(dm, C, np)
    for dm in mol.intor("int1e_r").reshape(3, mol.nao, mol.nao)
]
dipole_moment = np.asarray(dipole_moment)

# Create a tuple with the shape of the AO two-body elements
u_shape = (mol.nao for i in range(4))

h = transform_one_body_elements(hf.get_hcore(), C, np)

```

```

u = transform_two_body_elements(
    mol.intor("int2e").reshape(*u_shape),
    C,
    np,
)

noa = sum(hf.mo_occ[0] > 0)
nva = sum(hf.mo_occ[0] == 0)
nob = sum(hf.mo_occ[1] > 0)
nvb = sum(hf.mo_occ[1] == 0)
no = noa + nob
nv = nva + nvb

oa = slice(0, noa)
ob = slice(noa, no)
va = slice(no, no + nva)
vb = slice(no + nva, no + nv)

a_slices = [oa, va]
b_slices = [ob, vb]

# Create a combination of slices that should be zero in
# all matrix elements due to unequal spin-direction.
zero_slices = [(a, b) for a in a_slices for b in b_slices]
zero_slices += [(b, a) for a in a_slices for b in b_slices]

# Create a slice object for all indices, i.e., the ":" syntax in NumPy.
all_slice = slice(None, None)

# Explicitly set all cross-spin terms to zero
for s in zero_slices:
    h[s] = 0
    dipole_moment[(all_slice,) + s] = 0
    u[s + (all_slice, all_slice)] = 0
    u[(all_slice, all_slice) + s] = 0

# Convert to physicist's notation, from Mulliken notation
u = u.transpose(0, 2, 1, 3)

# Build a custom system from the integral elements
system = CustomSystem(n, 1, np=np)
system.set_h(h)
system.set_u(u, anti_symmetrize=True)
system.set_dipole_moment(dipole_moment)
system.set_nuclear_repulsion_energy(nuclear_repulsion_energy)

```

```
system.cast_to_complex()  
  
return system
```


Appendix D

Solving the Schrödinger Equation Analytically

Here we will illustrate how one can solve the time-independent Schrödinger equation analytically in three dimensions. By doing this exercise, we also see where the quantum numbers associated with an extra degree of freedom, that the introduction of an additional dimension entails. Here we also provide some motivation for the necessity of numerical approximations, as we introduce a few simple systems. Lastly, we give the solutions to the quantum harmonic oscillator, an important system in this thesis.

D.1 The Schrödinger Equation in Spherical Coordinates

Here we will solve the time-independent Schrödinger equation,

$$-\frac{\hbar^2}{2m}\nabla^2\Psi + V\Psi = E\Psi, \quad (\text{D.1})$$

by separation of variables. In Equation D.1, m is the mass of the particle in the system, \hbar is Planck's reduced constant, E is the eigenenergy, and Ψ is the eigenstate of the system. The squared differential operator ∇^2 becomes the following in spherical coordinates,

$$\nabla^2 = \frac{1}{r^2}\frac{\partial}{\partial r}\left(r^2\frac{\partial}{\partial r}\right) + \frac{1}{r^2\sin\theta}\frac{\partial}{\partial\theta}\left(\sin\theta\frac{\partial}{\partial\theta}\right) + \frac{1}{r^2\sin\theta}\left(\frac{\partial^2}{\partial\phi^2}\right), \quad (\text{D.2})$$

where we have used the coordinates r , θ and ϕ as the radius, polar angle and azimuthal angle, respectively. Inserting Equation D.2 into Equation D.1 yields,

$$-\frac{\hbar^2}{2m}\left[\frac{1}{r^2}\frac{\partial}{\partial r}\left(r^2\frac{\partial\Psi}{\partial r}\right) + \frac{1}{r^2\sin\theta}\frac{\partial}{\partial\theta}\left(\sin\theta\frac{\partial\Psi}{\partial\theta}\right) + \frac{1}{r^2\sin\theta}\left(\frac{\partial^2\Psi}{\partial\phi^2}\right)\right] + V\Psi = E\Psi. \quad (\text{D.3})$$

We look for solutions to this equations of the form

$$\Psi(r, \theta, \phi) = R(r)Y(\theta, \phi). \quad (\text{D.4})$$

Inserting this into Equation D.3 gives,

$$-\frac{\hbar^2}{2m} \left[\frac{Y}{r^2} \frac{d}{dr} \left(r^2 \frac{dR}{dr} \right) + \frac{R}{r^2 \sin \theta} \left(\sin \theta \frac{\partial Y}{\partial \theta} \right) + \frac{R}{r^2 \sin^2 \theta} \left(\frac{\partial^2 Y}{\partial \phi^2} \right) \right] + VRY = ERY, \quad (\text{D.5})$$

which we multiply by $-\frac{2mr^2}{RY\hbar^2}$,

$$\begin{aligned} & \left\{ \frac{1}{R} \frac{d}{dr} \left(r^2 \frac{dR}{dr} \right) - \frac{2mr^2}{\hbar^2} [V(r) - E] \right\} \\ & + \frac{1}{Y} \left\{ \frac{1}{\sin \theta} \frac{\partial}{\partial \theta} \left(\sin \theta \frac{\partial Y}{\partial \theta} \right) + \frac{1}{\sin \theta} \frac{\partial^2 Y}{\partial \phi^2} \right\} = 0, \end{aligned} \quad (\text{D.6})$$

where the first part is only dependent on r and the second part is only dependent on θ and ϕ . Notice that we have also assumed a spherical symmetric potential, i.e. $V = V(r)$. Next, we introduce the cleverly chosen separation constant $l(l+1)$,

$$\frac{1}{R} \frac{d}{dr} \left(r^2 \frac{dR}{dr} \right) - \frac{2mr^2}{\hbar^2} [V(r) - E] = l(l+1) \quad (\text{D.7})$$

$$\frac{1}{Y} \left\{ \frac{1}{\sin \theta} \frac{\partial}{\partial \theta} \left(\sin \theta \frac{\partial Y}{\partial \theta} \right) + \frac{1}{\sin^2 \theta} \frac{\partial^2 Y}{\partial \phi^2} \right\} = -l(l+1). \quad (\text{D.8})$$

D.1.1 The Angular Equation

Starting with Equation D.8, which dictates the dependence of Ψ on θ and ϕ , we have,

$$\frac{1}{\sin \theta} \frac{\partial}{\partial \theta} \left(\sin \theta \frac{\partial Y}{\partial \theta} \right) + \frac{1}{\sin^2 \theta} \frac{\partial^2 Y}{\partial \phi^2} = -l(l+1) \sin^2 \theta Y. \quad (\text{D.9})$$

We wish to make a further separation, by inserting $Y(\theta, \phi) = \Theta(\theta)\Phi(\phi)$ and dividing by $\Theta\Phi$,

$$\frac{1}{\Theta} \left[\sin \theta \frac{d}{d\theta} \left(\sin \theta \frac{d\Theta}{d\theta} \right) \right] + l(l+1) \sin \theta + \frac{1}{\Phi} \frac{d^2 \Phi}{d\phi^2} = 0, \quad (\text{D.10})$$

where we see that the variables have gathered in separate terms again. We therefore introduce the separation constant m^2 , which has nothing to do with the particle mass,

$$\frac{1}{\Theta} \left[\sin \theta \frac{d}{d\theta} \left(\sin \theta \frac{d\Theta}{d\theta} \right) \right] + l(l+1) \sin \theta = m^2 \quad (\text{D.11})$$

$$\frac{1}{\Phi} \frac{d^2 \Phi}{d\phi^2} = -m^2. \quad (\text{D.12})$$

Of these two Equation D.12 is instantly recognisable,

$$\frac{d^2 \Phi}{d\phi^2} = -m^2 \Phi, \quad (\text{D.13})$$

with the general solution

$$\Phi(\phi) = C_1 e^{im\phi} + C_2 e^{-im\phi}, \quad (\text{D.14})$$

but we will choose the more simpler solution

$$\Phi(\phi) = e^{im\theta}. \quad (\text{D.15})$$

We require periodicity, i.e. $\Phi(\phi + 2\pi) = \Phi(\phi)$, which means that m only takes integer values,

$$m = 0, \pm 1, \pm 2, \pm 3, \dots$$

The other angular equation, in Equation D.11, is not so simple,

$$\sin \theta \frac{d}{d\theta} \left(\sin \theta \frac{d\Theta}{d\theta} \right) + [l(l+1) \sin \theta - m^2] \Theta = 0. \quad (\text{D.16})$$

It has the more complicated solutions,

$$\Theta(\theta) = AP_l^m(\cos \theta), \quad (\text{D.17})$$

where P_l^m is the associated Legendre function,

$$P_l^m(x) \equiv (1-x^2)^{|m|/2} \left(\frac{d}{dx} \right)^{|m|} P_l(x), \quad (\text{D.18})$$

and P_l is the l th Legendre polynomial given by the Rodrigues formula,

$$P_l(x) \equiv \frac{1}{2^l l!} \left(\frac{d}{dx} \right)^l (x^2 - 1)^l. \quad (\text{D.19})$$

We see that for this function to take a value, we must have $l > 0$. Moreover, we see that if $|m| > l$ then $P_l^m = 0$. For a given l , there must be $2l+1$ possible values for m ,

$$l = 0, 1, 2, \dots \quad m = l, -l+1, \dots, -1, 0, 1, \dots, l-1, l.$$

A mathematician would at this point argue that because Equation D.11 is a second-order differential equation it should have two sets of solutions, not just the solution in Equation D.17. Another set of solutions exist but these are not sensible in the physical sense as they have singularities at $\theta = 0$ and $\theta = \pi$.

We would want to normalise the solutions we have found thus far. In spherical coordinates the volume element is

$$d^3\mathbf{r} = r^2 \sin \theta dr d\theta d\phi, \quad (\text{D.20})$$

this gives,

$$\int \int \int |\Psi|^2 r^2 \sin \theta dr d\theta d\phi = \int |R|^2 r^2 dr \int \int |Y|^2 \sin \theta dr d\theta d\phi = 1. \quad (\text{D.21})$$

We can normalise these parts separately,

$$\int_0^\infty |R|^2 r^2 dr = 1, \quad \int_0^{2\pi} \int_0^\pi |Y|^2 \sin \theta d\theta d\phi = 1. \quad (\text{D.22})$$

It so happens that the normalised angular wave functions are the spherical harmonics,

$$Y_l^m(\theta, \phi) = \epsilon \sqrt{\frac{2l+1}{4\pi}} \frac{(l-|m|)!}{(l+|m|)!} e^{im\phi} P_l^m(\cos \theta). \quad (\text{D.23})$$

A nice attribute of the spherical harmonics is that they are orthogonal.

D.1.2 The Radial Equation

For the type of spherical symmetric system we are dealing with, we have saved the best part for last, namely Equation D.7, which contains the potential V ,

$$\frac{d}{dr} \left(r^2 \frac{dR}{dr} \right) - \frac{2mr^2}{\hbar^2} [V(r) - E] R = l(l+1)R. \quad (\text{D.24})$$

To make our efforts less effortfull we make a variable change, $u(r) \equiv rR(r)$, such that

$$R = \frac{u}{r}, \quad \frac{dR}{dr} = \frac{1}{r} \frac{du}{dr} - \frac{u}{r^2}, \quad \frac{d}{dr} \left(r^2 \frac{dR}{dr} \right) = \frac{d^2u}{dr^2},$$

making Equation D.24,

$$-\frac{\hbar^2}{2m} \frac{d^2u}{dr^2} + \left[V + \frac{\hbar^2}{2m} \frac{l(l+1)}{r^2} \right] u = Eu, \quad (\text{D.25})$$

which is identical to one-dimensional Schrödinger equation, except for a new *effective* potential,

$$V_{\text{eff}} = V + \frac{\hbar^2}{2m} \frac{l(l+1)}{r^2}. \quad (\text{D.26})$$

For the radial equation with the substituted variable, we also require normalisation,

$$\int_0^\infty |u|^2 dr = 1. \quad (\text{D.27})$$

This is as far we get without specifying a potential.

D.2 Quantum Systems

There are several potentials that can be inserted into Equation D.24 in order to define a system. Some of these constitute mere toy models, like the “particle-in-a-box” potential, also called the infinite square well,

$$V(r) = \begin{cases} 0, & \text{if } r < a; \\ \infty & \text{if } r > a. \end{cases} \quad (\text{D.28})$$

Other potentials can approximate a natural system more properly, like the potential for the hydrogen atom.

The hydrogen atom consists of a heavy proton of charge e , together with a much lighter electron of charge $-e$, that orbits around it. The proton is essentially motionless, while the electron is bound by the mutual attraction between the opposite charges. The potential energy follows from Coulomb’s law,

$$V(r) = -\frac{e^2}{4\pi\epsilon_0} \frac{1}{r}. \quad (\text{D.29})$$

This gives a relatively simple radial equation,

$$-\frac{\hbar^2}{2m} \frac{d^2u}{dr^2} + \left[-\frac{e^2}{4\pi\epsilon_0} \frac{1}{r} + \frac{\hbar}{2m} \frac{l(l+1)}{r^2} \right] u = E_u. \quad (\text{D.30})$$

After Hydrogen, the next atom is helium. The Hamiltonian,

$$\hat{H} = \left\{ -\frac{\hbar^2}{2m} \nabla_i^2 - \frac{1}{4\pi\epsilon_0} \frac{2e^2}{r_1} \right\} + \left\{ -\frac{\hbar^2}{2m} \nabla_i^2 - \frac{1}{4\pi\epsilon_0} \frac{2e^2}{r_2} \right\} + \frac{1}{4\pi\epsilon_0} \frac{e^2}{|\mathbf{r}_1 - \mathbf{r}_2|}, \quad (\text{D.31})$$

consists of two hydrogen-like Hamiltonians, one for electron 1 and one for electron 2, inside curly braces. The last term describes the repulsion between the two electron, and causes trouble. If we ignore the last term, the Schrödinger equation separates, and we would get a ground state energy of -109 eV, but the experimentally measured value is -78.975 eVs [104]. We miss horribly by ignoring electron repulsion!

D.2.1 The Quantum Harmonic Oscillator

The quantum harmonic oscillator is the quantum mechanical analogue to the classical harmonic oscillator. Any arbitrary potential can be closely approximated as a harmonic potential about the equilibrium point, making the quantum harmonic oscillator one of the most important systems in quantum mechanics.

One Dimension

The hamiltonian of a one-dimensional harmonic oscillator is

$$\hat{H} = -\frac{\hbar^2}{2m} \nabla^2 + \frac{1}{2} m\omega^2 \hat{x}^2, \quad (\text{D.32})$$

where the potential function is a rewritten form of Hooke's law,

$$V(x) = \frac{1}{2} k \hat{x}^2 = \frac{1}{2} m\omega^2 \hat{x}^2, \quad (\text{D.33})$$

such that

$$\omega = \sqrt{\frac{k}{m}}.$$

The eigenstates of the one-dimensional harmonic oscillator is given by,

$$\Psi_n(x) = \frac{1}{\sqrt{2^n n!}} \left(\frac{m\omega}{\pi\hbar} \right)^{1/2} e^{-\frac{m\omega\hat{x}^2}{2\hbar}} H_n \left(\sqrt{\frac{m\omega}{\hbar}} x \right), \quad n = 0, 1, 2, 3, \dots, \quad (\text{D.34})$$

where the functions H_n are the Hermite polynomials,

$$H_n(z) = (-1)^n e^{z^2} \left(\frac{d}{dz} \right)^n (e^{-z^2}). \quad (\text{D.35})$$

The corresponding eigenenergies are,

$$E_n = \hbar\omega \left(n + \frac{1}{2} \right). \quad (\text{D.36})$$

Higher Dimensions

The three-dimensional harmonic oscillator can be solved in cartesian coordinates by separation of variables. The time-dependent Schrödinger equation for this system is,

$$-\frac{\hbar^2}{2m}\nabla^2\Psi + \frac{1}{2}m\omega^2\hat{r}^2\Psi = E\Psi, \quad (\text{D.37})$$

where $\hat{r} = \sqrt{\hat{x}^2 + \hat{y}^2 + \hat{z}^2}$. We insert

$$\Psi(x, y, z) = \xi(x)\eta(y)\zeta(z)$$

into Equation D.37 and divide by $\xi\eta\zeta$,

$$-\frac{\hbar^2}{2m}\frac{1}{\xi}\frac{\partial\xi}{x} + \frac{1}{2}m\omega^2\hat{x}^2 - \frac{\hbar^2}{2m}\frac{1}{\eta}\frac{\partial\eta}{y} + \frac{1}{2}m\omega^2\hat{y}^2 - \frac{\hbar^2}{2m}\frac{1}{\zeta}\frac{\partial\zeta}{z} + \frac{1}{2}m\omega^2\hat{z}^2 = E. \quad (\text{D.38})$$

In this expression we have two terms each of which depends on only one of the variables x , y and z , the sum of which is the constant E . In turn, each of the three groups of terms must be constant on its own. We can conclude that one three-dimensional harmonic oscillator is equivalent to three one-dimensional oscillators, in cartesian coordinates.

The general energy expression for a higher-dimensional quantum harmonic oscillator reads,

$$E_n = \left(n + \frac{d}{2}\right)\hbar\omega, \quad (\text{D.39})$$

where d is the number of dimensions. Unlike the one-dimensional quantum harmonic oscillator, a higher-dimension system will have energy degeneracies.

It is also possible to solve the harmonic-oscillator system in spherical coordinates, by inserting the potential

$$V(r) = \frac{1}{2}m\omega^2\hat{r}^2,$$

into the radial equation, specified in Equation D.7,

$$-\frac{\hbar^2}{2m}\frac{d^2u}{dr^2} + \left(\frac{1}{2}m\omega^2\hat{r}^2 + \frac{\hbar^2}{2m}\frac{l(l+1)}{r^2}\right)u = Eu. \quad (\text{D.40})$$

The solutions will be different, depending on the number of dimensions. In two dimensions we have eigenfunctions given by,

$$\Psi_{nm}(r, \theta) = N_{nm}ae^{im\theta}(ar)^{|m|}L_n^{|m|}(a^2r^2)e^{-a^2r^2/2}, \quad (\text{D.41})$$

where

$$a \equiv \sqrt{\frac{m\omega}{\hbar}},$$

N_{nm} is a normalisation constant given by,

$$N_{nm}\sqrt{\frac{n!}{\pi(n+|m|)!}},$$

and

$$L_{q-p}^p(x) \equiv (-1)^p \left(\frac{d}{dx} \right)^p L_q(x), \quad (\text{D.42})$$

is an associated Laguerre polynomial, where

$$L_q(x) \equiv e^x \left(\frac{d}{dx} \right)^q (e^{-x} x^q), \quad (\text{D.43})$$

is the q th Laguerre polynomial. The corresponding energy eigenvalues in two dimensions are

$$E_{nm} = \hbar\omega(2n + |m| + 1). \quad (\text{D.44})$$

In three dimensions the eigenfunctions are given by,

$$\Psi_{nlm}(r, \theta, \phi) = N_{nl} r^l e^{-a^2 r^2/2} L_n^{l+\frac{1}{2}}(a^2 r^2) Y_l^m(\theta, \phi), \quad (\text{D.45})$$

where N_{nl} is a normalisation constant, L are the associated Laguerre polynomials given by Equation D.42 and Y are the spherical harmonics given by Equation D.23. The corresponding energy eigenvalues in three dimensions are,

$$E_{nl} = \hbar\omega \left(2n + l + \frac{3}{2} \right). \quad (\text{D.46})$$

Notice that in two dimensions there are only two quantum numbers, while in three dimensions there are three quantum numbers. This derivation has completely disregarded spin and angular momentum, which would add further quantum numbers, because further degrees of freedom are introduced.

Bibliography

1. Kvaal, S. Ab Initio Quantum Dynamics Using Coupled-Cluster. *The Journal of Chemical Physics* **136**, 194109 (2012).
2. Myhre, R. H. Demonstrating that the Nonorthogonal Orbital Optimized Coupled Cluster Model Converges to Full Configuration Interaction. *The Journal of Chemical Physics* **148**, 094110 (2018).
3. Sun, Q. *et al.* PySCF: The Python-Based Simulations of Chemistry Framework 2017.
4. Parrish, R. M. *et al.* Psi4 1.1: An Open-Source Electronic Structure Program Emphasizing Automation, Advanced Libraries, and Interoperability. *Journal of Chemical Theory and Computation* **13**, 3185 (2017).
5. Kohn, W. Cyclotron Resonance and de Haas-van Alphen Oscillations of an Interacting Electron Gas. *Physical Review* **123**, 1242 (1961).
6. Schøyen, Ø. S. *Real-Time Quantum Many-Body Dynamics* MA thesis (2019).
7. Pederiva, G. *Computing the Lambda Scale of Pure Yang-Mills Theory from a Novel Lattice QCD Code with Gradient Flow* MA thesis (2018).
8. Vege, H. M. M. *Solving SU (3) Yang-Mills Theory on the Lattice: A Calculation of Selected Gauge Observables with Gradient Flow* MA thesis (2019).
9. Stende, J. A. *Constructing High-Dimensional Neural Network Potentials for Molecular Dynamics* MA thesis (2017).
10. Treider, H. V. *Speeding Up Ab Initio Molecular Dynamics with Artificial Neural Networks* MA thesis (2017).
11. Sand, O. P. *Massive Neutrinos and Spherical Collapse in LCDM and DGP Gravity* MA thesis (2016).
12. Hartree, D. R. The Wave Mechanics of an Atom with a Non-Coulomb Central Field. Part I. Theory and Methods. *Mathematical Proceedings of the Cambridge Philosophical Society* **24**, 89 (1928).
13. Fock, V. A. Näherungsmethode zur Lösung des Quantenmechanischen Mehrkörperproblems. *Zeitschrift für Physik* **61**, 126 (1930).
14. Szabo, A. & Ostlund, N. S. *Modern Quantum Chemistry: Introduction to Advanced Electronic Structure Theory* (Courier Corporation, 2012).

15. Kohn, W. & Sham, L. J. Self-Consistent Equations Including Exchange and Correlation Effects. *Physical Review* **140**, A1133 (1965).
16. Helgaker, T., Jorgensen, P. & Olsen, J. *Molecular Electronic-Structure Theory* (John Wiley & Sons, 2014).
17. Hammond, B. L., Lester, W. A. & Reynolds, P. J. *Monte Carlo Methods in Ab Initio Quantum Chemistry* (World Scientific, 1994).
18. Bartlett, R. J. & Purvis, G. D. Many-Body Perturbation Theory, Coupled-Pair Many-Electron Theory, and the Importance of Quadruple Excitations for the Correlation Problem. *International Journal of Quantum Chemistry* **14**, 561 (1978).
19. Pople, J. A., Binkley, J. S. & Seeger, R. Theoretical Models Incorporating Electron Correlation. *International Journal of Quantum Chemistry* **10**, 1 (1976).
20. Shavitt, I. & Bartlett, R. J. *Many-Body Methods in Chemistry and Physics: MBPT and Coupled-Cluster Theory* (Cambridge University Press, 2009).
21. Brueckner, K. A. & Levinson, C. A. Approximate Reduction of the Many-Body Problem for Strongly Interacting Particles to a Problem of Self-Consistent Fields. *Physical Review* **97**, 1344 (1955).
22. Goldstone, J. Derivation of the Brueckner Many-Body Theory. *Proceedings of the Royal Society of London. Series A - Mathematical and Physical Sciences* **239**, 267 (1957).
23. Coester, F. Bound States of a Many-Particle System. *Nuclear Physics* **7**, 421 (1958).
24. Coester, F. & Kümmel, H. Short-Range Correlations in Nuclear Wave Functions. *Nuclear Physics* **17**, 477 (1960).
25. Ratcliff, L. E. *et al.* Challenges in Large Scale Quantum Mechanical Calculations. *Wiley Interdisciplinary Reviews: Computational Molecular Science* **7**, e1290 (2017).
26. Ashoori, R. Electrons in artificial atoms. *Nature* **379**, 413 (1996).
27. Kristiansen, H. E. *Time Evolution of Quantum Mechanical Many-Body Systems* MA thesis (2017).
28. Kristiansen, H. E., Schøyen, Ø. S., Kvaal, S. & Pedersen, T. B. Numerically Stable Time-Dependent Coupled-Cluster Simulations of Many-Electron Dynamics in Intense Laser Pulses. (*In Preparation for Publication*) (2019).
29. Blackford, L. S. *et al.* An updated set of basic linear algebra subprograms (BLAS). *ACM Transactions on Mathematical Software* **28**, 135 (2002).
30. Anderson, E. *et al.* *LAPACK Users' Guide* Third. ISBN: 0-89871-447-8 (paperback) (Society for Industrial and Applied Mathematics, Philadelphia, PA, 1999).
31. Lam, S. K., Pitrou, A. & Seibert, S. Numba: A llvm-based python jit compiler. *Proceedings of the Second Workshop on the LLVM Compiler Infrastructure in HPC*, 7 (2015).

32. Helgaker, T. & Jørgensen, P. Analytical Calculation of Geometrical Derivatives in Molecular Electronic Structure Theory. *Advances in Quantum Chemistry* **19**, 183 (1988).
33. Arponen, J. Variational Principles and Linked-Cluster exp S Expansions for Static and Dynamic Many-Body Problems. *Annals of Physics* **151**, 311 (1983).
34. Ehrenfest, P. Bemerkung über die Angenäherte Gültigkeit der Klassischen Mechanik Innerhalb der Quantenmechanik. *Zeitschrift für Physik A - Hadrons and Nuclei* **45**, 455 (1927).
35. Dirac, P. A. M. *The Principles of Quantum Mechanics* (Oxford University Press, 1930).
36. Von Neumann, J. *Mathematical Foundations of Quantum Mechanics* (Berlin: Springer, 1932).
37. Helgaker, T. *et al.* Recent Advances in Wave Function-Based Methods of Molecular-Property Calculations. *Chemical Reviews* **112**, 543 (2012).
38. Joachain, C. J., Kylstra, N. J. & Potvliege, R. M. *Atoms in Intense Laser Fields* (Cambridge University Press, 2012).
39. Post, H. Individuality and Physics. *The Listener* **70**, 534 (1963).
40. Feynman, R. P. Nobel Lecture: The Development of the Space-Time View of Quantum Electrodynamics. <https://www.nobelprize.org/prizes/physics/1965/feynman/lecture/> (1965).
41. Leinaas, J. M. & Myrheim, J. On the Theory of Identical Particles. *Il Nuovo Cimento B (1971-1996)* **37**, 1 (1977).
42. Fierz, M. *Über die Relativistische Theorie Kräftefreier Teilchen mit Beliebigem Spin* PhD thesis (Birkhäuser, 1939).
43. Pauli, W. The Connection between Spin and Statistics. *Physical Review* **58**, 716 (1940).
44. Hilborn, R. C. Atoms in Orthogonal Electric and Magnetic Fields: A Comparison of Quantum and Classical Models. *American Journal of Physics* **63**, 330 (1995).
45. Pauli, W. Über den Zusammenhang des Abschlusses der Elektronengruppen im Atom mit der Komplexstruktur der Spektren. *Zeitschrift für Physik A Hadrons and Nuclei* **31**, 765 (1925).
46. Harris, F. E., Monkhorst, H. J. & Freeman, D. L. *Algebraic and Diagrammatic Methods in Many-Fermion Theory* (New York, NY (United States); Oxford University Press, 1992).
47. Slater, J. C. The Self Consistent Field and the Structure of Atoms. *Physical Review* **32**, 339 (1928).
48. Gaunt, J. A. A Theory of Hartree's Atomic Fields. *Mathematical Proceedings of the Cambridge Philosophical Society* **24**, 328 (1928).
49. Slater, J. C. Note on Hartree's Method. *Physical Review* **35**, 210 (1930).

50. Hartree, D. R. & Hartree, W. Self-Consistent Field, with Exchange, for Beryllium. *Proceedings of the Royal Society of London. Series A - Mathematical and Physical Sciences* **150**, 9 (1935).
51. Heitler, W. & London, F. Wechselwirkung Neutraler Atome und Homöopolare Bindung nach der Quantenmechanik. *Zeitschrift für Physik* **44**, 455 (1927).
52. Berthier, G. Extension de la Methode du Champ Moleculaire Self-Consistent a Letude des Etats a Couches Incompltes. *Comptes Rendus Hebdomadaires des Seances de l'Academie des Sciences* **238**, 91 (1954).
53. Pople, J. A. & Nesbet, R. K. Self-Consistent Orbitals for Radicals. *The Journal of Chemical Physics* **22**, 571 (1954).
54. Hochstuhl, D., Hinz, C. M. & Bonitz, M. Time-Dependent Multiconfiguration Methods for the Numerical Simulation of Photoionization Processes of Many-Electron Atoms. *The European Physical Journal Special Topics* **223**, 177 (2014).
55. Brillouin, L. Les Problèmes de Perturbations et les Champs Self-Consistents. *J. Phys. Radium* **3**, 373 (1932).
56. Wigner, E. P. On a Modification of the Rayleigh-Schrödinger Perturbation Theory. *Magyar Tudományos Akadémia Matematikai és Természettudományi Ertesítője* **53**, 477 (1935).
57. Rayleigh, J. W. S. The Theory of Sound, Article 88, vol. 1. *2nd revised edn. New York: Dover (reprint 1945)*, 110 (1894).
58. Schrödinger, E. Quantisierung als Eigenwertproblem. *Annalen der Physik* **385**, 437 (1926).
59. Hubbard, J. The Description of Collective Motions in Terms of Many-Body Perturbation Theory. *Proceedings of the Royal Society of London. Series A. Mathematical and Physical Sciences* **240**, 539 (1957).
60. Hugenholtz, N. M. Perturbation Theory of Large Quantum Systems. *Physica* **23**, 481 (1957).
61. Kümmel, H. Origins of the Coupled Cluster Method. *Theoretica Chimica Acta* **80**, 81 (1991).
62. Čížek, J. On the Correlation Problem in Atomic and Molecular Systems. Calculation of Wavefunction Components in Ursell-Type Expansion Using Quantum-Field Theoretical Methods. *The Journal of Chemical Physics* **45**, 4256 (1966).
63. Paldus, J., Čížek, J. & Shavitt, I. Correlation Problems in Atomic and Molecular Systems. IV. Extended Coupled-Pair Many-Electron Theory and Its Application to the B H 3 Molecule. *Physical Review A* **5**, 50 (1972).
64. Sinanoglu, O. Many-Electron Theory of Atoms, Molecules and Their Interactions. *Advances in Chemical Physics*, 315 (1964).
65. Löwdin, P.-O. The historical development of the electron correlation problem. *International Journal of Quantum Chemistry* **55**, 77 (1995).

66. Purvis III, G. D. & Bartlett, R. J. A Full Coupled-Cluster Singles and Doubles Model: The Inclusion of Disconnected Triples. *The Journal of Chemical Physics* **76**, 1910 (1982).
67. Thouless, D. J. Stability Conditions and Nuclear Rotations in the Hartree-Fock Theory. *Nuclear Physics* **21**, 225 (1960).
68. Einstein, A. *et al.* The Foundation of the General Theory of Relativity. *Annalen der Physik* **49**, 769 (1916).
69. Campbell, J. E. On a Law of Combination of Operators (Second Paper). *Proceedings of the London Mathematical Society* **1**, 14 (1897).
70. Baker, H. F. Alternants and Continuous Groups. *Proceedings of the London Mathematical Society* **2**, 24 (1905).
71. Hausdorff, F. Die Symbolische Exponentialformel in der Gruppentheorie. *Berichte über die Verhandlungen der Königlich-Sächsischen Gesellschaft der Wissenschaft zu Leipzig, Mathematisch-Physische Klasse* **58**, 19 (1906).
72. Kvaal, S. Variational Formulations of the Coupled-Cluster Method in Quantum Chemistry. *Molecular Physics* **111**, 1100 (2013).
73. Fink, M. A New Method for Evaluating the Density Matrix and its Application to the Ground State Form Factors of ${}^4\text{He}$ and ${}^{16}\text{O}$. *Nuclear Physics A* **221**, 163 (1974).
74. Feynman, R. P. Forces in Molecules. *Physical Review* **56**, 340 (1939).
75. Helgaker, T. & Jørgensen, P. Configuration-Interaction Energy Derivatives in a Fully Variational Formulation. *Theoretica Chimica Acta* **75**, 111 (1989).
76. Bartlett, R. J. & Noga, J. The Expectation Value Coupled-Cluster Method and Analytical Energy Derivatives. *Chemical Physics Letters* **150**, 29 (1988).
77. Arponen, J. S., Bishop, R. F. & Pajanne, E. Extended Coupled-Cluster Method. I. Generalized Coherent Bosonization as a Mapping of Quantum Theory into Classical Hamiltonian Mechanics. *Physical Review A* **36**, 2519 (1987).
78. Krylov, A. I., Sherrill, C. D., Byrd, E. F. C. & Head-Gordon, M. Size-Consistent Wave Functions for Nondynamical Correlation Energy: The Valence Active Space Optimized Orbital Coupled-Cluster Doubles Model. *The Journal of Chemical Physics* **109**, 10669 (1998).
79. Pedersen, T. B., Koch, H. & Hättig, C. Gauge Invariant Coupled Cluster Response Theory. *The Journal of Chemical Physics* **110**, 8318 (1999).
80. Gross, E. K. U. & Runge, E. Many-particle theory (1986).
81. Jørgensen, M. H. *Many-Body Approaches to Quantum Dots* MA thesis (2011).
82. Lohne, M. P. *Coupled-Cluster Studies of Quantum Dots* MA thesis (2010).
83. Loss, D. & DiVincenzo, D. P. Quantum Computation with Quantum Dots. *Physical Review A* **57**, 120 (1998).
84. Reimann, S. M. & Manninen, M. Electronic Structure of Quantum Dots. *Reviews of Modern Physics* **74**, 1283 (2002).

85. Anisimovas, E. & Matulis, A. Energy Spectra of Few-Electron Quantum Dots. *Journal of Physics: Condensed Matter* **10**, 601 (1998).
86. Fock, V. Bemerkung zur Quantelung des harmonischen Oszillators im Magnetfeld. *Zeitschrift für Physik A Hadrons and Nuclei* **47**, 446 (1928).
87. Darwin, C. G. The Diamagnetism of the Free Electron. *Mathematical Proceedings of the Cambridge Philosophical Society* **27**, 86 (1931).
88. Pulay, P. Convergence Acceleration of Iterative Sequences. The Case of SCF Iteration. *Chemical Physics Letters* **73**, 393 (1980).
89. Pedersen, T. B. & Kvaal, S. Symplectic Integration and Physical Interpretation of Time-Dependent Coupled-Cluster Theory. *The Journal of Chemical Physics* **150**, 144106 (2019).
90. Golub, G. H. & Welsch, J. H. Calculation of Gauss Quadrature Rules. *Mathematics of Computation* **23**, 221 (1969).
91. Hairer, E., Lubich, C. & Wanner, G. *Geometric Numerical Integration: Structure-Preserving Algorithms for Ordinary Differential Equations* (Springer Science & Business Media, 2006).
92. Li, X. *et al.* A time-Dependent Hartree-Fock Approach for Studying the Electronic Optical Response of Molecules in Intense Fields. *Physical Chemistry Chemical Physics* **7**, 233 (2005).
93. Zanghellini, J., Kitzler, M., Brabec, T. & Scrinzi, A. Testing the Multi-Configuration time-dependent Hartree–Fock method. *Journal of Physics B: Atomic, Molecular and Optical Physics* **37**, 763 (2004).
94. Miyagi, H. & Madsen, L. B. Time-Dependent Restricted-Active-Space Self-Consistent Field Theory for Laser-Driven Many-Electron dynamics. *Physical Review A* **87**, 062511 (2013).
95. Jensen, F. *Introduction to computational chemistry* (John Wiley & Sons, 2017).
96. Brey, L., Johnson, N. F. & Halperin, B. I. Optical and Magneto-Optical Absorption in Parabolic Quantum Wells. *Physical Review B* **40**, 10647 (1989).
97. Lai, M.-Y. & Pan, X.-Y. The generalized harmonic potential theorem in the presence of a time-varying magnetic field. *Scientific reports* **6**, 35412 (2016).
98. Heitmann, D. & Kotthaus, J. P. The Spectroscopy of Quantum Dot Arrays. *Physics Today* **46**, 56 (1993).
99. Meurer, B., Heitmann, D. & Ploog, K. Single-Electron Charging of Quantum-Dot Atoms. *Physical Review Letters* **68**, 1371 (1992).
100. Nielsen, E., Muller, R. P. & Carroll, M. S. Configuration Interaction Calculations of the Controlled Phase Gate in Double Quantum Dot Qubits. *Physical Review B* **85**, 035319 (2012).
101. Vorrath, T. & Blümel, R. Electronic Structure of Three-Dimensional Quantum Dots. *The European Physical Journal B - Condensed Matter and Complex Systems* **32**, 227 (2003).

102. Kristiansen, H. E., Schøyen, Ø. S., Winther-Larsen, S. G. & Hjorth-Jensen, M. Time Evolution of Quantum Dot Systems. (*In Preparation for Publication*) (2019).
103. Monkhorst, H. J. Calculation of Properties with the Coupled-Cluster Method. *International Journal of Quantum Chemistry* **12**, 421 (1977).
104. Griffiths, D. J. & Schroeter, D. F. *Introduction to quantum mechanics* (Cambridge University Press, 2018).